



If you have discovered material in AURA which is unlawful e.g. breaches copyright, (either yours or that of a third party) or any other law, including but not limited to those relating to patent, trademark, confidentiality, data protection, obscenity, defamation, libel, then please read our [Takedown Policy](#) and [contact the service](#) immediately

WEB STRENGTH  
OF  
ROLLED STEEL JOISTS

BY

RAYMOND GRAHAM GUY B.Sc.

A THESIS SUBMITTED FOR THE DEGREE  
OF  
DOCTOR OF PHILOSOPHY

DEPARTMENT OF CIVIL ENGINEERING  
THE UNIVERSITY OF ASTON  
IN BIRMINGHAM

JULY 1977

## WEB STRENGTH OF ROLLED STEEL JOISTS

BY

RAYMOND GRAHAM GUY

THESIS SUBMITTED FOR THE DEGREE OF DOCTOR OF PHILOSOPHY 1977

## SUMMARY

This work is concerned with the behaviour of thin webbed rolled steel joists or universal beams when they are subjected to concentrated loads applied to the flanges. The prime concern is the effect of high direct stresses causing web failure in a small region of the beam.

The review shows that although many tests have been carried out on rolled steel beams and built up girders, no series of tests has restricted the number of variables involved to enable firm conclusions to be drawn.

The results of 100 tests on several different rolled steel universal beam sections having various types of loading conditions are presented. The majority of the beams are tested by loading with two opposite loads, thus eliminating the effects of bending and shear, except for a small number of beams which are tested simply supported on varying spans.

The test results are first compared with the present design standard (BS 449) and it is shown that the British Standard is very conservative for most of the loading conditions included in the tests but is unsafe for others.

Three possible failure modes are then considered, overall elastic buckling of the web, flexural yielding of the web due to large out of plane deflexions and local crushing of the material at the junction of the web and the root fillets. Each mode is considered theoretically and developed to establish the main variables, thus enabling a comparison to be made with the test results. It is shown that all three failure modes have a particular relevance for individual loading conditions, but that determining the failure load given the beam size and the loading conditions is very difficult in certain instances.

Finally it is shown that there are some empirical relationships between the failure loads and the type of loading for various beam serial sizes.

Beam, Buckling, Crushing, Joist, Web

## ACKNOWLEDGEMENTS

Page No.

The author wishes to express his thanks to Professor M. Holmes, B.Sc., Ph.D., C.Eng., F.I.C.E., F.I.Struct.E., F.I.Mun.E., head of the department of Civil Engineering, for permitting the research to be carried out. The author also wishes to express his gratitude to his supervisor, Mr. A. W. Astill, B.Sc., C.Eng., F.I.Struct.E., for his guidance and encouragement throughout the period of this research project.

Thanks are also due to Mr. W. Parsons and his team of technicians for their invaluable help with the laboratory work.

Finally the author wishes to thank the Science Research Council for providing the financial support.

10



## CONTENTS

	Page No.
Summary	(i)
Acknowledgements	(ii)
Contents	(iii)
Notation	(xiii)
CHAPTER 1 - REVIEW.	
1.1 Introduction.	1
1.2 British Standard 449 (BS 449).	2
1.3 Standard Elastic Plate Buckling Theory.	4
1.3.1 Uniform Edge Loading on Two Opposite Edges.	5
1.3.2 Concentrated Edge Loading on Two Opposite Edges.	6
1.4 Further Plate Buckling Theories.	7
1.4.1 Inelastic Plate Buckling.	10
1.5 Empirical Methods of Analysis and Published Test Results.	12
1.6 Conclusions from Previous Work.	14
CHAPTER 2 - EXPERIMENTATION AND PRESENTATION OF THE RESULTS.	
2.1 Introduction.	16
2.1.1 Test Beam Referencing.	16
2.1.2 Universal Beam Serial Sizes.	18
2.1.3 Tests Carried Out.	18
2.2 Material Properties.	24
2.2.1 Tensile Tests.	24
2.2.1.1 Large Tensile Test Specimens.	25
2.2.1.2 Small Tensile Test Specimens.	27
2.2.2 Results of Tensile Tests.	27

2.2.3	Observations from the Tensile Test Results.	31
2.3	Test Beam Preparation and Performance Under Test.	33
2.3.1	Test Beam Dimensions.	34
2.3.2	Strain Indicators.	37
2.3.2.1	Strain Distribution.	40
2.3.2.2	Strain Gauge Readings.	44
2.3.3	Deflexion Indicators.	55
2.3.3.1	Deflexion Recordings.	56
2.4	Test Details.	59
2.4.1	Load Applications.	59
2.4.2	Test Procedure.	63
2.4.3	Modes of Failure and Test Failure Loads.	65
2.4.3.1	Modes of Failure.	65
2.4.3.2	Test Failure Loads.	70
2.5	Conclusions from the Test Results.	78
CHAPTER 3 - DESIGN GUIDES AND OTHER AUTHORS' THEORIES.		
3.1	Introduction.	79
3.2	Current Design Practice.	80
3.2.1	Design to BS 449.	80
3.2.2	Comparison with the Test Results.	82
3.2.3	Conclusions from the Comparison.	90
3.3	Other Authors' Work.	91
3.3.1	Shedd (40).	91
3.3.2	Winter and Pian (32).	92
3.3.3	Delesques (33).	93
3.4	Conclusions.	94

## CHAPTER 4 - ELASTIC BUCKLING THEORY.

4.1	Introduction.	96
4.2	Elastic Buckling Analysis.	96
4.2.1	Plate with Two Opposite Uniformly Distributed Loads.	99
4.2.2	Plate with Two Opposite Partial Edge Loads.	103
4.2.3	Plate with Boundary Conditions Applicable to the Web of a Rolled Steel Beam.	105
4.3	Estimation of the Restraint Provided by the Flanges of a Rolled Steel Universal Beam.	115
4.4	Elastic Critical Test Load.	117
4.4.1	Strain Behaviour in the Web.	119
4.4.2	The Southwell Plot.	119
4.4.2.1	The Southwell Plot for the Tested Beams.	121
4.4.3	Conclusions from the Test Elastic Critical Loads.	129
4.5	Comparison of Developed Theory and the Test Results.	129
4.6	Conclusions from the Comparison.	138

## CHAPTER 5 - YIELD LINE THEORY.

5.1	Introduction.	140
5.2	Yield Line Method.	141
5.2.1	Mode 1.	141
5.2.2	Mode 2.	146
5.2.3	Mode 3.	151

	Page No.
5.2.4 Restraining Effects.	156
5.2.4.1 Flange Restraining Effects.	156
5.2.4.2 Web Restraining Effects.	159
5.3 The $\Delta/w_c$ Ratio.	160
5.3.1 Empirical Assessment of $\Delta/w_c$ .	161
5.4 Comparison with the Test Results.	162
5.5 Observations and Conclusions from the Comparison.	169
CHAPTER 6 - LOCAL CRUSHING AND EMPIRICAL ASSESSMENT OF THE TEST RESULTS.	
6.1 Introduction.	172
6.2 Local Crushing Theory.	172
6.3 Suitability of the Crushing Theory.	175
6.4 Empirical Assessment of the Test Results.	183
6.4.1 Series III.	183
6.4.2 Series V and VI.	184
6.5 Conclusions.	188
CHAPTER 7 - CONCLUSIONS AND SUGGESTIONS FOR FURTHER RESEARCH.	
7.1 Introduction.	192
7.2 Conclusions from the Test Results.	193
7.3 Conclusions from the comparisons of Individual Theories with the Test Results.	195
7.4 Summary.	200
7.5 Suggestions for Further Research.	202
REFERENCES	204

## APPENDIX

A.1	Strain and Deflexion Recordings.	209
A.2	Elastic Analysis Details.	258

## LIST OF TABLES

## CHAPTER 2

Table 2.1	Beam serial sizes used in the tests.	20
Table 2.2		21-23
Table 2.3		28-30
Table 2.4		35-36
Table 2.5		71-72

## CHAPTER 3

Table 3.1		84-85
-----------	--	-------

## CHAPTER 4

Table 4.1	Typical results of the elastic analysis	112
Table 4.2	Results of the Southwell plot for beams tested in Series I and II.	125
Table 4.3	Results of the Southwell plot for selected beams in Series III to VI.	130

## CHAPTER 5

Table 5.1		163-164
-----------	--	---------

## CHAPTER 6

Table 6.1		177
Table 6.2		179
Table 6.3		184
Table 6.4	Series V	186
Table 6.5	Series VI	186

## APPENDIX

Table A.1		211-257
Table A.2		263-274

## LIST OF FIGURES

## CHAPTER 1

Figure 1.1 Plates with various loading conditions. 8

## CHAPTER 2

Figure 2.1 Summary of test Series I to VII. 19

Figure 2.2 Tensile test specimens and locations. 26

Figure 2.3 Variation of yield stress with section thickness. 32

Figure 2.4 Typical strain gauge locations and referencing. 39

Figure 2.5 41

Figure 2.6 43

Figure 2.7 Comparison of strains for Series I and III (at 200 KN). 45

Figure 2.8 Typical mid-depth strain distributions - Series I. 47

Figure 2.9 Typical mid-depth strain distributions - Series III. 48

Figure 2.10 Typical strain distributions - Series IV. 50

Figure 2.11 Typical strain distributions - Series V. 52

Figure 2.12 Test 96 (Series VII) web stresses at mid-span. 54

Figure 2.13 Typical load deflexion curves - Series I and III. 57

Figure 2.14 Series II load deflexion curves. 60

Figure 2.15 61

Figure 2.16 66

Figure 2.17 68

Figure 2.18 69

Figure 2.19	Typical pattern of retest failure loads for selective tests.	73
Figure 2.20	Typical variation of test failure loads with the variables investigated - Series I to IV.	75
Figure 2.21	Typical variation of test failure loads with the variables investigated - Series V and VI.	76
Figure 2.22	Typical variation of test failure loads with the variables investigated - Series VII.	77
CHAPTER 3		
Figure 3.1	Typical comparison of test failure loads and BS 449 ultimate loads - Series I and II.	86
Figure 3.2	Typical comparison of test failure loads and BS 449 ultimate loads - Series III and IV.	88
Figure 3.3	Typical comparison of Series V test failure loads and BS 449 ultimate loads.	89
CHAPTER 4		
Figure 4.1	Elastic buckling coefficient $K_1$ - various edge conditions.	100
Figure 4.2	Elastic buckling coefficient $K_1$ - free loaded edges (Woinowsky-Krieger (10))	101
Figure 4.3	Elastic buckling coefficient $K_1$ - restrained loaded edges (Bleich (12)).	102
Figure 4.4	Elastic buckling coefficient $K$ - various edge conditions.	104

Figure 4.5	Typical results obtained by Khan and Walker (20).	106
Figure 4.6	Plate deflected form used for the elastic analysis (free unloaded edges).	108
Figure 4.7	Typical form of the results of the elastic analysis.	113
Figure 4.8	Typical form of the results of the elastic analysis.	114
Figure 4.9		116
Figure 4.10		118
Figure 4.11	Typical Southwell plot for Series I beams.	122
Figure 4.12	Southwell plot for Series II beams.	123
Figure 4.13	Typical Southwell plot for Series III beams.	126
Figure 4.14		128
Figure 4.15	Series I test results compared with elastic buckling theory.	131
Figure 4.16	Series III test results compared with elastic buckling theory.	133
Figure 4.17	Variation of $K_u$ with flange thickness(T)	136
Figure 4.18	Series V test results compared with elastic buckling theory.	137
CHAPTER 5		
Figure 5.1	Possible failure modes dependent on flange restraint.	142
Figure 5.2	Mode 1 yield line patterns.	143
Figure 5.3	Mode 1 - Section through applied loads (diagrammatic).	145



	Page No.
Figure 5.4 Typical results of Mode 1 analysis.	147
Figure 5.5 Mode 2 yield line patterns.	148
Figure 5.6 Mode 2 - Section through applied loads (diagrammatic).	149
Figure 5.7 Typical results of Mode 2 analysis.	152
Figure 5.8 Flange yield line patterns.	153
Figure 5.9 Mode 3 - Section through applied loads (diagrammatic).	154
Figure 5.10 Typical results of flange contribution to Mode 3 analysis.	157
Figure 5.11 Typical results of Mode 3 analysis.	158
Figure 5.12 Yield line theory compared with Series I and III test results.	166
Figure 5.13 Yield line theory compared with Series V test results.	167
Figure 5.14 Yield line theory compared with test results (failure remote from the end).	168
Figure 5.15	170
CHAPTER 6	
Figure 6.1	173
Figure 6.2	176
Figure 6.3	178
Figure 6.4 Typical comparison of local crushing theory and Series III test results.	181
Figure 6.5 Typical comparison of local crushing theory and Series V test results.	182
Figure 6.6	185

Figure 6.7	Variation of failure loads for beam N with beam length, showing the effects of the applied load length.	187
Figure 6.8	Variation of failure loads for beam M with beam length, showing the effects of the applied load length.	189
APPENDIX		
Figure A.1	Main program	260
Figure A.2	Subroutine MINIM	261

# NOTATION

A	Half wave length.
A'	Area of a strut.
a	Width of a rectangular plate.
B	Joist flange width.
b	Depth of a rectangular plate (or strut).
C	Half length of applied load.
Co	Euler buckling load (BS-449) $= \pi^2 E / r_s^2$ .
Cr	Flange restraint.
$C_1, C_2$	Constants.
D	Plate flexural rigidity.
$D_t$	Overall depth of a rolled steel beam.
$D_t'$	Elastic portion of the overall depth of a rolled steel beam.
d	Web depth (between root fillets).
E	Youngs modulus.
e	Eccentricity.
f	Coefficient.
fb	Permissible ultimate stress (Perry formula).
fy	Yield stress.
$fy_f$	Flange yield stress.
$fy_r$	Root yield stress.
$fy_w$	Web yield stress.
$h_b$	Effective strut width.
$h_c$	Effective bearing length.
I	Moment of inertia.
$K, K_1$	Elastic plate buckling coefficients.
$\underline{K}$	Stiffness matrix.
Ke	Equivalent elastic plate buckling coefficient.

$K_u$	Equivalent plate buckling coefficient determined from the ultimate load.
$L$	Overall length of a beam.
$l$	Half width of a plate.
$l_a$	Length of applied load.
$l_c$	Arbitrary length.
$l_e$	Distance from end of beam to applied load.
$l_k$	Width of applied load.
$l_s$	Length of a strut.
$M_f$	Plastic moment of resistance for the flange.
$M_p$	Plastic moment of resistance.
$M_w$	Plastic moment of resistance for the web.
$m$	Half depth of a plate.
$N_{cr}$	Critical force per unit length.
$N_x$	Applied force per unit length in the x-direction
$N_y$	Applied force per unit length in the y-direction
$N_{xy}$	Applied shear force per unit length.
$n$	Factor (Perry formula).
$P$	Load.
$P(i)$ , etc.	Load for mode indicated.
$P_{cr}$	Critical load.
$P_{exp}$	Experimental load.
$P_f$	Load taken by the flanges.
$P_p$	Load required to produce post crushing web failure.
$P_{th}$	Theoretical load.
$P_u, P_{ult}$	Ultimate load.
$P_0, P_1$	Loads as defined in the text (Chapter 5).
$P_{yl}$	Load computed using Yield Line Theory.
$Q$	Constant.

$R$	Coefficient of restraint.
$R_1, R_2, \text{etc.}$	Functions of $R$ as defined in the text.
$r$	Root radius.
$r_s$	Slenderness ratio.
$S$	Constant.
$s$	Span.
$s_b$	Reduced flange width ( $B - t/2 - r$ ).
$T$	Flange thickness.
$t$	Web thickness.
$U$	Work.
$W$	Work.
$w$	Out of plane web deflexion.
$w_c$	Out of plane web deflexion at mid-depth.
$w_{c1}, w_{c2}$	Out of plane web deflexion at mid-depth for modes 1 and 2 respectively.
$w_o$	Initial web or plate deflexion.
$w_1, w_2$	Amplitude of buckled wave.
$x, y, z$	Cartezian coordinates.
$Z$	Function as defined in the text.
$\alpha$	Wave length ratio ( $= A/m$ in Chapter 4) or arbitrary angle.
$\beta$	Loaded length ratio ( $= C/m$ in Chapter 4) or arbitrary angle.
$Y, Y_1, Y_2$	Restraint at the end of a strut.
$\Delta$	Deflexion under the applied load or small quantity.
$\Delta_1, \Delta_2$	Deflexion under the applied load for modes 1 and 2 respectively.
$\eta$	Reduction factor (inelastic buckling).
$\theta$	Arbitrary angle.

$\lambda$	Coefficient.
$\nu$	Poissons ratio.
$\xi$	Coefficient of restraint (Bleich).
$\rho$	Aspect ratio for a rectangular plate ( $l/m$ ).
$\sigma$	Stress.
$\sigma_{cr}$	Critical stress.
$\sigma_x$	Stress in the x-direction.
$\sigma_y$	Stress in the y-direction.
$\sigma_{xy}, \tau_{xy}$	Shear stress.
$\sigma_x'$	Statically determinate stress in the x-direction.
$\sigma_y'$	Statically determinate stress in the y-direction.
$\sigma_{xy}'$	Statically determinate shear stress.
$\phi$	Stress function (Chapter 4) or arbitrary angle.
$\phi_1 - \phi_4$	Stability coefficients.
$\bar{\omega}$	Arbitrary angle.

## CHAPTER 1 - REVIEW

### 1.1 Introduction

There is a certain amount of doubt about the validity of current design practices for determining the web strength of rolled steel universal beams when subjected to concentrated loads applied to the flanges.

Hrennikoff (1) in a paper in 1961, when investigating the collapse of the Vancouver 2nd. Narrows Bridge believed that a lesson to be learnt was "the inapplicability of the usual column formulae for the design of the webs of the grillage beams in buckling". In the presented work he showed the results of tests on short lengths of the I-beam section used in the failed grillage and showed some then current design codes to give unsatisfactory safe load factors. These tests in fact were conducted with the flanges held rigid, which presented more stable conditions than those in the actual collapse where the top flanges of the beams moved laterally with respect to the bottom flanges. He also showed that the use of plywood packing in the beam grillage could quite easily lead to the formation of plastic hinges in the flanges thus weakening the section.

More recently the report of the collapse of the falsework for the River Loddon Viaduct (2) concluded that defects in the beam grillage and its supports led to partial failure of the grillage which initiated the overall collapse. The buckled and twisted shape of the beams after the collapse, increases the overall possibility of the collapse being initially due to buckling of the webs of the rolled

steel beams.

The present range of rolled steel universal beams available was introduced in the early sixties, and gives a greater variation of section properties for each standard depth size than the British Standard Beams (BSB) or Rolled Steel Joists (RSJ) which they superceded. This made available lighter sections for a desired bending strength. In 1964 Holmes(3) pointed out an example of the possible dangers in accepting the new lighter sections without consideration of effects usually negligible with old heavier sections. He showed that in the case of I-beams used as runway beams, the local bending stresses in the flanges could be as important a factor in design as the more usual overall bending stresses and corresponding deflexions.

As an example of the sectional property changes, the maximum web depth to web thickness ratio ( $d/t$ ) rose from 37.35 to 56.67 with the new lighter sections compared to British Standard Beams.

## 1.2 British Standard 449 (BS 449)

B.S.449, 'The Use of Structural Steel in Building'(4) was first introduced in 1932 and has been revised several times since. It is the most widely used design standard for steelwork in Britain and is used almost without limitation for such applications as formwork superstructures and water tower grillages. However the former example will shortly be included in a new Code of Practice(5) in course of preparation.



Prior to publication of BS449 in 1932, Glanville(6) at the request of the British Steelwork Association conducted 10 tests with rolled steel beams to determine the 'advisability of providing web stiffeners for steel I-beams'. He concluded that from such a few tests it was impossible to formulate a basis for design but drew general conclusions from the work.

The clauses which deal with rolled steel beams when subjected to concentrated loads in the current edition of BS449 are different to those in the original publication. Both editions considered two criteria, the overall buckling of the web and local crushing in the vicinity of the applied load. The depth to which dispersion of the load through the beam can be taken has changed when considering web buckling and the provision of web stiffeners at points of concentrated loads is now only necessary if certain conditions are not met.

Further reference to BS449 will imply the latest edition together with any amendments(4a) at the time of writing.

The web buckling clause in BS449 is 28(a)(i) in Chapter 4. It is based on the Perry formula (see for example reference (7)) for the elastic buckling of struts with a limitation on the stress at the outer fibre due to bending. The 'strut' has a length equal to  $d$ , the depth of the web between the root fillets and is assumed to be effectively restrained at each end, thus the effective length is  $d/2$ . The width is an 'effective' width being the distance obtained by taking a dispersion of  $45^{\circ}$  from the point of application of the load to the level of the

neutral axis or the end of the beam whichever is the shortest. This effective width can be increased by the length of any stiff bearing, flange plate or seating angle, but the  $45^\circ$  dispersion still applies. This method of designing for web buckling is very similar to the design codes of many other countries, the main variations being either the dispersion angle or the level of the beam to which the dispersion is taken.

The web crushing design clause in BS449 is 27e in Chapter 4. It is based on the assumption that the most likely place for crushing to occur in a beam loaded on its flanges is in the web at its junction with the root radius. An effective length along which crushing will occur is determined by assuming a  $30^\circ$  dispersion angle to the plane of the flange, to meet the junction of the web and root radius or edge of the beam, whichever is shortest. The allowable bearing stress is also specified.

### 1.3 Standard Elastic Plate Buckling Theory

As indicated in the previous section most design codes introduce a factor of safety against the elastic buckling of an effective strut or uniformly loaded plate when considering the effect of a concentrated load on a universal beam.

In fact the web of a universal beam would seem to be more likely to act as a rectangular plate subjected to complicated in-plane loading and boundary conditions, the resulting elastic stability analysis therefore being much more complex. Since two dimensions are much larger

than the third plate behaviour would appear to be indicated.

### 1.3.1 Uniform Edge Loading on Two Opposite Edges

As most design codes simplify the web of a universal beam to a uniformly loaded rectangular plate or strut, the analysis of the actual boundary conditions with a simplified uniform load would be useful.

Several authors have investigated the analyses of rectangular plates subjected to uniform in-plane loads (figure 1.1(a)) since the early work of Bryan (8) in 1891. Some authors have analysed plates with complex boundary conditions such as Stowell (9) who analysed a rectangular plate with free unloaded edges and either clamped or simply supported loaded edges. He showed that the non-dimensional plate buckling factor  $K_1$  is less than 4.0 and 1.0 respectively as would be expected by comparison with the corresponding values for struts. Woinowsky-Kreiger (10) analysed a rectangular plate with the unloaded edges simply supported and the loaded edges free in which he showed that the loaded edges could either remain in line or move laterally, and in the latter the buckling coefficient  $K_1$ , is greatly reduced.

Some authors, among them Timoshenko (11), Bleich (12), Stowell (13) and Gerard and Becker (14) have collected together the work of several authors for various analyses which consider many different boundary conditions. These works provide a good summary of the present state of knowledge and the method of determining the plate buckling factor in each case. Bleich (12) includes a very good

section dealing with elastically restrained loaded edges, considering the full range of restraint, with the coefficient of restraint varying from zero (clamped) to infinity (simply supported). He shows how the restraint coefficient can be determined from the dimensions of the restraining member.

The determination of the elastic buckling coefficient  $K_1$  is based on the fundamental St. Venant differential equation for the deflexion  $w$  of a thin plate under the action of forces in its middle plane:

$$\nabla^4 w = \frac{\partial^4 w}{\partial x^4} + 2 \frac{\partial^4 w}{\partial x^2 \partial y^2} + \frac{\partial^4 w}{\partial y^4} = - \frac{t}{D} \left( \sigma_x \frac{\partial^2 w}{\partial x^2} + 2 \sigma_{xy} \frac{\partial^2 w}{\partial x \partial y} + \sigma_y \frac{\partial^2 w}{\partial y^2} \right) \quad \dots 1.1$$

or by an energy method using the integral equation:

$$\Delta W = \frac{D}{2} \iint \left\{ \left( \frac{\partial^2 w}{\partial x^2} + \frac{\partial^2 w}{\partial y^2} \right)^2 - 2(1-\nu) \left[ \frac{\partial^2 w}{\partial x^2} \frac{\partial^2 w}{\partial y^2} - \left( \frac{\partial^2 w}{\partial x \partial y} \right)^2 \right] \right\} dx dy$$

$$- \frac{t}{2} \iint \left[ \sigma_x \left( \frac{\partial w}{\partial x} \right)^2 + 2 \tau_{xy} \frac{\partial w}{\partial x} \frac{\partial w}{\partial y} + \sigma_y \left( \frac{\partial w}{\partial y} \right)^2 \right] dx dy \quad \dots 1.2$$

either of which needs a determination of the initial state of stress. Some of the analyses require the use of an approximate energy method if the deflected shape is not known, such as when the boundary conditions are complicated.

### 1.3.2 Concentrated Edge Loading on Two Opposite Edges

As well as considering the web of a universal beam as a rectangular plate subjected to a uniform load, it could be considered as a wide plate subjected to an isolated concentrated load on its edge.

When considering a rectangular plate subjected to a concentrated load, the differential equation 1.1 has variable coefficients which makes its solution difficult. Hence in this case an energy method will need to be employed whatever the boundary conditions.

Timoshenko (11) analysed the case of a plate, simply supported on the unloaded edges and either clamped or simply supported on the loaded edges and subjected to two opposite concentrated point loads, centrally on each edge as in figure 1.1(b). He used a strain energy method but assumed that the only stresses in the plate were in the direction of the line of action of the two external forces.

Legget (15) later analysed accurately the same problem but only when the loaded edges were simply supported. He found Timoshenko's results to be in error by up to 12½%.

Yamaki (16) has analysed the case when the loaded edges are clamped and his results show Timoshenko's results to be in even greater error.

Zetlin (17) using the Rayleigh-Ritz procedure analysed a simply supported plate loaded as shown in figure 1.1(c) in which he assumed the shear stress distribution to be parabolic. He produced results for 3 different lengths of edge loading and 3 different plate aspect ratios. He used these 9 series of results to provide design graphs and subsequently compared them with a few selected tests which although having the same basic form were considerably in error.

#### 1.4. Further Plate Buckling Theories.

The previous section considered what has firmly been

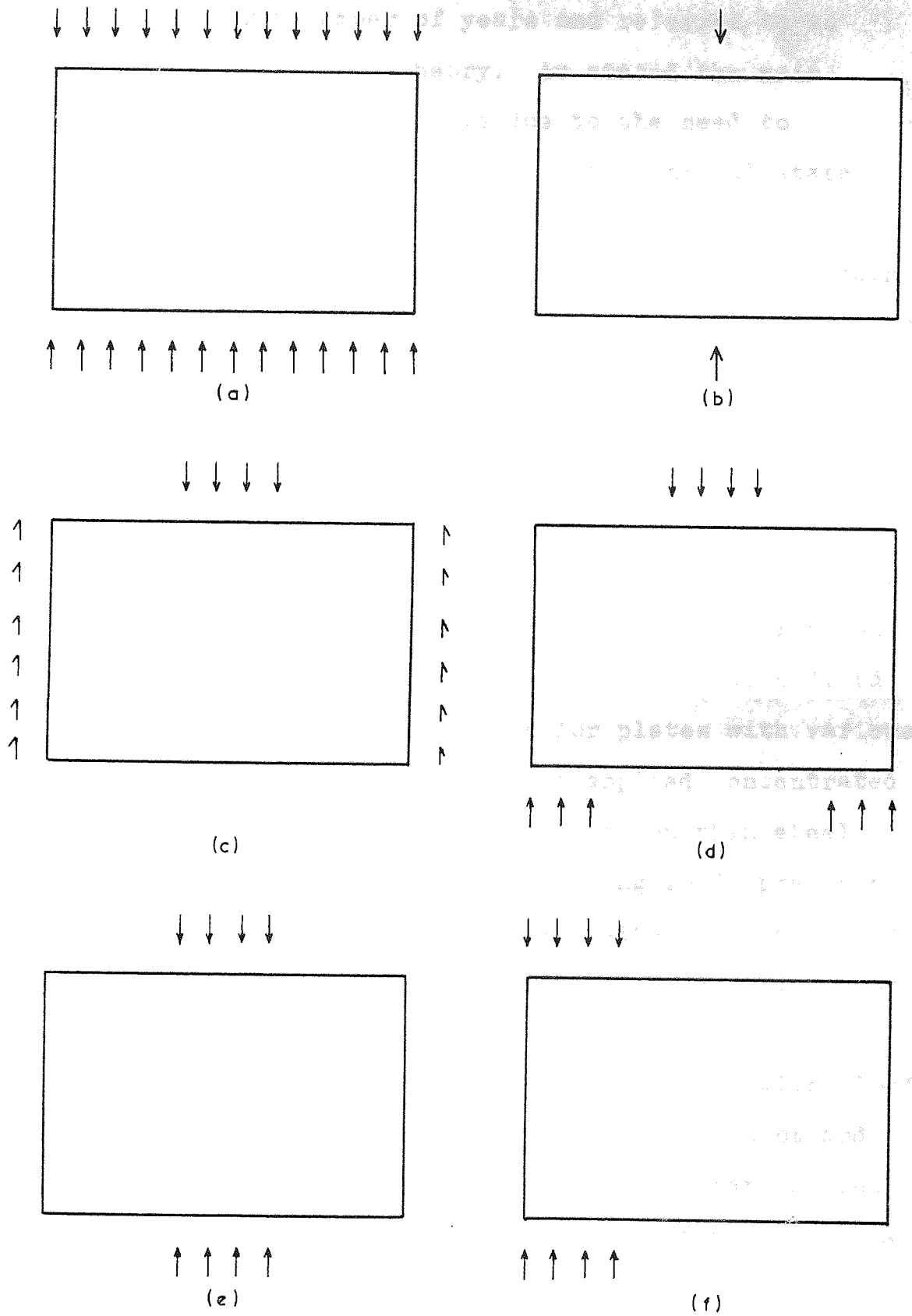


Figure 1.1 Plates with various loading conditions.

established over a number of years and referred to as Classical Plate Buckling Theory. As stated the main difficulties in the analysis is due to the need to determine a deflected shape and also the initial state of stress.

However in two excellent papers Alfutov and Balabukh (18,19) recast equation 1.2 in a form which did not require a determination of the initial state of stress. It does impose some boundary conditions and still requires the deflected shape, but even so much simplifies the mathematical analyses.

Khan and Walker (20) have very recently adopted this method to analyse rectangular plates simply supported all round and subjected to the forces shown in figures 1.1(d) and 1.1(e). They produced results for plates with various aspect ratios and several lengths of applied concentrated loads, and compared them with some tests on thin steel plates. They concluded that the buckling loads predicted in the analysis showed good agreement with the test loads at which the plates showed their maximum rate of increase of lateral deflexions. They also showed there to be a parametric relationship between the elastic buckling load during the test as determined by the Southwell plot and the test ultimate load. They also proposed that the method of analysis could be extended to more complicated loading and plate boundary conditions.

Due to the complicated nature of elastic plate buckling problems with non-standard boundary and loading conditions, the finite element method has been considered as a method of analysis.

In 1966 Kapur and Hartz (21) showed the manner in which plate stability problems could be solved using finite elements. They showed the approach as the use of stability coefficient matrices in conjunction with the more familiar stiffness matrices, and that the insertion of the boundary conditions is a comparably simple matter.

White and Cottingham (22) used a finite difference analysis to solve the plate stability problem shown in figure 1.1(e), with both simply supported and clamped edges. They analysed 7 different load combinations for aspect ratios from  $\frac{1}{3}$  to 3.

In 1969 Rockey and Bagchi (23) presented results for a plate with flanges on two edges, using the finite element method. They showed how the interaction of the flange and web affected the stress distribution in the web and also the overall buckling load. The results presented were for limited ranges of the variables.

#### 1.4.1. Inelastic Plate Buckling.

It is possible for a plate to buckle when the material has passed its elastic limit. This is referred to as elasto-plastic buckling or plastic buckling, depending on the state of stress in the plate. Quite clearly, introducing the non-linear stress-strain relationship for the material beyond the elastic limit introduces further complications into the analysis, and together with non-linear effects due to concentrated loading the potential analysis of the problem is fearsome.



Several authors have researched this particular non-linear effect. Ilyushin (24) solved, by developing work in a previous publication of his (25), the case when a rectangular plate is compressed by two opposite uniform loads with standard boundary conditions.

In 1946 Gerard (26) using a secant modulus method solved the case for a simply supported plate subjected to a uniform edge loading. He verified the results with small scale tests on aluminium alloy specimens, which showed very good agreement with the theory.

Stowell (27) in 1948 presented a table of reduction factors  $\eta$  by which the computed critical stress calculated by elastic buckling theory should be multiplied to obtain the critical stress for the plastic case. The value of  $\eta$  is determined in a different way for various edge conditions and aspect ratios and is always in terms of the secant modulus of elasticity, the tangent modulus of elasticity and the linear elastic modulus of elasticity. He compared some of the results with experimental results obtained by other authors and showed good agreement.

Several other authors have published works of lesser importance and many are summarised by Gerard and Becker (14) to which the reader is referred and so it is felt that no further comment is needed here.

Introducing such factors  $\eta$  as those obtained by Stowell (27) for plates loaded with complicated loading and boundary conditions would be a formidable task, and a finite element method of analysis would probably be more manageable. However in this case it is thought that introducing another approximate method into an already approximate finite element

stability analysis for plates could lead to serious errors.

However, the authors have found

### 1.5 Empirical Methods of Analysis and Published Test Results

Many tests have been reported

Many tests have been reported on steel beams, subjected to concentrated loads, and have sometimes been accompanied by empirical or semi-empirical theories. The most common semi-empirical formulae are based on the angle of distribution of stress through the beam.

Moore (28) in 1913 published the results of 40 tests carried out on I-beams with various loading conditions. In the report he stressed the importance of deciphering the initial mode of failure and that it was very difficult to distinguish between the final failure pattern and the initial cause of failure. He showed a table listing the results of 9 tests which in his opinion finally failed due to initial web failure. He also made some observations of the variation of steel strength with its location in the beam cross-section.

In 1916 Moore and Wilson (29) reported the results of 8 tests performed with built up girders. They chose the particular beams used in order to ensure that the primary failure would be in the web. The photographs in the report clearly show two types of failure, diagonal shear buckling of the web and torsional buckling of the beam, rotating in plan about a vertical axis at mid-span.

Much later Lyse and Godfrey (30) published the results of 14 tests on rolled steel beams and welded plate girders. They concluded that for beams with web depth to thickness ( $d/t$ ) ratios of up to 70 there was no danger of web buckling,

but that the maximum load sustained decreased with an increase of this ratio. However, the authors were mostly concerned with the incidence of shear buckling. (35).

In 1931, Glanville (3) as previously mentioned reported the results of ten tests carried out for the British Steelwork Association, but came to no firm conclusions.

Wastlund and Bergman (31) conducted 11 tests on built up I-beams in considerable detail. They gave design recommendations for web buckling based on the results of the tests, but said that it had been found that the theoretical load of plane web plates bears no direct relation to the ultimate load and that the ratio of the ultimate load to the theoretical critical load increases with the slenderness ratio. They showed that only 2 tests showed any indication of the elastic stability phenomena during the tests.

Winter and Pian (32) performed tests on 136 cold formed steel sections loaded as shown in figure 1.1(d), (e) and (f). Although cold formed sections were used, which had quite weak, radiused flange to web connexions, the dependent variables determined may be comparable with those for hot rolled sections. They concluded that all the beams tested failed due to crushing and that the failure loads were irrespective of the depths of the sections. They fitted an empirical straight line relationship between the ultimate load and certain variables of the form:

$$P = (15 + 3.25\sqrt{l_a/t}) t^2 f_y \quad 1.3$$

for beams loaded remote from the end and;

$$P = (10 + 1.25\sqrt{l_a/t}) t^2 f_y \quad 1.4$$

for beams loaded at the end.

Delesques (33) in 1974 investigated the results of tests performed by several researchers, the most relevant to this work being Bergfelt (34) and Bergfelt and Hovik (35). Delesques attempted to determine the main parameters concerned with the ultimate load carrying capacity of I-beams. He assembled the results from 60 tests in all and used as a reference the value  $P_{ult}/E_t$ . He found that this value did not vary appreciably with  $f_y$ ,  $d/t$ ,  $L/D_t$  and the conditions for supporting the load. He finally produced a whole range of design guides for use with beams in certain ranges of the variables.

#### 1.6 Conclusions from Previous Work

The behaviour of rolled steel universal beams when subjected to concentrated loads on the flanges is very complex. There are many variables involved including:

1. Stresses due to loading conditions, bending, shear, and direct stresses.
2. Beam dimensions and properties, depth, web thickness, yield stress etc.

The published works reviewed here have gone part of the way towards investigating these. However many of the works have contained too many variables to be able to draw firm conclusions. One exception is Winter and Pian (32) whose many tests clarified the situation for their particular range of variables and whose results are used in American design practices for cold formed sections.

The work by Delesques (33) also attempted to consider the results of many tests but because the results were

drawn from such a wide field and were not conducted for one specific investigation he found it difficult to find relationships between the results.

This review therefore indicates the need for a wide range of tests in the form of those conducted by Winter and Pian. It indicates the necessity for a systematic series of tests designed to examine a limited number of variables at any one time. By varying more than one parameter in a study related to stability, the particular parameter which causes any change in critical load values is not always discernable.

By this reasoning it is proposed to carry out a series of tests on rolled steel universal beams subjected to concentrated loads in the following manner.

1. To limit the types of stress imposed in the first instance.
2. To investigate the influence of additional stresses keeping all other variables constant.
3. To vary dimensional properties of the section with constant loading conditions.

Finally the theories usually associated with the strength of universal beams can be compared with the systematic test results to determine which is most applicable and possibly to develop further theories or semi-empirical theories which better represent the effects of each variable.

The complete range of every variable would obviously be too great for a limited study as presented here and so limited ranges will be considered. Any limitations imposed will be indicated and discussed in the final chapter.

## CHAPTER 2 - EXPERIMENTATION AND PRESENTATION OF THE TEST RESULTS

### 2.1 Introduction

It is inevitable that when conducting such a large number of tests as are included in the present work, the experimental procedures and methods will vary. In this work changes were made in such factors as the number of strain gauges, location of deflexion gauges etc., and it would therefore be impractical to present the experimental details and procedures for each individual test. This chapter therefore refers to the general experimental details employed and encompasses the recordings made for all tests. This means that many tests do not show recordings for some of the measurements referred to in the text.

Grade 43 rolled steel universal beam sections were used throughout and were taken randomly from a local steel stockholder. All obvious imperfections such as flame cut ends, dents and bends were removed from each length by cold sawing.

#### 2.1.1 Test Beam Referencing

The tests are divided into seven series denoted I to VII according to the type of loading, the points of application of the loads and the variables investigated.

Series I - Beams loaded by two opposite concentrated point loads applied to the flanges at mid-length, perpendicular to the plane of the flanges, and in line with

the centre of the web. Beam serial size varied, and the length varied for each serial size.

Series II - Beams loaded by two opposite concentrated point loads applied to the flanges at mid-length, perpendicular to the plane of the flanges and with a known eccentricity to the centre of the web. Beam serial size and length constant but eccentricity varied.

Series III - Beams loaded by two opposite knife edge loads applied to the flanges at mid-length, across their width, perpendicular to the plane of the flanges. Beam serial size varied, and the length varied for each serial size.

Series IV - Beams loaded by two opposite knife edge loads applied to the flanges across their width, perpendicular to the plane of the flanges. Beam serial size and length constant but distance from the knife edges to the end of the beam varied.

Series V - Beams loaded by two opposite uniformly distributed loads applied to the flanges at mid-length, across their width, perpendicular to the plane of the flanges. Beam serial size varied. Beam length constant for each serial size and the length of the applied load varied.

Series VI - Beams loaded by two opposite uniformly distributed loads applied to the flanges at mid-length, across their width, perpendicular to the plane of the flanges. Beam serial size varied and for each serial size the length of the beam varied for several different lengths of the uniformly distributed load.

Series VII - Beams simply supported on two knife edges and loaded by a third at mid-span. Loads applied across



the width of the flanges and perpendicular to their plane. Beam serial size and overhang at the supports kept constant but span varied.

These seven series are summarised in figure 2.1.

There is a certain amount of cross referencing, for instance Series III and IV will coincide when  $l_a$ , the length of the uniformly distributed load is zero and the beam length  $L$  is the same. Any coincident results will be shown with both series where necessary.

### 2.1.2 Universal Beam Serial Sizes

Universal beams for the tests were chosen to give a wide range of web depth to thickness ( $d/t$ ) ratios. The most slender webbed universal beam section available is 406mm x 140mm x 39 Kg/m, which was used for about 30% of the total number of tests. Table 2.1 shows the eleven different beam sizes used together with the empirical size and the depth to thickness ratios of the webs.

### 2.1.3 Tests Carried Out

A complete list of the beams tested in this work is given in Table 2.2, which shows the tests carried out in each series, the variables investigated, the value of the variables for each test, the test number and the reference letter of the 12 metre length from which each beam length was cut. The suffix R indicates the beams which were retested in the manner to be described in Section 2.4.2.

Series I and III account for approximately half of all



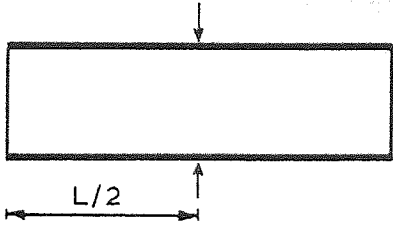

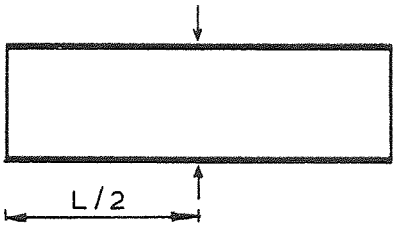

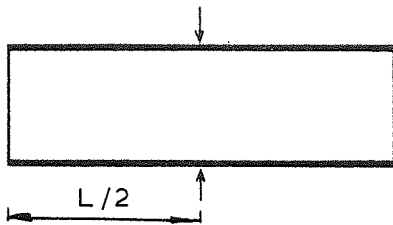

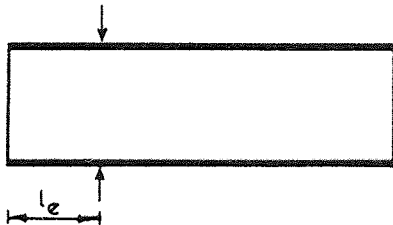

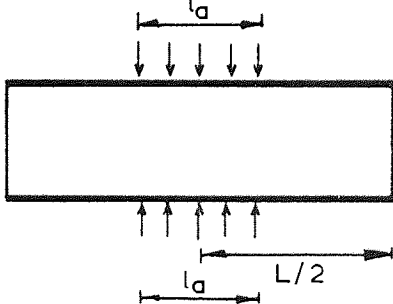

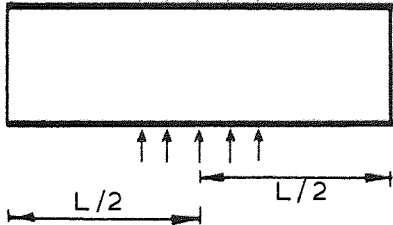

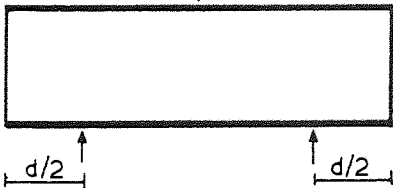

Series. No.	Loading Arrangement	Details
I		 Two opposite concentrated point loads. $L$ , Serial size vary.
II		 Two opposite concentrated point loads. $e$ varies.
III		 Two opposite knife edge loads. $L$ , Serial size vary.
IV		 Two opposite knife edge loads. $l_e$ varies.
V		 Two opposite uniformly distributed loads. $l_a$ , Serial size vary.
VI		 Two opposite uniformly distributed loads. $L, l_a$ , Serial size vary.
VII		 Simply supported on two knife edges and loaded at mid-span by a third. $L$ varies.

Figure 2.1 Summary of test Series I to VII.

Metric U.B. Size D <sub>t</sub> (mm) x B (mm) x Kg/m	Imperial U.B. Size D <sub>t</sub> (ins) x B (ins) x Lbs/ft	Web Depth to Thickness Ratio
457 191 98	18 7.5 66	35.4
406 140 39*	16 5.5 26*	56.7
406 140 39	16 5.5 26	56.7
305 165 46	12 16.5 31	39.2
305 165 40	12 16.5 27	43.1
305 102 25	12 4 16.5	47.4
254 146 43	10 5.75 29	29.6
254 146 37	10 5.75 25	33.7
254 102 22	10 4 15	38.6
203 133 30	8 5.25 20	27.0
102 64 9.65	4 2.5 6.5	17.8

\* Indicates flange thickness reduced.

Table 2.1 Beam serial sizes used in the tests.

Test Series	Test No.	Serial Size D <sub>t</sub> (mm) x B(mm) x Kg/m	Beam Ref.	Variables Investigated	Value of Variables
I	1	406 x 140 x 39	A	L/d	0.5
I	2	406 x 140 x 39	A	L/d	1.0
I	3	406 x 140 x 39	A	L/d	2.0
I	4	406 x 140 x 39	A	L/d	3.0
I	5	406 x 140 x 39	A	L/d	4.0
I	6	254 x 146 x 37	G	L/d	0.5
I	7	254 x 146 x 37	G	L/d	1.0
I	8	254 x 146 x 37	G	L/d	2.0
I	9	254 x 146 x 37	G	L/d	3.0
I	*10	254 x 146 x 37	G	L/d	4.0
I	11R	305 x 102 x 25	K	L/d	0.5
I	12	305 x 102 x 25	K	L/d	1.0
I	13R	305 x 102 x 25	K	L/d	2.0
I	14	305 x 102 x 25	K	L/d	3.0
I	*15	305 x 102 x 25	K	L/d	3.0
I	16R	305 x 165 x 46	L	L/d	0.5
I	17R	305 x 165 x 46	L	L/d	1.0
I	18R	305 x 165 x 46	L	L/d	2.0
I	19R	305 x 165 x 46	L	L/d	3.0
I	20	254 x 102 x 22	J	L/d	0.5
I	21	254 x 102 x 22	J	L/d	1.0
I	22	254 x 102 x 22	J	L/d	2.0
I	23	254 x 102 x 22	J	L/d	3.0
I	24	203 x 133 x 30	H	L/d	0.5
I	25	203 x 133 x 30	H	L/d	1.0
I	26	203 x 133 x 30	H	L/d	2.0
I	27	203 x 133 x 30	H	L/d	3.0
I	28	254 x 146 x 43	R	L/d	1.0
I	*29	254 x 146 x 43	R	L/d	2.5
* Load spread by 75mm square plate.					
II	1	406 x 140 x 39	A	e	0
II	30	406 x 140 x 39	B	e	5mm
II	31	406 x 140 x 39	B	e	10mm
II	32	406 x 140 x 39	B	e	20mm

R: Failed beam retested.

Table 2.2

Test Series	Test No.	Serial Size $D_t(\text{mm}) \times B(\text{mm})$ $\times \text{Kg/m}$	Beam Ref.	Variables Investigated	Value of Variables
III	33	406 x 140 x 39	A	L/d	0.5
III	34	406 x 140 x 39	A	L/d	1.0
III	35	406 x 140 x 39	A	L/d	2.0
III	36	406 x 140 x 39	A	L/d	3.0
III	37	254 x 146 x 37	G	L/d	0.5
III	38	254 x 146 x 37	G	L/d	1.0
III	39	254 x 146 x 37	G	L/d	2.0
III	40	254 x 146 x 37	G	L/d	3.0
III	41R	305 x 102 x 25	K	L/d	0.5
III	42R	305 x 102 x 25	K	L/d	1.0
III	43R	305 x 102 x 25	K	L/d	2.0
III	44R	305 x 102 x 25	K	L/d	3.0
III	45	305 x 165 x 46	L	L/d	0.5
III	46R	305 x 165 x 46	L	L/d	1.0
III	47R	305 x 165 x 46	L	L/d	2.0
III	48R	305 x 165 x 46	L	L/d	3.0
III	49R	254 x 102 x 22	J	L/d	0.5
III	50R	254 x 102 x 22	J	L/d	1.0
III	51R	254 x 102 x 22	J	L/d	2.0
III	52R	254 x 102 x 22	J	L/d	3.0
III	53	203 x 133 x 30	H	L/d	0.5
III	54	203 x 133 x 30	H	L/d	1.0
III	55	203 x 133 x 30	H	L/d	2.0
III	56	203 x 133 x 30	H	L/d	3.0
III	57	254 x 146 x 43	R	L/d	1.0
III	58	254 x 146 x 43	R	L/d	2.0
III	59	254 x 146 x 43	R	L/d	2.5
III	60	406 x 140 x 39	B	L/d	3.0
III	†61R	406 x 140 x 39	E	L/d	3.0
III	†62R	406 x 140 x 39	E	L/d	3.0
III	†63R	406 x 140 x 39	E	L/d	3.0
III	†64R	406 x 140 x 39	E	L/d	3.0
III	78R	254 x 146 x 43	N	L/d	3.0
III	83R	305 x 165 x 40	M	L/d	3.0
III	65R	102 x 64 x 9.65	P	L/d	3.0
III	66R	457 x 191 x 98	S	L/d	3.0
†Flange properties varied.					
IV	36	406 x 140 x 39	A	$l_e/d$	1.5
IV	60	406 x 140 x 39	B	$l_e/d$	1.5
IV	67	406 x 140 x 39	B	$l_e/d$	1.0
IV	68	406 x 140 x 39	B	$l_e/d$	0.5
IV	69	406 x 140 x 39	B	$l_e/d$	0.25
IV	70	406 x 140 x 39	C	$l_e/d$	0.07

Table 2.2 (cont.)

Test Series	Test No.	Serial Size $D_t(\text{mm}) \times B(\text{mm})$ $\times \text{Kg/m}$	Beam Ref.	Variables Investigated	Value of Variables
V	36	406 x 140 x 39	A	$l_a/L$	0
V	60	406 x 140 x 39	B	$l_a/l$	0
V	71	406 x 140 x 39	A	$l_a/L$	0.083
V	72	406 x 140 x 39	B	$l_a/L$	0.167
V	73	406 x 140 x 39	B	$l_a/L$	0.333
V	74	406 x 140 x 39	B	$l_a/L$	0.667
V	40	254 x 146 x 37	G	$l_a/L$	0
V	75R	254 x 146 x 37	G	$l_a/L$	0.167
V	76R	254 x 146 x 37	G	$l_a/L$	0.333
V	77R	254 x 146 x 37	G	$l_a/L$	0.667
V	78R	254 x 146 x 43	N	$l_a/L$	0
V	79R	254 x 146 x 43	N	$l_a/L$	0.167
V	80R	254 x 146 x 43	N	$l_a/L$	0.333
V	81R	254 x 146 x 43	N	$l_a/L$	0.667
V	82R	254 x 146 x 43	N	$l_a/L$	1.0
V	83R	305 x 165 x 40	M	$l_a/L$	0
V	84R	305 x 165 x 40	M	$l_a/L$	0.167
V	85R	305 x 165 x 40	M	$l_a/L$	0.333
V	86R	305 x 165 x 40	M	$l_a/L$	0.667
V	87R	305 x 165 x 40	M	$l_a/L$	1.0
VI	88R	254 x 146 x 43	N	$l_a/d, L/d$	0.5, 2
VI	79R	254 x 146 x 43	N	$l_a/d, L/d$	0.5, 3
VI	89R	254 x 146 x 43	N	$l_a/d, L/d$	0.5, 4
VI	80R	254 x 146 x 43	N	$l_a/d, L/d$	1.0, 3
VI	90R	254 x 146 x 43	N	$l_a/d, L/d$	1.0, 4
VI	91R	254 x 146 x 43	N	$l_a/d, L/d$	1.0, 5
VI	92R	305 x 165 x 40	M	$l_a/d, L/d$	0.5, 2
VI	84R	305 x 165 x 40	M	$l_a/d, L/d$	0.5, 3
VI	93R	305 x 165 x 40	M	$l_a/d, L/d$	0.5, 4
VI	85R	305 x 165 x 40	M	$l_a/d, L/d$	1.0, 3
VI	94R	305 x 165 x 40	M	$l_a/d, L/d$	1.0, 4
VI	95R	305 x 165 x 40	M	$l_a/d, L/d$	1.0, 5
VII	36	406 x 140 x 39	A	$s/d$	0
VII	60	406 x 140 x 39	B	$s/d$	0
VII	96R	406 x 140 x 39	C	$s/d$	1.0
VII	97R	406 x 140 x 39	C	$s/d$	2.0
VII	98	406 x 140 x 39	D	$s/d$	3.72
VII	99R	406 x 140 x 39	F	$s/d$	4.9
VII	100	406 x 140 x 39	F	$s/d$	7.0

Table 2.2 (cont.)

the beams tested, and utilise all eleven section sizes used. This was to enable the section properties to be related to the load carrying capacity with a good degree of certainty. It would then be unnecessary to use such a variation of section sizes for the other series, and so other variables could then be investigated.

## 2.2 Material Properties

From each 12 metre length of universal beam section, a sample length was cold sawn and used to determine the material characteristics. Each 12 metre length is referred to alphabetically, and so tensile test results and test beams will refer to the particular beam from which it was cut when necessary.

The material characteristics required were the yield stress, ultimate stress and the modulus of elasticity for each 12 metre length. It was also considered necessary to investigate the variation of material strength with various locations in the cross-section.

### 2.2.1 Tensile Tests

Two types of tensile tests were employed, one using small specimens and the other using large specimens. The large specimens, which required the least preparation time were used to determine the general strength of the section and the small specimens to determine the strength of the section at a particular location.

For some of the small section sizes it was not

possible to take the large specimens, in which case the small specimens were taken as a matter of course.

For 2 of the 12 metre lengths of 406 x 140 x 39 Kg/m section, both types of specimens were taken as a cross-check of the results obtained.

#### 2.2.1.1 Large Tensile Test Specimens

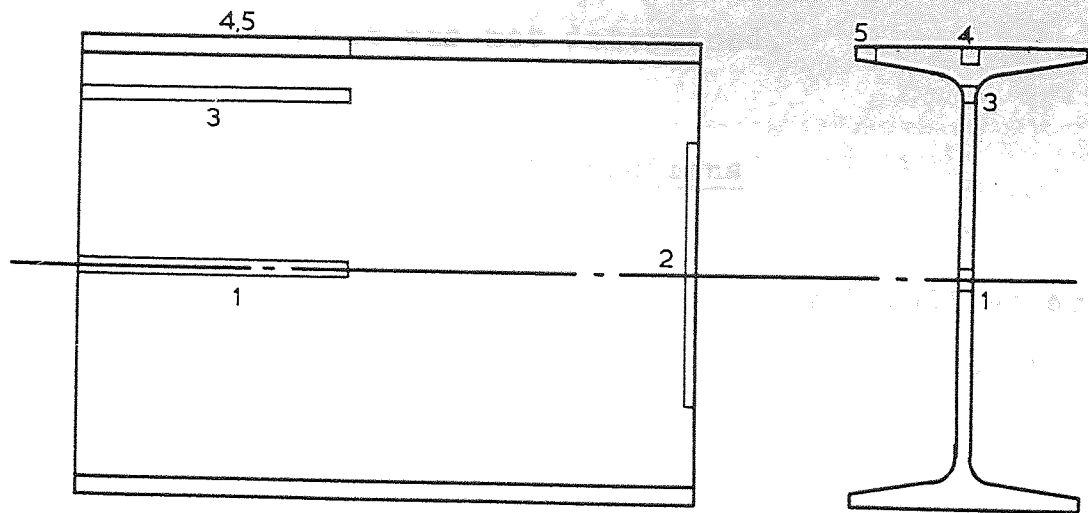
Specimens 250-300 millimetres long were cold sawn from each sample length at the locations shown in figure 2.2(a), and tested in an Avery-Dennison hydraulic compression-tension testing machine which incorporates a 50 millimetre gauge length strain recorder and automatic plotter. Beams with overall depths  $D_t$  of less than 250mm could not have these specimens taken as they would have been too short to ensure adequate grip in the jaws of the testing machine.

The cold sawn specimens were subsequently machined to a uniform section. Specimen numbers 1, 2 and 5 of figure 2.2(a) were machined along the two sawn edges to form a rectangular section of approximately 10mm wide by the thickness of the web or flange. Specimen numbers 2 and 4 were machined on all sides to form a section approximately 10mm square.

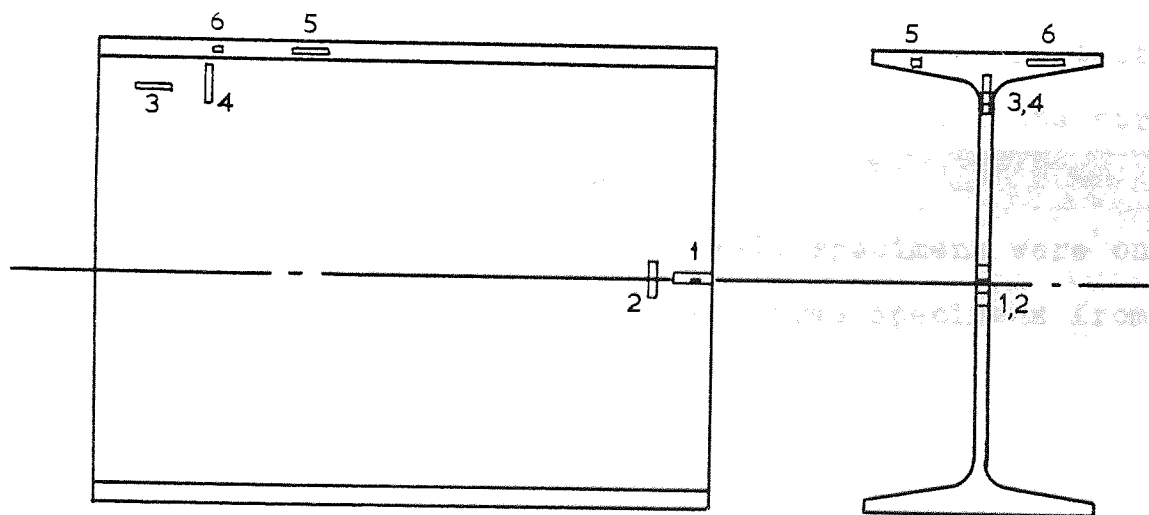
The resultant specimen dimensions were recorded to the nearest 0.01mm. Utilising the automatic strain recording from the tensile test, the yield stress, ultimate stress and modulus of elasticity were obtained for each of the 5 specimens.

The value of the modulus of elasticity was quite consistent for a large number of tests and so for some of

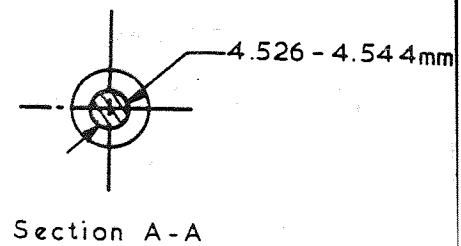
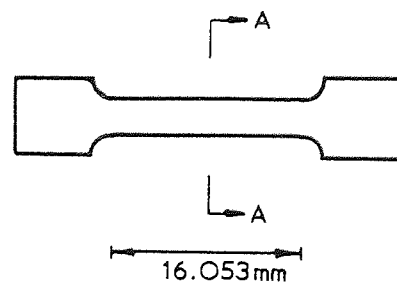




(a) Large tensile test specimen locations.



(b) Small tensile test specimen locations.



(c) Hounsfield tensile specimen No.12.

Figure 2.2 Tensile test specimens and locations.



the later tests it was not determined.

#### 2.2.1.2 Small Tensile Test Specimens

Small specimens were cold sawn from localised areas at the locations shown in figure 2.2(b), machined to the shape and dimensions of a Hounsfield Specimen Size No. 12 as shown in figure 2.2(c), and tested in a Hounsfield Tensometer. These small specimens were taken from two beams as a check on the results obtained by the previous method, and also to investigate any variation in material strength with location in the beam cross-section.

From the strain recording obtained during the tests on these small specimens the yield stress and ultimate stress of each specimen was obtained.

As testing proceeded these small specimens were only taken when the beam size prevented large specimens from being taken.

#### 2.2.2 Results of Tensile Tests

The resulting yield stresses and ultimate stresses for the tensile tests carried out on the specimens taken from each 12 metre length of steel used are shown in Table 2.3. The reference letter is that used in Table 2.1, which enables the strength of any test beam to be determined. Also shown are the average yield and ultimate stresses for the web and flange and also a value for the section as a whole.

The modulus of elasticity was determined for

Location	Yield Stress	Ult. Stress	Location	Yield Stress	Ult. Stress
406 x 140 x 39 Kg/m			Beam reference A		
1	396.80	575.36	1	367.34	466.71
2	407.96	580.94	2	409.93	530.83
Small Samples 3	319.92	497.24	Large Samples 3	345.22	505.31
4	330.46	518.32	4	324.34	495.94
5	328.60	497.86	5	336.38	493.15
6	344.10	509.64			
Average web	363.78	542.96	Average web	366.93	502.04
Average flange	336.35	503.75	Average flange	330.36	494.54
Overall	350.07	523.36	Overall	348.64	498.29
406 x 140 x 39 Kg/m			Beam reference B		
1	404.86	564.94	1	428.57	553.13
2	425.94	581.05	2	436.38	552.38
Small Samples 3	320.54	530.87	Large Samples 3	357.85	519.02
4	311.59	520.34	4	346.42	525.13
5	325.50	531.49	5	355.77	511.27
6	343.48	530.25			
Average web	365.72	549.30	Average web	395.16	535.89
Average flange	334.49	539.77	Average flange	351.09	518.20
Overall	350.11	544.54	Overall	373.13	527.04
406 x 140 x 39 Kg/m Ref. C			406 x 140 x 39 Kg/m Ref. D		
1	397.15	518.58	1	402.80	530.58
2	404.27	523.32	2	407.57	544.35
Large Samples 3	331.83	481.76	Large Samples 3	330.45	510.87
4	351.64	495.72	4	335.35	506.16
5	340.88	489.25	5	375.37	523.18
Average web	366.27	501.35	Average web	367.82	524.17
Average flange	346.26	492.48	Average flange	355.36	514.67
Overall	356.26	496.92	Overall	361.59	519.42

All stresses in  $N/mm^2$ .

Table 2.3

Location	Yield Stress	Ult. Stress	Location	Yield Stress	Ult. Stress
406 x 140 x 39 Kg/m Ref. E			406 x 140 x 39 Kg/m Ref. F		
1	407.55	538.16	1	409.89	530.39
2	411.86	538.21	2	409.44	526.63
Large 3	333.30	505.79	Large 3	343.46	503.31
Samples 4	345.87	506.36	Samples 4	328.27	495.67
5	357.38	509.67	5	351.17	497.42
Average web	371.50	521.99	Average web	376.56	515.91
Average flange	351.62	508.01	Average flange	339.72	496.54
Overall	361.56	515.00	Overall	358.14	506.23
254 x 146 x 37 Kg/m Ref. G			203 x 133 x 30 Kg/m Ref. H		
1	389.48	558.43	1	365.82	556.53
2	399.36	565.85	2	354.93	549.61
Small 3	327.09	540.21	Small 3	364.83	557.18
Samples 4	325.85	538.99	Samples 4	313.81	473.80
5	339.75	534.95	5	311.61	514.15
6	325.85	525.69	6	321.04	515.39
Average web	360.44	550.86	Average web	349.85	534.28
Average flange	332.80	530.32	Average flange	316.32	514.77
Overall	346.62	540.59	Overall	339.09	524.52
254 x 102 x 22 Kg/m Ref. J			305 x 102 x 25 Kg/m Ref. K		
1	353.61	513.35	1	355.79	516.91
2	362.23	506.92	2	358.37	509.26
Large 3	306.67	503.49	Large 3	323.22	491.86
Samples 4	337.67	507.96	Samples 4	332.72	511.24
5	339.64	511.92	5	331.70	502.29
Average web	332.29	506.82	Average web	340.15	502.47
Average flange	338.65	509.94	Average flange	332.20	506.67
Overall	335.47	508.38	Overall	336.18	504.62

All stresses in  $\text{N/mm}^2$ .

Table 2.3 (cont.)

Location	Yield Stress	Ult. Stress	Location	Yield Stress	Ult. Stress
305 x 165 x 46 Kg/m Ref. L			305 x 165 x 40 Kg/m Ref. M		
1	378.92	537.12	1	424.64	526.23
2	385.21	568.02	2	411.63	512.05
Large	281.76	480.44	Large	352.76	476.43
Samples	289.84	518.59	Samples	315.16	467.83
5	308.85	491.36	5	299.45	427.02
Average web	331.91	516.50	Average web	385.45	497.78
Average flange	299.34	504.97	Average flange	307.30	447.42
Overall	315.63	510.74	Overall	346.38	472.60
254 x 146 x 43 Kg/m Ref. N			102 x 64 x 9.66 Kg/m Ref. P		
1	331.67	523.30	1	359.44	508.84
2	350.76	523.11	2	347.80	511.91
Large	308.92	509.14	Small	356.37	509.46
Samples	305.08	499.23	Samples	347.19	516.92
5	313.62	504.74	5	359.44	508.22
Average web	325.07	516.17	6	339.84	510.07
Average flange	309.35	501.98	Average web	352.70	511.78
Overall	317.21	509.08	Average flange	349.64	509.15
254 x 146 x 43 Kg/m Ref. R			457 x 191 x 98 Kg/m Ref. S		
1	294.53	488.02	1	284.81	482.45
2	304.33	482.51	2	278.45	463.86
Small	305.05	491.40	Large	272.77	472.91
Samples	277.38	473.94	Samples	257.45	477.11
5	305.78	492.95	5	285.17	470.07
6	291.47	484.35	Average web	277.20	472.67
Average web	295.32	483.97	Average flange	271.31	473.59
Average flange	298.62	488.65	Overall	274.25	473.31
Overall	296.97	486.31			

All stresses in N/mm<sup>2</sup>.

Table 2.3 (cont.)

approximately half of the tensile tests but it is not considered necessary to show the results here as it was consistently found to be  $200 \text{ KN/mm}^2$  to within 1 or 2%. This value will be used throughout the work where necessary without further comment.

### 2.2.3 Observations from the Tensile Test Results

Tensile tests of both types were used for beams A and B and so their results can be compared. Beam A shows the results of both types of test to give almost identical results for yield stresses while beam B gives results 6.6% higher for the large specimens than for the small specimens. However this variation is small and so results from both types of test are quite comparable. The results for beams A-F, which were all of the same serial size gave very consistent results.

The general trend of the results is that the thinner the section, the greater the yield stress, as shown in figure 2.3, whilst the ultimate stress remains constant. This possibly indicates that the yield stress is affected by the hot rolling process during manufacture due to the rate of dispersion of heat from the section when cooling. It could also be affected to some extent by cold working. This would also explain the lower yield stress for some sections at the junction of the flange and web because of the increased thickness provided by the root radii.

The manufacturers' guaranteed tensile yield stress for a grade 43 rolled steel beam is  $250 \text{ N/mm}^2$  whereas the average yield stress indicated by these tests is that

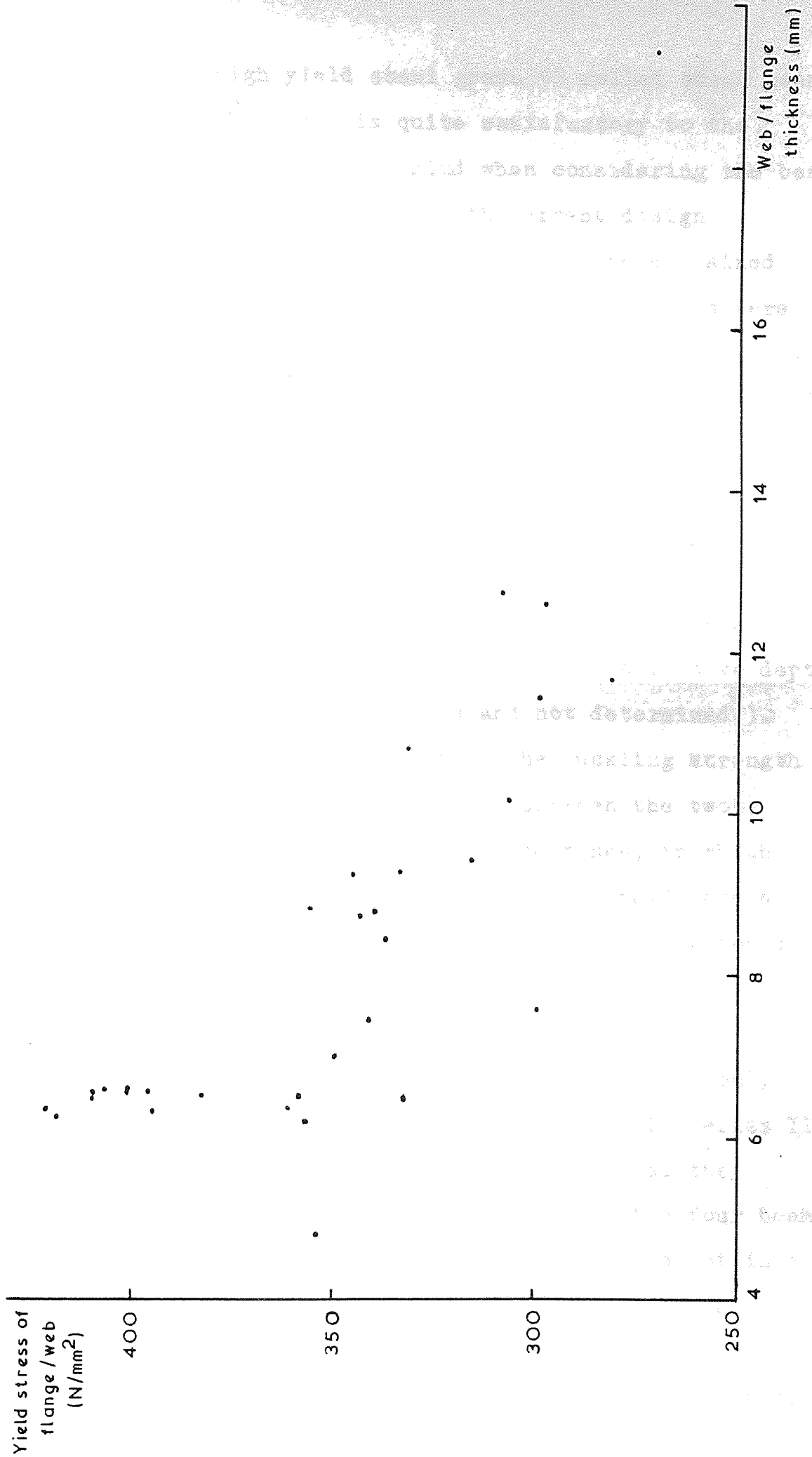


Figure 2.3 Variation of yield stress with section thickness.



specified for a high yield steel grade 50 rolled steel beam which is  $350 \text{ N/mm}^2$ . This is quite satisfactory to the consumer but must be borne in mind when considering the beam test results and comparing them with current design practice. This higher stress could perhaps be explained when considering that the superceded R.S.J. sections were consistently thicker than the universal beam sections, and by reference to figure 2.3 would have had a yield stress of approximately  $300 \text{ N/mm}^2$ .

### 2.3 Test Beam Preparation and Performance Under Test

For virtually all the tests, each beam length was intentionally cold sawn to a multiple of the effective depth  $d$  ( as quoted by the manufacturers and not determined ). This was because it was thought that the buckling strength of the web when considered as a plate between the two flanges, might prove to be of prime importance, in which case the plate to be analysed theoretically would have a convenient aspect ratio, and also because the dimension  $d$  is a constant for small ranges of universal beam serial sizes.

Apart from cold sawing to the required length, only four test beams had their properties altered. In Series III four beams of serial size 406 x 140 x 39 Kg/m had the thicknesses of both flanges reduced. Each of the four beams had their thicknesses reduced to varying sizes to obtain a range of flange to web thickness ( $T/t$ ) ratios. As the test beams were relatively short, and the flanges quite straight it was possible to machine them to a variation of thickness

in the length of  $\pm 0.125\text{mm}$ , by machining small areas at a time.

### 2.3.1 Test Beam Dimensions

The test beams were sawn to an accuracy of  $\pm 0.5\text{mm}$  which for the shortest length gives a maximum possible error of less than  $\pm 0.5\%$ , which is considered satisfactory.

The overall depth, flange widths, flange thicknesses and web thickness of every test beam were recorded at a maximum of 0.5 metre intervals along the length. This was so that a comparison could be made between the manufacturers specified dimensions and the actual dimensions, and also to include the actual dimensions in any relevant theory when considered. The resultant average values of these 4 variables were then determined and are shown in Table 2.4. Some sections had very little variation of these dimensions for the whole 12 metre length, and where this occurred the average value is shown applicable to several test beams.

The overall depth and flange widths were measured with a vernier caliper to an accuracy of  $0.01\text{mm}$ . The flange thicknesses were measured midway between the web and the flange edge with a micrometer to an accuracy of  $0.01\text{mm}$ .

The web thickness was measured with a micrometer in three places, the mid-depth and adjacent to each root radius. The dimension shown in Table 2.4 is that at mid-depth which was always found to be the thinnest point. The web is thicker adjacent to each flange, usually over a depth of approximately  $40\text{mm}$ , than at the centre by 3-5%.

Selected beams were measured to record any initial



Test No.	Overall Depth $D_t$	Flange Width $B$	Flange Thickness $T$	Web Thickness $t$	Length $L$	Web Ecc'y
1	400.63	140.16	9.01	6.56	178.5	
2	401.18	139.97	9.36	6.56	357	.15
3	401.15	139.64	9.37	6.52	714	.25
4	401.00	140.30	9.32	6.65	1071	.15
5	401.09	139.44	9.29	6.53	1428	.30
6	259.14	145.64	10.86	6.53	108	.02
7	259.38	146.06	10.78	6.28	216	.11
8	259.26	145.74	10.78	6.45	432	.06
9	259.21	144.16	10.73	6.80	648	.39
10	259.35	145.88	10.81	6.52	864	.30
11	304.92	102.56	6.47	6.19	138	
12					275	
13					550	
14					827	
15					825	
16	307.10	165.67	11.43	6.53	132	
17					262	
18					526	
19					790	
20					104	
21	258.20	103.05	8.43	6.48	224	
22					446	
23					672	
24					85	.24
25					170	.01
26	209.45	133.13	9.29	6.20	340	.10
27	209.50	132.94	9.35	6.32	510	.07
28	257.06	146.47	12.60	7.56	216	.07
29	256.78	146.31	12.57	7.61	540	.01
30	398.35	140.63	8.46	6.50	1071	1.33
31	398.36	140.42	8.47	6.52	1071	1.34
32	398.51	140.46	8.46	6.50	1071	1.00
33	401.55	140.40	9.21	6.56	178.5	
34	401.07	139.85	9.40	6.55	357	.15
35	401.08	139.88	9.28	6.69	714	.42
36	400.97	139.72	9.37	6.46	1071	.33
37	259.02	144.45	10.84	6.98	108	.28
38	259.28	146.06	10.76	6.36	216	0
39	259.25	145.83	10.74	6.46	432	.40
40	259.33	145.90	10.78	6.48	648	.31
41	304.92	102.56	6.47	6.19	136	
42					275	
43					550	
44					825	
45					132	
46	307.10	165.67	11.43	6.52	262	
47					526	
48					825	
49					102	
50					224	

All dimensions in mm

Table 2.4

Test No.	Overall Depth $D_t$	Flange Width $B$	Flange Thickness $T$	Web Thickness $t$	Length $L$	Web Ecc'y
51}	258.20	103.05	8.43	6.48	448	
52}					672	
53	209.32	133.04	9.24	6.28	85	.15
54	210.08	133.15	9.50	6.41	170	.28
55	209.31	133.59	9.55	6.37	340	.17
56	209.47	132.93	9.39	6.33	510	.03
57	257.10	146.56	12.58	7.65	216	.07
58	256.98	146.49	12.55	7.60	432	.08
59	257.33	146.24	12.57	7.58	540	.02
60	400.18	141.94	8.80	6.30	1071	
61	397.48	142.12	7.12	6.50	1071	
62	394.13	141.69	5.47	6.62	1071	
63	390.63	141.75	3.69	6.51	1071	
64	387.90	141.06	2.18	6.50	1071	
65	101.84	63.76	6.99	4.78	294	
66	465.58	192.96	19.40	11.66	1212	
67	401.20	142.20	8.77	6.34	1071	.75
68	400.92	142.12	8.77	6.31	1071	.62
69	401.17	141.90	8.66	6.30	1071	.68
70	401.31	138.73	9.27	6.53	1071	.53
71	401.01	139.95	9.38	6.56	1071	.05
72	398.63	140.97	8.43	6.58	1071	.74
73	400.83	142.43	8.77	6.20	1071	.47
74	401.23	141.77	8.84	6.31	1071	.55
75}	259.24	145.53	10.78	6.54	562	
76}					648	
77}					648	
78	261.12	147.57	12.68	7.43	648	
79	261.17	147.57	12.69	7.45	648	
80	261.08	147.51	12.72	7.46	648	
81	261.20	147.56	12.72	7.43	648	
82	261.12	147.73	12.70	7.42	648	
83	305.03	165.51	10.28	6.22	789	
84	305.10	165.70	10.31	6.26	789	
85	305.83	165.88	10.25	6.25	789	
86	305.72	165.88	10.20	6.19	789	
87	305.10	165.83	10.34	6.24	789	
88	260.89	147.55	12.71	7.45	432	
89	261.19	147.46	12.74	7.47	864	
90	261.28	147.61	12.74	7.45	864	
91	261.24	147.61	12.74	7.43	1080	
92	305.17	165.85	10.34	6.25	526	
93	304.71	166.24	10.32	6.21	1052	
94	304.88	165.89	10.22	6.17	1052	
95	305.07	165.45	10.31	6.23	1315	
96	401.25	138.56	9.23	6.59	714	.32
97	400.96	138.87	9.21	6.56	1071	.56
98	400.66	141.62	8.82	6.57	1685	
99	400.81	138.66	9.49	7.20	2107	
100	400.14	141.73	8.65	6.47	2857	

All dimensions in mm.

Table 2.4 (cont.)

curvature in the web. To enable this to be done, the centres of the web at its junction with each flange were taken as reference points. The distance from the line joining these two points to the centre of the web at mid-depth was recorded in the following way. The beam was set with its flange edges on a perfectly flat machine table and the distance from the machine table to the web face at the three points under consideration measured. The beam was then inverted and the procedure repeated. Utilising the web thicknesses previously determined the required dimension could then be found. The maximum eccentricity of the web itself was found to be 1.34mm for test beam 31, but this was an exception. It was generally found that the more slender the web, the greater the initial eccentricity. The eccentricities recorded are shown in Table 2.4.

### 2.3.2 Strain Indicators

The stress and consequently strain distribution through an elastic medium when it is subjected to a concentrated load is very complex, as can be observed in many photoelasticity text books (Frocht (36), Cokez (37) et al). It was decided therefore that to try to determine accurately the strain distribution through the flange and web of a universal beam would be beyond the scope of the present work, and that an approximate distribution would be determined from a minimum of strain measurements.

Electrical resistance linear strain gauges were attached to virtually all the test beams but in varying numbers. Generally for the early tests, several gauges were

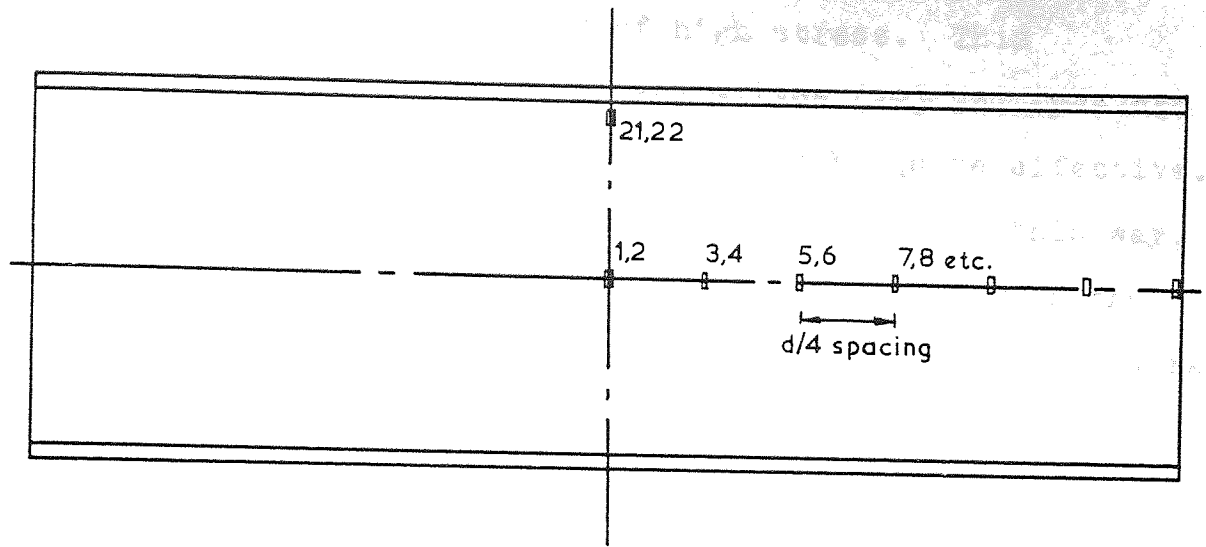
attached, but the number was reduced for later tests as the information obtained was shown to be consistent. For the early tests gauges were attached at the locations shown in figure 2.4(a) for beams in Series I to VI and figure 2.4(b) for beams in Series VII, on both sides of the web to account for direct and bending strains. Attaching strain gauges at these locations achieves two objectives. Firstly the progression of the area of the web which has yielded from the load application point would be indicated and secondly the decrease of strain at the web mid-depth away from the load application point would also be indicated. For some series ( Series I to VI ) the strains recorded are principal strains because of the symmetry of the system.

To obtain further useful strain recordings would necessitate the use of many strain gauge rosettes and the information so obtained is not thought to justify the additional cost in both time and money.

The linear strain gauges used throughout were 5mm long and were bonded to the test beams after first grinding the beam to a smooth surface at the appropriate locations.

For later tests only two linear strain gauges were attached to the test beams, at the mid-depth of the web along the line of action of the centres of the applied loads and on each side of the web. These were attached to record any sudden change in stress in the beam web, for instance due to buckling or yielding. This location was expected to be the point of maximum stress on the mid-depth line and would therefore show any sudden change in stress clearer than any other location.

As well as recording some actual strains and hence

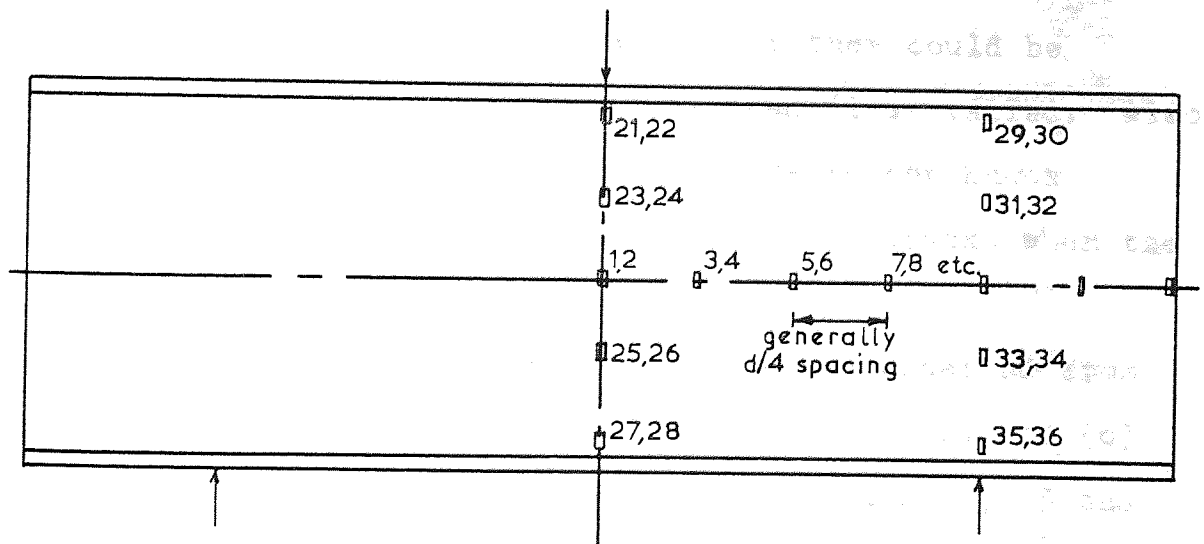


(a) Series I to VI

Reference numbers:

Odd numbers one face

Even numbers other face.



(b) Series VII

Figure 2.4 Typical strain gauge locations and referencing.

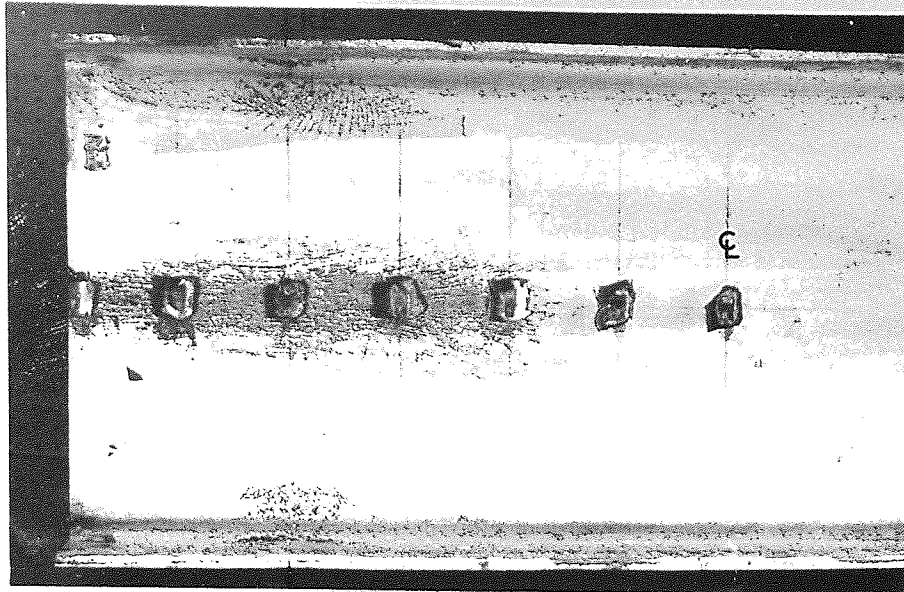
enabling the stresses to be calculated, some beams were whitewashed to indicate areas of high stress. This technique was adopted by Moore and Wilson (29) and Lyse and Godfrey (30) amongst others and shown to be quite effective. Whilst not being able to record actual strains in this way, it has been shown that definite crack lines appear in the whitewash at high strains. For the early tests in this work beams were whitewashed in addition to the attachment of strain gauges. This was when a general distribution of the stress throughout the section was required, but for later tests the method was only employed in selective tests.

#### 2.3.2.1 Strain Distribution

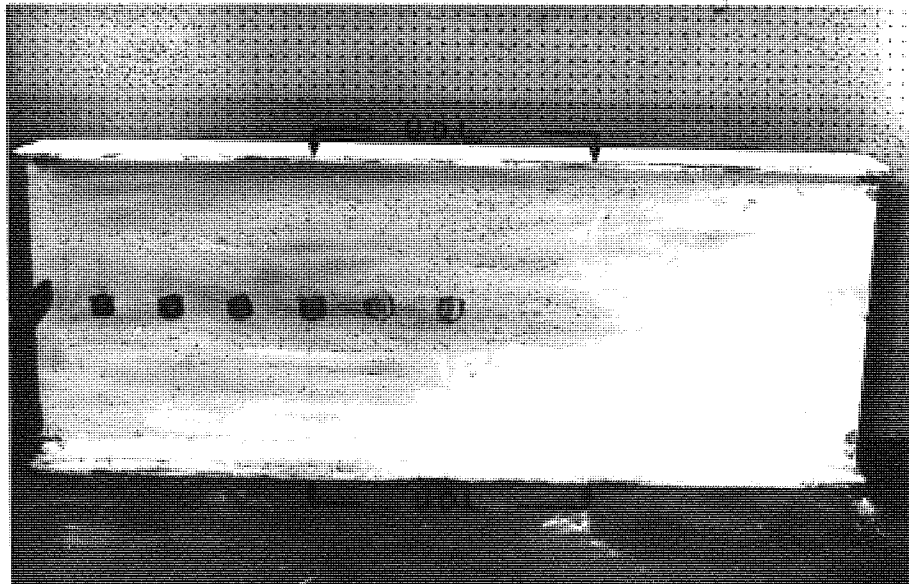
The information gained from the crack lines in the whitewash must be regarded as approximate as they are those present after failure. This means that they could be different to those present when the beam first failed. Also the strain at which the whitewash cracks is not known exactly although it will be assumed that it cracks when the material yields.

The general strain distribution can be observed from the pattern in the whitewash. Figure 2.5(a), (b) and (c) shows the pattern after failure for test beams 68, 73 and 74 respectively, which were loaded as shown. Areas of very high strain are indicated by the larger areas of flaked whitewash. The strain gauge positions are the larger dark areas at the intersection of the grid reference lines. The crack lines at mid-depth are always along the mid-depth line, which confirms that the direction of principal strain

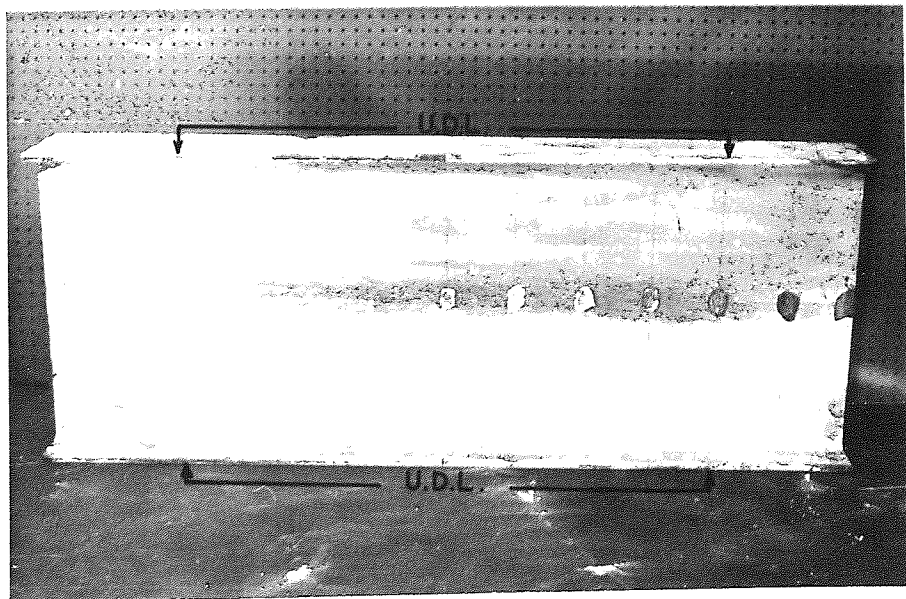




(a) Two opposite Knife Edge Loads.



(b) Two opposite Uniformly Distributed Loads.



(c) Two opposite Uniformly Distributed Loads.

Figure 2.5

is perpendicular to this mid-depth line. The grid lines are at  $d/4$  intervals.

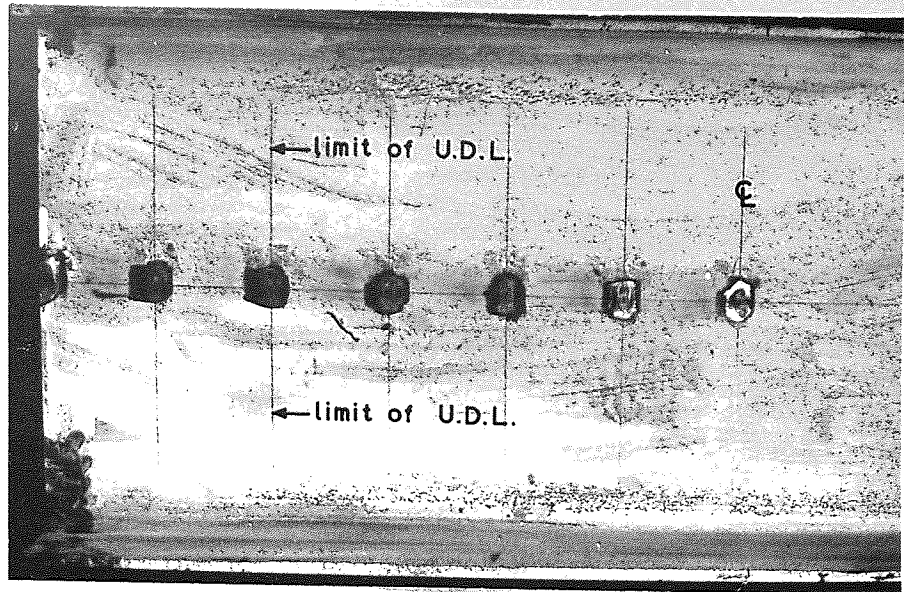
Figure 2.5(a) shows a region of yield in the web and the flange in the vicinity of the applied loads, and also a dispersion of strain into the web. The angle that this dispersion line makes with the plane of the flange can be seen to be in the region of  $30^0$ , although this angle may well differ further into the web. The strain gauge readings confirm the observation from figure 2.5(a) that the strain in the web at mid-depth is very small at a distance of between  $d/2$  and  $3d/4$  from the line of action of the applied loads.

Figures 2.5(b) and (c) show different lengths of yielded regions at the mid-depth line, corresponding to different lengths of the applied loads. In each case the length of the crack lines in the whitewash are between  $d/4$  and  $d/8$  greater than the length of the applied uniformly distributed loads. Comparing this with the length of the crack lines in figure 2.5(a), which was for a knife edge load condition, would indicate that the stress dispersion is greater for a shorter length of applied load.

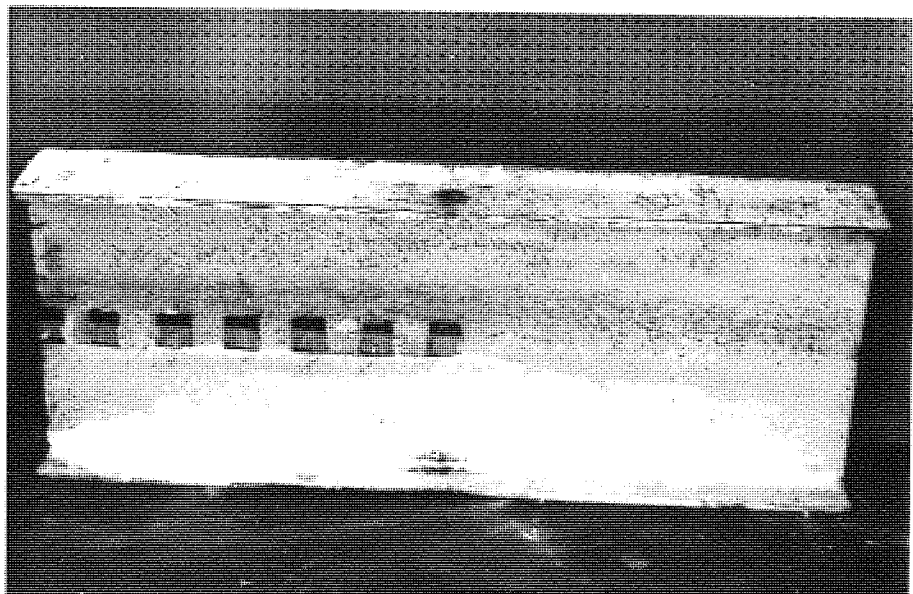
Figure 2.6(a) shows the crack lines in the whitewash in the region of the applied loads for test 74, which was loaded with a uniformly distributed load. The lengths of the crack lines are very similar to those at the mid-depth, which were on the reverse side and were shown in figure 2.5(c). The lines do have a slight curvature away from the centre of the applied load.

Figure 2.6(b) shows the strains in the web for test 32, which was loaded eccentrically by ball bearings on each

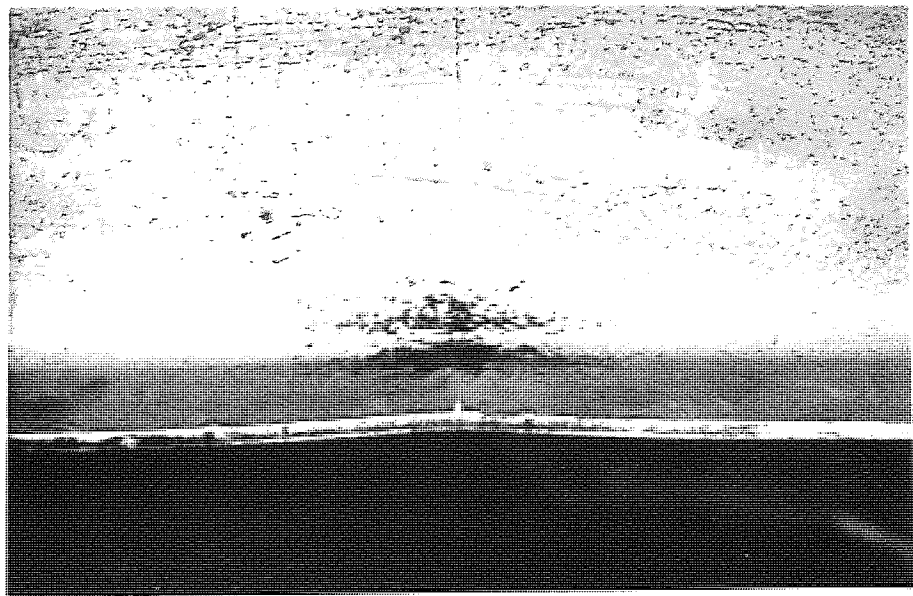




(a) Two opposite Uniformly Distributed Loads.



(b) Two opposite point loads (eccentricity = 20mm)



(c) Two opposite point loads (eccentricity = 20mm)

flange ( Series II ). The crack lines are more dense at the centre and get increasingly more sparse towards the beam edge. The extent of local yielding can be seen, which is shown in greater detail in figure 2.6(c). The ball bearing has penetrated the flange due to its location at 20 millimetres eccentricity to the web.

### 2.3.2.2 Strain Gauge Readings

The strain gauge readings for all tests are shown in the appendix. The reference numbers are consistent for all beams. Some general observations from the strain measurements will be included here. As gauges were always used in pairs, one on each side of the web, the resulting bending and direct strains will be used where necessary. The stresses will not normally be quoted as the necessary conclusions can be drawn from the strains. Hence readings which have exceeded the 'yield strain' will be shown with 'Y' alongside. The yield strain is that determined from the tensile test results.

Figure 2.7 shows a comparison between the strains ( direct and bending ) for tests 4 and 36 at the same applied load of 200KN. Each beam is identical except for the type of applied loads, test 4 having no restraint against rotation because of the ball loading, but test 36 having restraint provided by the knife edge loads applied across the flanges. The direct strains are quite comparable with the strain at the beam centre being slightly higher for test 36 due to the smaller radius on the knife edges compared to the radius of the ball bearings. The bending

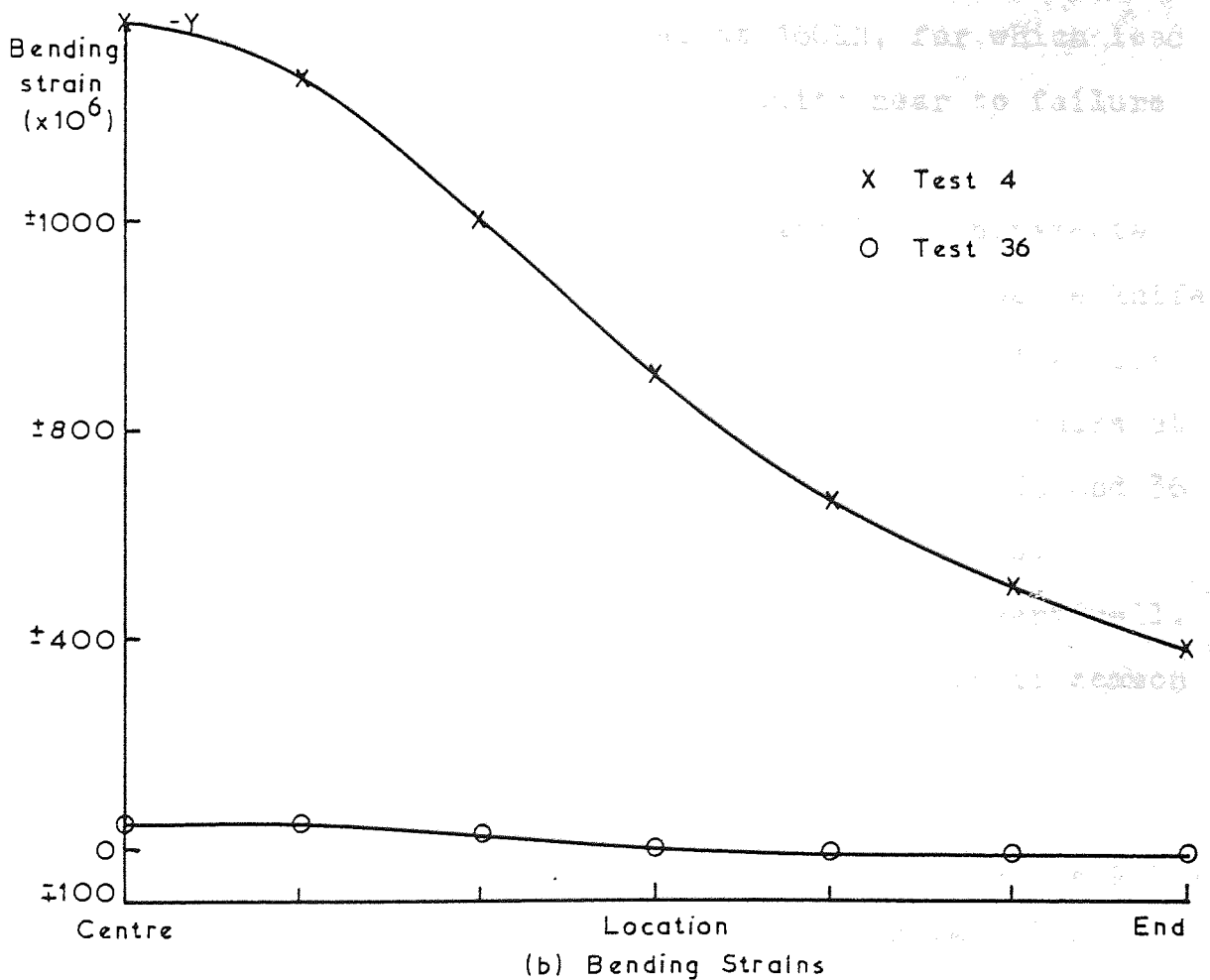
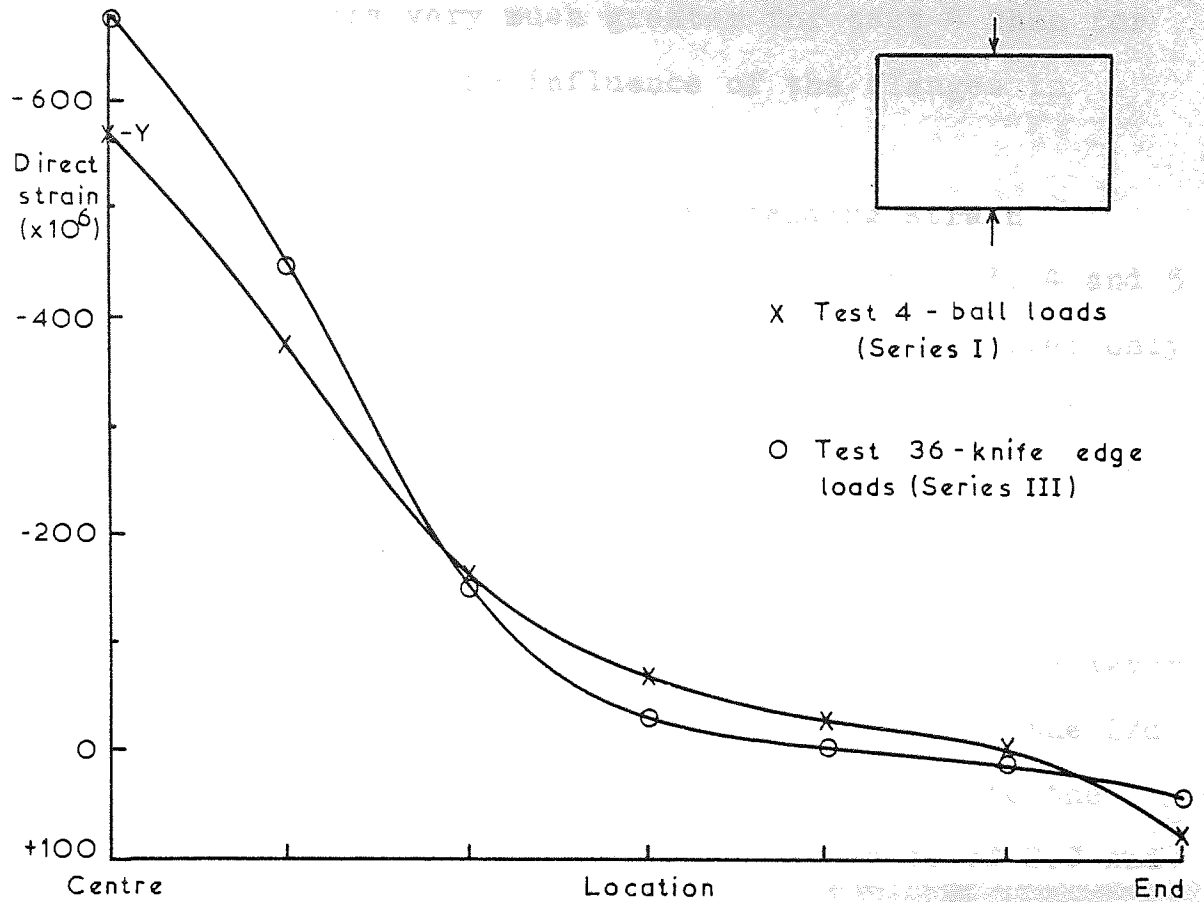


Figure 2.7 Comparison of strains for Series I and III (at 200KN).

strains however are very much greater for test 4 than for test 36, thus showing the influence of the flanges in preventing bending of the web.

Figure 2.8 shows the direct and bending strain distributions along the mid-depth line for tests 3, 4 and 5 at the same applied load of 160KN. These tests differ only in the length of the test beam, each being loaded by two opposite ball loads. All show very similar direct strain distributions, which shows that, for beams with length to effective depth ratios ( $L/d$ ) of 2.0 or greater, the distribution of direct strain is almost identical. However the bending strains are reduced for an increase in the  $L/d$  ratio, but the reduction is not linearly related to the increase in length. In fact between  $L/d$  ratios of 2.0 and 3.0 the change in bending strains is quite marked. However this could be due to the fact that at 160KN, for which load figure 2.8 is drawn, test 3 beam was quite near to failure compared to tests 4 and 5.

Comparison of the strains at certain load increments for beams tested in Series III (loaded by two opposite knife edge loads at mid-length) is not as straightforward as for those in Series I above. The bending and direct strains at two loading increments are compared for tests 34, 35 and 36 in figure 2.9. They were each of different lengths.

The direct strains in figure 2.9(a) compare very well. At 200KN the strains are almost identical over their common length, but at 300KN there is a certain amount of distribution of the strain for the longer beams thus reducing their maximum strain, which is as one would expect.

Comparison of the bending strains in figure 2.9(b)

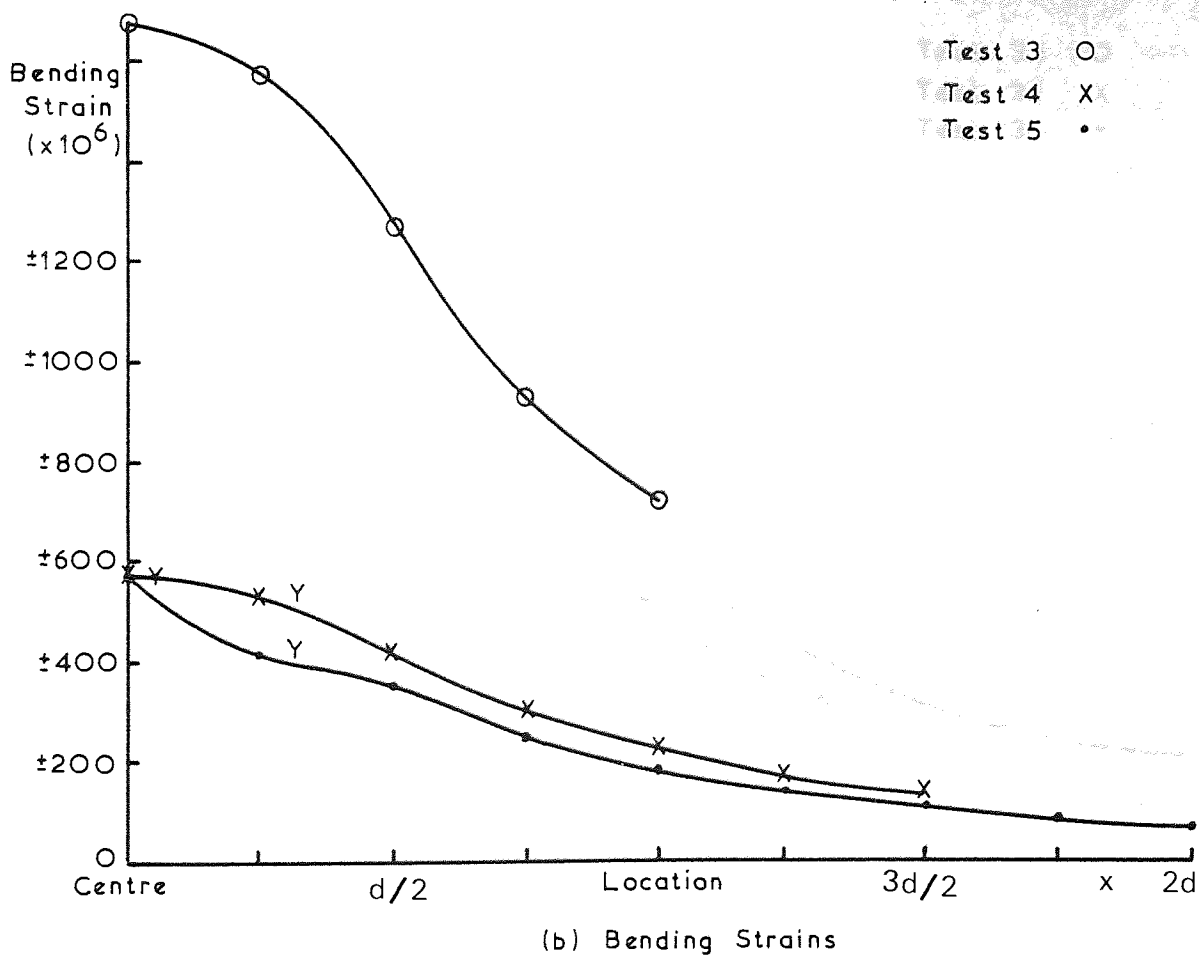
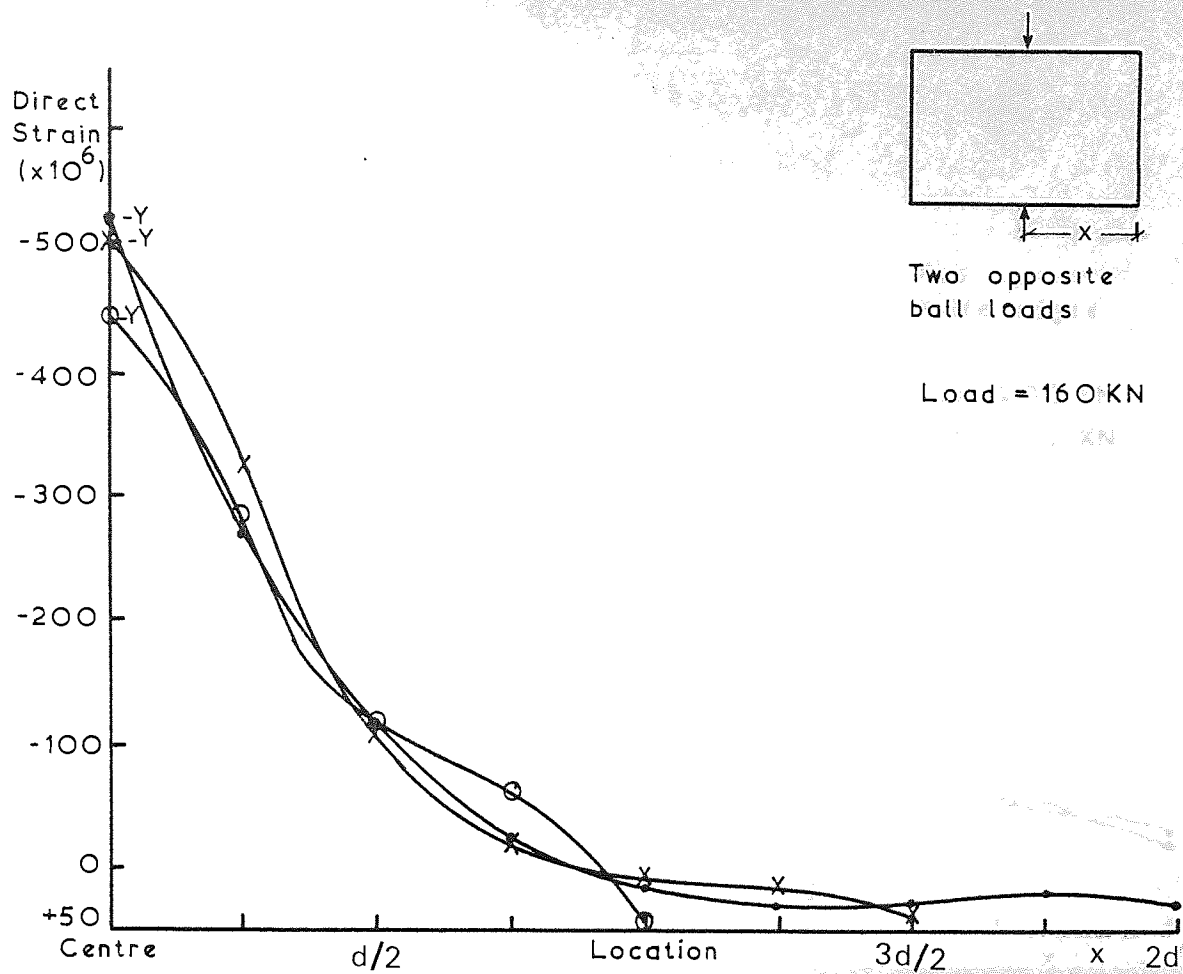


Figure 2.8 Typical mid-depth strain distributions - Series I.



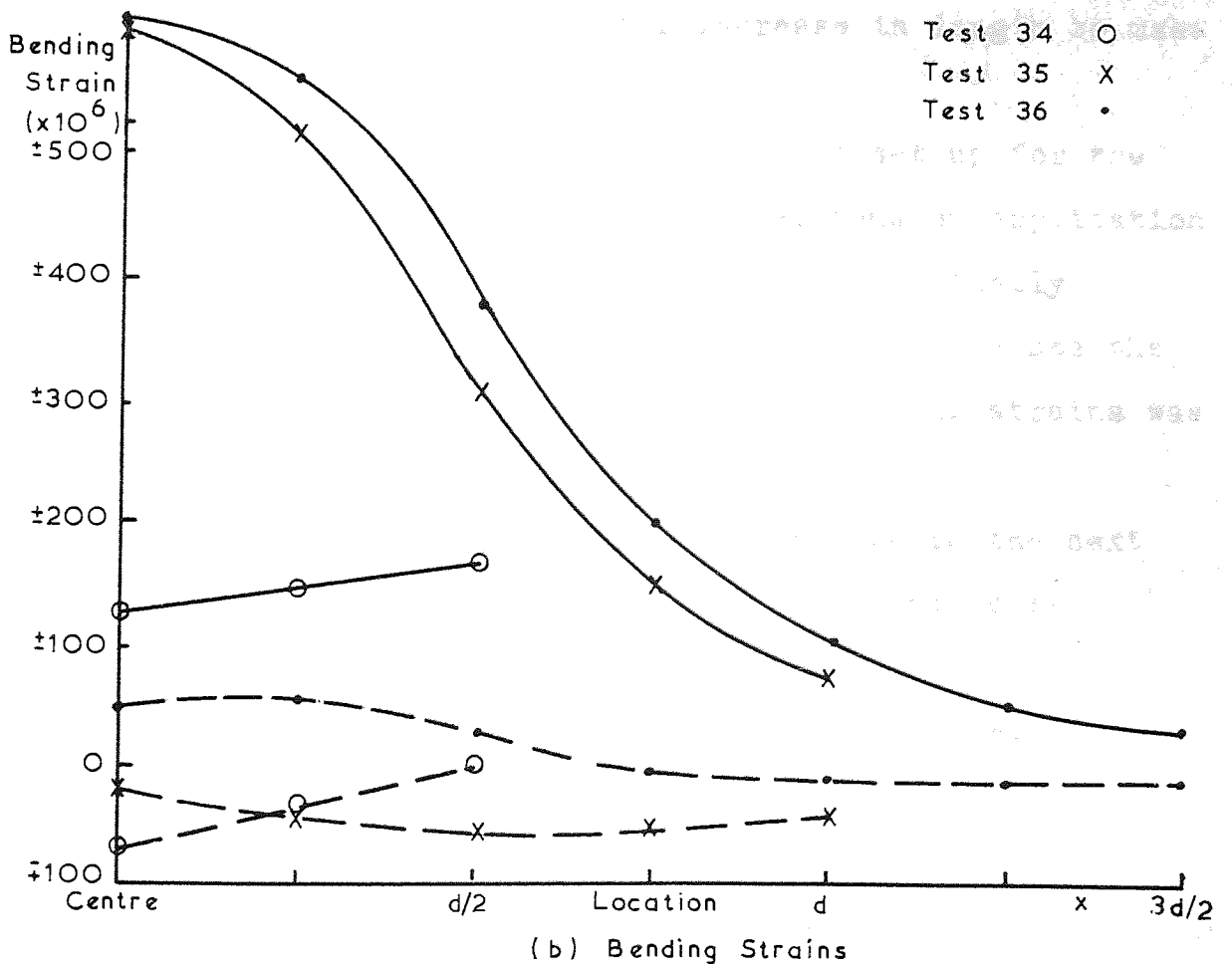
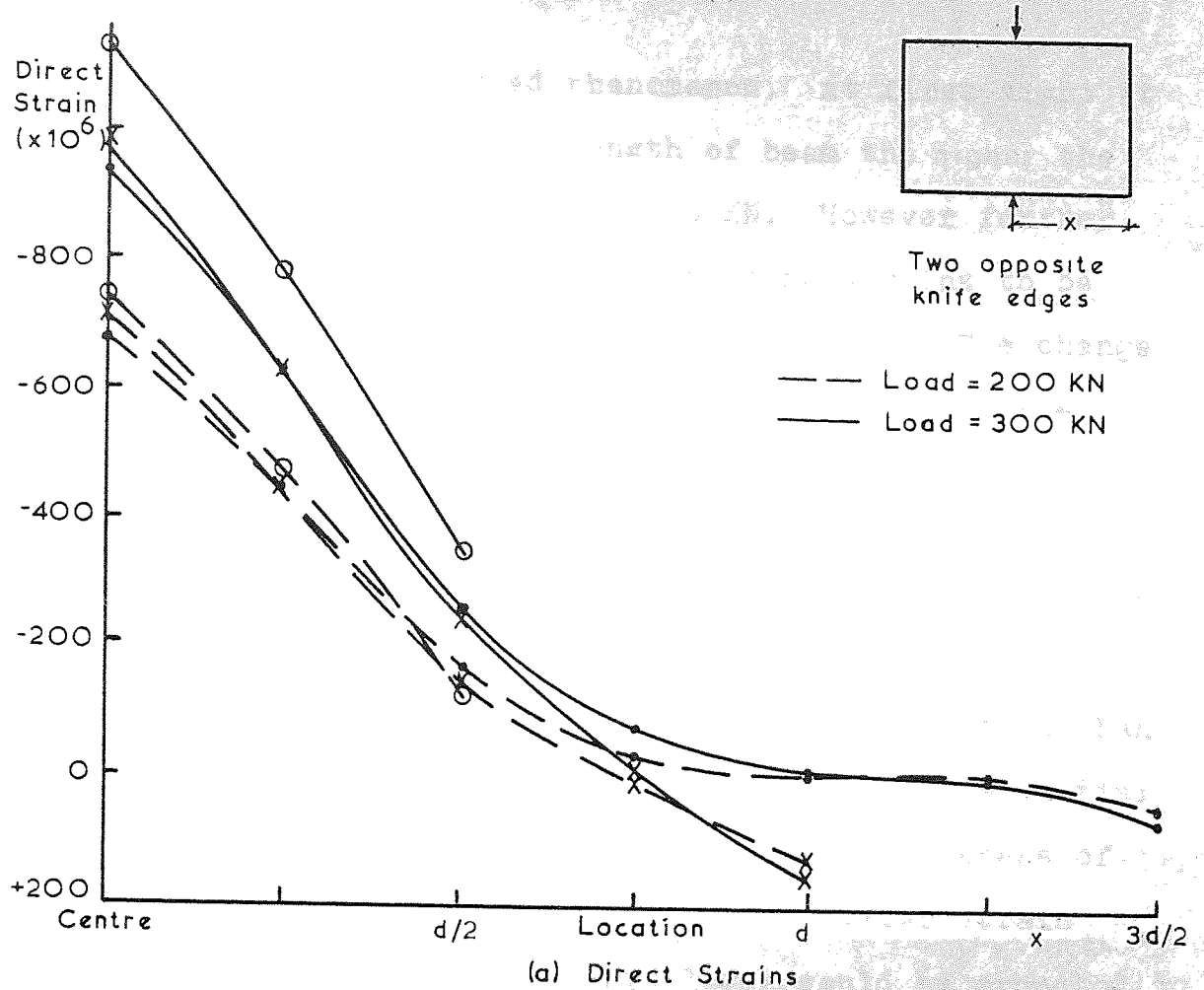


Figure 2.9 Typical mid-depth strain distributions - Series III.

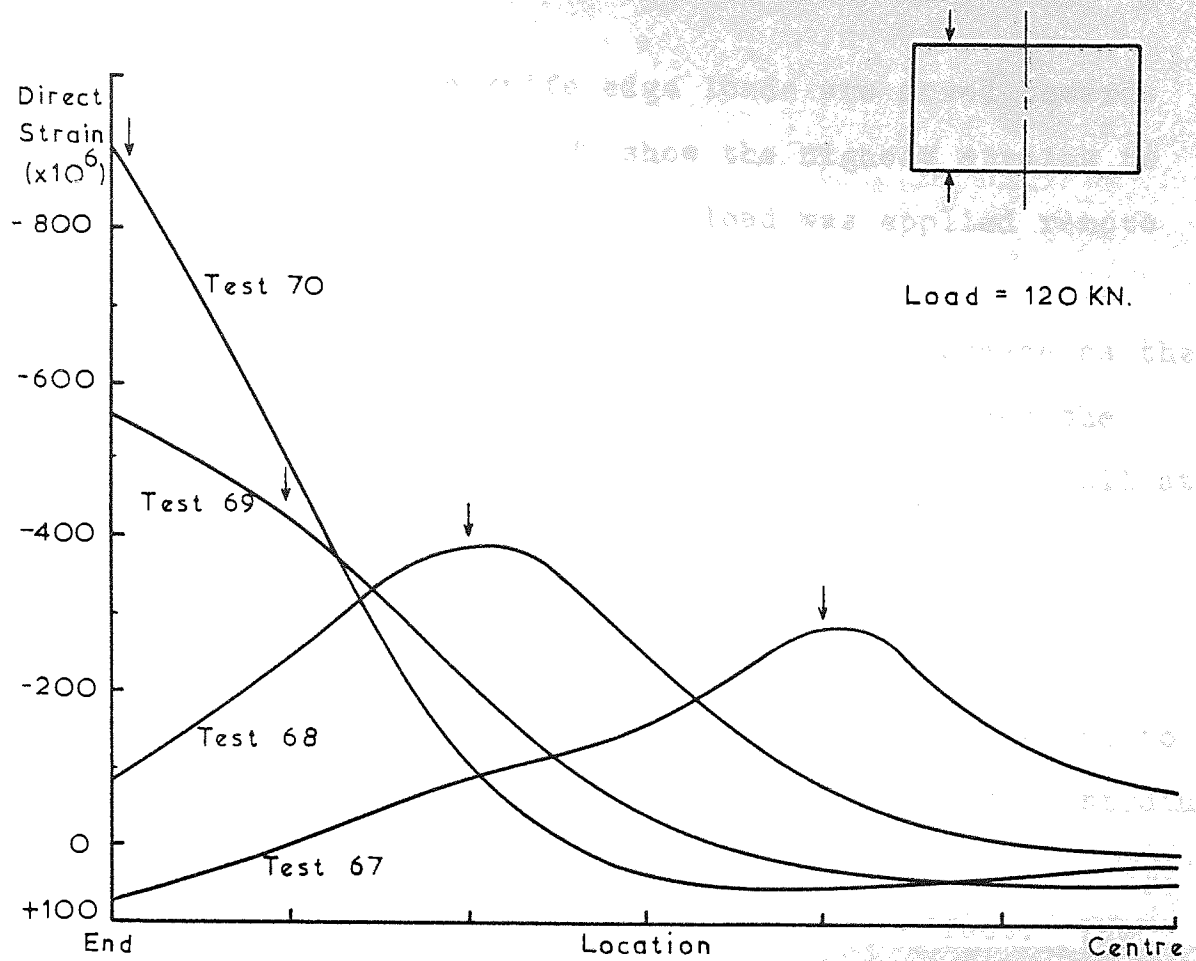
however shows an unexpected phenomenon. At first sight it appears that the longer the length of beam the higher the bending strain, on comparison at 300KN. However further comparison at 200KN shows all the bending strains to be similar ( on average and ignoring the signs ). The change in bending strain between 200 and 300KN shows that the longer the beam the greater is the increase in bending strain.

In trying to account for this it can be said, firstly, as the bending strains are relatively small at 200KN it would be erroneous to compare them in any more detail than above. Secondly, no account has been taken of the initial eccentricities of the webs, nor the out of squareness of the section. Tests 35 and 36 have very similar strain distributions, and so the failure loads would be expected to be very similar, and any further increase in length to make very little difference.

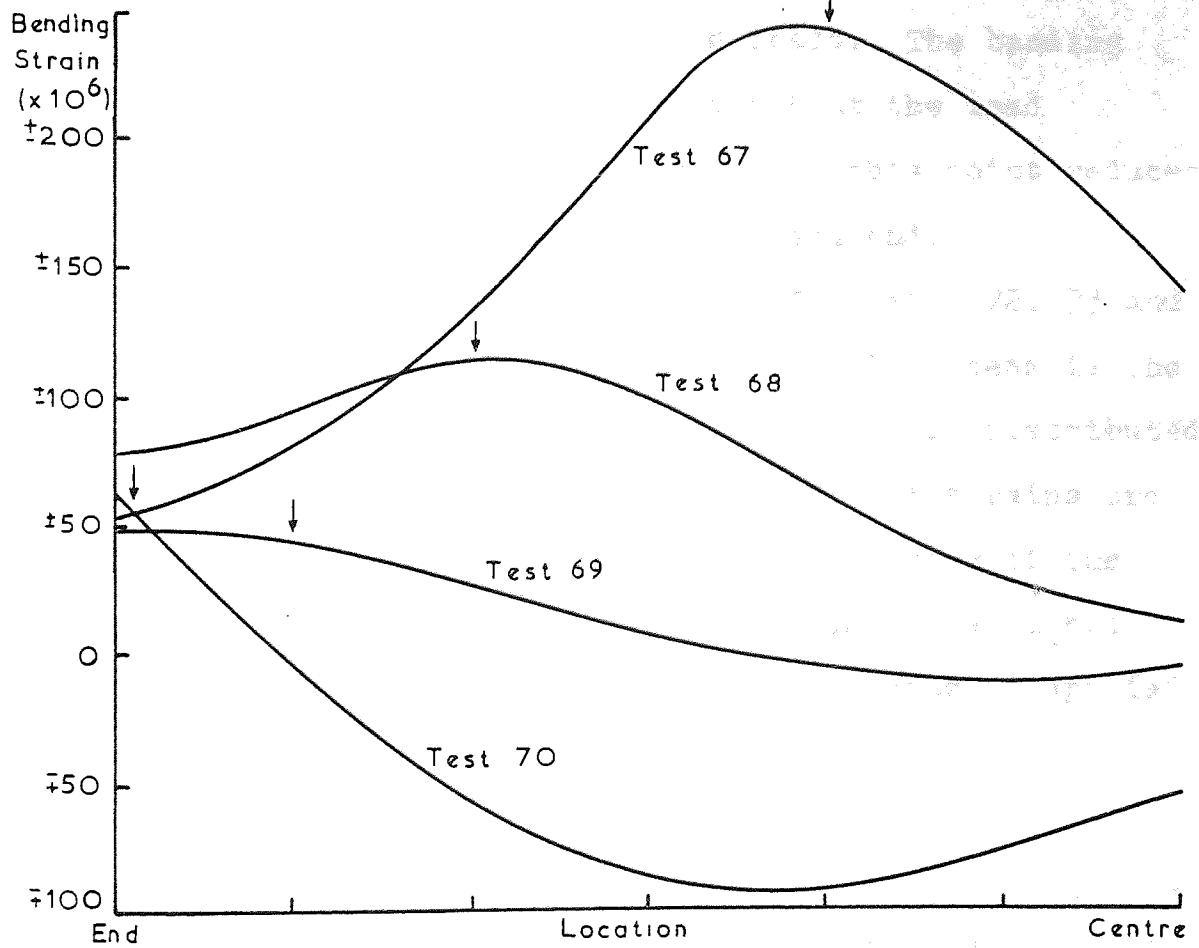
It is possible that when test 34 was set up for the test, that the flanges were not square, thus on application of the load they were twisted square which virtually corrected any initial eccentricity of the web. Hence the increase of deflexions and consequently bending strains was very small compared to tests 35 and 36.

Examination of the deflexion recordings in the next section will help to show whether this hypothesis is possible.

Figure 2.10 shows the bending and direct strain distributions along the mid-depth of the web for test numbers 67-70 ( Series IV ) at the same load of 120KN. This shows the influence on the direct and bending strains in the



(a) Direct strains



(b) Bending strains

Figure 2.10 Typical strain distributions - Series IV.

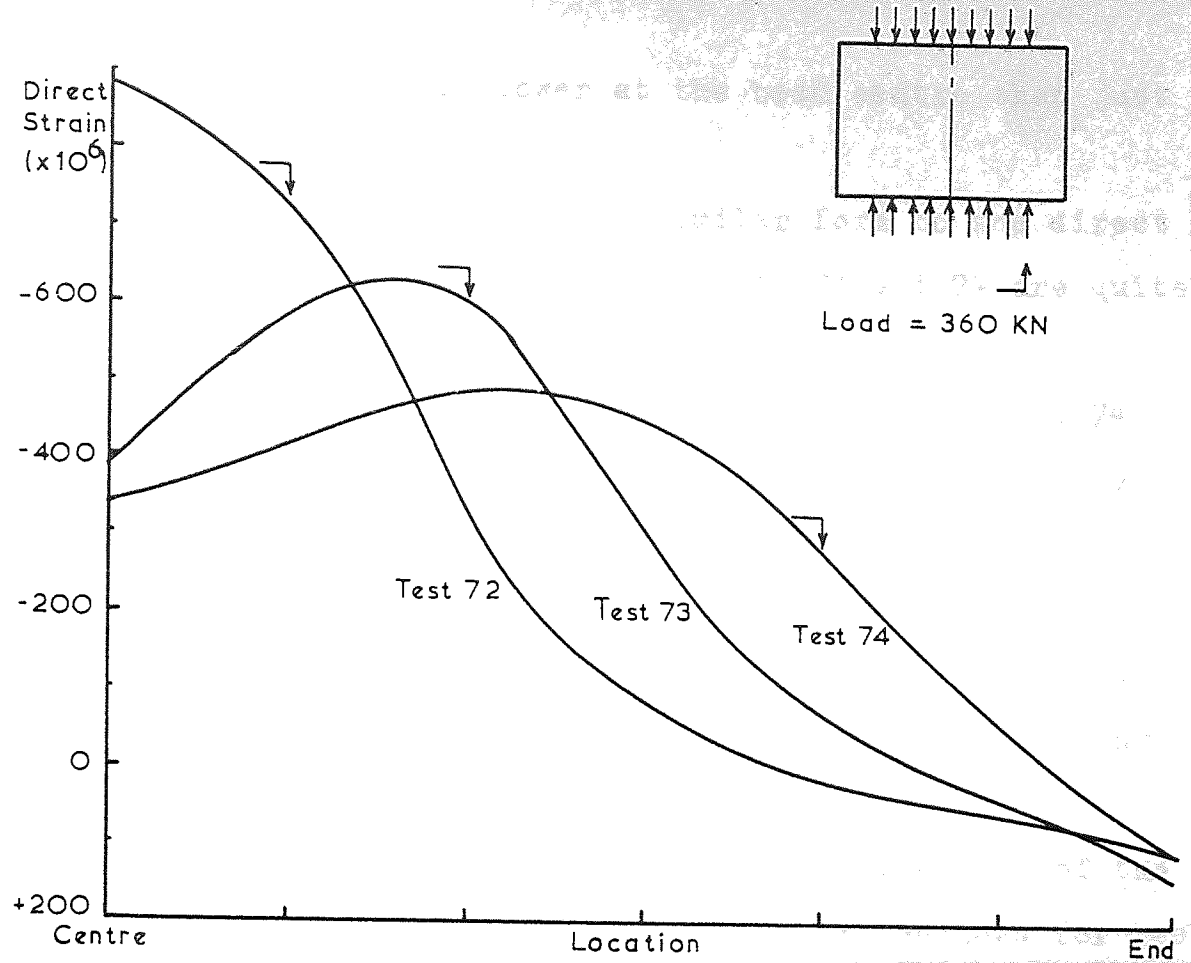


web as the two opposite knife edge loads are moved towards the beam end. Tests 69 and 70 show the highest strains to be at the beam end even though the load was applied remote from the end.

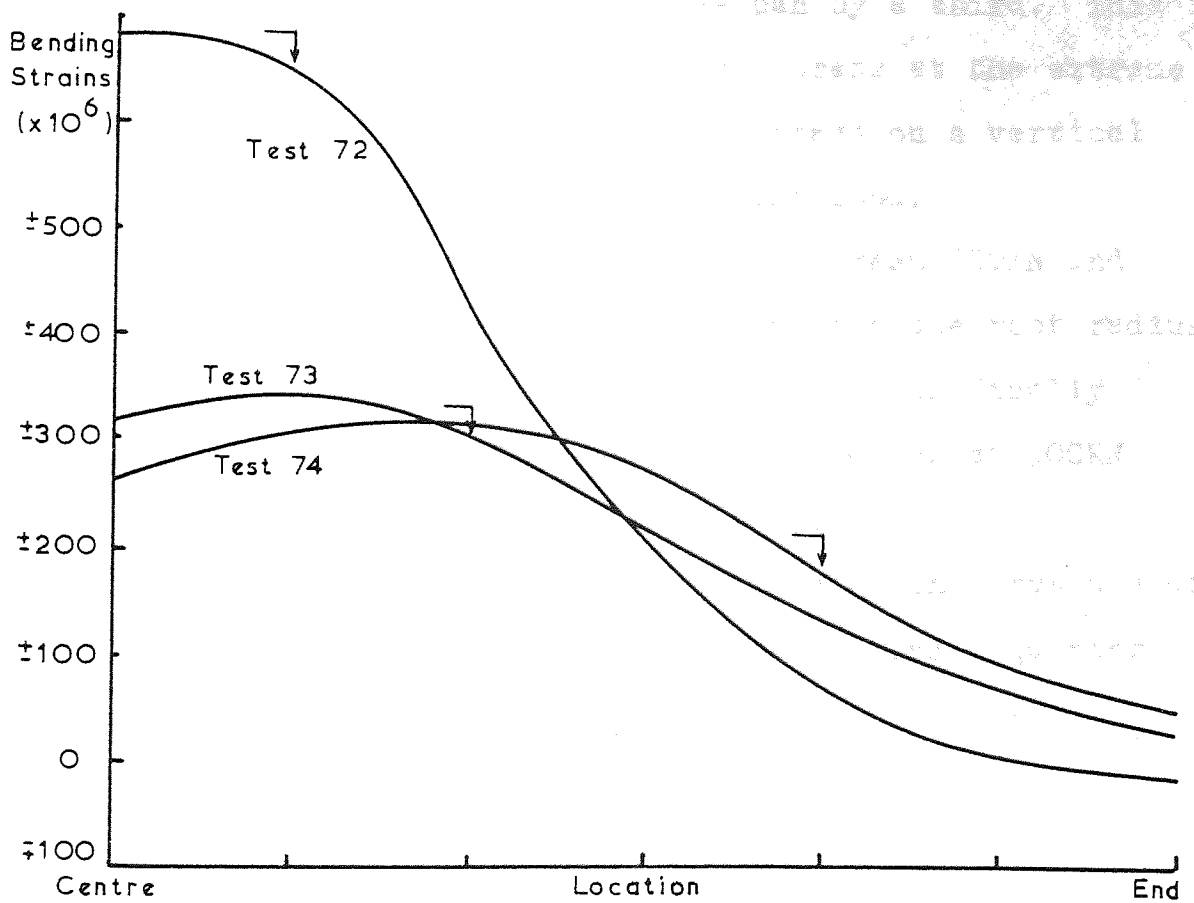
The maximum direct strains are shown to increase as the knife edge loads move towards the beam end. However the direct strain on this mid-depth line is always very small at a distance of between  $d$  and  $3d/2$  from the load application point. This shows that the distance along the beam over which the stress or strain disperses does not alter significantly as the load application point moves nearer to the beam end, although the intensity of the stress or strain is greater for the same applied load.

The bending strains show an interesting effect. The bending strains at the beam end are all very similar whatever the position of the applied loads. The bending strains are highest at the web mid-depth at the load application point and the actual value at this point reduces as the applied loads move towards the beam end.

The plot of the mid-depth strains for tests 72, 73 and 74 ( Series V ) are shown in figure 2.11. Each beam is the same length and loaded by two opposite uniformly distributed loads, the length of which varies. The direct strains are as one would expect, high strains in the vicinity of the applied loads and decreasing away from them. The direct strain curves are flatter for increasing lengths of applied load and it would be expected to be almost horizontal for a uniformly distributed load along the whole length. The direct strains for the tests with the two longest lengths of uniformly distributed loads are shown to have the peculiar



(a) Direct strains.



(b) Bending strains

Figure 2.11 Typical strain distributions - Series V.

characteristic of being lower at the beam centre than just away from the centre.

The bending strains show a similar form to the direct strains. The bending strains for tests 73 and 74 are quite similar.

For both direct and bending strains tests 73 and 74 show the maximum strains to be between the centre of the beam and the end of the uniformly distributed load. This may be due to any unintentional effects such as bending of the flat plate used to provide the uniformly distributed load or variations in the overall depth of the beam along its length.

The state of stress in the web in the vicinity of the load can be examined from the strain gauge readings for test number 96 (Series VII), which was simply supported on two knife edge loads and loaded at mid-span by a third. This is shown in figure 2.12 which shows the stress at the extreme fibre due to bending and the direct stress on a vertical section of the web at the central point load.

The direct stresses show that at between 200KN and 240KN the web yields near its junction with the root radius at the central load point. The yielded region finally extends to one quarter of the depth of the web at 300KN ( approximately 95% of the final load ).

The bending stresses indicate a change in curvature of the loaded beam between the top of the web and a quarter depth. This could indicate a deflected shape of the following form:

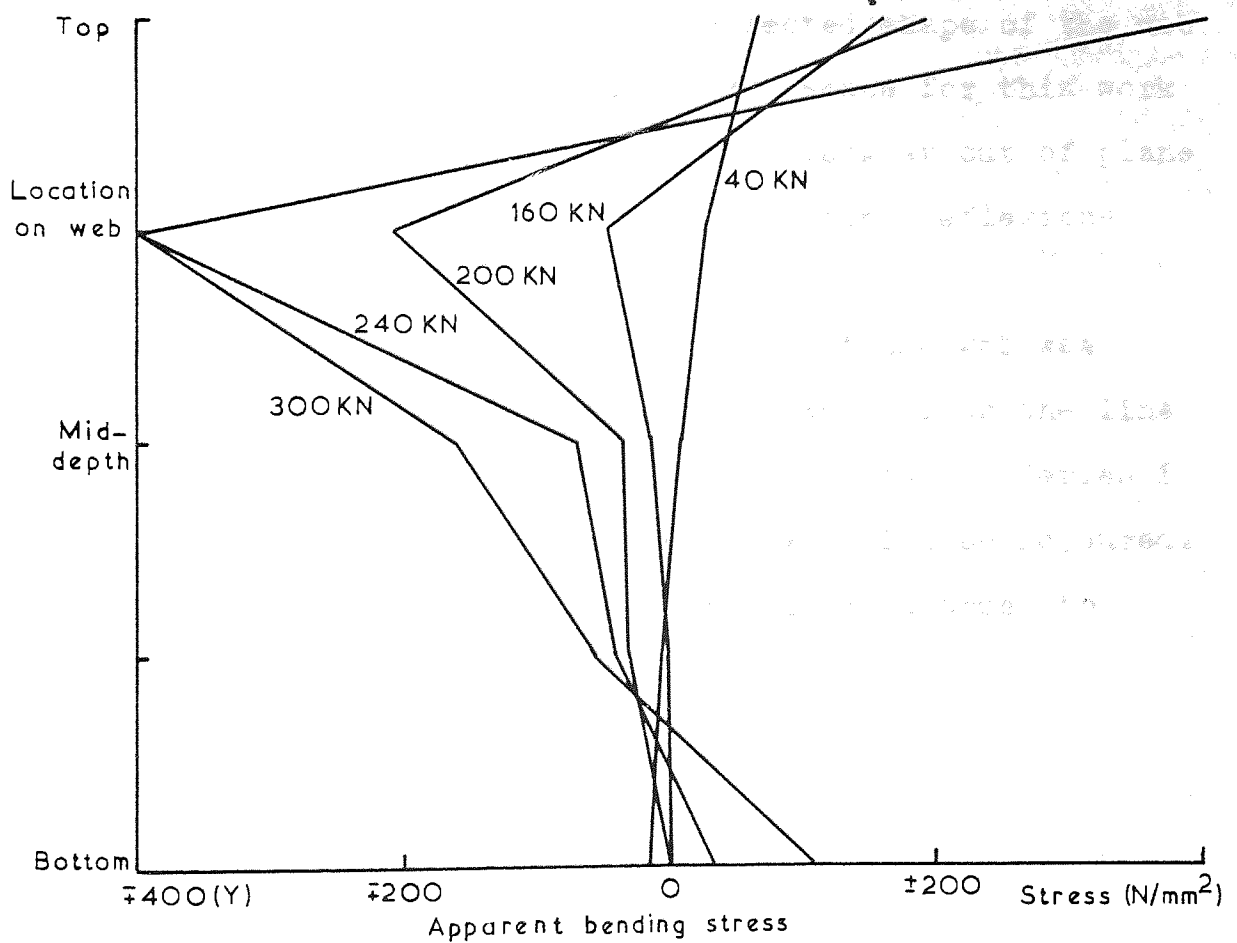
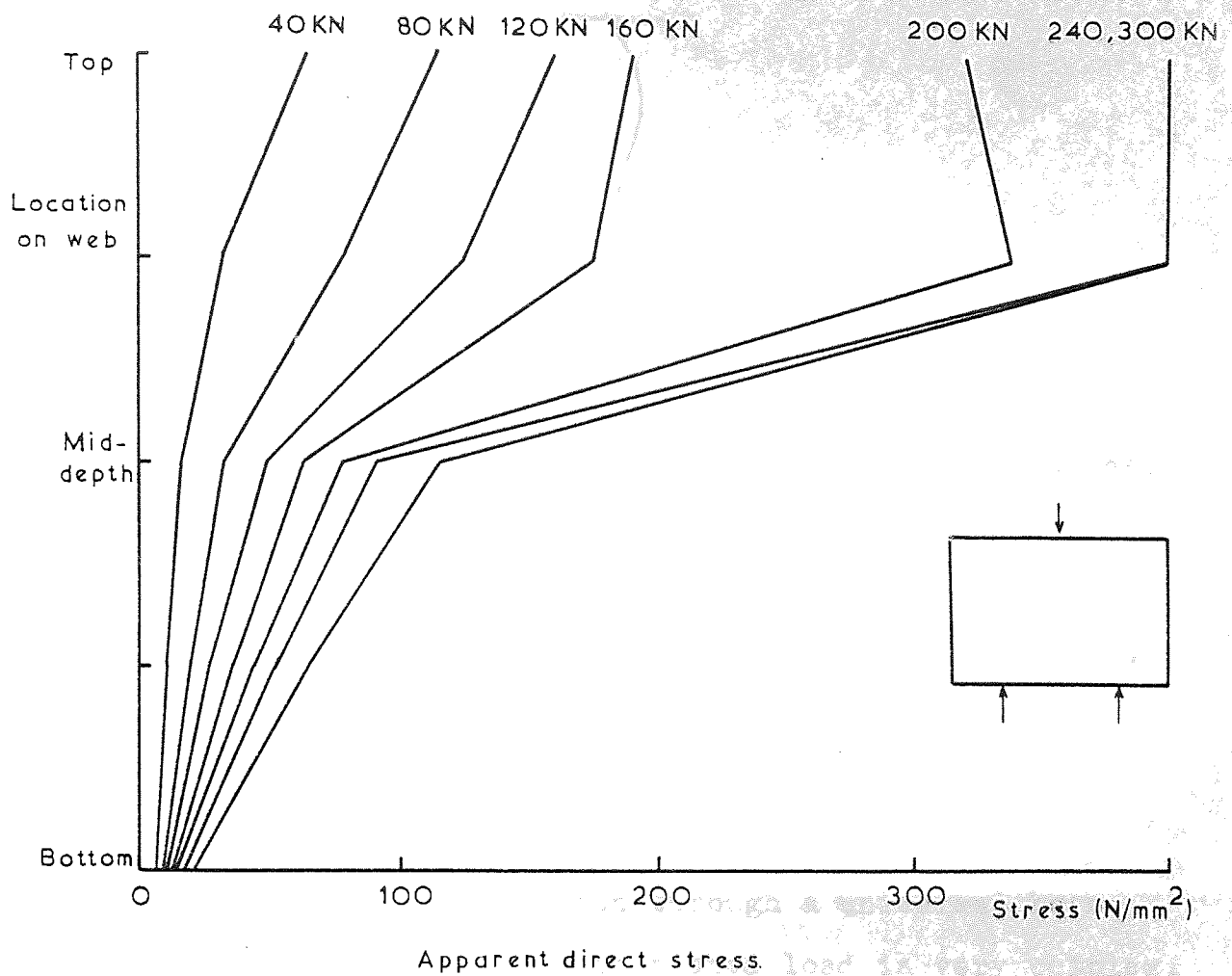


Figure 2.12. Test 96 (Series VII) web stresses at mid-span.



The strains in the tests tend to show gradual changes. Very rarely is there an instance of a sudden change in strains, and this usually occurs for beams of very short length or for long lengths of uniformly distributed loads.

### 2.3.3 Deflexion Indicators

As the strain distribution through a universal beam when it is subjected to a concentrated load is very complex, it follows that the out of plane deflected shape of the web and the flanges will also be complex. Hence for this work it was decided to measure the expected largest out of plane deflexion of the web together with any other deflexions which were considered important.

The largest out of plane deflexion of the web was expected to be at the mid-depth of the web, along the line of action of the centres of the applied loads for Series I to VI. In many tests this was the only deflexion measured. At least one deflexion was always measured in order to record any sudden change, and also for possible use in determining the elastic buckling load at a later date. For Series VII many more deflexion gauges were placed along the mid-depth line but away from the applied loads. For this

series the vertical deflexion of the beam at the mid-span was also recorded, at both sides of the web position to account for any twisting or warping of the section.

All deflexion gauges used were mechanical dial gauges with divisions of 0.01mm so that each reading could be taken to the nearest 0.005mm if required.

#### 2.3.3.1 Deflexion Recordings

The deflexion recordings for each test beam are shown with the strain gauge recordings in the appendix. The readings will be used here to illustrate various points.

The central deflexion gauge for many tests showed a relatively large increase of the lateral deflexion of the web at a very small load. The deflexions then increased very gradually at a slower rate until near failure when they increased at a very fast rate and in some tests the gauges became unreadable. The initial large deflexions were mainly due to 'squaring up' of the flanges between the applied loads as the initial load increment was applied. This was evident even when great care was taken to pack the applied loads to make even contact with the flanges.

Typical load-deflexion curves for beams tested with two opposite loads at their mid-length (Series I and III) are shown in figures 2.13(a) and (b). Figure 2.13(a) shows, for beams tested by ball loads, that as the beam length increases so the deflexion at each load increment decreases and also that the deflexion prior to failure is increased. This is due to the restraining effect of the additional length of beam, and also the availability of a certain amount of beam



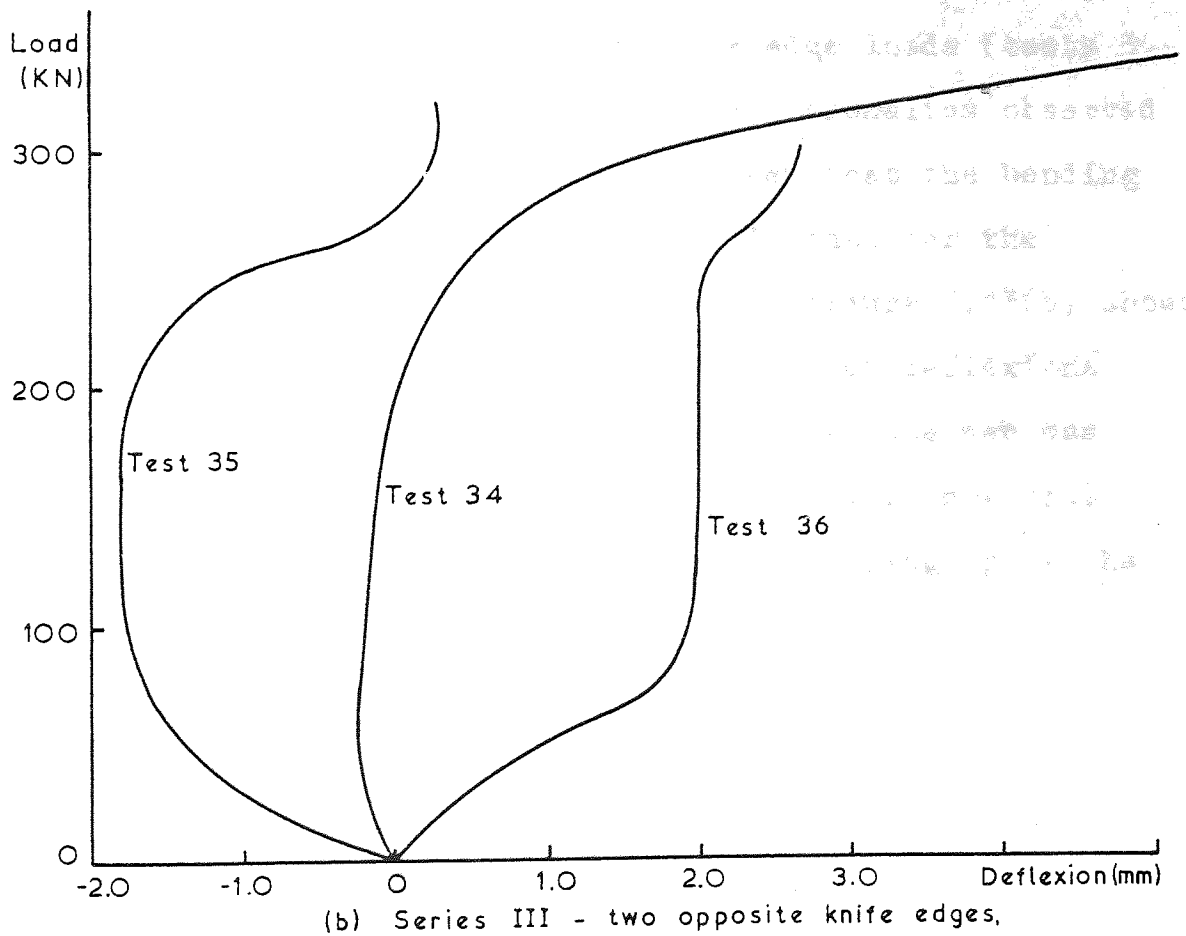
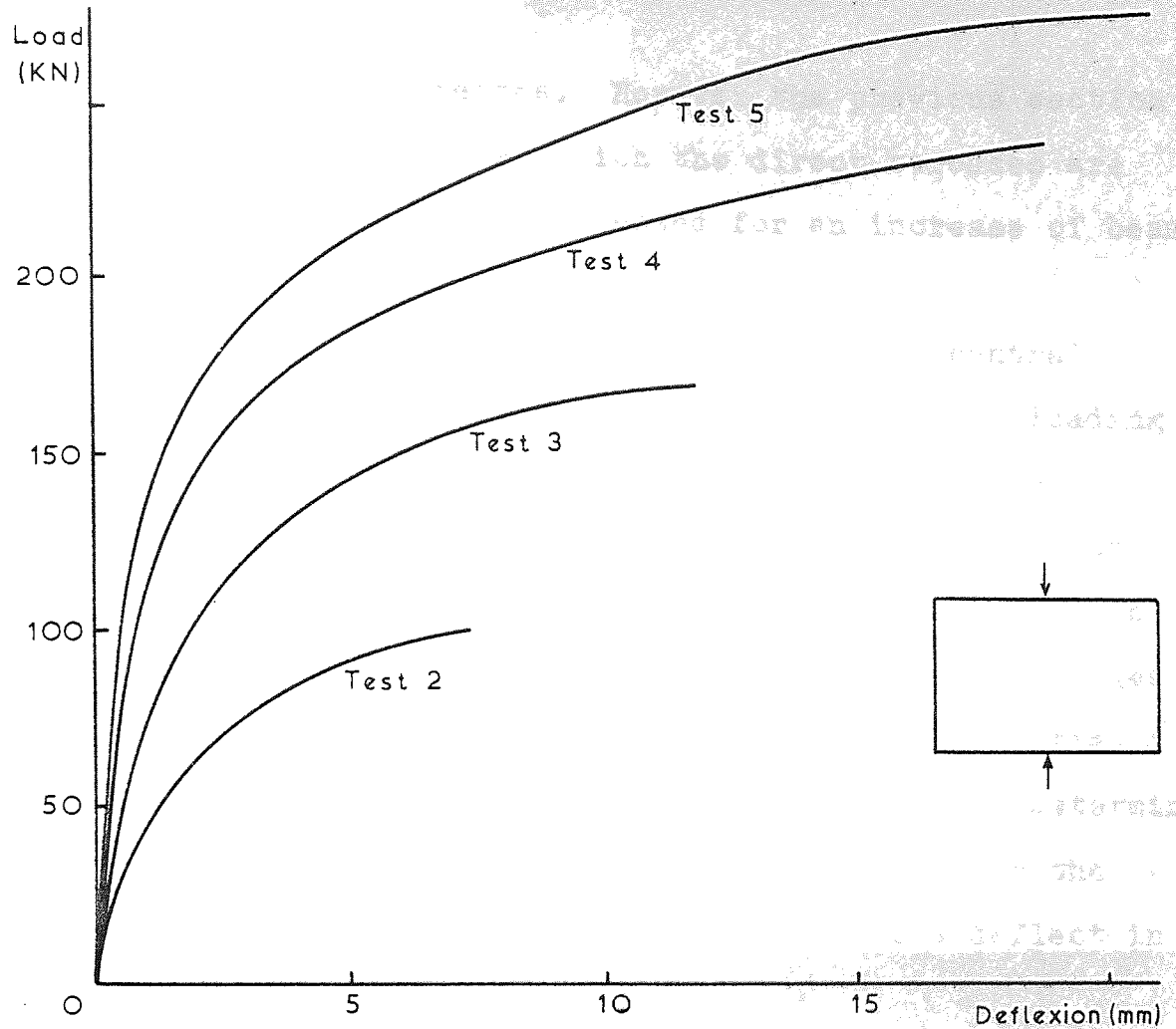


Figure 2.13 Typical load deflexion curves - Series I & III.

to redistribute the stresses. However the previous section showed that the length over which the direct stresses are distributed is not greatly increased for an increase of beam length.

Figure 2.13(b) shows the comparison of the central deflexions for increasing lengths of beam tested by loading with two opposite knife edge loads (Series III). The deflexion just prior to failure does not seem to show any relationship with the length of the test beam. Obvious in figure 2.13(b) is the initial bedding-in of the knife edges and consequent squaring up of the flanges causing initial large deflexions. However this does not seem to predetermine the failure pattern as some beams finally deflect in the direction of the initial deflexions while others deflect in the opposite direction.

These observations of the deflexion gauge recordings for beams loaded by two opposite knife edge loads (tests 34-36) confirm the reasons for the apparent anomalies observed previously in figure 2.9(b). It was seen that the bending strains were greater for tests 35 and 36 than for the shorter beam in test 34. Examination of figure 2.13(b) shows that test 34 had virtually no increase in web deflexions between 100KN and 250KN thus indicating that the web was practically vertical. Tests 35 and 36 however show that their deflexions increase after initial squaring up of the flanges.

The central deflexion gauge did not always record the maximum out of plane deflexions of the web, as originally intended. It was found that for some beams the maximum deflexion was nearer to the top of the web.



Figure 2.14(a) shows the comparison between the load-deflexion curves for beams tested with two opposite ball loads applied eccentrically to the web (Series II). This shows, as one would expect that the greater the eccentricity of the applied loads, the greater the initial out of plane deflexion of the web for each load increment. However the final web deflexion at mid-depth is approximately the same for all four tests, although the exact deflexion at failure could not be recorded. The different slopes of the load-deflexion curves are more consistent when observed in figure 2.14(b) which shows the deflexion of the web in relation to the line of action between the two forces.

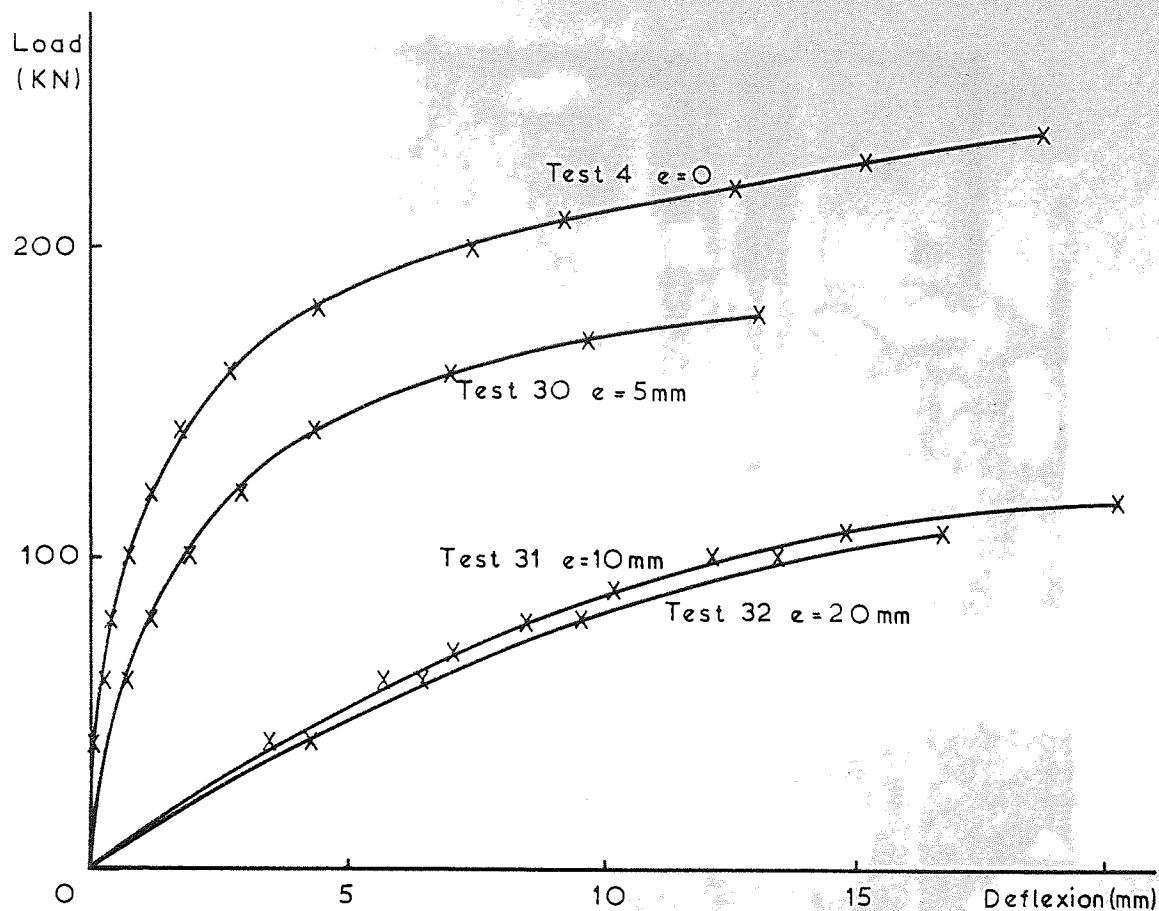
## 2.4 Test Details

Testing was carried out using one of the three hydraulic testing machines shown in figure 2.15, the selection depending on the expected failure load of the test beams and the type of loading required. All tests incorporating two opposite loads (Series I to VI) were carried out in the 500KN or 2500KN capacity machines shown in figures 2.15(a) and 2.15(b) respectively. The simply supported beams of Series VII were tested in the 1000KN ram shown in figure 2.15(c).

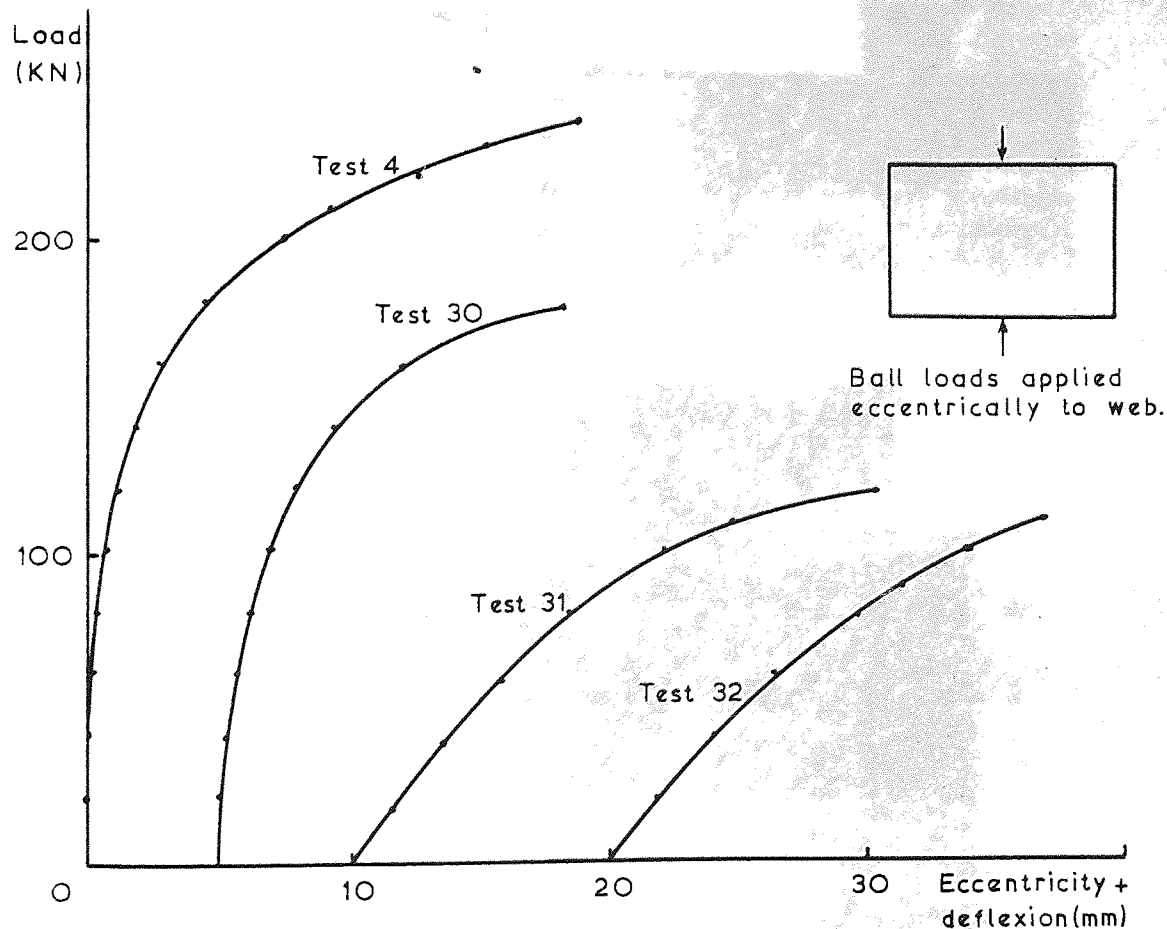
### 2.4.1 Load Applications

Three loading types were used throughout the tests.

1. Concentrated Point Load - This type of loading was achieved by applying the load through a 20mm diameter ball

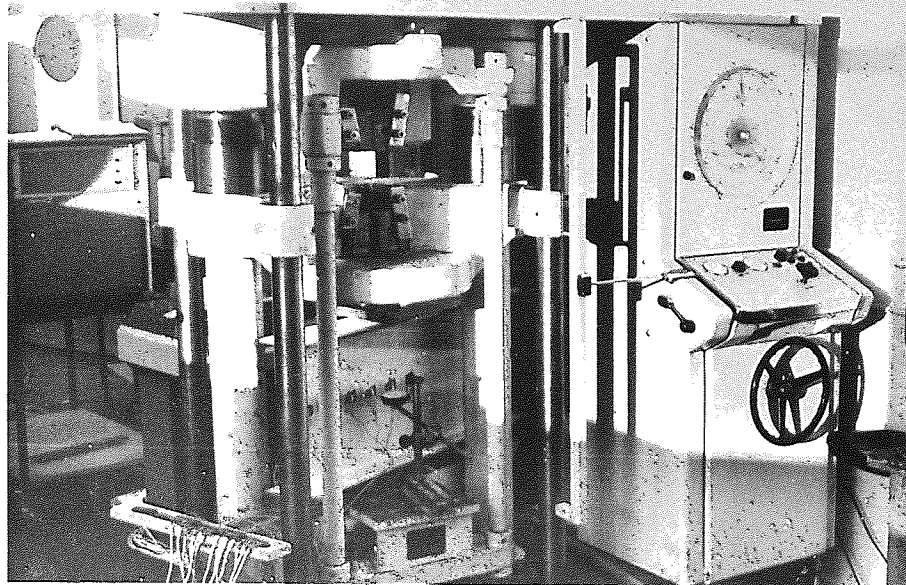


(a)

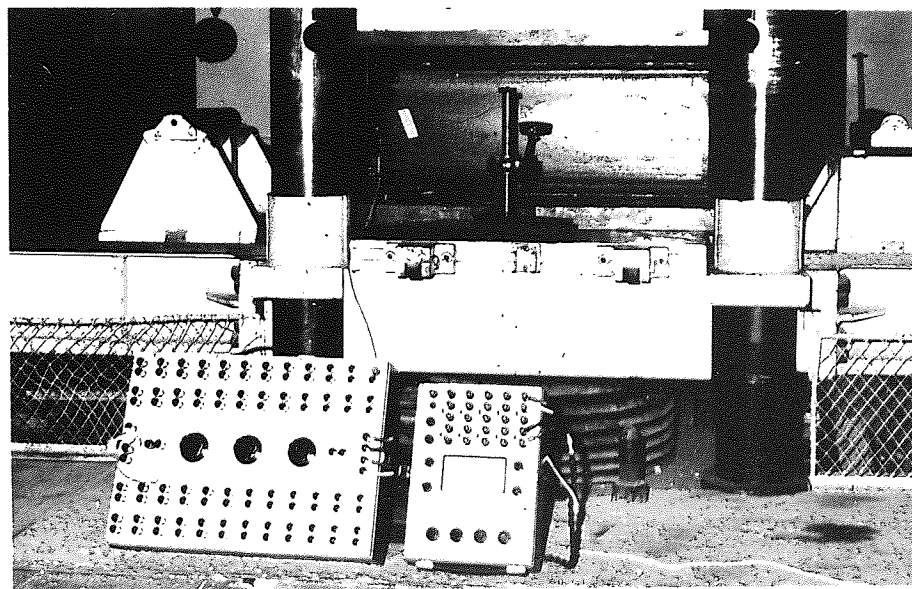


(b)

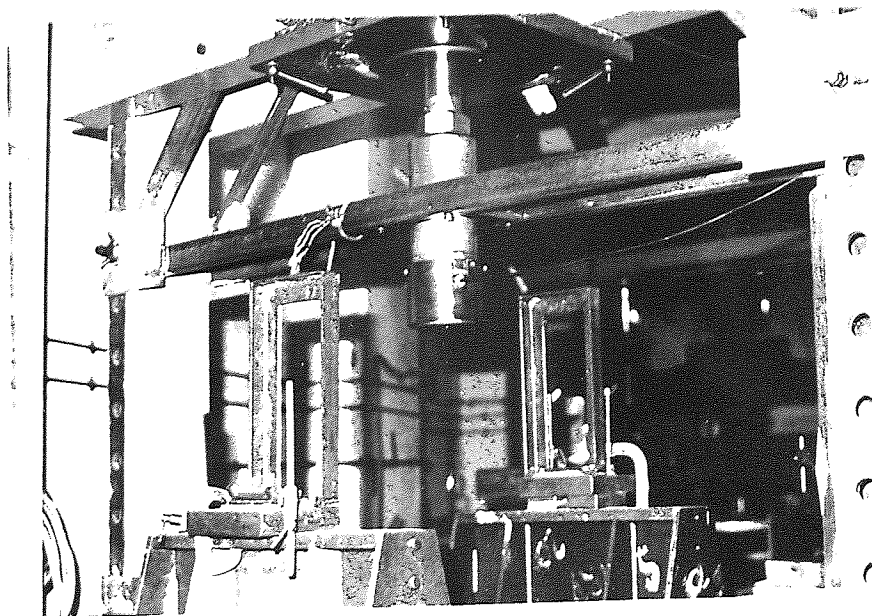
Figure 2.14 Series II load-deflection curves.



(a) Dennison - 500 KN capacity.



(b) Avery - 2500 KN capacity.



(c) Testing Rig - 1000 KN capacity.

bearing. This was placed directly onto the flange in line with the web centre or at a known eccentricity.

It was found that the ball bearing embedded slightly into the test beam for all tests and so when it was considered to be detrimental to the performance of the beam, the test was repeated using small spreader plates. The use of a ball bearing was considered to be the most suitable method of applying a concentrated load without imposing any restraint against rotation on the flanges. This is because even when embedded slightly there would be a spherical surface between the ball bearing and the test beam along which rotation could occur. Experiments using a more concentrated load than a ball bearing were shown to restrict the flange rotation due to considerable penetration by the loads.

2. Knife Edge Load - The knife edges used throughout were manufactured with a radius bearing edge of small diameter. They were made from mild steel and hardened prior to use. They proved very successful and did not distort or flatten in subsequent tests even at very high loads. The area in contact with the flange was very small and is assumed to be zero. The knife edge loads were not attached to the test beam in any way, the only restraint provided being due to friction on the contact area. The flanges could have lifted off the knife edges if such a mode of failure were possible.

3. Uniformly Distributed Load - This was effected by placing 25mm thick plates of the required length in the appropriate position. Again for this type of loading the flanges could lift off the loading plate if such a failure



mode were possible.

#### 2.4.2 Test Procedure

Due to imperfections inherent in universal beam sections because of the hot rolling process, difficulties arise when setting the test beam prior to testing. All rolled steel beams have a degree of 'out of squareness' of the cross section, which means that the flanges are not necessarily at right angles to the web. This degree of out of squareness can also vary along the length of the beam, as can the overall depth  $D_t$ . The test beams can therefore be set for testing in either of two ways. Firstly, the web can be set vertical and secondly the bottom flange can be set horizontally across its width.

To set the web vertical is difficult when loading by means of flat plates on each flange. In this case packing pieces would be required to compensate for the contour of each flange over the area of the loading plates. This would be very difficult, and the degree of accuracy of setting the web vertical could not be guaranteed.

To add to this difficulty, there is also the fact that the web is not perfectly flat and so the effectiveness of setting it vertical is questionable. Setting the web vertical along the whole length of the beam may not always be possible because of the variation in shape along the length.

Hence for tests using two opposite knife edge loads or two opposite concentrated ball loads, the beams were set with the centres of the web, at its junction with the

flanges, in a vertical plane at the point of application of the loads. The knife edge loads were packed as accurately as possible to ensure even contact with the flanges. For tests using two opposite uniformly distributed loads, the test beams were set with the bottom flange horizontal, and resting on the bottom plate. The flange which was most square to the web was set on the bottom plate and the top plate packed to try to ensure even contact with the beam as far as was possible. For simply supported beams, the beams were set with the web vertical at the mid-span. Certain tests using two opposite knife edge loads were repeated with the bottom flange horizontal and consequently the web not vertical. The implications of this and the effect of the different ways of setting the test beams are discussed in Chapters 5 and 7.

All test beams were set with the bottom flange horizontal with respect to the length and the centres of the applied loads plumb.

Loading during all tests was effected in small increments at a constant rate until failure. Failure for this purpose being determined by the failure of the specimen to take any further increase in load and usually accompanied by corresponding rapid increases of deflexions. At failure the load was reduced as quickly as possible to avoid excessive deformations. The load was then either removed, or if the beam was to be retested, reduced to approximately 5% of the failure load. The beams which were retested were usually reloaded three times or until either the deflexions became excessive or the reduction in failure loads for successive retests was small. Repeat loading cycles were

only carried out for a selected number of tests.

At each loading increment strain gauge readings were recorded automatically using a Compulog Data Logger, except when only two strain gauges were attached, in which case a Peekel was used to take readings manually. Dial gauge deflexion readings were recorded manually at each loading increment. It was not usually possible to record strain gauge readings or dial gauge readings at failure due to their high rate of increase. However an approximate dial gauge reading was sometimes possible. During reloading cycles only dial gauge readings were recorded, again where possible.

During each test, observations were made of the performance of the test beam. The appearance of crack lines in the whitewash, when used, was recorded. The same effect could sometimes be observed in beams which were not whitewashed by the behaviour of the scale.

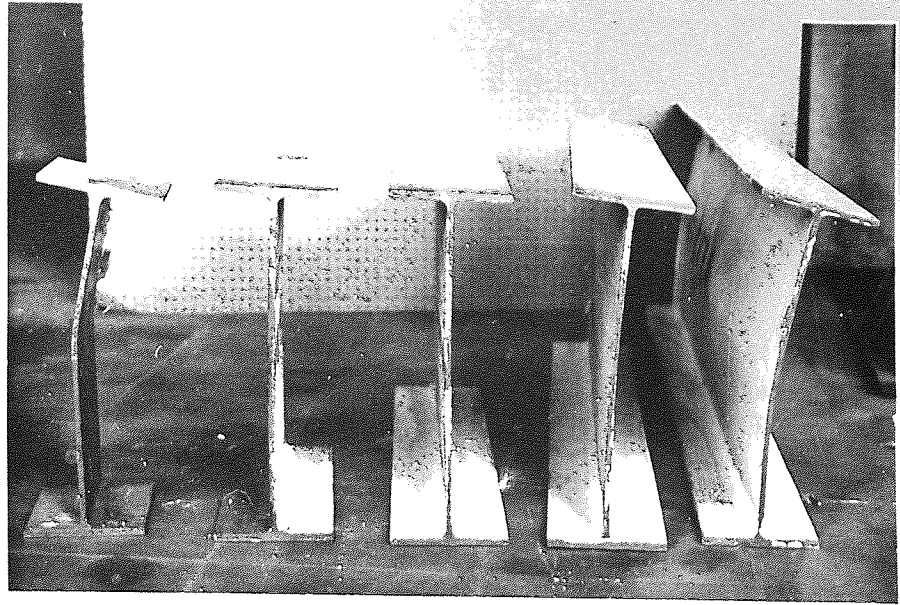
Any distortions which would not be recorded by the measuring devices were noted, such as flange rotation or bending.

#### 2.4.3 Modes of Failure and Test Failure Loads

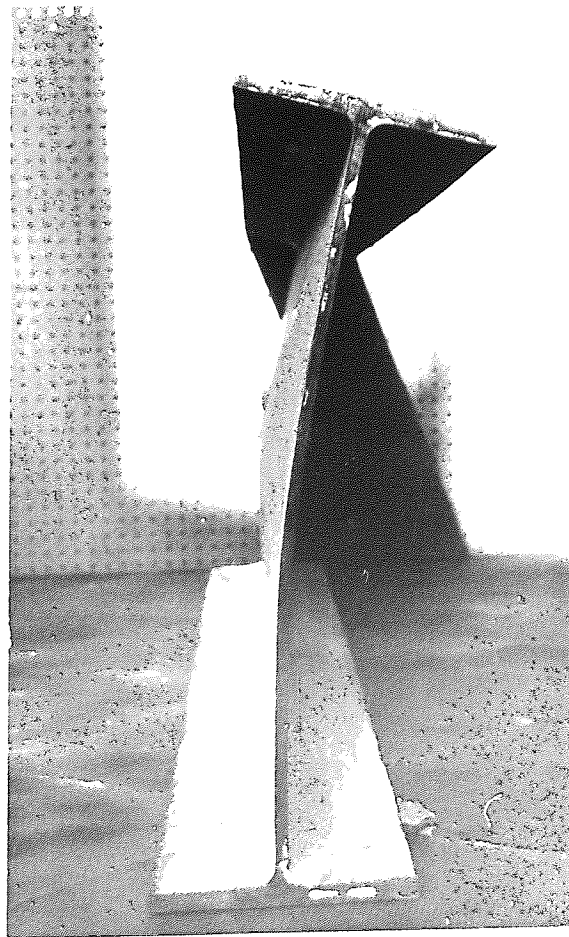
##### 2.4.3.1 Modes of Failure

Several modes of failure were observed during the tests some of which can be verified by an investigation of the strain recordings taken during the tests.

Mode 1 - This failure mode is shown in figure 2.16 and virtually all beams tested in Series I and II failed in this



(a)



(b)

Figure 2.16



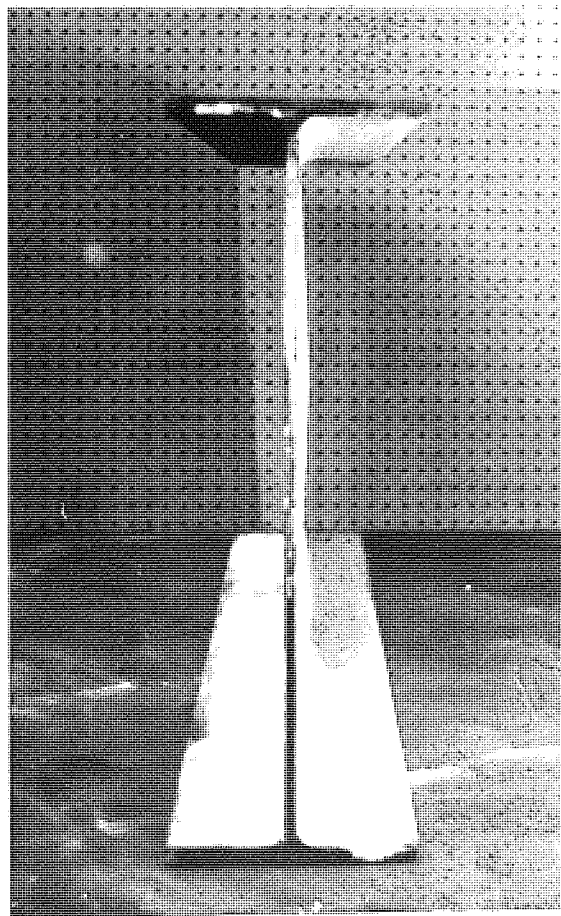
way. At failure the rate of increase of lateral deflexions of the web increased considerably and because of the type of applied loads the flanges were free to rotate. The web lateral deflexions were greatest at the mid-depth and decreased towards each flange. Along the length of the beam the web lateral deflexions were either constant at each particular depth for short beams or were at a maximum at the centre and reduced towards each end for longer beams. The actual deflexions after failure for each beam cannot be compared as they will be dependant upon the speed at which the loading system was removed.

Mode 2 - This failure mode is shown in figure 2.17. The lateral deflexions of the web had the same form as for Mode 1 but the flange deflexions varied. For short lengths of beam the flanges remained straight and the failure was confined only to the web, but for long lengths there was a definite flange distortion at the load point which can be seen in figure 2.17(a), and can be seen to be one sided. In fact the flange is seen to have lifted off one side of the knife edge load. This flange distortion is confined to a small region of the beam in the vicinity of the applied load. Figure 2.17(b) shows that at the ends of the beam the section is virtually unchanged by the test.

Mode 3 - This failure mode is shown in figures 2.18(a) and (b). This failure mode is characterised by the out of plane deflexions of the web being confined to a small area near to a load application point and sometimes accompanied by a distortion in the flanges. This distortion of the flange is also confined to a small region and is across the whole width of the flange rather than the one sided flange

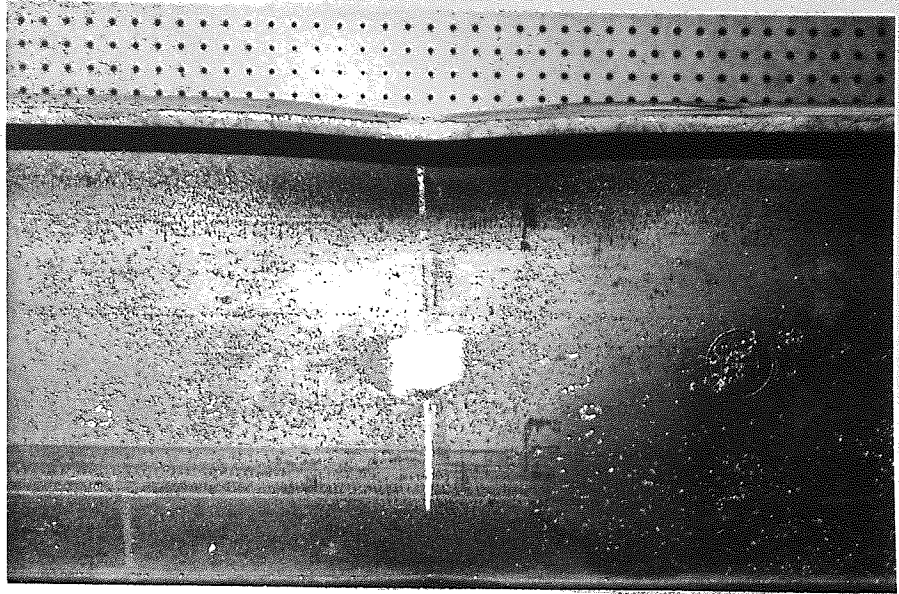


(a)

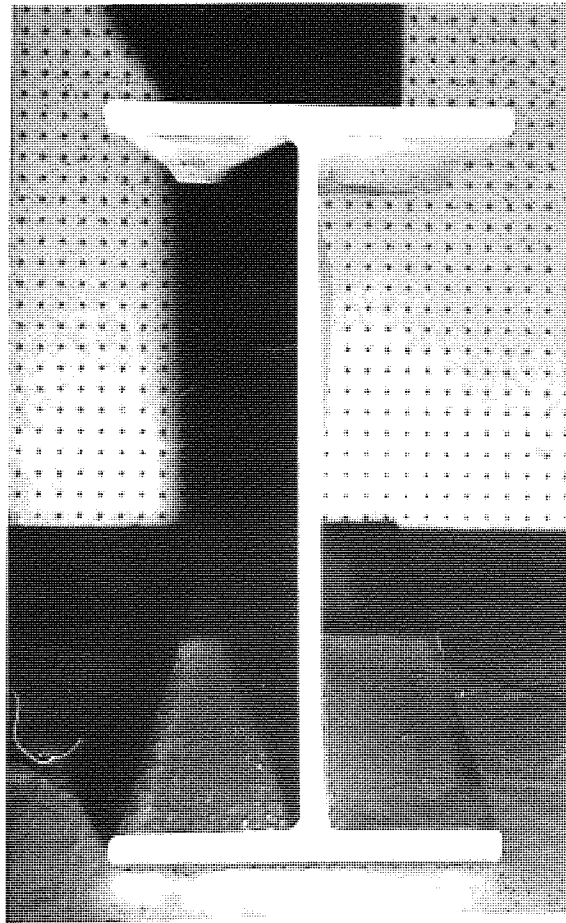


(b)

Figure 2.17



(a)



(b)

Figure 2.18

failure of Mode 2. This failure mode is consistent with that indicated by the strain gauge recordings shown previously.

#### 2.4.3.2 Test Failure Loads

The test failure loads for all 100 tests are shown in Table 2.5. The value of the failure loads for beams which were retested are also shown, together with the mode of failure as outlined in Section 2.4.3.1.

Examination of the loads attained for beams which were retested can provide more information on the type of failure. Short beams loaded by concentrated loads and long beams loaded by long uniformly distributed loads behave similarly. Both lead to a very sudden failure with strain and deflexion measuring devices unreadable at the instant of failure, followed by a very distorted section which upon retesting only attains approximately half of the initial failure load. Long beams loaded by concentrated loads lead to a relatively slow failure with the measuring devices readable at the onset of failure, with the retest failure loads reducing by only a small amount each time.

The former failure type could be indicative of an elastic failure, with the subsequent retest failure loads reducing to a load at which the section has become plastic. The latter type could be the load at which the section has become plastic, being a much lower load than the elastic buckling load. Figure 2.19 shows the loading cycles for failures which illustrate these points, and also a test failure which falls somewhere between these two extremes.



Test No.	Failure Load	Retest 1 Load	Retest 2 Load	Retest 3 Load	Failure Mode
1	62.6				1
2	108.8				1
3	179.4				1
4	239.2				1
5	279.0				1
6	98.2				1
7	127.1				1
8	236.9				1
9	308.4				1
10	298.4				1
11	48.0	40.3	32.7		1
12	117.2	--	43.4		1
13	178.4	86.2			1
14	159.9				1
15	280.0				1
16	54.7	46.1			1
17	127.7	101.6	39.1		1
18	236.2	122.1	72.7		1
19	216.9	166.7			1
20	107.3				1
21	159.4				1
22	255.1				1
23	292.8				1
24	109.3				1
25	173.6				1
26	249.5				1
27	272.2				1
28	218.6				1
29	264.6				1
30	187.3				1
31	123.0				1
32	115.6				1
33	219.2				2
34	323.8				2
35	355.2				2
36	360.2				2
37	210.1				2
38	279.0				2
39	327.3				2
40	344.8				2
41	123.8	29.3			2
42	175.6	122.8			2
43	211.0	177.4	155.0		2
44*	215.6	212.3	203.4	187.1	2
45	215.7				2
46	320.2	87.2			2
47	371.0	324.9	314.9	284.0	3
48*	359.5	348.0	338.9		2
49	150.0	63.0			2
50	224.7	99.6			2

All loads in KN.

\* Indicates central deflexion gauge reading recorded for each retest.

Table 2.5

Test No.	Failure Load	Retest Load 1	Retest Load 2	Retest Load 3	Failure Mode
51	260.1	227.2	210.8		2
52*	276.2	257.2	248.2	238.4	2
53	159.1				2
54	236.5				2
55	277.7				3
56	306.9				3
57	341.1				3
58	382.7				2
59	398.6				2
60	287.4				2
61	268.7	228.9	220.7		2
62*	241.6	237.4	231.5	227.6	2
63	219.2	205.0	172.0	159.0	2
64	193.8	160.5	136.0	130.0	2
65	156.6	128.8	122.6		2
66	921.8	822.5	810.0	792.5	2
67	277.8				2
68	271.6				2
69	219.2				2
70	155.6				2
71	450.8				2
72	416.0				2
73	515.7				2
74	784.7				2
75*	470.8	436.0	413.5	406.1	2
76	613.8	586.9	504.7	480.8	2
77	911.8	525.7	453.4	406.1	2
78*	452.8	433.5	407.2	393.3	2
79	601.9	578.0	540.6	513.2	2
80	797.2	705.0	607.9	587.9	2
81	1220.7	830.0	605.0	480.0	2
82	1484.8	521.2	448.4	418.5	2
83*	348.5	312.9	301.4	289.0	2
84	397.7	386.1	358.7	348.8	2
85	563.0	513.2	465.4	445.9	2
86	827.1	607.9	387.6	338.8	2
87	997.2	488.3	411.6	384.6	2
88	544.1	520.0	497.5	475.0	2
89	614.8	567.5	532.5	512.5	2
90	774.3	740.0	730.0	715.0	2
91	732.4	715.0	703.0	655.0	2
92	383.6	372.0	365.0	375.0	2
93	402.6	390.0	362.5	357.5	2
94	543.1	505.0	475.0	420.0	2
95	552.1	507.5	478.0	441.0	2
96*	317.0	311.0	303.2	298.6	3
97*	311.3	293.2	286.0	277.6	3
98†	385.0				3
99	305.0	260.0			3
100	275.0				3

All loads in KN.

† Indicates load spread over 100mm.

\* Indicates central deflexion gauge reading recorded for each retest.

Table 2.5 (cont.)

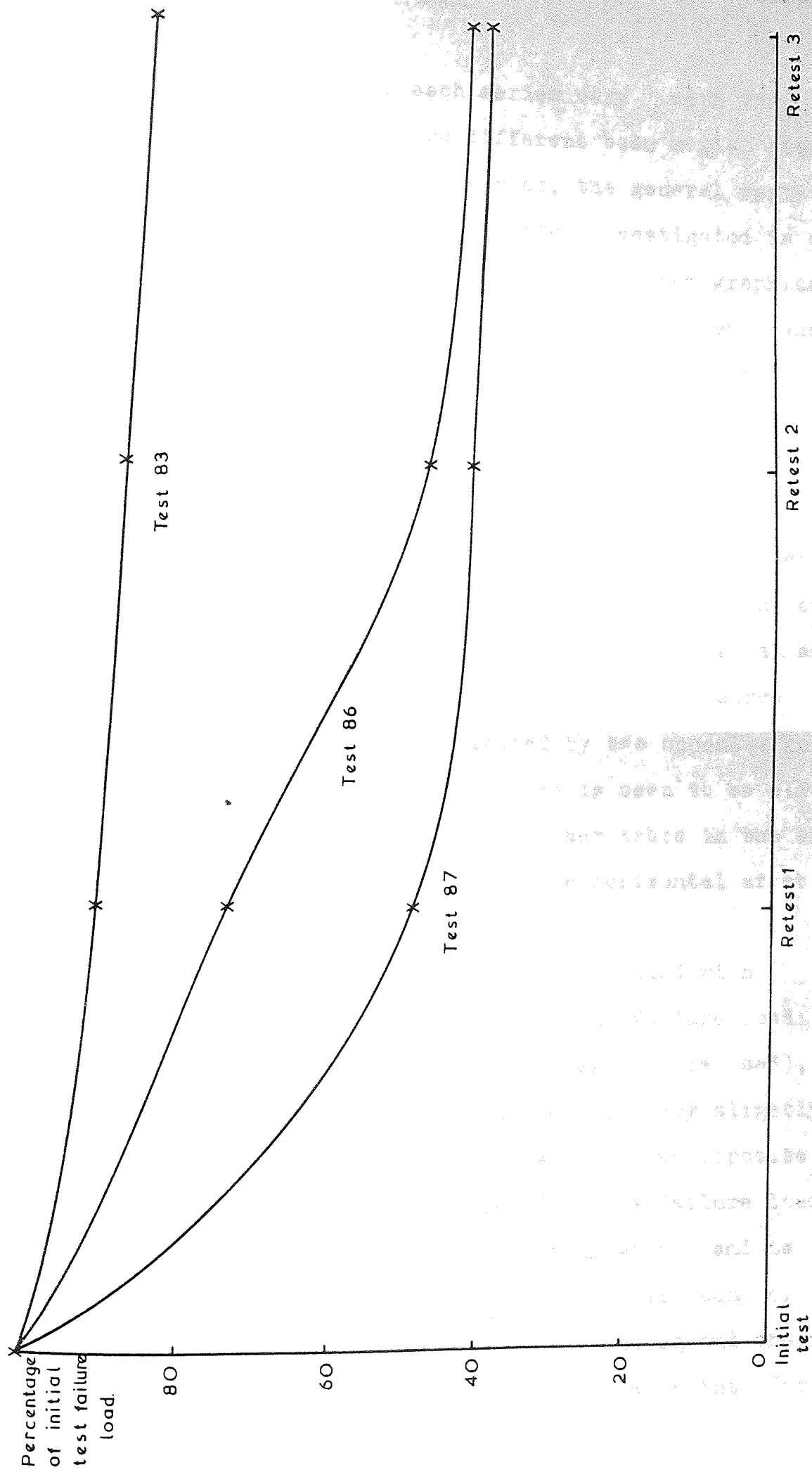


Figure 2.19 Typical patterns of retest failure loads for selective tests.

The failure loads for each series vary with the variables investigated. Where different beam serial sizes have been used in a particular series, the general variation of the ultimate load with the variables investigated is of the same form. Figures 2.20, 2.21 and 2.22 show graphically the effect of each of the variables for each series. Where convenient two or more series are shown on one graph.

Series I (beams tested by two opposite ball loads) shows that for each increase of the length of the beam there is a corresponding increase in the failure load. For some beam serial sizes the curve is horizontal at an  $L/d$  (length to effective depth) ratio of between 3.0 and 4.0. The curve shown in figure 2.20(a), however, is not horizontal at an  $L/d$  ratio of 4.0 but the slope is reducing. The curve illustrating Series III (beams tested by two opposite knife edges) test results in the same figure is seen to be almost horizontal at an  $L/d$  ratio of 2.0. Other tests in the same series show the same curve always to be horizontal at at least an  $L/d$  ratio of 2.5.

Figure 2.20(b) shows that for beams loaded with increasing eccentricities (Series II), the failure load reduces almost linearly (for the beam serial size used), up to a certain eccentricity, and then reduces very slightly for further increases. For beams loaded by two opposite knife edges near to the end (Series IV), the failure load reduces, and the load sustained by a beam at its end is approximately half that it would sustain at its centre.

Figure 2.22 shows the influence of bending and shear on the failure load of a beam (Series VII). Two points for zero span have been plotted because their dimensional



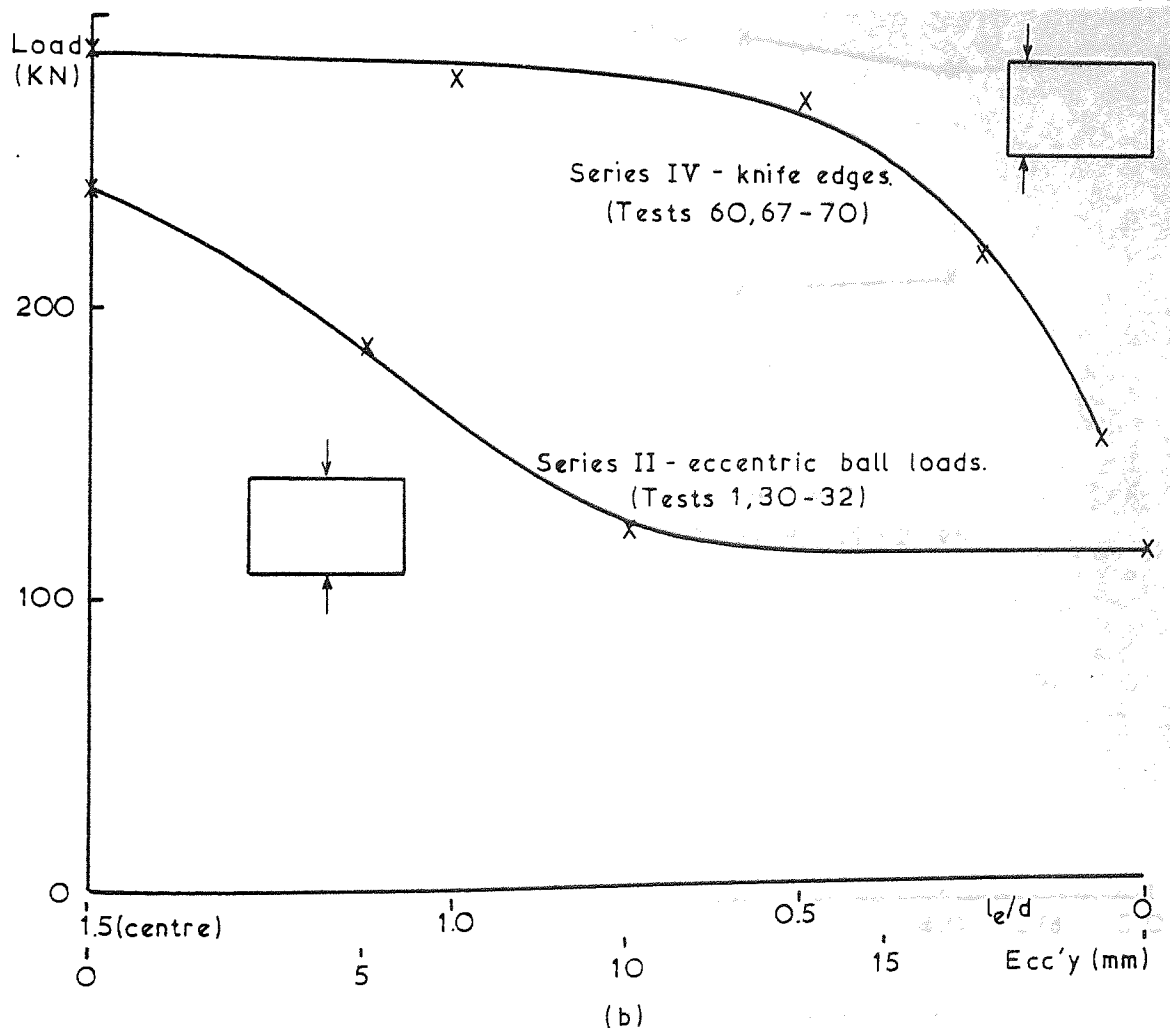
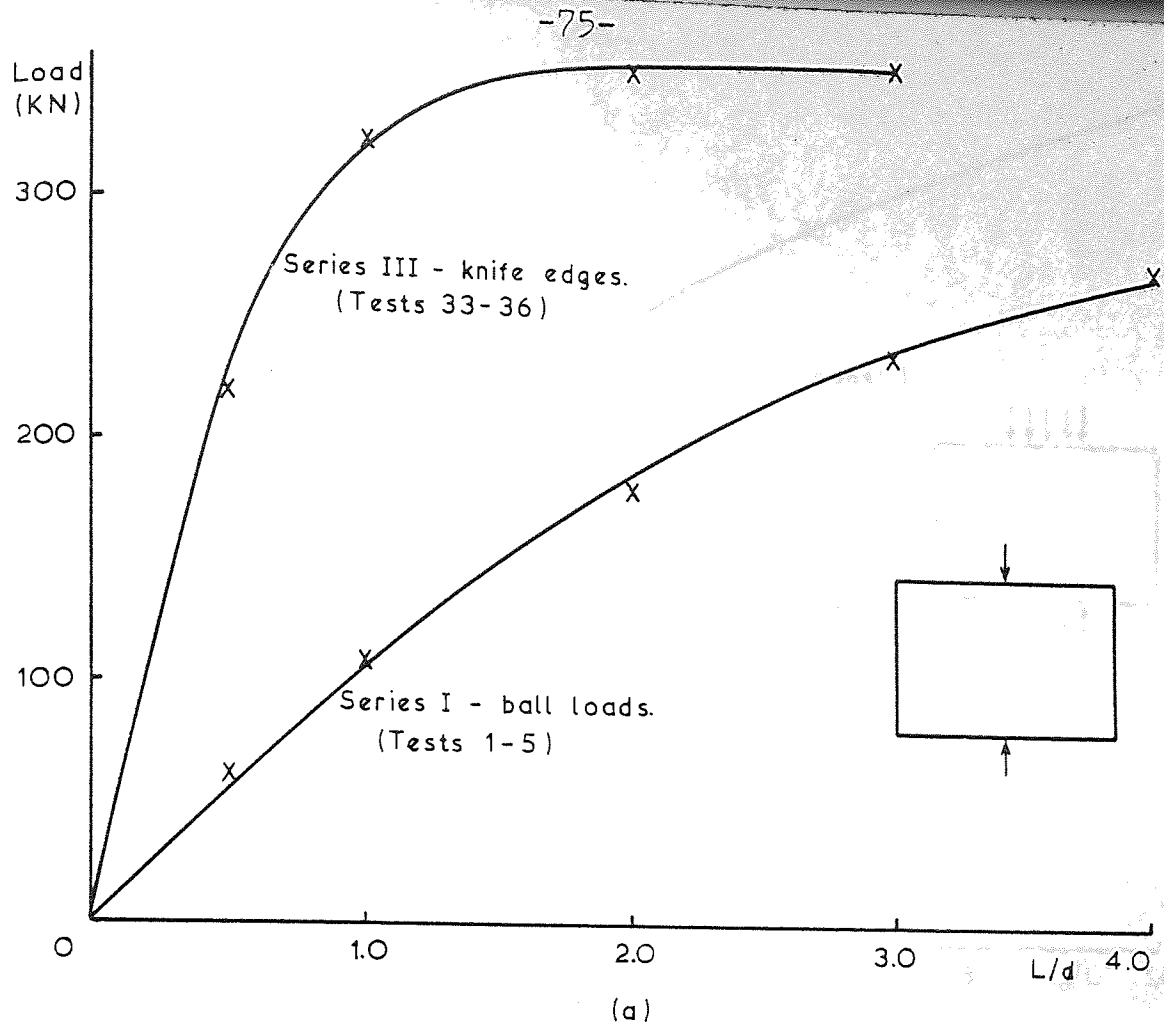


Figure 2.20 Typical variation of test failure loads with the variables investigated - Series I to IV.

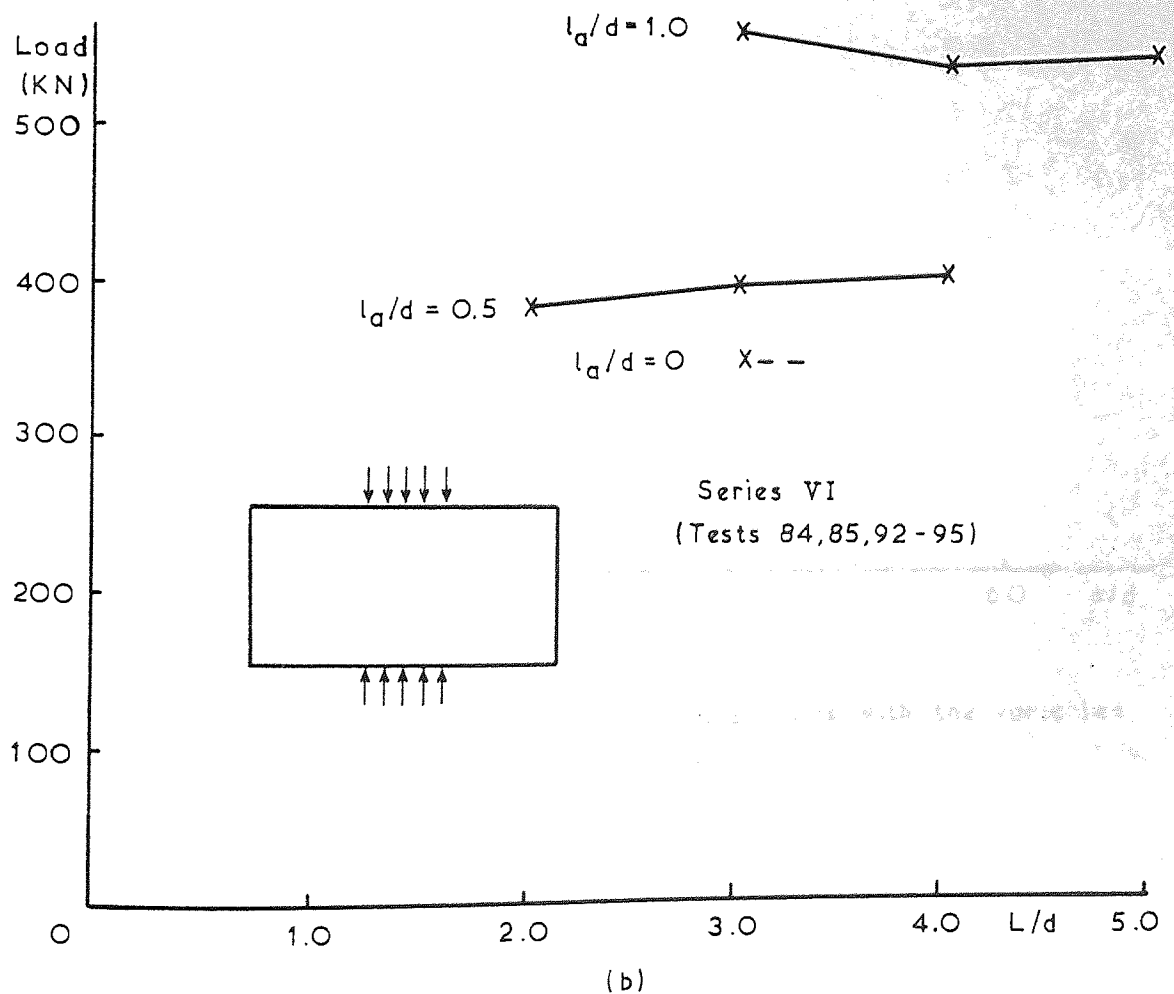
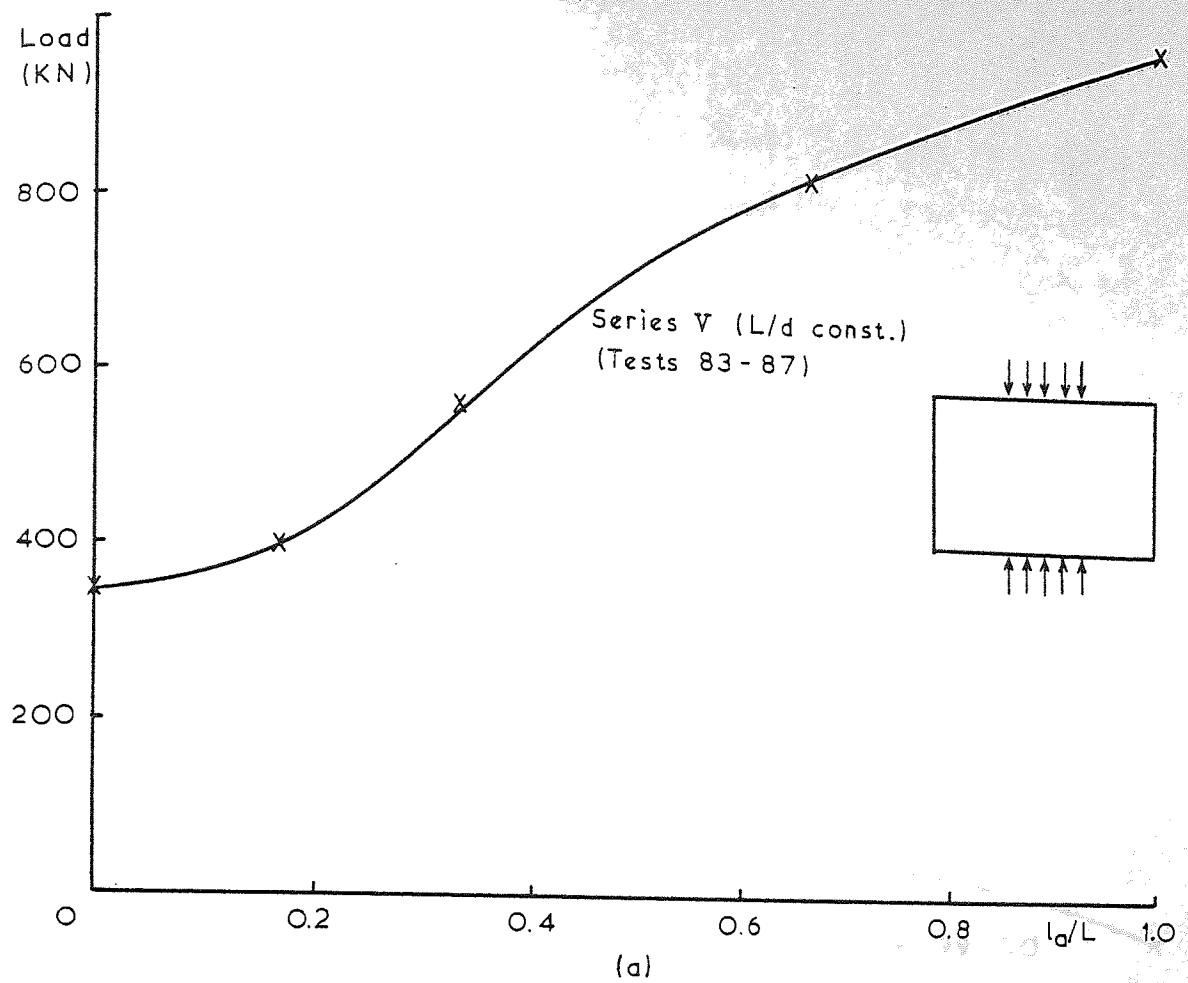


Figure 2.21 Typical variation of test failure loads with the variables investigated - Series V and VI.

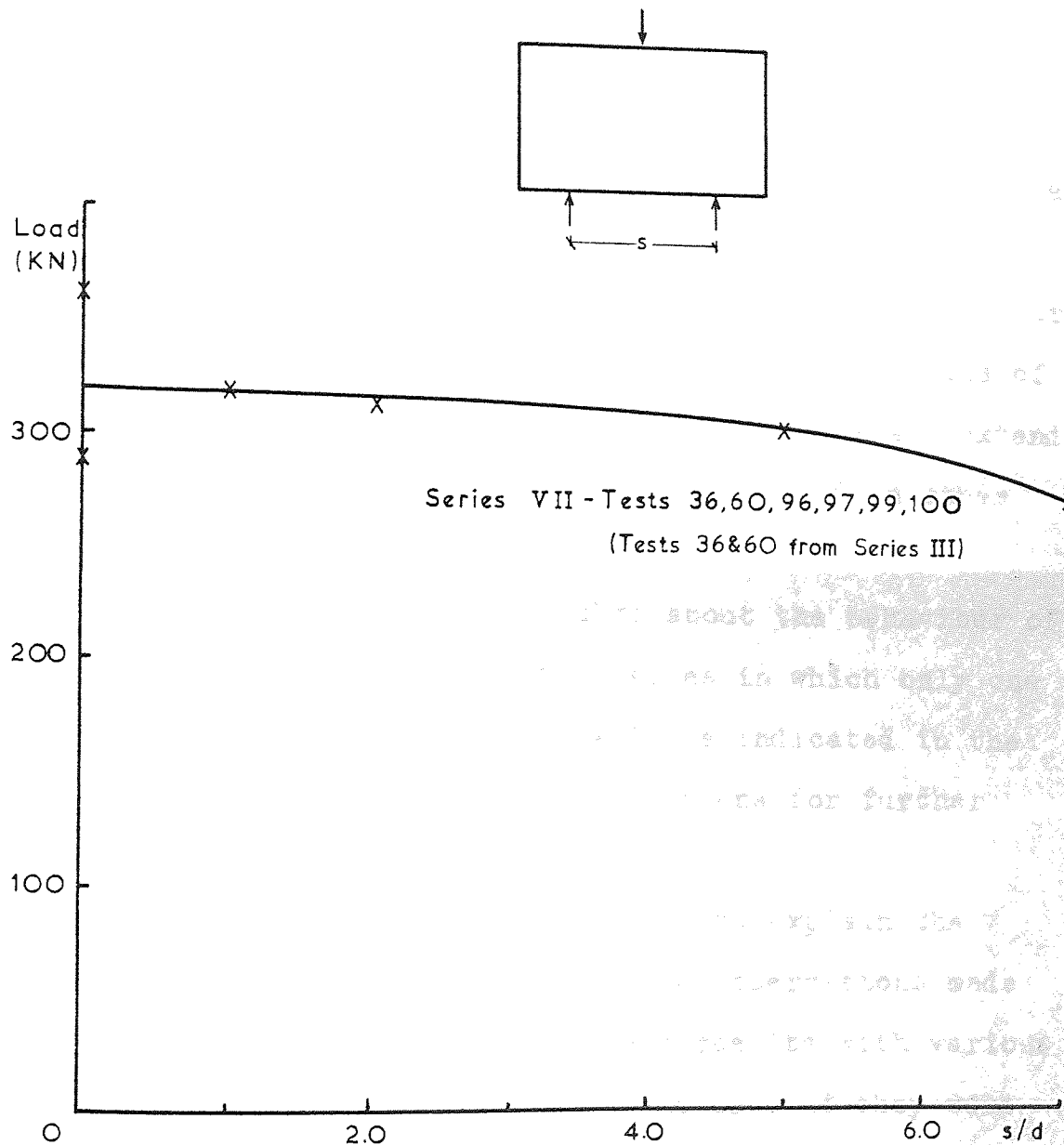


Figure 2.22 Typical variation of test failure loads with the variables investigated - Series VII.

properties differ even though they have the same serial size. This shows that for Mode 3 failure patterns, the effects of bending and shear do not appear to have much influence on the failure load for the spans investigated here.

## 2.5 Conclusions From the Test Results

For the simplest types of loading, the test results are presented for several beam sizes and many show similar behaviour patterns. It should therefore be possible to draw conclusions with reasonable certainty from the results of the tests covering a range of beam serial sizes and extend these to predict the behaviour of beams tested in other ways.

Obviously there will be doubts about the behaviour of other beam section sizes for the series in which only one serial size was tested and this will be indicated in the final chapter when considering suggestions for further research.

Several hypotheses were presented to explain the behaviour of some of the beams and the observations made during the tests. Comparing the test results with various analytical approaches later should indicate if they were correct.

## CHAPTER 3 - DESIGN GUIDES AND OTHER AUTHORS' THEORIES

### 3.1 Introduction

Most current design standards have clauses limiting the applied stresses in the web of a steel beam when subjected to concentrated loads. The effects of both 'web bearing', the local crushing of the web in the vicinity of the loaded portion of the flange and 'web buckling', the induced stresses due to axial force and out of plane deflexions of the web are usually considered.

Several of the current design standards are based on the semi-empirical load dispersion technique, but all have variations, such as the angle of dispersion, the allowable stresses and the depth to which dispersion may be taken. The most widely used design standard in this country is British Standard 449 (BS 449), 'The Use of Structural Steel in Building'.

Some empirical and semi-empirical theories for determining the load carrying capacity of steel beams subjected to concentrated loads have been developed to satisfy the results from tests and are therefore untried for beams with considerably different characteristics.

This chapter therefore examines the suitability of current design standards and the load dispersion technique, and in particular BS 449 in the light of the results from the tests conducted for this work. It also examines in some detail the theories presented by other authors.

### 3.2 Current Design Practice

As stated in the previous section, most design standards base the relevant sections dealing with web bearing and web buckling on the load dispersion technique. However there is a considerable variation between codes on the way in which the load disperses through the flanges of the beam. One Dutch report by Voorn (38) has suggested that when considering web bearing, the angle of dispersion through the flange should vary with the length of the stiff bearing applied to the flange, whereas most design guides have a constant angle of dispersion.

As BS 449 is based on the load dispersion technique, and is most commonly used in this country, this code will be examined in detail. In this way the suitability of the standard can be assessed, and also any shortcomings of the load dispersion method. Further, the suitability or effectiveness of suggestions such as those made by Voorn can also be examined.

At the time of writing BS 449, the 1969 edition in metric units is in use, together with 'Amendment Slip Number 5, published 31st. July 1975' (4a). The amendment was introduced to give closer control over the webs of beams at points of concentrated loads when considering web buckling.

#### 3.2.1 Design to BS449

BS 449 contains clauses which limit the stresses at certain points in the web of a beam due to buckling and

bearing when the beam is subjected to concentrated loads applied to the flanges or at points of support.

The ultimate load due to web buckling is determined from:

$$P = t \, f_b \, h_b \quad 3.1$$

where  $f_b$  is the average stress as determined from the Perry formula:

$$f_b = \frac{f_y + (n+1)C_o}{2} - \sqrt{\left(\frac{f_y + (n+1)C_o}{2}\right)^2 - f_y C_o} \quad 3.2$$

and:  $n = 0.3 (r_s/100)^2$

$$C_o = \pi^2 E / r_s^2$$

$$r_s = \text{slenderness ratio}$$

Values are shown in Table 17 in BS 449 for some standard grade steels.

An appropriate factor of safety is usually incorporated in  $f_b$  to arrive at a permissible working load but has been omitted here as the comparison with the test results will involve ultimate loads.

The dimension  $h_b$  is an effective strut width and is defined as 'the length of the stiff portion of bearing plus the additional length given by dispersion at  $45^\circ$  to the level of the neutral axis, plus the thickness of flange plates at the bearing and the thickness of the seating angle (if any)'.

The slenderness ratio  $r_s$  is defined as  $d\sqrt{3}/t$ , which assumes a fully end restrained strut of length  $d$ , but if the loaded flange is not restrained against lateral movement or is allowed to rotate then the slenderness ratio  $r_s$  should be increased accordingly.

If the load is applied out of the line of the mid-plane



of the web then the effect of the induced bending stresses should be taken into account.

The ultimate load due to web bearing or crushing is:

$$P = t f_y h_c \quad 3.3$$

where  $f_y$  is the yield stress of the beam.

The dimension  $h_c$  is an effective bearing length and is the length of stiff bearing plus the additional length given by dispersion at  $30^\circ$  to the plane of the flanges to the level of the junction of the web and root radius. The effects of flange plates may also be included.

The minimum yield stress for a grade 43 steel is taken as  $250 \text{ N/mm}^2$ .

### 3.2.2 Comparison with the Test Results

The yield stress of  $250 \text{ N/mm}^2$  is the guaranteed minimum yield stress as quoted by the manufacturer. BS 4360 (39) for control tensile testing gives the manufacturer the option of taking the control specimen from the flange or web of a universal beam. Thus, although the tensile strength of the beams used in the tests reported here was always greater than  $250 \text{ N/mm}^2$ , it does not imply that there is always a further material safety factor incorporated by assuming the yield strength to be  $250 \text{ N/mm}^2$  at the design stage. The observations from Chapter 2 have indicated that if a beam has a satisfactory control specimen when taken from the web or flange, the yield strength at another location in the section could be below the guaranteed minimum.

For the purposes of the comparison, the yield stress obtained from the tensile test specimens at the relevant



location in the beam cross section will be used when calculating the ultimate loads in accordance with BS 449.

The theoretical BS 449 ultimate loads due to buckling and bearing are shown for all 100 test cases in Table 3.1, together with the actual failure loads. Also shown is the ratio of the minimum theoretical load to the actual failure load as a percentage. The ratio is less than 100% for 88 of the 100 tests, and so for those the BS 449 method is conservative by varying amounts. Consequently for 12 of the 100 tests the ratio is greater than 100%, which means that the BS 449 method gives a less than satisfactory factor of safety at working load in these cases.

The general observations from Table 3.1 show that for very short lengths of concentrated load the method is very conservative, for long lengths of applied load the method is unsatisfactory and for intermediate lengths of applied load the method effects a suitable factor of safety against failure.

A typical comparison of theoretical failure loads determined in this way and actual failure loads for beams in Series I (in which the method of testing permitted flange rotations) is shown in figure 3.1(a), and for beams in Series II (which incorporated eccentrically applied loads) in figure 3.1(b). Both show that for long beams loaded by short lengths the method is very conservative. However in both cases the basic form of the theoretical buckling failure loads is very similar to the form of the test failure loads.

The short beams in figure 3.1(a) with  $L/d$  ratios of 0.5 and 1.0 show the test failure loads to be closer to the

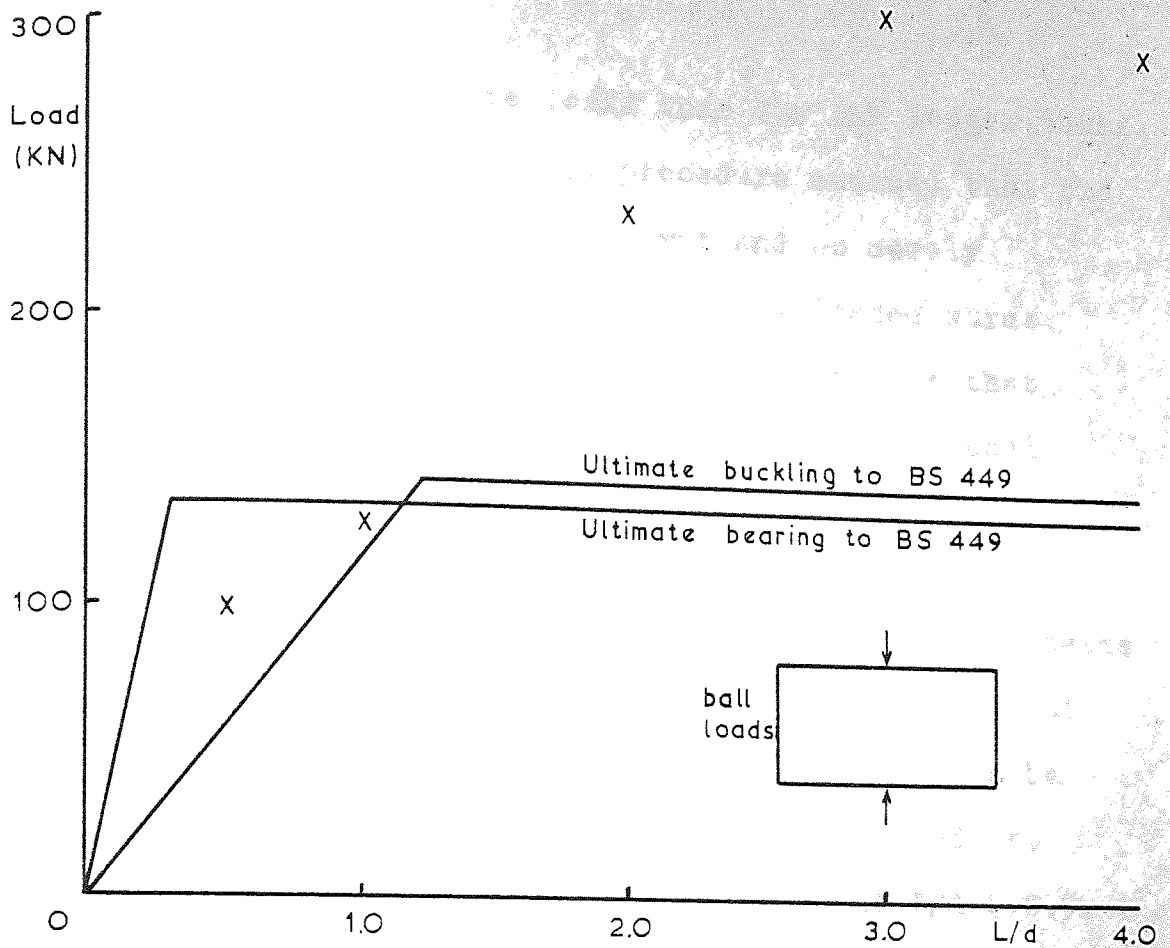
Test No.	BS 449 Ultimate Load(KN) Buckling	BS 449 Ultimate Load(KN) Bearing	Lowest Mode Buck./ Bear.	Test Ult. Load (KN)	$\frac{P(BS 449)}{P_{exp}}\%$
1	43.7	141.5	B	62.6	69.8
2	87.3	141.5	B	108.8	80.2
3	98.1	141.5	B	179.4	54.7
4	98.1	141.5	B	239.2	41.0
5	98.1	141.5	B	279.0	35.2
6	59.7	134.9	B	98.2	60.8
7	119.5	134.9	B	127.1	94.0
8	143.4	134.9	C	236.9	56.9
9	143.4	134.9	C	308.4	43.7
10	143.4	134.9	C	298.4	45.2
11	47.8	97.5	B	48.0	99.6
12	95.5	97.5	B	117.2	81.5
13	105.9	97.5	C	178.4	54.7
14	105.9	97.5	C	159.9	61.0
15	105.9	97.5	C	280.0	34.8
16	52.4	129.6	B	54.7	95.8
17	104.8	129.6	B	127.7	82.1
18	122.4	129.6	B	236.2	51.8
19	122.4	129.6	B	216.9	56.4
20	60.7	110.3	B	107.3	56.6
21	121.5	110.3	C	159.4	69.2
22	140.0	110.3	C	255.1	43.2
23	140.0	110.3	C	292.8	37.7
24	64.8	116.4	B	109.3	59.3
25	129.6	116.4	C	173.6	67.1
26	159.8	116.4	C	249.5	46.7
27	159.8	116.4	C	272.2	42.8
28	178.0	146.6	C	218.6	67.1
29	211.7	146.6	C	264.6	55.4
30	17.2	130.9	B	187.3	9.2*
31	9.5	130.9	B	123.0	7.7*
32	5.0	130.9	B	115.6	4.3*
33	199.5	141.6	C	219.2	64.6
34	399.0	141.6	C	323.8	43.7
35	448.3	141.6	C	355.2	39.9
36	448.3	141.6	C	360.0	39.3
37	210.8	134.4	C	210.1	64.0
38	421.6	134.4	C	279.0	48.2
39	505.9	134.4	C	327.3	41.1
40	505.9	134.4	C	344.8	39.0
41	188.9	97.5	C	123.8	78.8
42	377.8	97.5	C	175.6	55.5
43	418.9	97.5	C	211.0	46.2
44	418.9	97.5	C	215.6	45.2
45	208.2	129.4	C	215.7	60.0
46	416.5	129.4	C	320.2	40.4
47	486.3	129.4	C	371.0	34.9
48	486.3	129.4	C	359.5	36.0
49	198.7	110.3	C	150.0	73.5
50	397.3	110.3	C	224.7	49.1

\*Bending stress incorporated using BS 449 interaction formula

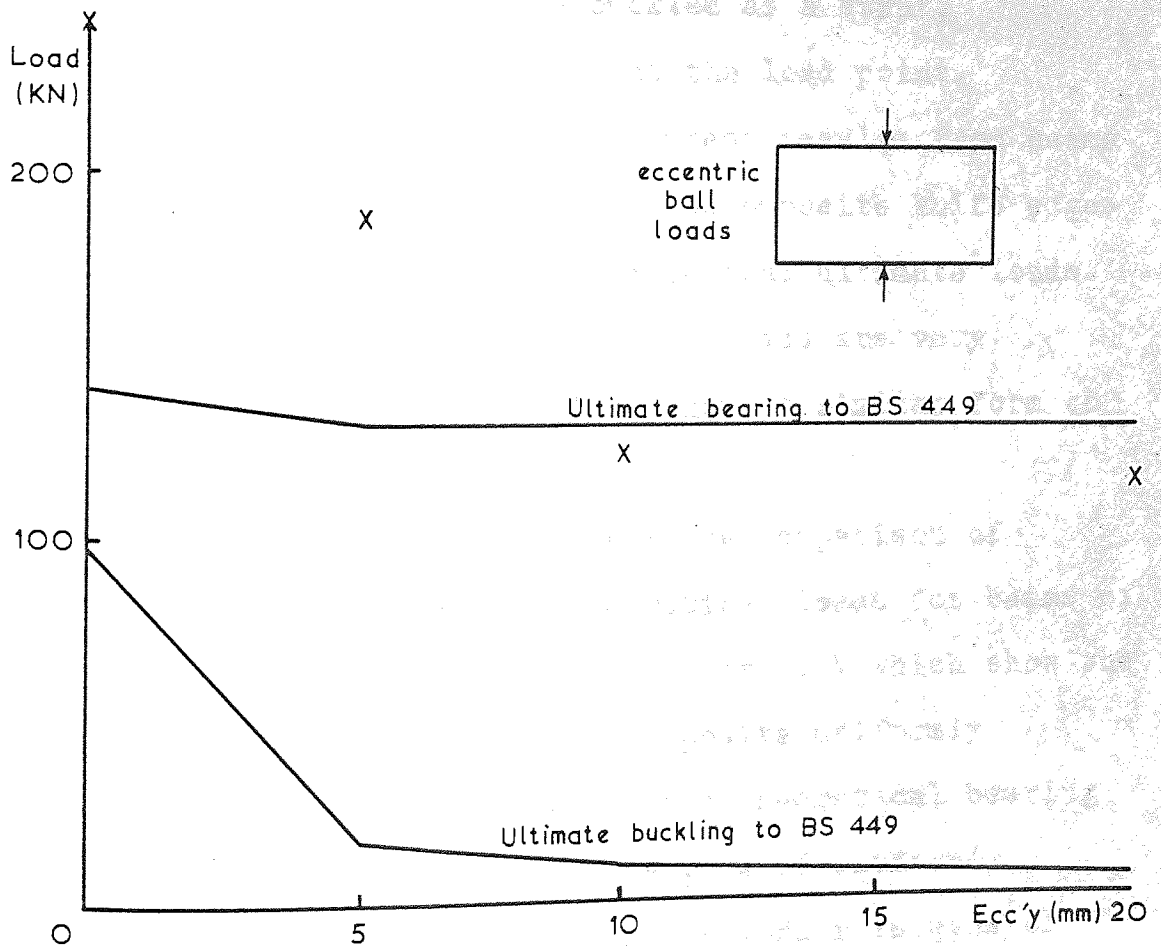
Table 3.1

Test No.	BS 449 Ultimate Load(KN) Buckling	BS 449 Ultimate Load(KN) Bearing	Lowest Mode Buck./ Bear.	Test Ult. Load (KN)	$\frac{P(\text{BS 449})}{P_{\text{exp}}}\%$
51	458.0	110.3	C	260.1	42.4
52	458.0	110.3	C	276.2	39.9
53	171.8	117.5	C	159.1	73.8
54	343.7	117.5	C	236.5	49.7
55	423.5	117.5	C	277.7	42.3
56	423.5	117.5	C	306.9	38.3
57	437.8	147.5	C	341.1	43.2
58	521.3	147.5	C	382.7	38.5
59	521.3	147.5	C	398.6	37.0
60	406.7	129.2	C	287.4	45.0
61	418.1	130.0	C	268.7	48.4
62	454.1	119.8	C	241.6	49.6
63	411.5	104.4	C	219.2	47.6
64	408.0	92.9	C	193.8	47.9
65	167.7	83.9	C	156.6	53.6
66	1266.6	326.1	C	921.8	35.4
67	411.4	129.1	C	277.8	46.5
68	389.3	129.1	C	271.6	47.5
69	274.7	129.1	C	219.2	58.9
70	224.9	127.2	C	155.6	81.7
71	548.1	329.6	C	450.8	73.1
72	658.3	498.3	C	416.0	119.8
73	737.9	817.9	B	515.7	143.1
74	1060.8	1532.0	B	784.7	135.2
75	718.0	364.6	C	470.8	77.4
76	930.1	594.7	C	613.8	96.9
77	1272.6	1055.0	C	911.8	115.7
78	563.6	161.6	C	452.8	35.7
79	796.7	409.8	C	601.9	68.1
80	1029.7	658.0	C	797.2	82.5
81	1398.4	1154.5	C	1220.7	94.6
82	1398.4	1489.3	B	1484.8	94.2
83	485.8	146.2	C	348.5	42.0
84	694.9	435.7	C	397.6	109.6
85	904.1	725.1	C	563.0	128.8
86	1254.8	1304.0	B	827.1	151.7
87	1254.8	1736.8	B	997.2	125.8
88	796.7	409.8	C	544.1	75.3
89	796.7	409.8	C	614.8	66.7
90	1029.7	658.0	C	774.3	85.0
91	1029.7	658.0	C	732.4	89.8
92	694.9	435.7	C	383.6	113.6
93	694.9	435.7	C	402.6	108.2
94	904.1	725.1	C	543.1	133.5
95	904.1	725.1	C	552.1	131.3
96	433.8	146.7	C	317.0	46.3
97	433.8	146.7	C	311.3	47.1
98	563.4	359.1	C	385.0	93.3
99	433.8	146.7	C	305.0	48.1
100	433.8	146.7	C	275.0	53.3

Table 3.1 (cont.)



(a) Series I - Tests 6-10.



(b) Series II - Tests 4,30-32.

Figure 3.1 Typical comparison of test failure loads and BS 449 ultimate loads - Series I and II.

theoretical buckling failure loads than for the longer beams. At these lengths the BS 449 design procedure assumed that the whole of the beam would act as a strut and so merely indicated the failure load for a uniformly loaded strut using the Perry formula. It is therefore possible that these two tests did buckle and were unaffected by local crushing at the load point.

Figure 3.2(a) shows the typical comparison of the actual failure loads and theoretical failure loads for beams tested in Series III, by two opposite knife edge loads at mid-length. The theoretical bearing load is shown to be very conservative and the theoretical buckling loads to overestimate for long beam lengths. However at  $L/d = 0.5$ , the Perry formula predicts the failure load almost exactly and again this beam could have buckled as a strut, unaffected by the local yielding at the load point.

Figure 3.2(b) compares typical test results from beams in Series IV, which were loaded by two opposite knife edges near to the beam end, with the theoretical ultimate loads. Again the theoretical bearing failure loads are very conservative and the buckling loads have a similar form to the actual failure loads.

Figures 3.3(a) and 3.3(b) show the comparison of typical test results with the theoretical loads for beams of two different serial sizes tested in Series V which show the effects of varying lengths of two opposite uniformly distributed loads. These show how the theoretical bearing loads are conservative for short lengths of uniformly distributed loads and overestimate for longer lengths of load. The theoretical buckling loads are always

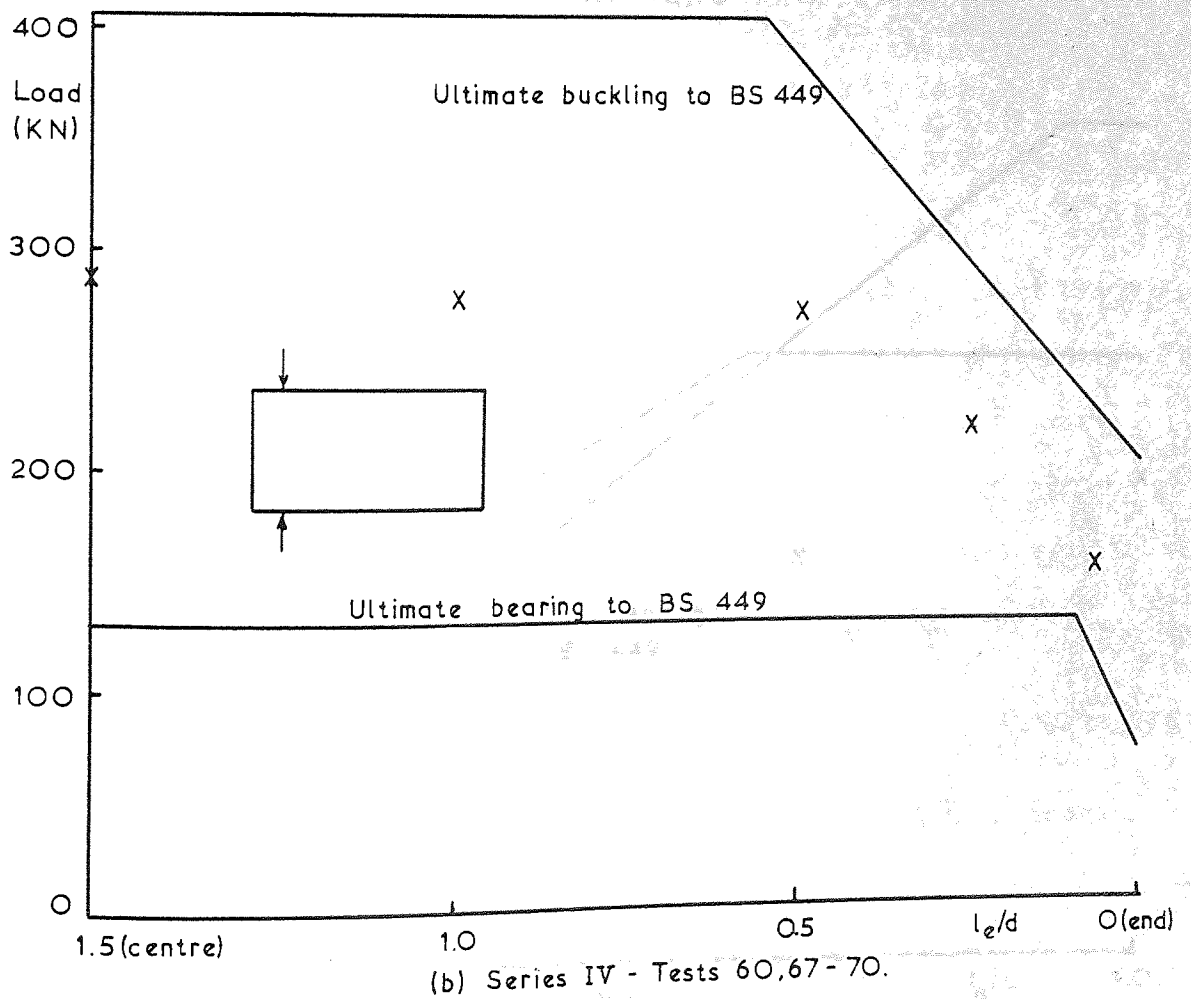
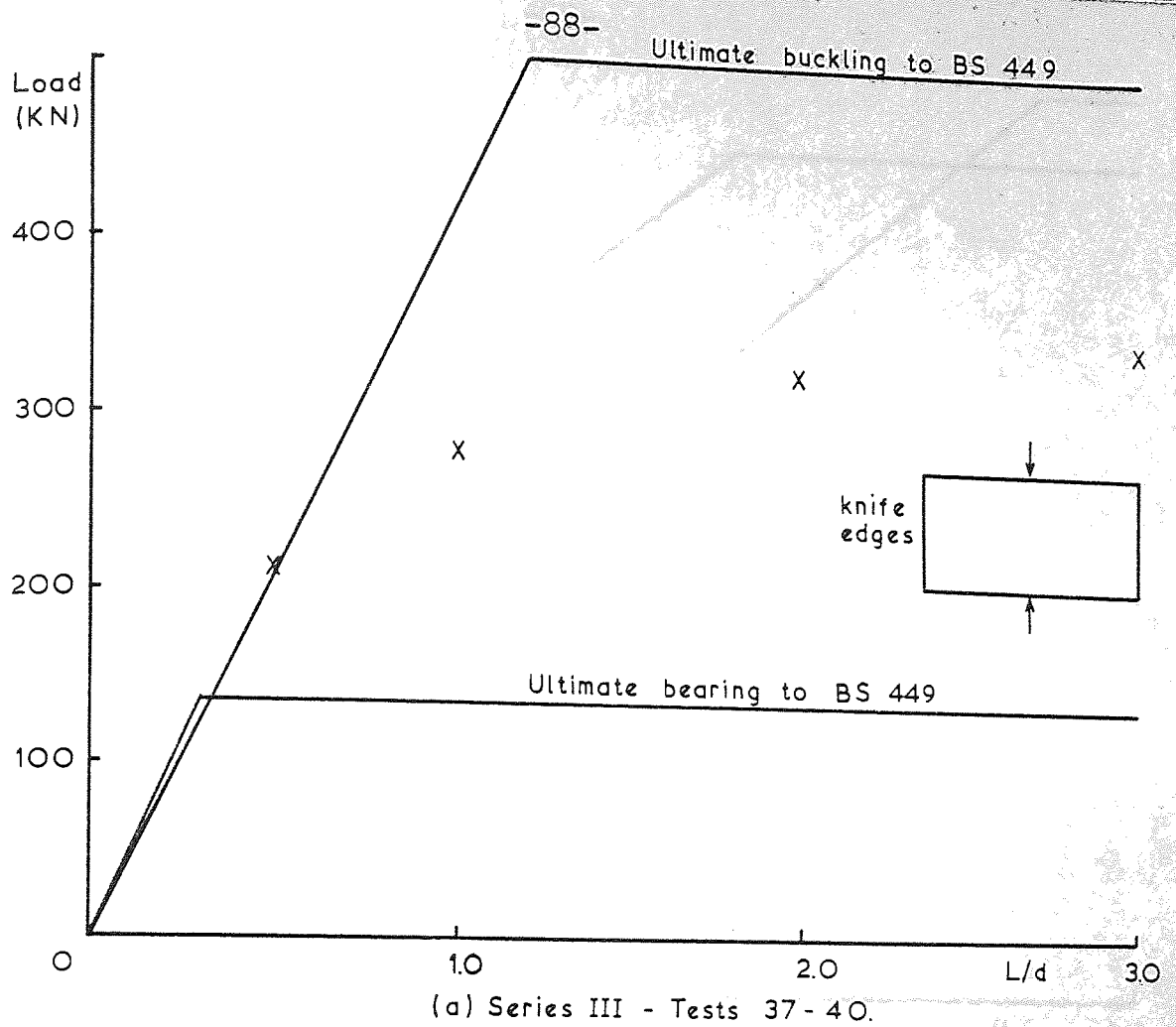


Figure 32 Typical comparison of test failure loads and BS 449 ultimate loads - Series III and IV.

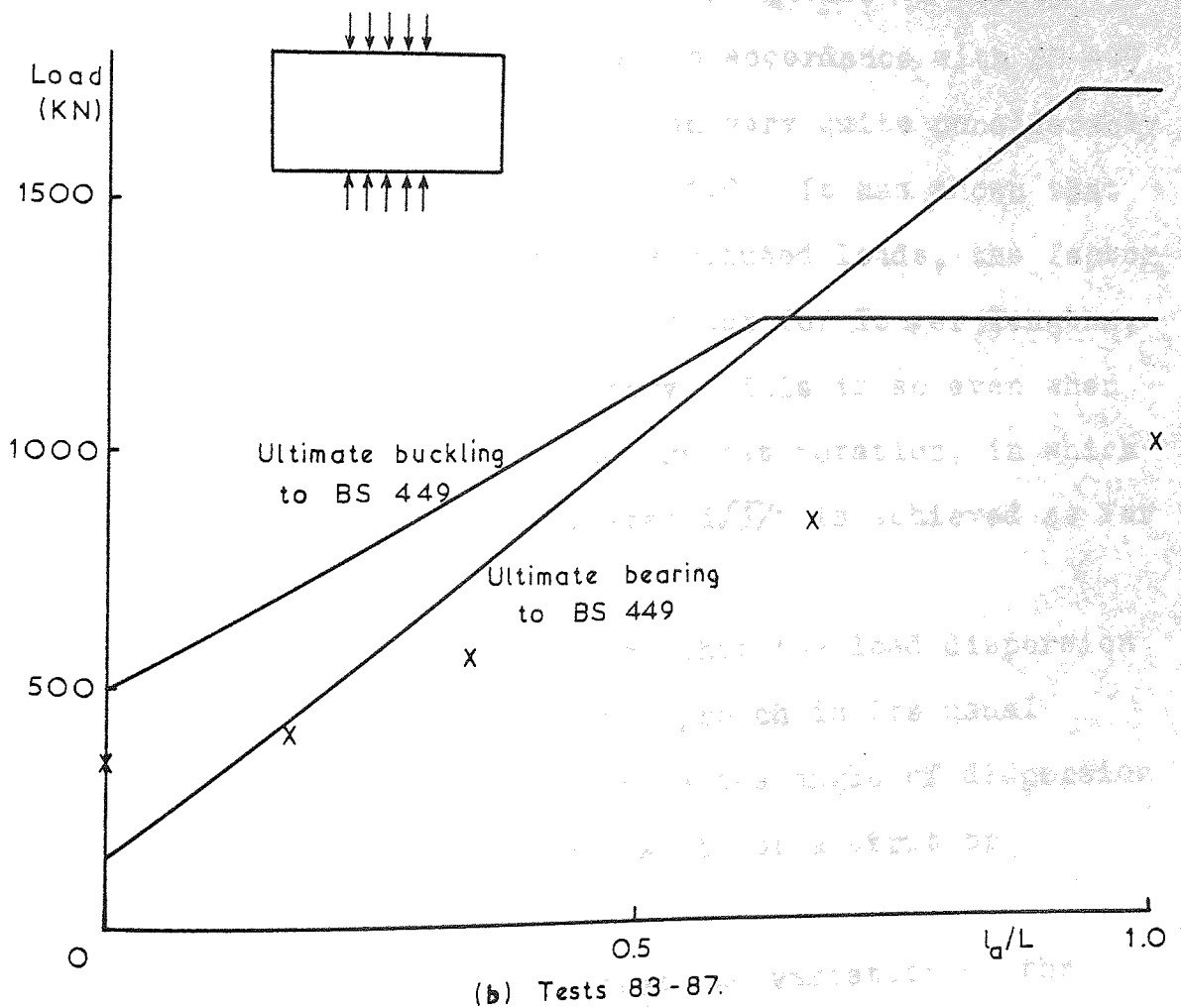
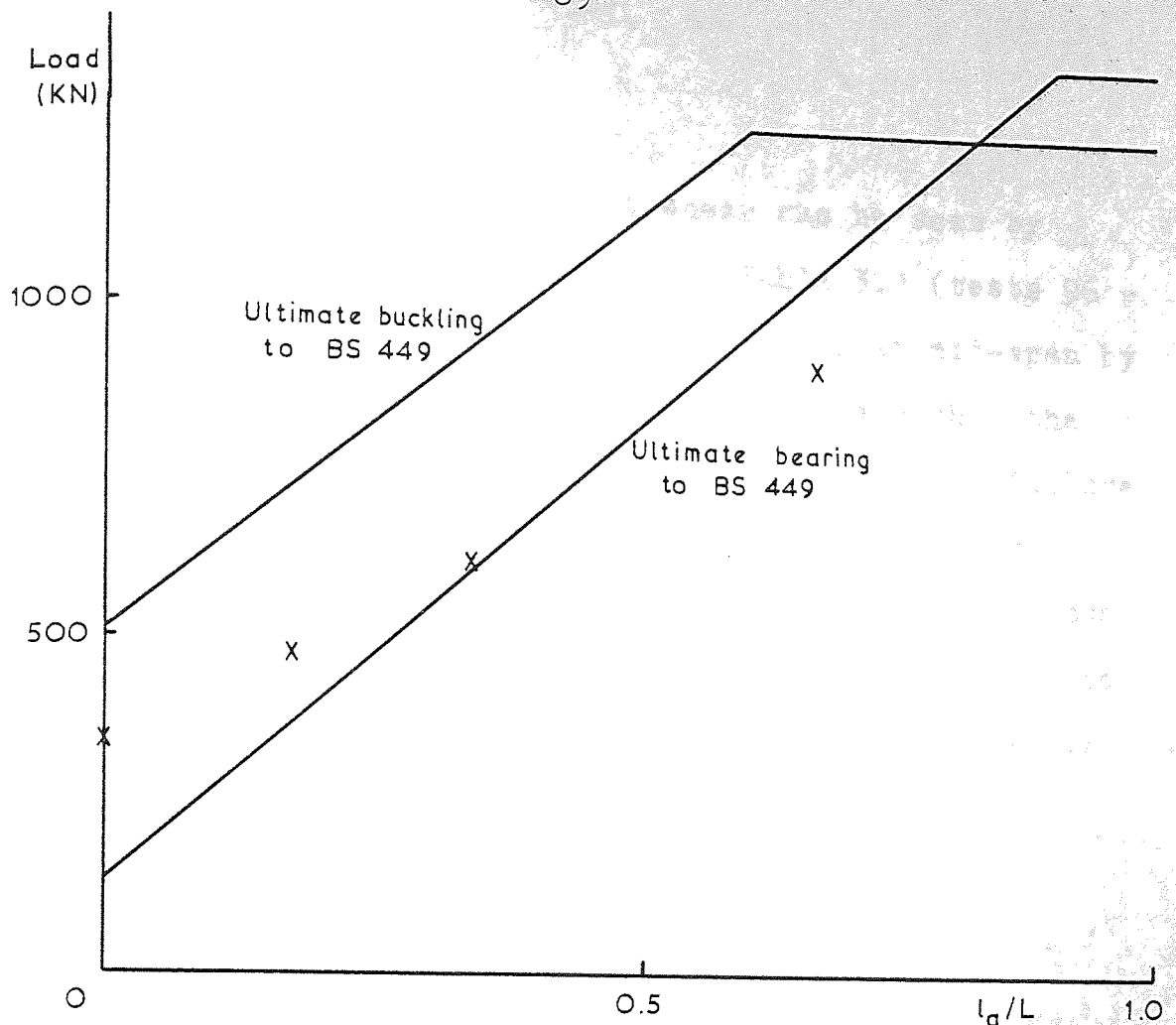


Figure 3.3 Typical comparison of Series V test failure loads and BS 449 ultimate loads.



conservative in this case.

The influence of bending and shear can be seen by considering the Series VII results in Table 3.1 (tests 96 - 100), which were simply supported and loaded at mid-span by knife edges. From these results it can be seen that the bending of a beam does not significantly affect its failure load, as the errors in the theoretical loads are very similar to those beams tested in other series. This shows that for short spans the effects of bending can be ignored when considering the effects of concentrated loads, as in fact the theoretical analysis does.

### 3.2.3 Conclusions From the Comparison

The comparison has shown that the factor of safety against failure in beams designed in accordance with BS 449 for web buckling and web bearing can vary quite considerably and in some cases can be less than 1.0. It has shown that for short lengths of uniformly distributed loads, the factor of safety is greater than necessary but for longer lengths, the design method is unsatisfactory. This is so even when the flanges are fully restrained against rotation, in which case the effective length envisaged  $d\sqrt{3}/t$  is achieved as far as possible.

The comparison also indicates that the load dispersion method is not a practical design approach in its usual simple form, as the only variable is the angle of dispersion and consequently the 'effective' width of a strut or 'effective' bearing length.

It has already been shown that the variation of the

load with the length of stiff bearing is not linear which along with other factors would necessitate a variable angle of dispersion if the load dispersion approach were to be used.

It is also interesting to note that in one instance, for a beam loaded along its whole length and with the flanges fully restrained against rotation, both the bearing load and the buckling load overestimated the failure load. This could indicate that even when full restraint to the flanges is attained, the flange to web connexion is insufficient to achieve a fixed ended strut condition, in which case an effective length of  $d\sqrt{3}/t$  is erroneous.

These factors indicate that an approach such as the load dispersion method would need to have many complications to cater for the variations investigated in the tests reported here. This tends to defeat the object of a simplified approach. It would therefore be better to examine the problem afresh and once failure loads can be predicted with reasonable accuracy, then an empirical or semi-empirical simplified design approach can be formulated.

### 3.3 Other Authors' Work

#### 3.3.1 Shedd (40)

In 1934 Shedd gave design guides in his text book on structural design in steel. In it he gave design guides for web buckling and web bearing in rolled steel beams (similar to those outlined above in BS 449) which he based on previously published American work. He used a load

dispersion approach, allowing for various types of failure vis. flanges moving laterally or rotating or a combination of both. At the time of Shedd's publication, BS 449 specified the use of web stiffeners at points of concentrated loads.

Shedd's specifications for the load dispersion approach were much more conservative than those in the now current BS 449. For web buckling he gave the dispersion angle as  $45^\circ$  but only allowed the dispersion to one quarter of the overall depth of the beam. For web bearing he recommended no dispersion angle from the load application point, the length of web immediately below the load resisting the direct stress.

Comparing the ultimate loads by this method with the test results would lead to more generous safety factors for beams loaded with short lengths of uniformly distributed loads, and the same disadvantages as BS 449 for long lengths of uniformly distributed loads.

### 3.3.2 Winter and Pian (32)

Winter and Pian have performed many tests in a similar way to those presented in this report but on cold-formed steel beams. From the results of their tests they deduced two empirical formulae for beams subjected to concentrated loads applied either at the end or remote from the end.

The formulae they derived were, for a beam loaded at the end:

$$P = (10 + 1.25\sqrt{l_a/t}) t^2 f_y \quad 3.4$$

and for a beam loaded remote from the end:

$$P = (15 + 3.25\sqrt{l_a/t}) t^2 f_y \quad 3.5$$

Both formulae are irrespective of the type of loading and the depth of the section, although the type of load application they employed in their tests was constant.

Although they cannot be used directly for comparison with the results of the tests conducted for this work, the formulae show several interesting characteristics. The total load is dependent on the sum of two quantities, only one being dependent on the length of the applied load, and both independent of the depth of the section.

The cold formed sections used in their tests were made from a uniform thickness of metal, so that the contributions of the flange and web thicknesses cannot be detected in the above formulae.

Their test results showed a considerable amount of scatter, and the web junction with the flange was not as strong as that inherent in rolled steel beams and joists.

Hence any comparison between predicted test loads using the formulae and the results of the tests conducted for this report would be misleading.

### 3.3.3 Delesques (33)

Delesques used the results of tests carried out by several investigators to try to develop design guides for beams subjected to concentrated loads.

The results he utilised from papers by Bergfelt (34) and Bergfelt and Hovik (35) are of particular interest because of the variations in flange and web properties involved in a total of 51 tests. However the results of tests are not directly comparable as they had far more

slender webs than universal beam sections. The depth to thickness ratios of the webs varied from 150 to 350 compared to a maximum of approximately 60 for the beams tested in this work.

Delesques attempted to find a relationship between the failure loads for the tests and the section variables. He plotted several of the variables against  $P/Et^2$ . He showed the following to have no appreciable influence:

1. The elastic limit of the web ( $f_{yw}$ ).
2. The aspect ratio of the panel ( $L/d$  or  $s/d$ ).
3. The stiffness of the flanges and conditions for supporting the load.
4. The slenderness of the web.

However from the analysis of the results of the tests performed for this work in Chapter 2 it was shown that some of these factors appeared to influence the failure loads. It is possible that the factors which affect the failure load for less slender webs, such as those of universal beams vary considerably from those which affect the failure load for very slender webs such as those considered by Delesques.

### 3.4 Conclusions

Of the works considered here, only BS 449 was intended for use with rolled steel universal beams, and this was shown to be unsuitable for certain loading conditions and very conservative for others.

The simple load dispersion theory for the effective width of a strut and the effective bearing length are consequently inadequate in their present forms, particularly

for long bearing lengths.

Many investigators have drawn conclusions from a small number of specialised tests and shown that certain variables do not affect the load carrying capacity, whereas an examination of the test results presented in Chapter 2 shows that for universal beams some of these variables do have a considerable influence.

The empirical approach by Delesques showed the difficulties in determining any relationships which may exist between the properties of a beam and its physical characteristics.

## CHAPTER 4 - ELASTIC BUCKLING THEORY

### 4.1 Introduction

It is very difficult to state with any certainty what initiated the failure of the rolled steel universal beams under test, and there are several possibilities. Most design practices assume that the failure can be due to either local crushing in the vicinity of the applied load or overall elastic buckling of part of the web as a uniformly loaded plate or strut.

The purpose of this chapter is to investigate the validity of assuming overall elastic buckling of the web. The elastic plate buckling theory for the conditions which best represent the actual conditions of the web plates under test will be developed and compared with the test results. The elastic critical loads for each test will be determined where possible (otherwise the ultimate load attained will be assumed as the elastic critical load) for the comparison.

### 4.2 Elastic Buckling Analysis

The web of a universal beam will be considered as a rectangular plate with two free unloaded edges and two elastically restrained loaded edges due to the effect of the flanges. A prediction of the restraint provided by the flanges is very important in the elastic stability analysis. For example a strut of length  $b$  having restraint at its ends will have an elastic critical load of between  $\pi^2 EI/b^2$  and  $4\pi^2 EI/b^2$  depending on the amount of restraint. To examine



the effect of the variation that could be expected in plate analyses due to loaded edge restraint some standard results will be presented.

The value of the elastic critical load for a strut was presented above in the form:

$$P_{cr} = (\text{factor}) \times \pi^2 EI / b^2 \quad 4.1$$

where the factor is usually referred to as an elastic buckling coefficient. For plates, an elastic buckling coefficient is also used and is here denoted  $K_1$ :

$$N_{cr} = \sigma_{cr} t = K_1 \pi^2 D / b^2 \quad 4.2$$

where:

$$D = E t^3 / 12 (1 - \nu^2) \quad 4.3$$

the modulus of rigidity of the plate. The critical load in 4.2 is a load per unit length, the reason for which can be seen by comparing  $D$  with  $EI$  from 4.1.

The total critical load is:

$$N_{cr} a = K_1 \frac{\pi^2 D}{b} \frac{a}{b}$$

and if:

$$K = K_1 \frac{a}{b}$$

then:

$$P_{cr} = K \pi^2 D / b \quad 4.4$$

In the following work both  $K$  and  $K_1$  will be used where convenient for presenting results. In general  $K$  is used when concentrated loads are considered and  $K_1$  when uniformly distributed loads are considered.

The St. Venant differential equation of the deflected

surface for the buckled plate when no body forces are present was presented in Section 1.3.1. Hence:

$$D \nabla^4 w = N_x \frac{\partial^2 w}{\partial x^2} + N_y \frac{\partial^2 w}{\partial y^2} + 2 N_{xy} \frac{\partial^2 w}{\partial x \partial y} \quad 4.5$$

as presented by Timoshenko (11). The elastic critical load is the solution of this equation for the various boundary conditions. If the stresses  $N_x$ ,  $N_y$  and  $N_{xy}$  are not constant throughout the plate then equation 4.5 has variable coefficients and the solution of the equation is more difficult, but the principle remains the same.

An alternative to solving the equation is to use the energy method. In this method the plate is given a small lateral deflexion and the strain energy of bending equated to the work done by the forces acting in the middle plane of the plate. By equating the strain energy of bending to the work done, the plate is assumed to be in equilibrium and so the unstable form of equilibrium, when the plate has a deformed shape, can be found. The general energy equation was presented as equation 1.2:

$$\begin{aligned} & - \frac{1}{2} \iint \left[ N_x \left( \frac{\partial w}{\partial x} \right)^2 + N_y \left( \frac{\partial w}{\partial y} \right)^2 + 2 N_{xy} \frac{\partial w}{\partial x} \frac{\partial w}{\partial y} \right] dx dy \\ & = \frac{D}{2} \iint \left\{ \left[ \frac{\partial^2 w}{\partial x^2} + \frac{\partial^2 w}{\partial y^2} \right]^2 - 2(1-\nu) \left[ \frac{\partial^2 w}{\partial x^2} \frac{\partial^2 w}{\partial y^2} - \left( \frac{\partial^2 w}{\partial x \partial y} \right)^2 \right] \right\} dx dy \end{aligned}$$

.....4.6

It is necessary to find an expression for the lateral deflexion of the plate  $w$  which satisfies the boundary conditions and makes the variation of the energy equation a minimum. For certain boundary and loading conditions exact solutions for  $K_1$  can be found, but for complicated loading

and boundary conditions it is necessary to use an approximate method of analysis such as the Rayleigh-Ritz method.

#### 4.2.1 Plate With Two Opposite Uniformly Distributed Loads

When a rectangular plate is subjected to two opposite uniformly distributed loads only, then the terms involving  $N_y$  and  $N_{xy}$  disappear from equations 4.5 and 4.6 and the problem is somewhat simplified. The remaining complication is the boundary conditions.

If an exact expression for the deflected shape is known for a given set of boundary conditions then an exact solution for  $K_1$  can be found. If such an expression is not known then an approximate deflected shape must be utilised and a variational approach will lead to an approximate solution. The exact solutions are now known as standard cases. Many non-standard solutions for plates with two opposite uniformly distributed loads have been determined by several investigators for a whole range of boundary conditions. Some of the results are shown graphically in figures 4.1, 4.2 and 4.3. The author's name is given for the results which are not yet generally found in current text books.

The results presented are shown as the variation of  $K$  and  $K_1$  with the aspect ratio  $a/b$  and not as usually presented in text books as the variation of  $K$  and  $K_1$  with the aspect ratio  $b/a$ . This is because text books are usually more concerned with long strut-like plates which can buckle into many wave forms rather than wide plates which

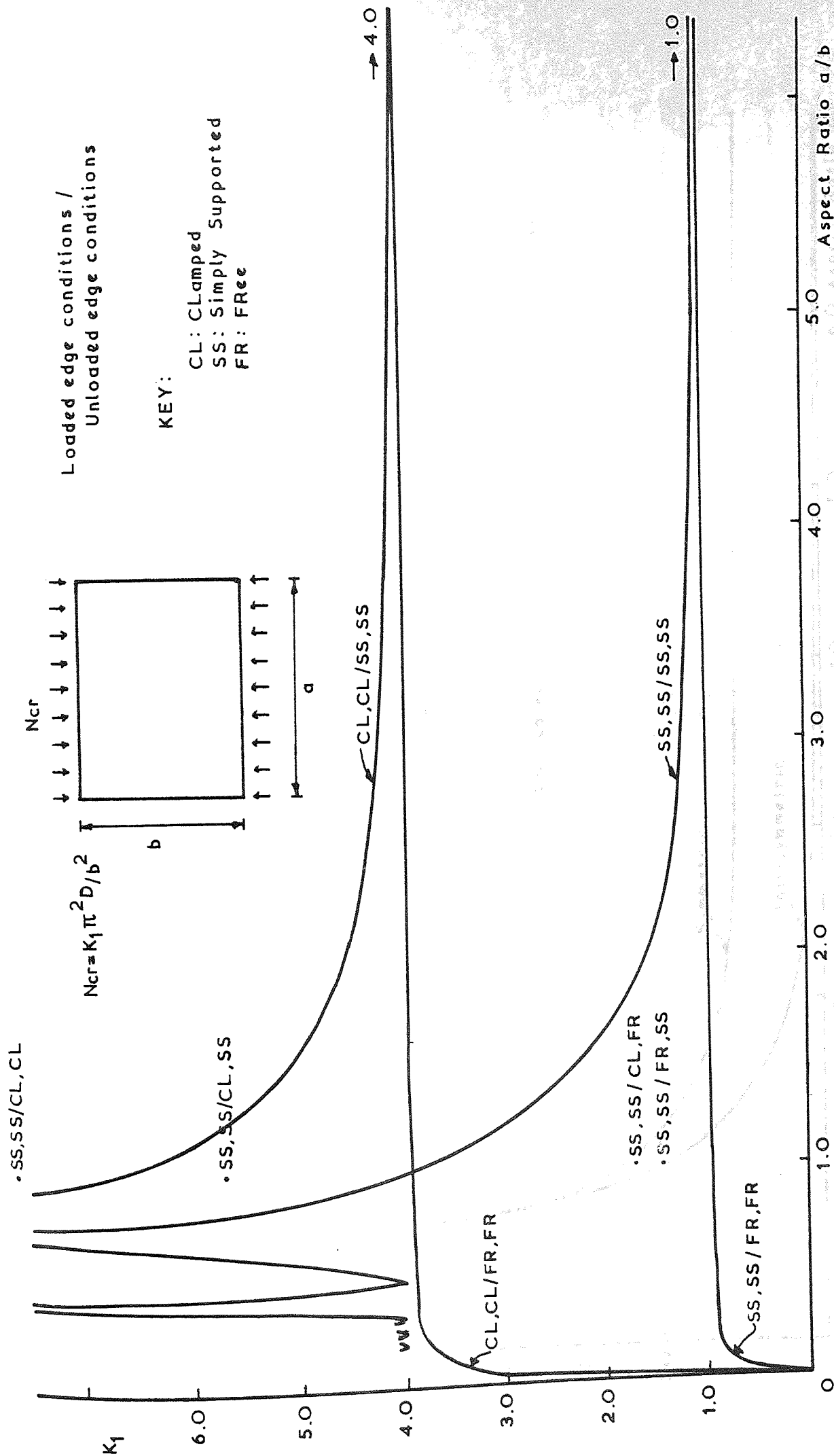


Figure 4.1 Elastic buckling coefficient  $K_1$ -various edge conditions.

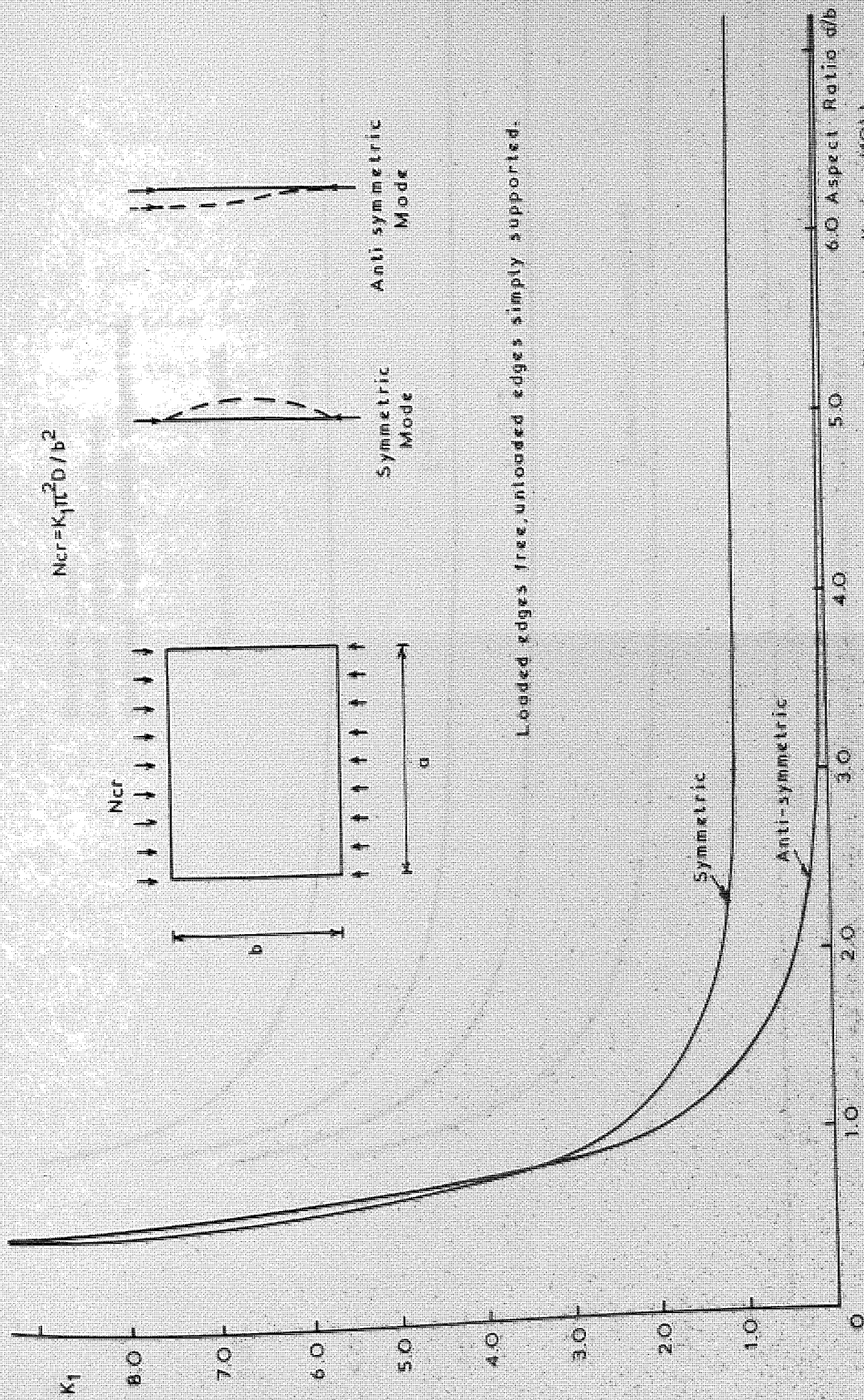


Figure 4.2 Elastic buckling coefficient  $K_1$ -free loaded edges (Woinowsky-Krieger (10) )



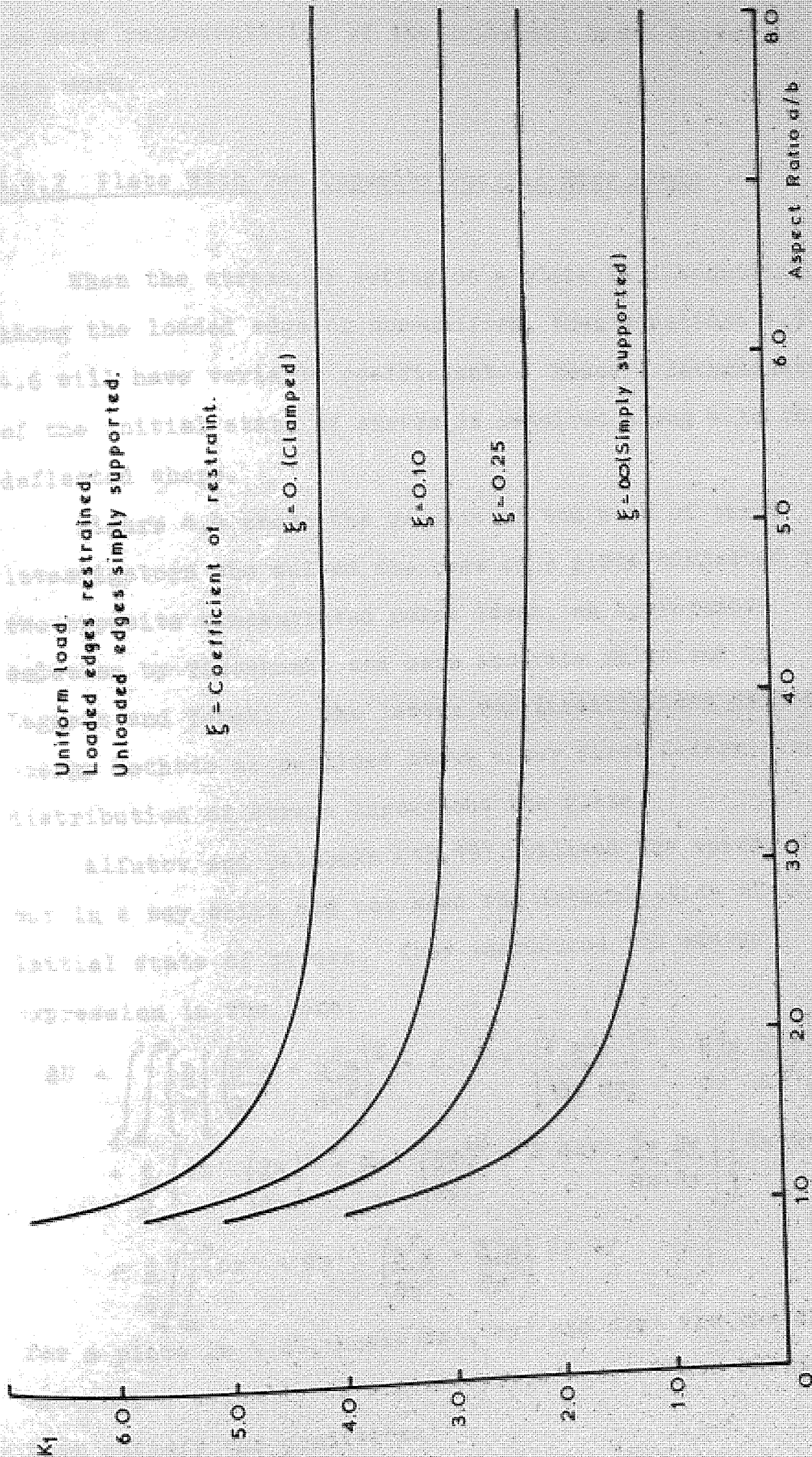


Figure 4.3 Elastic buckling coefficient  $K_1$ -restrained loaded edges (Bleich (12)).

are more representative of the universal beams tested in this work.

#### 4.2.2 Plate With Two Opposite Partial Edge Loads

When the stress  $N_x$  acting on a plate is discontinuous along the loaded edge or non-uniform, then equations 4.5 and 4.6 will have variable coefficients. Hence a determination of the initial state of stress is required along with the deflected shape.

Figure 4.4 shows the results of the work of three investigators who solved the case of a plate subjected to two opposite concentrated point loads, an approximate solution by Timoshenko and more accurate solutions by Leggett and Yamaki. The latter two investigators utilised energy methods as outlined above after first determining a distribution of stress throughout the plate.

Alfutov and Balabukh (18,19) utilised the energy method but in a way which did not need the determination of the initial state of stress. They reproduced the energy expression in the form:

$$\begin{aligned} \delta U = & \iint_{-m}^m \left\{ \frac{D}{2} \left[ \left( \frac{\partial^2 w}{\partial x^2} + \frac{\partial^2 w}{\partial y^2} \right)^2 + 2(1-\nu) \left[ \left( \frac{\partial^2 w}{\partial x \partial y} \right)^2 - \frac{\partial^2 w}{\partial x^2} \frac{\partial^2 w}{\partial y^2} \right] \right. \right. \\ & + \frac{t}{2} \left[ \sigma_x' \left( \frac{\partial w}{\partial x} \right)^2 + \sigma_y' \left( \frac{\partial w}{\partial y} \right)^2 + 2 \sigma_{xy}' \frac{\partial w}{\partial x} \frac{\partial w}{\partial y} \right] \Big\} dx dy \\ & - \frac{t}{E} \iint_{-m}^m (\sigma_x' + \sigma_y') \left( \frac{\partial^2 w}{\partial x^2} + \frac{\partial^2 w}{\partial y^2} \right) dx dy \end{aligned} \quad 4.7$$

for a plate  $2m \times 2l$ , where  $\sigma_x'$ ,  $\sigma_y'$  and  $\sigma_{xy}'$  are the applied external statically determinate stresses. These stresses must satisfy the conditions:



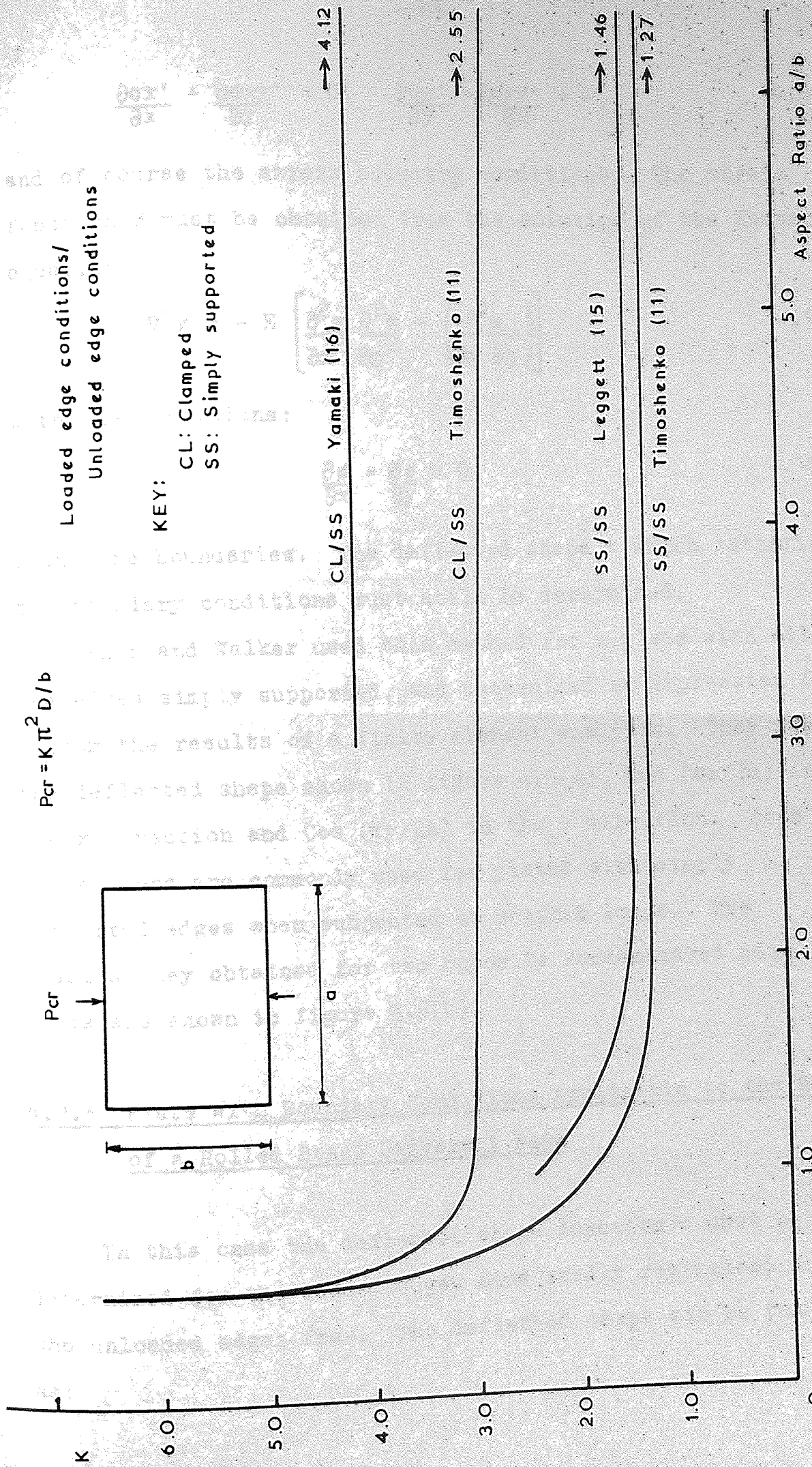


Figure 4.4 Elastic buckling coefficient  $K$  - various edge conditions.

$$\frac{\partial \sigma_x'}{\partial x} + \frac{\partial \sigma_{xy}'}{\partial y} = 0, \quad \frac{\partial \sigma_y'}{\partial y} + \frac{\partial \sigma_{xy}'}{\partial x} = 0 \quad 4.8$$

and of course the stress boundary conditions. The stress function  $\phi$  must be obtained from the solution of the Karman equation:

$$\nabla^4 \phi = -E \left[ \frac{\partial^2 w}{\partial x^2} \frac{\partial^2 w}{\partial y^2} - \left( \frac{\partial^2 w}{\partial x \partial y} \right)^2 \right] \quad 4.9$$

with the conditions:

$$\frac{\partial \phi}{\partial x} = \frac{\partial \phi}{\partial y} = 0 \quad 4.10$$

along the boundaries. The deflected shape  $w$  which satisfies the boundary conditions must still be determined.

Khan and Walker used this method for a plate with all the edges simply supported, and determined an expression for  $w$  from the results of a finite element analysis. They used the deflected shape shown in figure 4.5(a),  $\cos(\pi x/2m)$  in the  $x$  direction and  $\cos(\pi y/2A)$  in the  $y$  direction. Both expressions are commonly used for plates with simply supported edges when subjected to uniform loads. The results they obtained for two opposite concentrated edge loads are shown in figure 4.5(b).

#### 4.2.3 Plate With Boundary Conditions Applicable to the Web of a Rolled Steel Universal Beam

In this case the deflected shape function  $w$  must be determined for the loaded edges elastically restrained and the unloaded edges free. The deflected shape can be taken as:



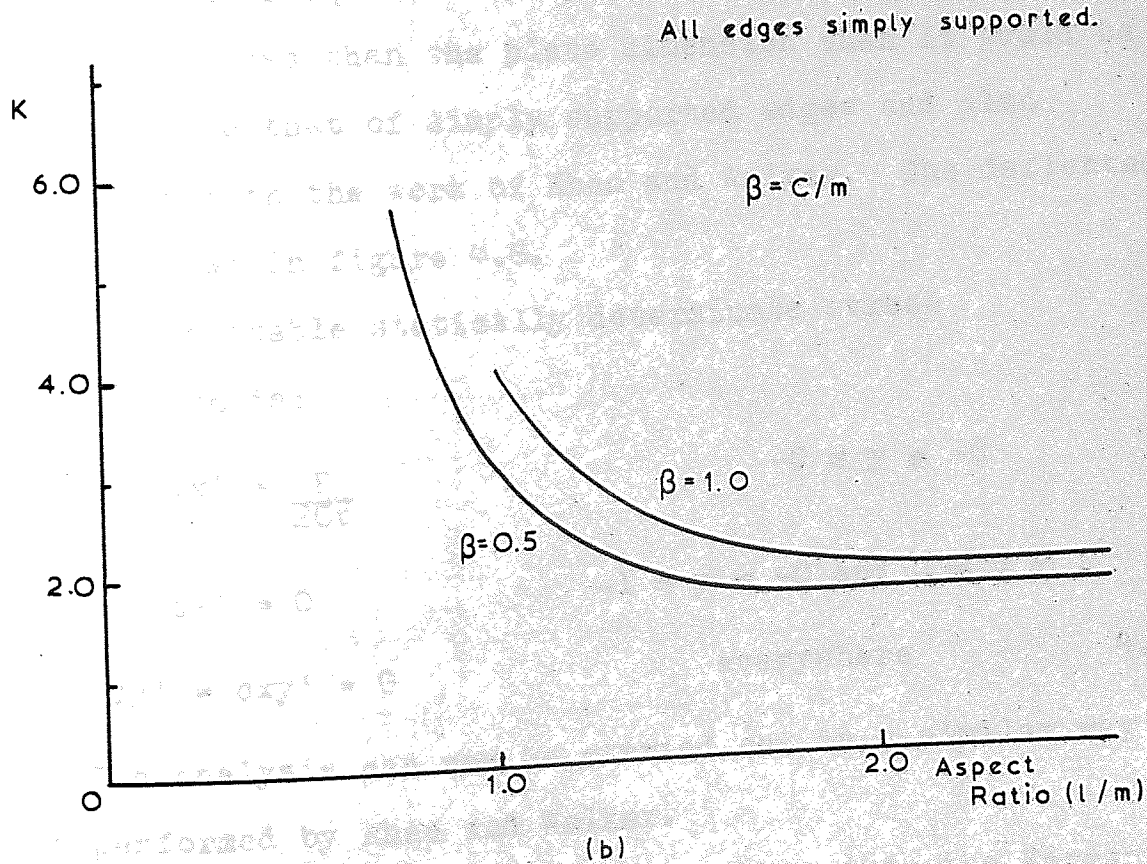
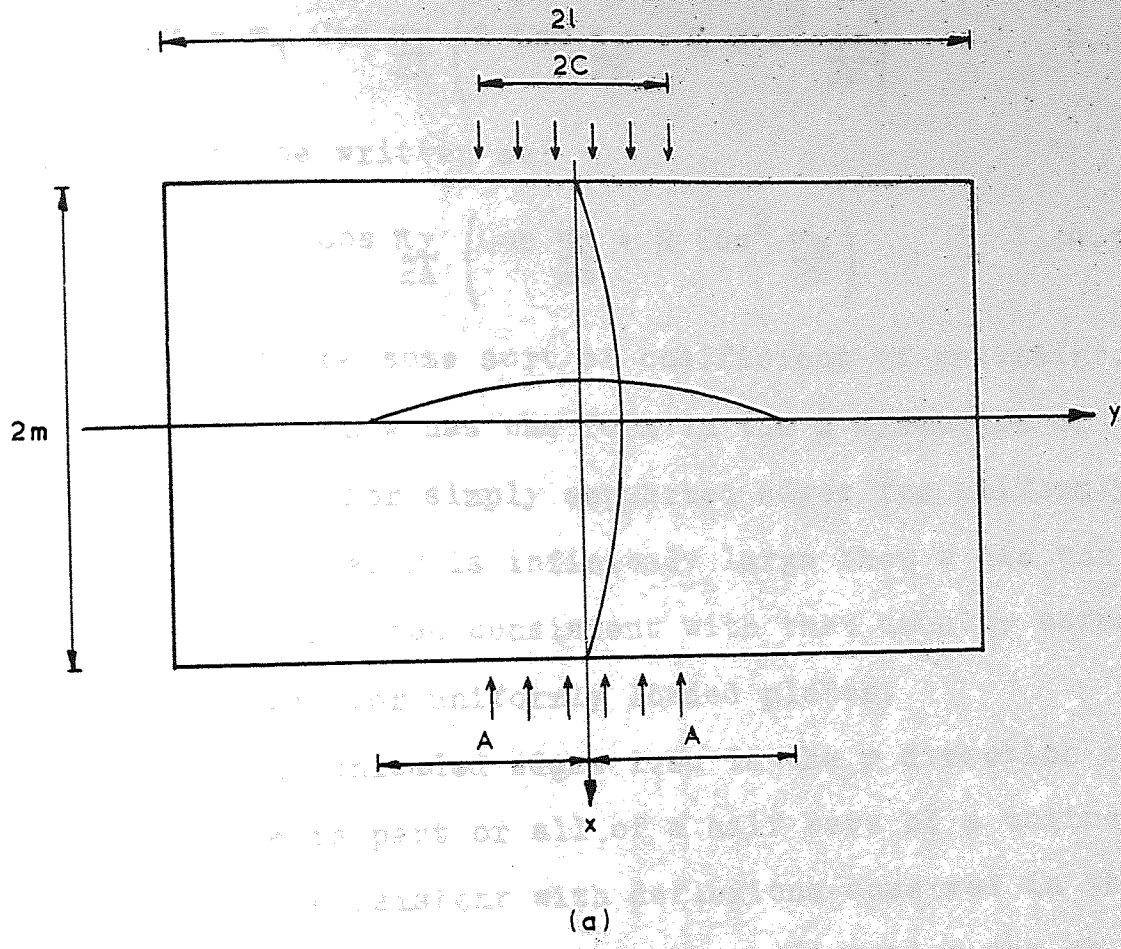


Figure 4.5 Typical results obtained by Khan & Walker (20).

$$w = w_1 \cos \frac{\pi y}{2A} \left( S \cos \frac{\pi x}{2m} + Q \cos^2 \frac{\pi x}{2m} \right) \quad 4.11$$

which can also be written as:

$$w = w_2 \cos \frac{\pi y}{2A} \left( \cos \frac{\pi x}{2m} + R \cos^2 \frac{\pi x}{2m} \right) \quad 4.12$$

which shows R to be some sort of coefficient of restraint. When R is zero then w has the form in the x direction of that usually used for simply supported edges for uniformly loaded plates. When R is infinitely large then w has the form in the x direction consistent with that usually assumed for clamped edges for uniformly loaded plates.

Between the unloaded edges i.e. in the y direction the deflected shape is part or all of a half wave of a cosine curve, which is consistent with deflexions observed in the tests. The length of the wave in the y direction can be greater than or equal to the plate dimension. If the wave length were less than the plate dimension then it would be equivalent to that of simply supported edges and also consistent with the work of Khan and Walker. The deflected form is shown in figure 4.6.

An applicable statically determinate stress distribution is:

$$\sigma_x' = \frac{P}{2Ct}$$

$$-C \leq y \leq +C$$

$$\sigma_x' = 0$$

$$-1 \leq y \leq -C \text{ and } C \leq y \leq 1$$

$$\sigma_y' = \sigma_{xy}' = 0$$

$$\text{everywhere}$$

$$4.13$$

The analysis can now be carried out in a similar way to that performed by Khan and Walker. Substitution of the expression for w into the Karman equation 4.9 gives:



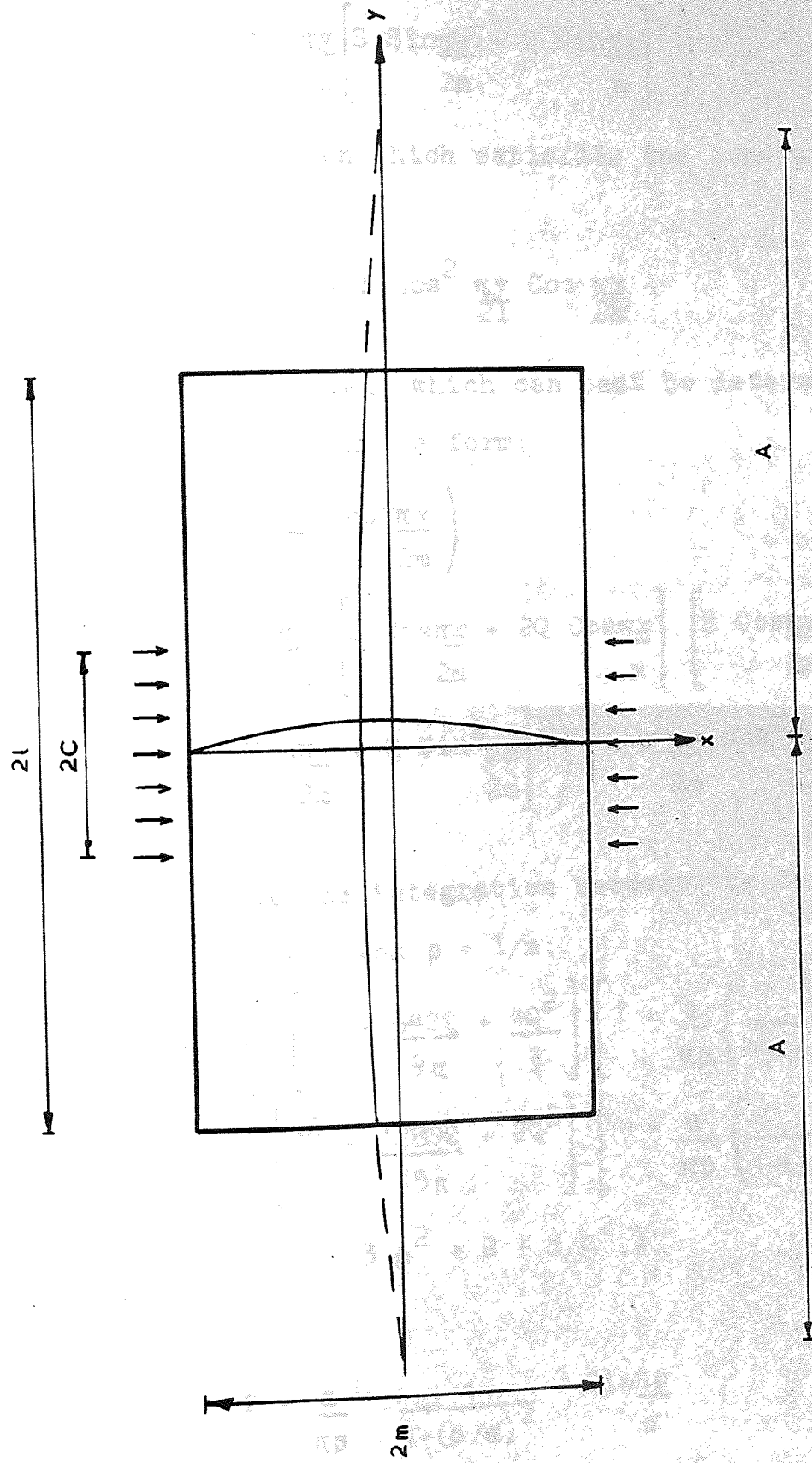


Figure 4.6 Plate deflected form used for the elastic analysis (free unloaded edges).

$$\nabla^4 \phi = -\frac{E\pi^4 w_1^2}{16A^2 m^2} \left( \cos^2 \frac{\pi y}{2A} \left[ \frac{S \cos \frac{\pi x}{2m} + 2Q \cos \frac{\pi x}{m}}{2m} \right] \left[ \frac{S \cos \frac{\pi x}{2m} + Q \cos^2 \frac{\pi x}{2m}}{2m} \right] - \sin^2 \frac{\pi y}{2A} \left[ \frac{S \sin \frac{\pi x}{2m} + Q \sin \frac{\pi x}{m}}{2m} \right]^2 \right) \quad 4.14$$

A stress function which satisfies the conditions 4.8 is:

$$\phi = f \cos^2 \frac{\pi y}{2A} \cos \frac{\pi x}{2m} \quad 4.15$$

where f is a coefficient which can best be determined from Galerkin's equation in the form:

$$\int_{-l}^l \int_{-m}^m \left\{ \nabla^4 \left( f \cos^2 \frac{\pi y}{2A} \cos \frac{\pi x}{2m} \right) + \frac{E\pi^4 w_1^2}{16A^2 m^2} \left( \cos^2 \frac{\pi y}{2A} \left[ \frac{S \cos \frac{\pi x}{2m} + 2Q \cos \frac{\pi x}{m}}{2m} \right] \left[ \frac{S \cos \frac{\pi x}{2m} + Q \cos^2 \frac{\pi x}{2m}}{2m} \right] - \sin^2 \frac{\pi y}{2A} \left[ \frac{S \sin \frac{\pi x}{2m} + Q \sin \frac{\pi x}{m}}{2m} \right]^2 \right) \right\} \cos^2 \frac{\pi x}{2m} \cos^2 \frac{\pi y}{2A} dx dy = 0 \quad \dots\dots 4.16$$

Carrying out the integration between the correct limits and denoting  $\alpha = A/m$  and  $\rho = l/m$ :

$$f = \left( \frac{-Ew_1^2 \rho^2}{8 \alpha^2} \left\{ 3 \left[ S^2 + \frac{64SQ}{9\pi} + \frac{4Q^2}{3} \right] \left[ 1 + \frac{\alpha}{\pi\rho} \left( \frac{1}{1-(\rho/\alpha)^2} \right) \frac{\sin \pi\rho}{\alpha} \right] - \left[ S^2 + \frac{128SQ}{15\pi} + 2Q^2 \right] \left[ 1 - \frac{\alpha}{\pi\rho} \left( \frac{1}{1-(\rho/\alpha)^2} \right) \frac{\sin \pi\rho}{\alpha} \right] \right\} \right) / (3\rho^2 + 2 + 3/\rho^2)$$

and if:

$$Z = \frac{\alpha}{\pi\rho} \frac{1}{1-(\rho/\alpha)^2} \frac{\sin \pi\rho}{\alpha}$$

then:



$$\phi = \left( - \frac{E w_1^2 \rho^2}{8 \alpha^2} \left\{ 3 \left( S^2 + \frac{64 S Q}{9 \pi} + \frac{4 Q^2}{3} \right) (1+Z) - \left( S^2 + \frac{128 S Q}{15 \pi} + 2 Q^2 \right) (1-Z) \right\} \cos^2 \frac{\pi x}{2m} \cos^2 \frac{\pi y}{2A} \right) / (3 \rho^2 + 2 + 3/\rho^2) \quad 4.17$$

Now by using equation 4.7 and substituting for the partial derivatives of  $\phi$  and  $w$ , the value of  $K$  can be determined, where  $K = \frac{2 m P c r}{\pi^2 D}$ .

It is important to integrate between the correct limits. Doing so, and putting  $\beta = C/m$ ; and also re-introducing  $R$ :

$$K = \frac{\left( \frac{\pi \rho}{\alpha} + \frac{\sin \pi \rho}{\alpha} \right) \left( \alpha^2 R_1 + 2 + \frac{R_2}{\alpha^2} \right) - 4 (1-v) \frac{\sin \pi \rho}{\alpha}}{\frac{\alpha^2}{\beta} \left( \frac{\beta \pi}{\alpha} + \frac{\sin \beta \pi}{\alpha} \right) - \frac{\rho}{\beta \alpha} \frac{\sin \beta \pi}{\rho} \frac{[3 R_3 (1+Z) - R_4 (1-Z)]}{(3 \rho^2 + 2 + 3/\rho^2)}} \quad \dots\dots 4.18$$

where:

$$\begin{aligned} R_5 &= 1 + \frac{16 R}{3 \pi} + R^2 \\ R_1 &= \left( 1 + \frac{16 R}{3 \pi} + 4 R^2 \right) / R_5 \\ R_2 &= \left( 1 + \frac{16 R}{3 \pi} + \frac{3 R^2}{4} \right) / R_5 \\ R_3 &= \left( 1 + \frac{64 R}{9 \pi} + \frac{4 R^2}{3} \right) / R_5 \\ R_4 &= \left( 1 + \frac{128 R}{15 \pi} + 2 R^2 \right) / R_5 \end{aligned}$$

The only variable is  $\alpha$  for a particular aspect ratio. Hence equation 4.18 can be minimised with respect to  $\alpha$  and so the condition that  $K$  is a minimum is:

$$(\text{Denominator}) \times \frac{d}{d\alpha} (\text{Numerator})$$

$$- (\text{Numerator}) \times \frac{d}{d\alpha} (\text{Denominator}) = 0$$

Numerator and Denominator refer to expression 4.18.

The resulting expression is shown in the appendix. A computer program has been written to solve this problem, the flow diagram for which is also shown in the appendix.

Results for various conditions of edge restraint and aspect ratios are shown tabulated in Table 4.1 and graphically in figures 4.7 and 4.8. A fuller tabulation of the results is included in the appendix.

As can be seen from the results of the analysis, for a particular length of loading, the wave length is very large for a narrow plate. This means that the plate remains practically straight in the y direction and performs as a strut. As the aspect ratio increases so the wave length reduces so that for a very wide plate the deflected wave form is localised to a small region and the effect of the unloaded edges is small. This shows in the way that K in figures 4.7 and 4.8 is asymptotic to the values obtained by Khan and Walker for a plate simply supported on all four edges.

This can also be seen from the analysis, for if  $\alpha = \rho$  so that the wave length is equal to the width of the plate and the restraint coefficient  $R = 0$  so that the loaded edges are simply supported then:

$$K = \frac{\left( \frac{\pi \rho}{\alpha} + \sin \frac{\pi \rho}{\alpha} \right) \left( \alpha + \frac{1}{\alpha} \right)^2}{\frac{\alpha^2}{\beta} \left( \frac{\beta \pi}{\alpha} + \sin \frac{\beta \pi}{\alpha} \right) - \left( \frac{4}{\beta} \sin \frac{\beta \pi}{\alpha} \right) / (3\alpha^2 + 2 + 3/\alpha^2)}$$

....4.19



Aspect Ratio $l/m$	Buckling Coefficient $K$	Wave Length Ratio $A/m$
Loaded length ratio $C/m = 0.1$		
Restraint coefficient $R = 0.0$		
0.10	0.100	11.210
0.30	0.301	11.210
0.50	0.502	11.366
0.70	0.703	11.421
0.90	0.902	11.466
1.10	1.100	11.422
1.30	1.277	3.469
1.50	1.406	2.675
1.70	1.497	2.407
1.90	1.562	2.315
2.10	1.615	2.306
2.30	1.618	-
Restraint coefficient $R = 1.0$		
0.10	0.182	11.210
0.30	0.545	11.210
0.50	0.908	11.367
0.70	1.271	11.423
0.90	1.632	11.469
1.10	1.975	3.405
1.30	2.204	2.178
1.50	2.320	1.898
1.70	2.385	1.839
1.90	2.339	-
Restraint coefficient $R = \text{infinitely large}$		
0.10	0.400	11.210
0.30	1.202	11.210
0.50	2.003	11.365
0.70	2.803	11.420
0.90	3.598	5.434
1.10	4.135	1.690
1.30	4.239	-

Table 4.1 Typical results of the elastic analysis.

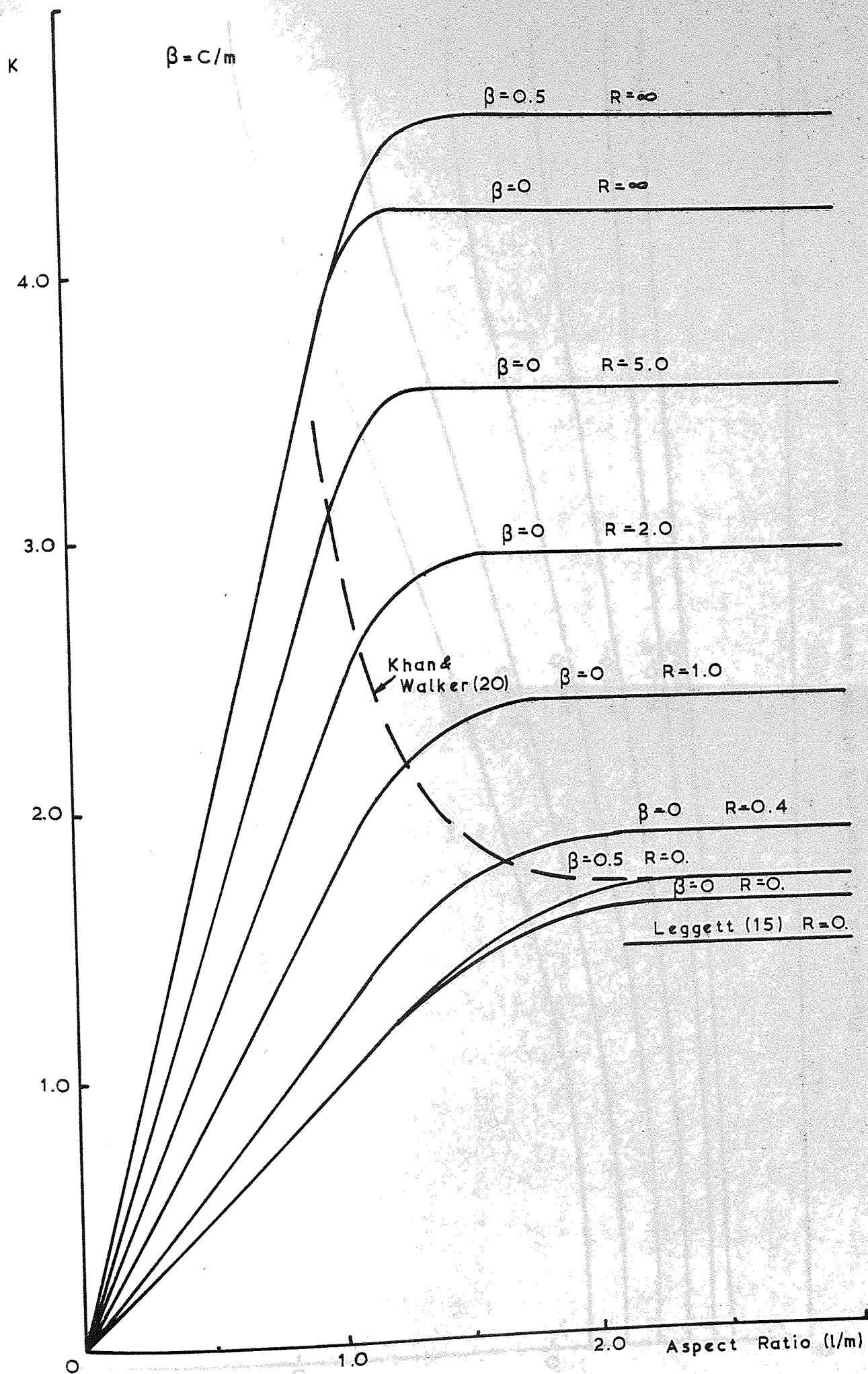


Figure 4.7 Typical form of the results of the elastic analysis.

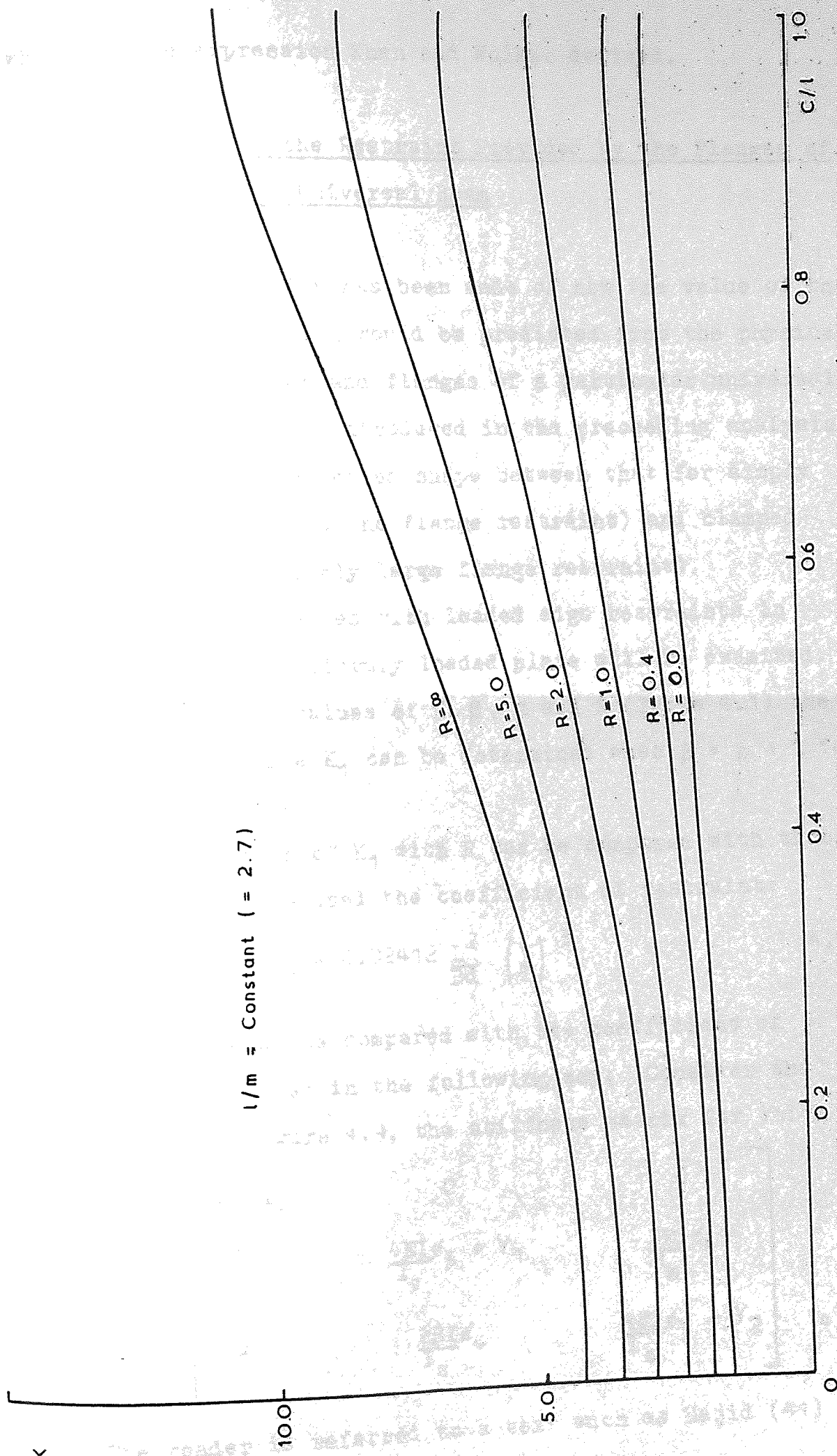


Figure 4.8 Typical form of the results of the elastic analysis.



which is the expression Khan and Walker derived.

#### 4.3 Estimation of the Restraint Provided by the Flanges of a Rolled Steel Universal Beam

So far no mention has been made of how the value of the restraint coefficient  $R$  would be predicted from the physical properties of the web and flanges of a particular universal beam. The value of  $R$  introduced in the preceeding analysis merely varied the deflected shape between that for simply supported loaded edges (no flange restraint) and clamped loaded edges (infinitely large flange restraint).

To see how  $R$  varies with loaded edge restraints in other analyses, a uniformly loaded plate will be examined. From the tabulated values of  $K$ ,  $\beta$ ,  $\alpha$  and  $R$  (Table 4.1) the value of  $K$  and hence  $K_1$  can be determined when  $\beta = \rho = 1$  for various values of  $R$ .

This variation of  $K_1$  with  $R$  can be compared with that of Bleich (12). He used the coefficient of restraint:

$$\xi = 0.02412 \frac{L^2}{Bd} \left( \frac{t}{T} \right)^3 \quad 4.20$$

This can also be compared with the coefficient of restraint determined in the following way: Consider the strut shown in figure 4.9, the stiffness matrix for which is

$$\begin{bmatrix} EA'/l_s & 0 & 0 \\ 0 & \frac{4EI\phi_3}{l_s} + \gamma_1 & \frac{2EI\phi_4}{l_s} \\ 0 & \frac{2EI\phi_4}{l_s} & \frac{4EI\phi_3}{l_s} + \gamma_2 \end{bmatrix} \quad 4.21$$

The reader is referred to a text such as Majid (41) for



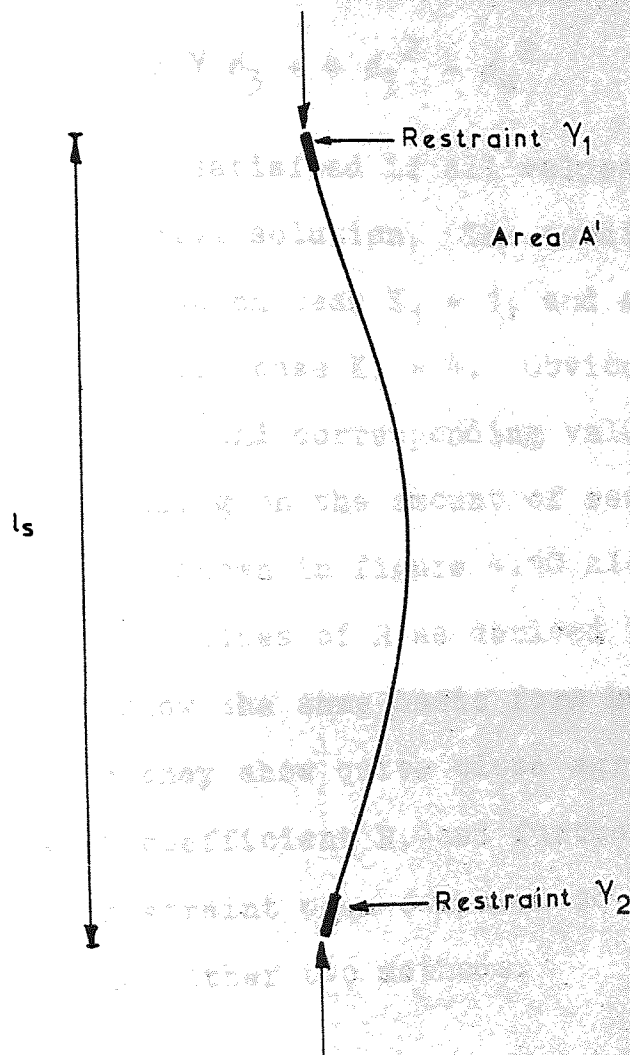


Figure 4.9

the derivation of this. The condition for stability is that the determinant of the stiffness matrix should be zero, and if the stiffness at both ends of the member is the same and is equal to  $\gamma/(EI/l_s)$  i.e. the relative stiffness, then:

$$|\underline{K}| = 0 = \gamma^2 + 2 \gamma \phi_3 + 4 \phi_3^2 - \phi_4^2 \quad 4.22$$

This condition is satisfied if all values are zero and hence  $K_1 = 0$ , the trivial solution. The condition is also satisfied if  $\gamma = 0$  in which case  $K_1 = 1$ , and also if  $\gamma$  is infinitely large in which case  $K_1 = 4$ . Obviously there is a whole range of  $\gamma$  values and corresponding values of  $K_1$  between 1 and 4 depending on the amount of restraint.

These values are shown in figure 4.10 along with those due to Bleich and the values of  $R$  as derived in the previous section. They all show the same basic form but are slightly different. However they show quite close agreement for low values of restraint coefficient  $R$ , and further,  $R$  rarely overestimates the restraint when compared to the restraint coefficient from the other two methods.

#### 4.4 Elastic Critical Test Load

The theoretical elastic buckling load factor  $K$  has been determined for certain plate boundary and loading conditions. It is now necessary to determine the load at which the web of the beam in each test attained its elastic critical load, for comparison. Two ways of establishing the elastic buckling load from test results are available.

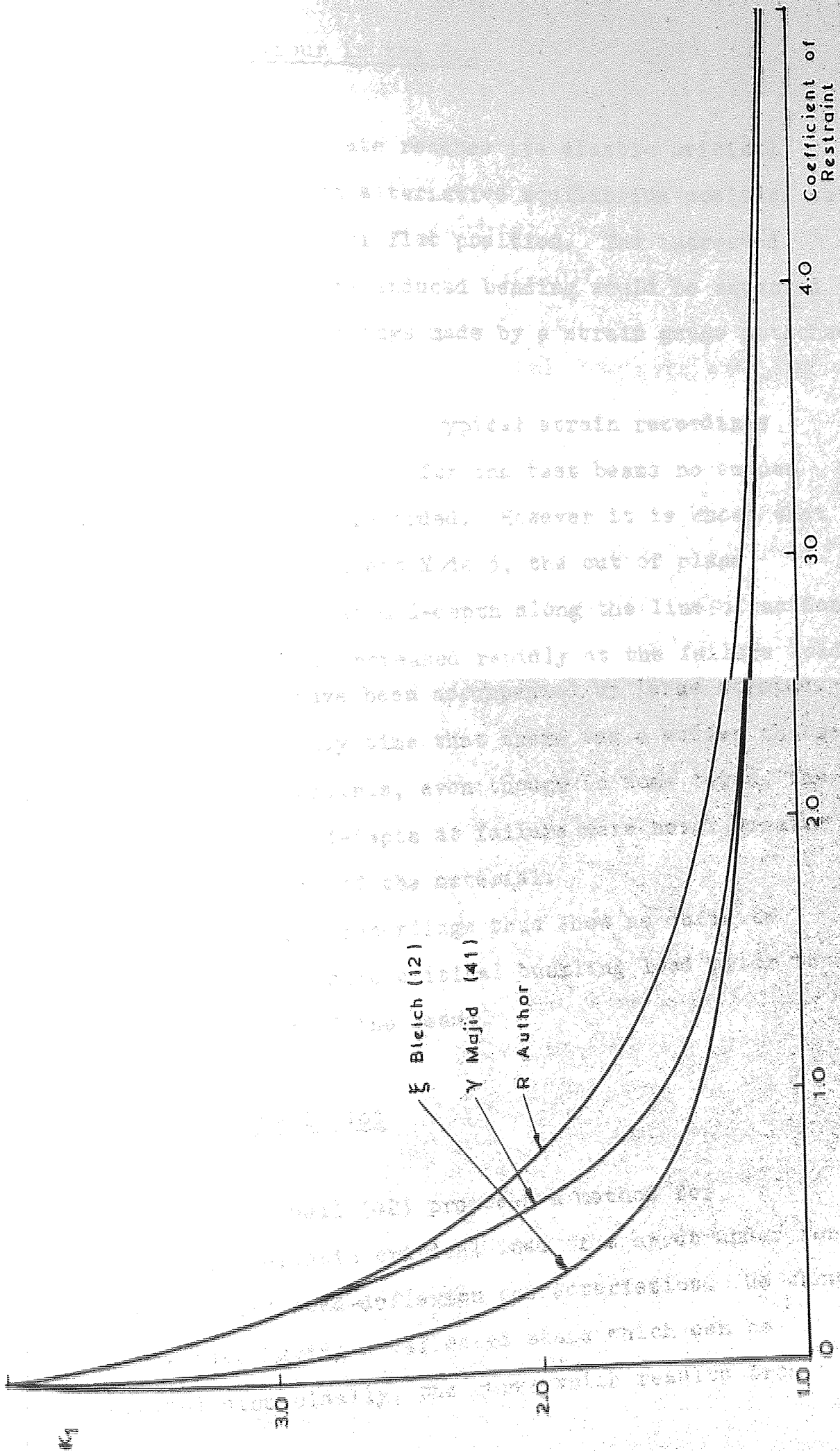


Figure 4.10



#### 4.4.1 Strain Behaviour in the Web

When a strut or plate reaches its elastic critical buckling load it has an alternative equilibrium position to the perfectly straight or flat position. The increased deflexions and therefore induced bending would be expected to reflect in the recordings made by a strain gauge attached to its extreme fibres.

It can be seen from the typical strain recordings presented in Chapter 2 that for the test beams no sudden changes in strain were recorded. However it is known that in all failure modes except Mode 3, the out of plane deflexions of the web at mid-depth along the line of action of the applied loads, increased rapidly at the failure load, and must therefore have been accompanied by large strains. Hence this was the only time that there was a sudden change in strain gauge recordings, even though in some tests, the strains at the web mid-depth at failure were never greater than the yield strain of the material.

The strain gauge recordings thus show no definite indications of an elastic critical buckling load prior to the overall failure of the beams.

#### 4.4.2 The Southwell Plot

In 1932 Southwell (42) proposed a method for determining the elastic critical load of a strut under test from the recorded load-deflexion characteristics. He showed that for struts having a deflected shape which can be approximated sinusoidally, the curve which results from

plotting the applied load against the central lateral deflexion, can be represented by a rectangular hyperbola. The asymptotes to the rectangular hyperbola are then the zero deflexion line and the critical load. However this only holds when the material is elastic and the deflexions are neither too small to have sufficient accuracy nor too large as to introduce secondary effects.

By changing the axes of the curve, the straight line relationship:

$$P_{cr} \frac{w}{P} = w + w_0 \quad 4.23$$

is obtained, where  $P$  and  $w$  are the load and corresponding deflexion respectively at any time and  $w_0$  any original deflexion that may be present. Hence by plotting  $w/P$  versus  $w$  from the test results, the value of  $P_{cr}$  can be obtained as the inverse of the slope of the resulting straight line.

Timoshenko et. al. (11, 43, 44) have since proposed the method for use with shells, plates and frameworks.

In practice, due to experimental errors, the plot of  $w/P$  versus  $w$  results in a certain amount of scatter and the best fit straight line has to be drawn through the points. If any initial deflexion is large, and hence more dominant than the deflexions incurred under load, the origin of the rectangular hyperbola must be shifted to avoid the initial deflexion to see if the resulting plot yields a better straight line. When the restraint to the loaded ends is altered, there is a corresponding change in slope of the Southwell plot, as was observed by Southwell in his original paper.

#### 4.4.2.1 The Southwell Plot for the Tested Beams

It has been observed from the tests that beams which failed in Modes 1 and 2 had a sinusoidal wave form between the two loaded flanges. However there is necessarily an effect of yield in the vicinity of the applied loads of the test beams, which will affect the applicability of the Southwell plot procedure. There is also the effect of the rotation of the flanges during the test and the possibility of their yielding also.

Figure 4.11 shows the typical Southwell plot for beams tested in Series I. All have very similar forms, showing an initial curve followed by one definite straight line. As the plots show such definite straight lines, it is very likely that the beams in Series I did buckle elastically, the initial curvatures in figure 4.11 possibly being due to the effects of friction on the ball bearing which was used to apply the loads. If the beams did buckle elastically then the effects of the yield area of the beam in the vicinity of the applied loads did not affect the buckling loads significantly, otherwise a change in slope of the plot would probably been apparent.

Figure 4.12 shows the Southwell plot for beams tested in Series II, which were tested by loading with two opposite ball loads as for Series I but applied eccentrically to the web. The two beams with the smallest eccentricities show similar characteristics to beams tested in Series I. However the beam with the largest eccentricity shows, after an initial curve, two straight lines. The second straight line indicates a lower elastic buckling load than the first.



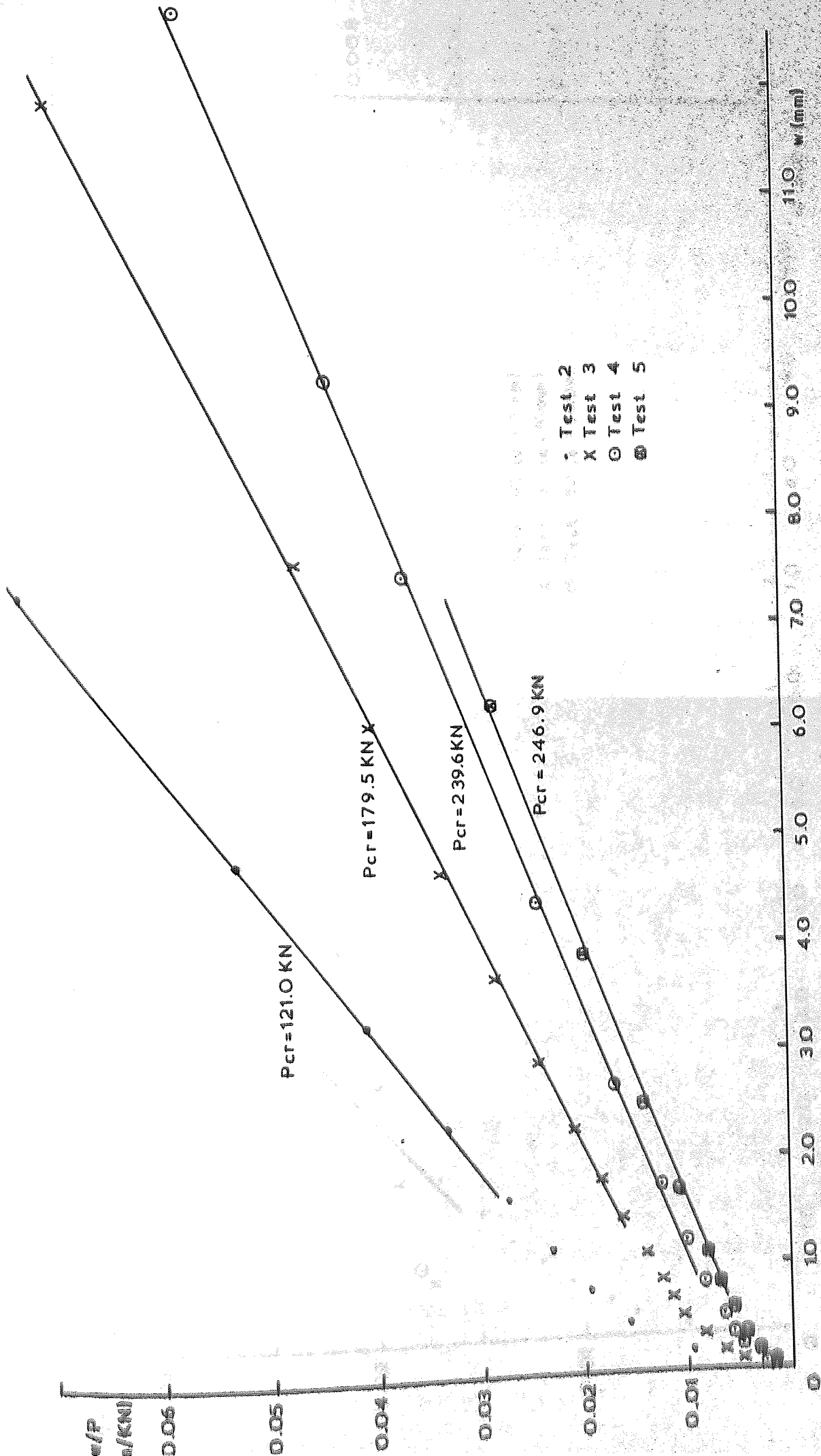


Figure 4.11 Typical Southwell plot for Series I beams.

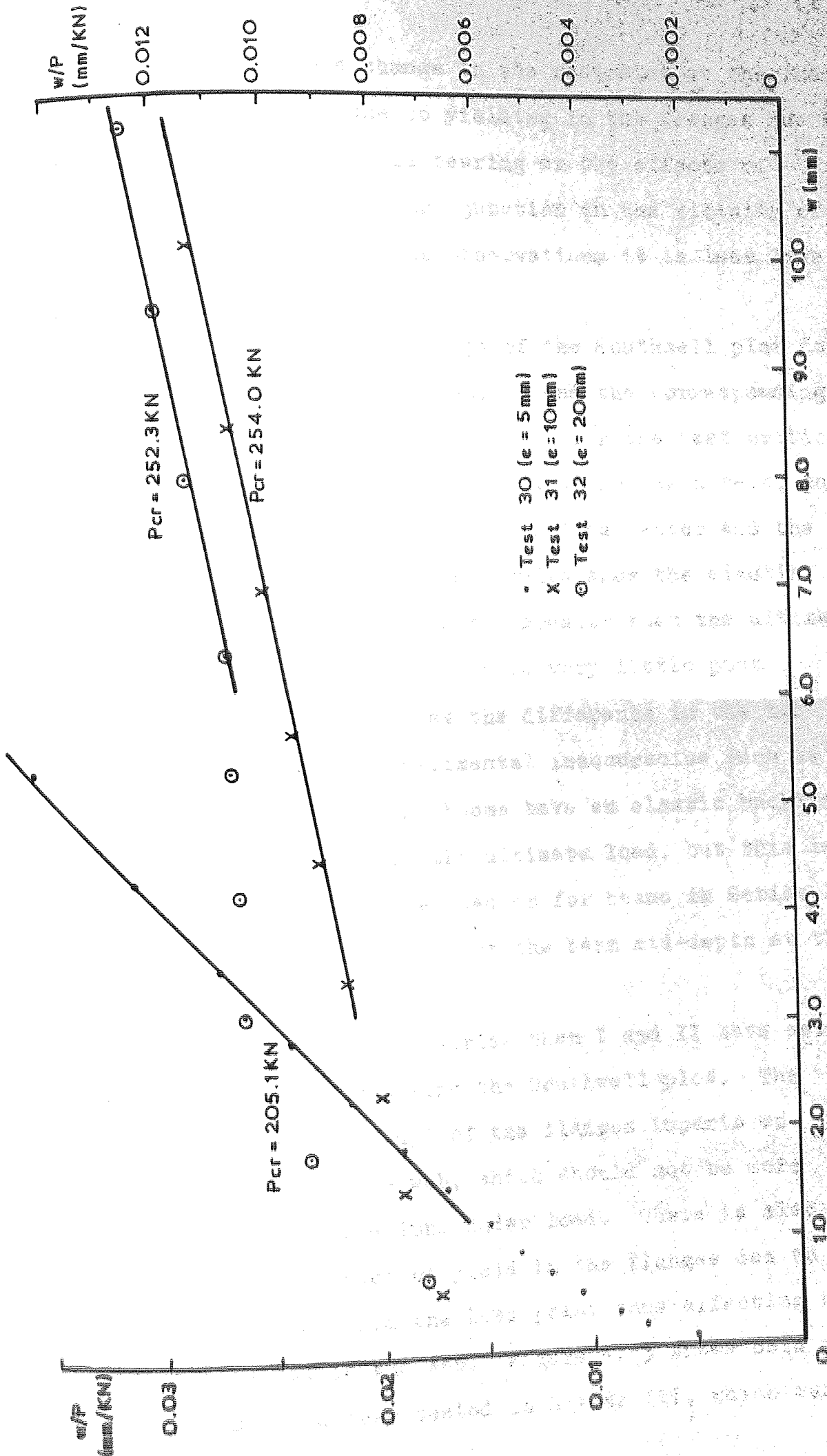


Figure 4.12 Southwell plot for Series II beams.

which could indicate a change in the restraint at the loaded edges. This could be due to yielding in the flanges due to the penetration of the ball bearing or the effects of yielding at the web to flange junction in the vicinity of the load. From the previous observations it is less likely to be the latter.

Table 4.2 shows the results of the Southwell plot for all beams tested in Series I and II and the corresponding value of the plate buckling factor  $K_e$  for the test critical loads. Also shown is the ultimate load for each test, the corresponding value of the plate buckling factor and the ratio of  $K_e / K_u$ . Most of the results show the elastic buckling test load to be slightly greater than the ultimate load. This shows the beams to have very little post buckling strength, if any, as the difference in the two values could be due to experimental inaccuracies such as an initial eccentricity. Some beams have an elastic buckling test load much higher than the ultimate load, but this is due to either spreading the load or for beams in Series II, the onset of yield in the web at the beam mid-depth at the extreme fibres.

Beams tested in other series than I and II have several complications when performing the Southwell plot. The effect of the 'squaring up' of the flanges imparts an initial deflexion to the web, which should not be more dominant than the deflexions under load. There is also the possibility of the onset of yield in the flanges due to their rotation away from the load point thus affecting the restraint provided to the web. Figure 4.13 shows both of these effects for a beam tested in Series III, which was

Test No.	L/d Ratio	Elastic Critical Load (KN)	$K_e$	Ultimate Test Load (KN)	$K_u$	$K_e/K_u$
1	1/2	-	-	62.6	.48	-
2	1	121.0	.93	108.8	.83	1.11
3	2	179.5	1.38	179.3	1.37	1.00
4	3	239.6	1.84	239.1	1.83	1.00
5	4	246.9	1.90	279.0	2.13	.88
6	1/2	97.5	.49	98.2	.50	.99
7	1	153.4	.78	127.0	.64	1.21
8	2	273.2	1.38	236.9	1.20	1.15
9	3	350.9	1.77	308.4	1.56	1.14
10	4*	369.7	2.16	298.5	1.74	1.24
11	1/2	53.8	.37	48.0	.33	1.12
12	1	124.7	.87	117.2	.81	1.07
13	2	145.3	1.01	178.4	1.24	.81
14	3	191.8	1.33	159.9	1.11	1.20
15	3*	-	-	280.0	1.94	-
16	1/2	53.6	.32	54.7	.32	.98
17	1	167.1	.99	127.7	.76	1.31
18	2	203.4	1.20	236.2	1.40	.86
19	3	265.2	1.57	216.9	1.28	1.22
20	1/2	114.9	.58	107.3	.54	1.07
21	1	173.9	.88	159.4	.81	1.09
22	2	222.2	1.13	255.1	1.29	.87
23	3*	384.6	2.25	292.8	1.71	1.31
24	1/2	138.9	.62	109.3	.49	1.27
25	1	197.2	.88	173.6	.77	1.13
26	2	265.5	1.18	249.5	1.11	1.06
27	3	295.0	1.32	272.2	1.21	1.08
28	1	226.0	.70	218.6	.68	1.03
29	2 1/2*	330.4	1.19	264.6	.95	1.25
30	3+	205.1	1.65	187.3	1.50	1.09
31	3+	254.0	2.03	123.0	.99	2.06
32	3+	252.3	2.02	115.6	.93	2.18

\* Load spread by 75mm plate.

+ Load applied eccentrically to web.

Table 4.2 Results of the Southwell plot for beams tested in Series I and II.

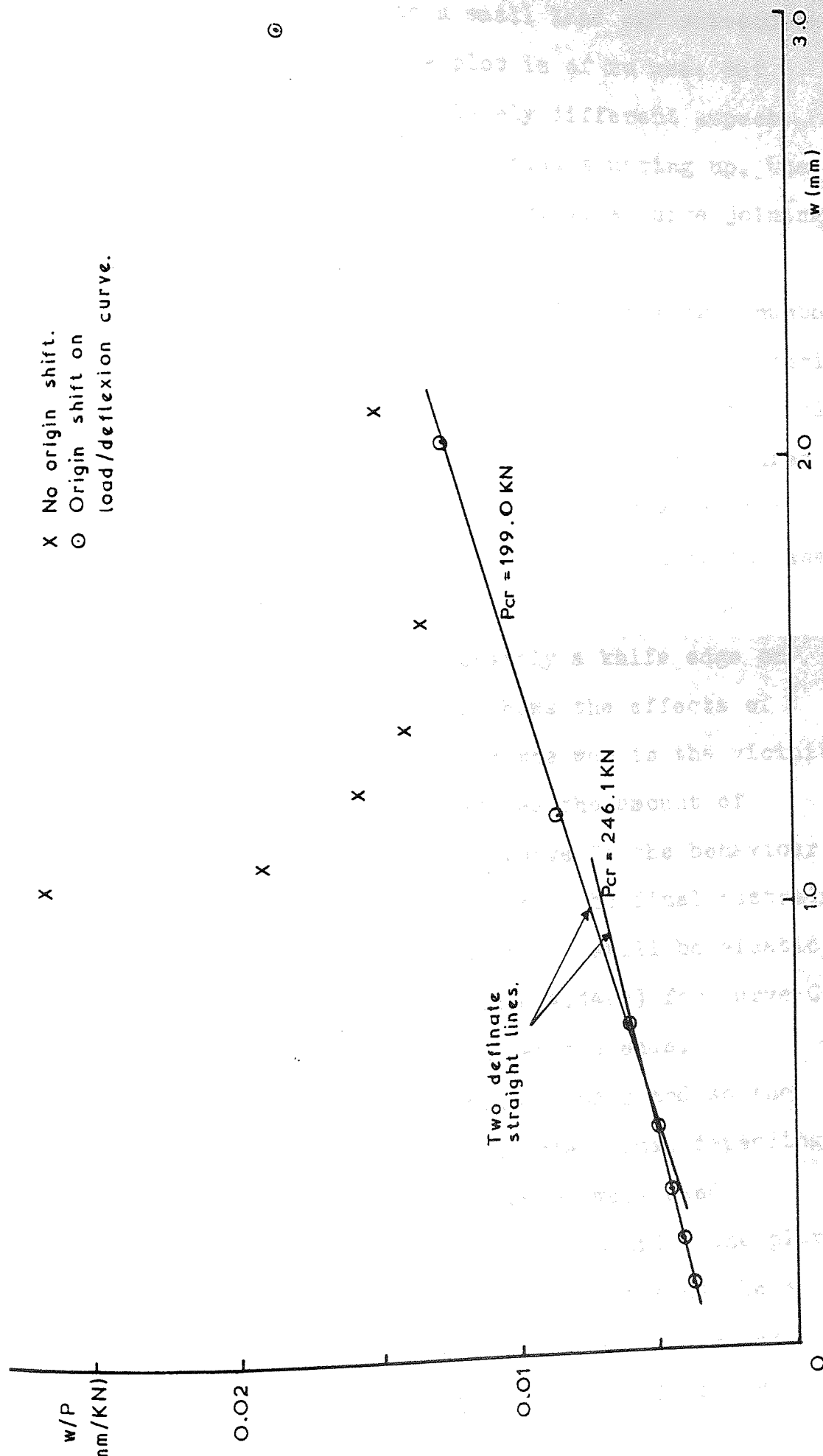


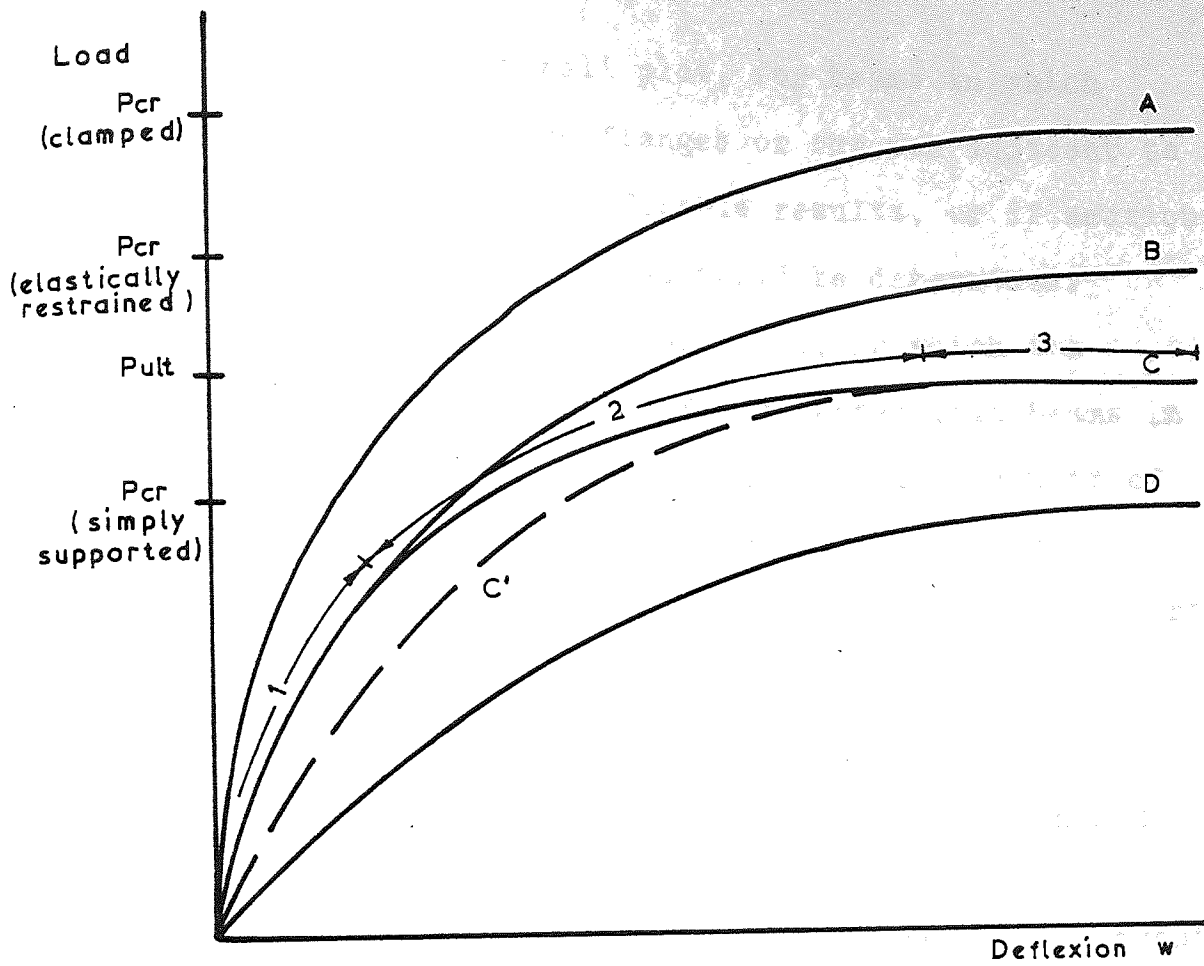
Figure 4.13 Typical Southwell plot for Series III beams.



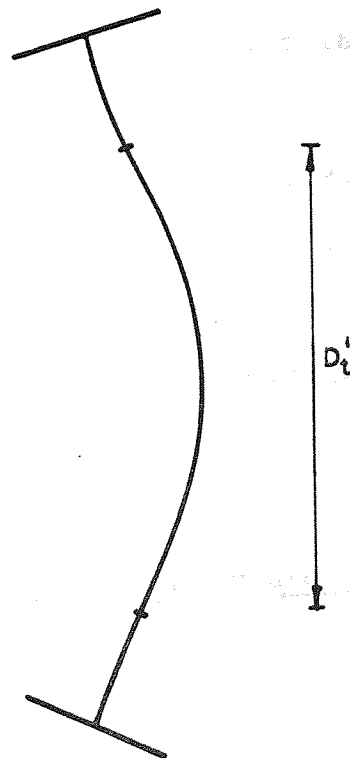
loaded by two opposite knife edge loads at mid-length. When the initial deformation due to a small load and subsequent flange movement is included the plot is of no use; but shifting the origin shows a completely different aspect. After removing the effect of the initial squaring up, the plot shows two straight lines, or possibly a curve joining all the points.

The possibility of the Southwell plot showing a number of straight lines or a curve can be explained by considering the curves of figure 4.14(a). Curves A and D show typical load-deflexion curves for a plate having the loaded edges fully restrained and simply supported respectively, the plate remaining elastic everywhere. Curve B shows the same thing for an ideally fully elastic plate having some restraint on the loaded edges, possibly a knife edge on elastic flanges. However curve C shows the effects of plasticity in either the flanges or the web in the vicinity of the loads which effectively reduces the amount of restraint on the loaded edges, and curve C' the behaviour which would be observed if the beam had the final restraint in curve C at zero load. The beam would still be elastic over the depth  $D_t$  as shown in figure 4.14(b) for curve C but would have an unknown restraint at the ends.

Curve C is asymptotic to both C' and B and so the Southwell plot could have three possible forms, depending on which points on the load-deflexion curve were used. Referring to figure 4.14(a), for lengths 1 and 3 the plot would be a straight line and for length 2 it would be a curve. The lengths of all sections 1, 2 and 3 are variable and the difference between the load at B and C is also



(a)



(b)

Figure 4.14

variable. Hence the Southwell plot, for beams in which there is any yielding in the flanges or the web adjacent to the flanges would lead to undefinable results, or if section 3 were used only the failure load would be determined.

These points are shown in Table 4.3, in which the Southwell plot results are shown for selected test beams in Series III to VI. The majority merely show the results of the inverse slope of the best fit straight line when approximating section 3 of curve C in figure 4.14(a) to part of a rectangular hyperbola.

#### 4.4.3 Conclusions from the Test Elastic Critical Loads

From this section it can be seen that the only relevant comparison with the theory will be the failure load for Series III to VI and the load obtained from the Southwell plot for Series I and II, although the latter was found to be very near to the failure load.

The test ultimate loads were generally attained while the stresses at the web mid-depth were lower than the yield stress of the steel, and so comparing the ultimate loads with the elastic buckling theory would seem to be most beneficial.

#### 4.5 Comparison of Developed Theory and the Test Results

The value of  $K_u$  for beams in Series I (tested by two opposite ball loads at mid-length) are compared with the elastic buckling theory in figure 4.15. The discontinuous theoretical curve is an approximation of the continuation of

Test No.	Elastic Critical Load (KN)	$K_e$	Ultimate Test Load (KN)	$K_u$	$K_e/K_u$
34	261.1	2.05	323.8	2.54	.81
35	326.4	2.56	355.2	2.79	.92
36	327.4	2.57	360.2	2.83	.91
37	209.4	1.03	210.1	1.03	1.00
39	327.9	1.61	327.3	1.61	1.00
40	327.9	1.61	344.8	1.69	.95
41	153.2	1.09	123.8	.88	1.24
42	199.0	1.41	175.6	1.25	1.13
43	225.0	1.60	211.0	1.50	1.07
44	247.9	1.76	215.6	1.53	1.15
45	200.0	1.22	215.7	1.32	.93
46	324.2	1.99	320.2	1.96	1.01
47	289.3	1.77	371.0	2.27	.78
48	373.1	2.29	359.5	2.20	1.04
49	145.6	.76	149.8	.79	.97
50	222.2	1.17	224.7	1.18	.99
51	319.6	1.68	260.1	1.36	1.23
52	348.4	1.83	276.2	1.45	1.26
53	181.6	.83	159.1	.73	1.14
54	303.6	1.39	236.5	1.09	1.28
55	280.1	1.29	277.7	1.28	1.01
60	307.7	2.72	287.4	2.54	1.07
61	260.4	2.09	268.7	2.16	.97
62	227.2	1.71	241.6	1.81	.94
63	198.5	1.56	219.2	1.72	.91
64	164.8	1.29	193.8	1.51	.85
66	927.6	1.51	921.8	1.50	1.01
67	311.0	2.73	277.8	2.44	1.12
68	278.0	2.44	271.6	2.39	1.02
69	216.5	1.90	219.2	1.92	.99
70	153.5	1.22	155.6	1.24	.99
71	411.7	3.28	450.8	3.59	.91
72	480.4	3.72	416.0	3.22	1.16
73	534.2	4.97	515.7	4.80	1.03
74	989.2	8.78	784.7	6.97	1.26
78	449.9	1.58	452.8	1.59	.99
79	625.0	2.19	601.9	2.11	1.04
80	854.7	3.00	797.2	2.80	1.07
81	1250.0	4.38	1220.7	4.28	1.02
83	336.5	2.36	348.5	2.45	.97
84	339.2	2.38	397.6	2.79	.85
85	684.9	4.81	563.0	3.95	1.22
86	1136.4	7.98	827.1	5.81	1.37
87	2156.3	15.14	997.2	7.00	2.16

Table 4.3 Results of the Southwell plot for selected beams in Series III to VI.

$$\beta = C/m = 0.$$

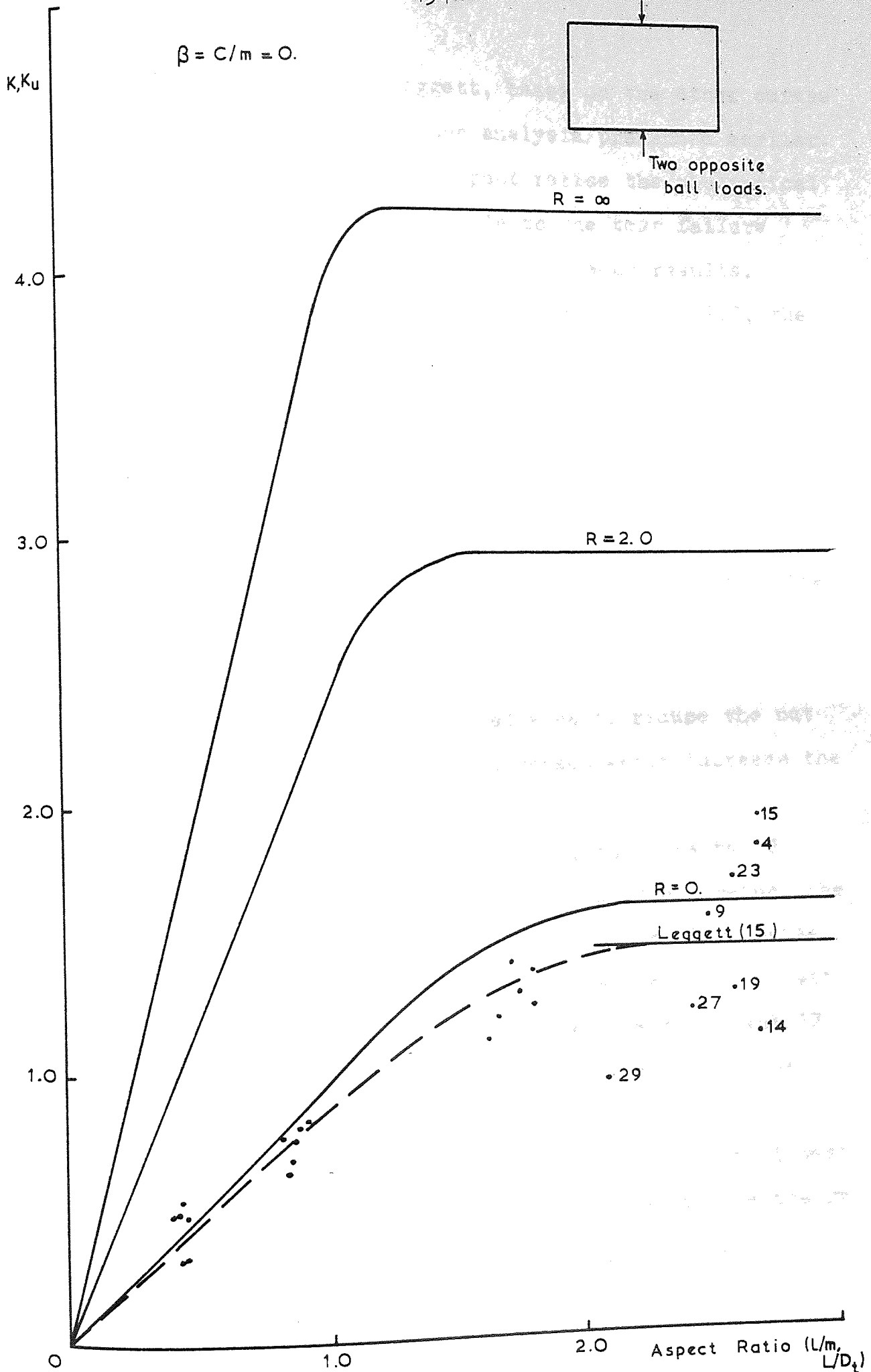


Figure 4.15 Series I test results compared with elastic



the exact solution due to Leggett, based on the other curves for varying values of  $R$  from the analysis presented earlier. It can be seen that for small aspect ratios the theoretical elastic buckling load is comparable to the test failure loads, with a small amount of scatter between results.

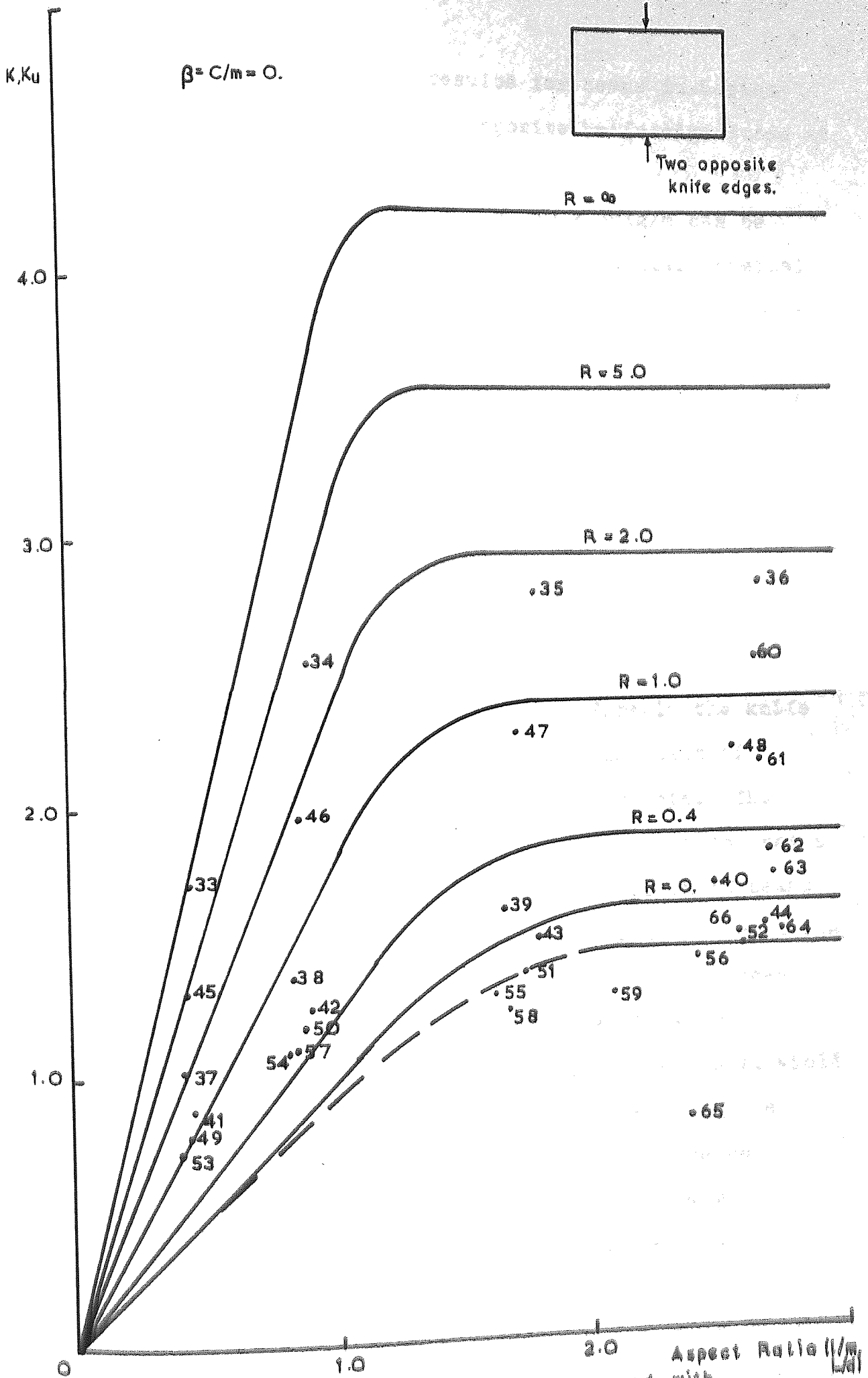
For aspect ratios greater than approximately 2.0, the difference between the theory and the test results is considerably greater, and with a much greater scatter. However several of the results in that region can be explained.

Tests 15 and 23 were loaded by a ball bearing on a spreader plate 75mm long which would therefore increase the ratio  $\rho$  in the analysis and hence increase the buckling load. For long beams one would also expect the resistance of the flanges away from the loaded area to reduce the out of plane deflexions of the web and consequently increase the buckling load.

For aspect ratios greater than 2.0, the effects of yielding in the region of the applied loads could reduce the elastic buckling load of the section. Test 14 illustrates this fact, as the beam tested was identical to that of test 15 which utilised a small spreader plate. Tests 19 and 27 could be lower just due to scatter, or they too could be influenced by local yielding.

The only apparently inexplicable result is that of test 29 which gives a very low result when compared to the theory even though the load was applied through a spreader plate. However, it is possible that this beam crushed under the load point even with the spreader plate.

Figure 4.16 shows the comparison of the elastic



buckling theory and the test results for beams in Series III, which were tested with two opposite knife edge loads at mid-length.

The beams of serial size 406 x 140 x 39Kg/m can be considered first. Tests 33 - 36 had very similar physical properties but varied in length, whereas tests 36 and 60 - 64 were all the same length but had varying flange thicknesses. It can be seen that for a short length of beam the result shows the flanges to fully restrain the web at its loaded edges. The restraint reduces for an increase in beam length, until it finally remains constant. It can be seen that reducing the flange thickness reduces the restraint for longer lengths of beam.

There are two reasons for the reduction of the restraint for increases in beam length. Firstly the knife edge loading prevents flange rotation at its point of application, but elsewhere the flanges can rotate. The knife edges would therefore restrict flange rotation over a greater fraction of the length of the beam for short beams than for long beams and hence effectively fully restrain the whole of the loaded edges for a short beam. The flanges could also yield for the longer beams thus allowing considerable flange rotation. Secondly, the web could yield at its junction with the root radius, thus reducing the resistance to bending of the web at that point, hence reducing the restraint to the web. This would be more pronounced for longer lengths due to the higher loads involved.

This second point would also explain the tests which have reduced flange thicknesses as the stress concentration

at the web root would be greater and hence the resistance to bending of the web less. The relationship between  $K_u$  and the value of  $T$  to various powers is shown in figure 4.17, which seems to indicate that  $K_u$  is proportional to either  $T^2$  or  $T^3$ . However as the other properties of the sections are quite similar this is approximately the same as saying that  $P_u$  is proportional to  $T^2$  or  $T^3$ .

Tests 45 - 48 show similar characteristics to those mentioned above as do tests 37 - 40, although even for short lengths the restraint to the loaded edges is less than full restraint. The other test results show similar characteristics also, but at long lengths fall on the zero restraint curve or just slightly below. The reasons for the reduction of the restraint to the loaded edges can be explained as previously for tests 33 - 36.

It is the least slender sections which have the lowest restraint for short lengths. This could mean that for a less slender section the thickness of the flanges would have to be increased by a very large amount to create the fully restrained condition, or that the effects of crushing at the load point is considerable due to the high loads involved.

Test number 65 cannot be explained at this stage, and can be seen to fall well below the zero restraint curve even though it failed in a Mode 2 pattern.

Figure 4.18 shows the comparison between the theory and the test results for beams in Series V, which were tested with two opposite uniformly distributed loads at mid-length. Also shown on the same graph are some relevant results from Series III, in which case the length of the uniformly distributed load is zero. All four beam serial sizes shown

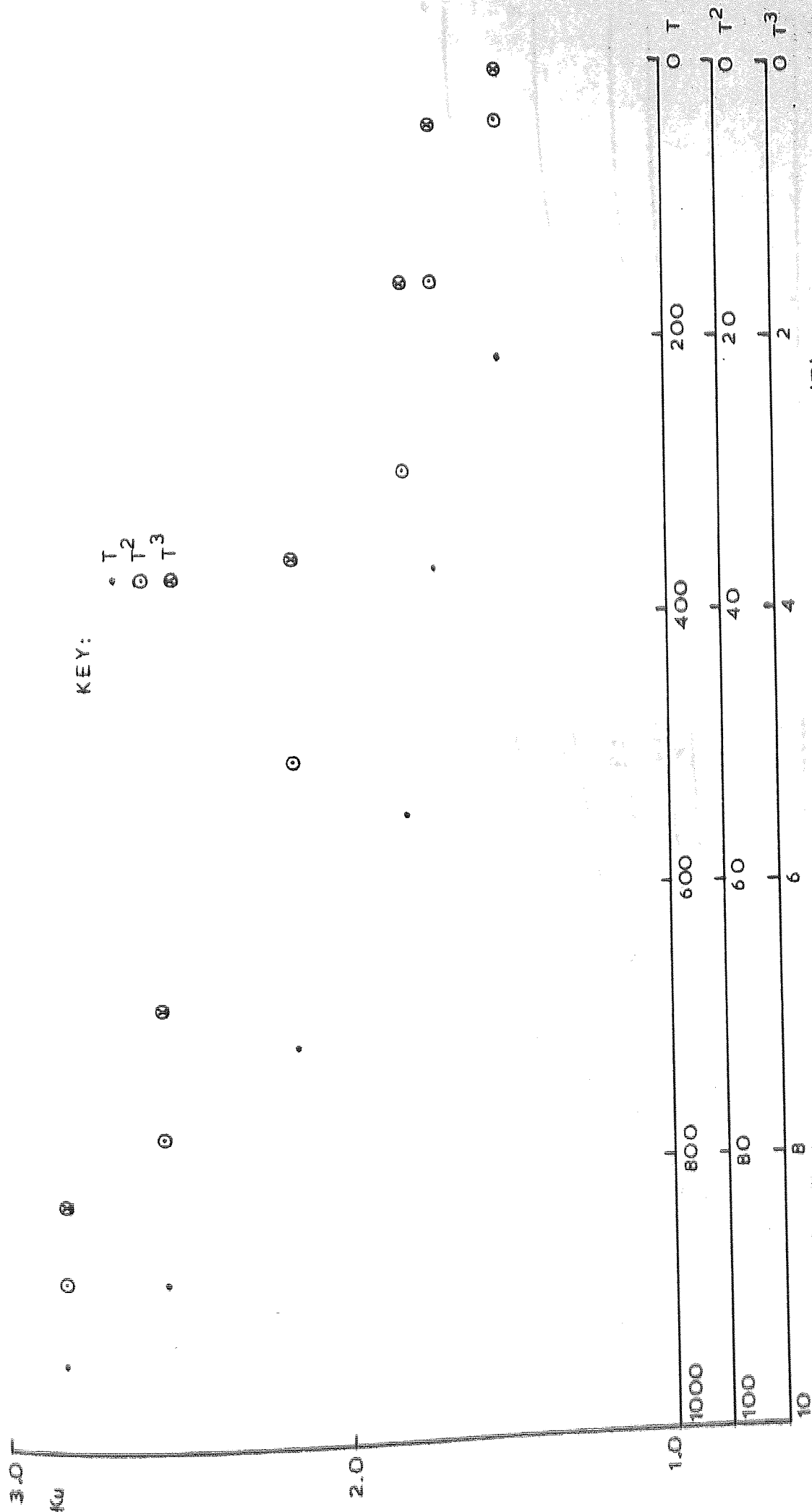


Figure 4.17 Variation of Kw with flange thickness (T).



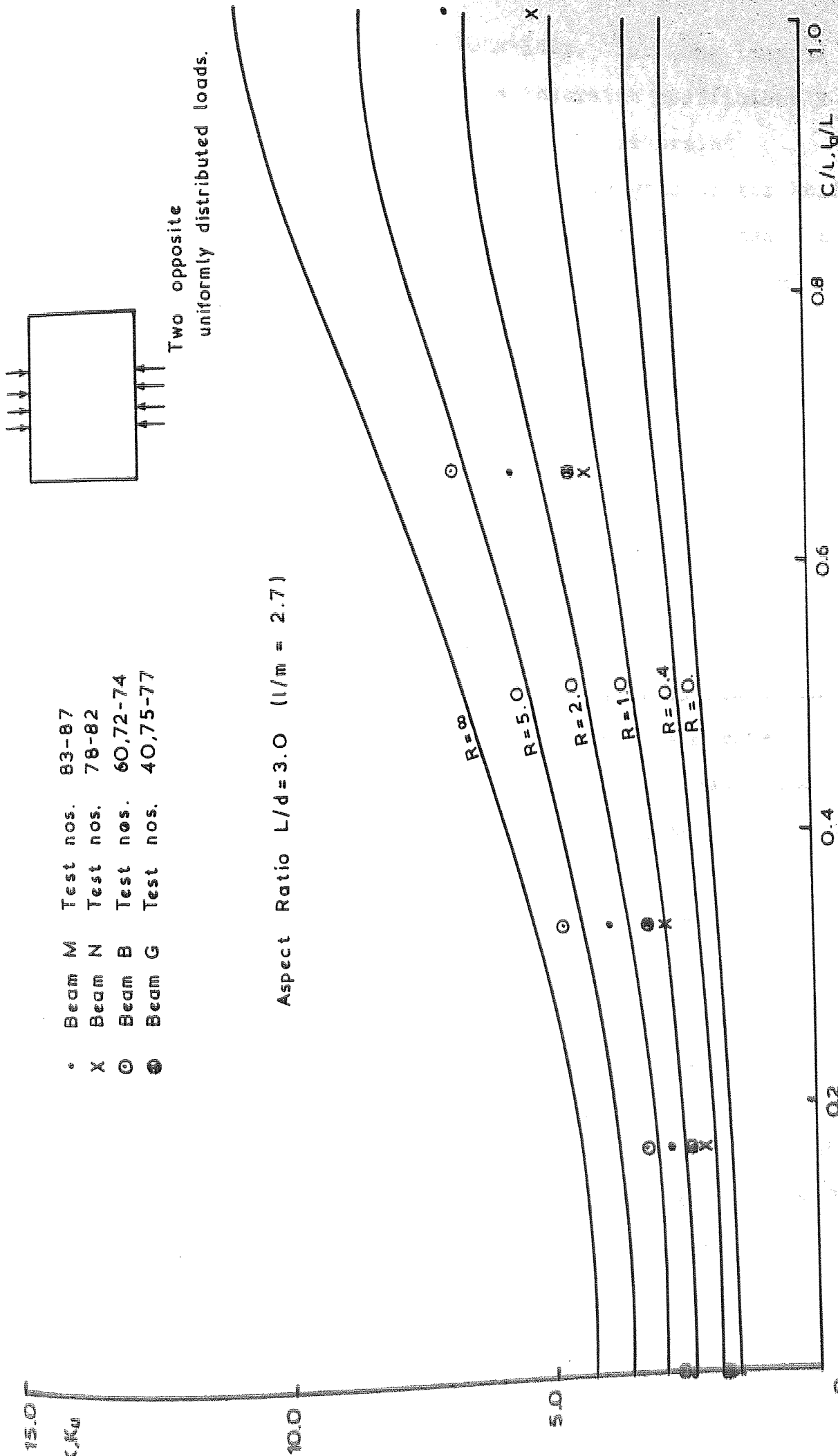


Figure 4.18 Series V test results compared with elastic buckling theory.

on the graph exhibit the same behaviour. For long lengths of uniformly distributed load, the restraint coefficient  $R$  for each beam is almost constant, but the restraint coefficient is reduced for short loaded lengths or for knife edge loads. This is a similar pattern to that of beams in Series III. The value of  $R$  for beams with long uniformly distributed loads from figure 4.18 would be expected to be the same as that for short beams loaded by knife edges. This can be observed for beam reference G.

#### 4.6 Conclusions from the Comparison

Whatever the loading conditions, it can be seen that, from the comparisons of the test results with the developed theory, the less slender beams always show less restraint provided by the flanges. Assuming that the beam webs buckled elastically, then this indicates that less slender beams would need flanges of considerably greater dimensions than slender beams to effect the same restraint to the loaded edges. It is possible therefore that the less slender webbed beams, despite having thicker flanges than the slender beams used in the tests conducted for this work, have flanges far smaller than necessary to provide any substantial restraint to the loaded edges. If all the beam webs did buckle elastically, then the previous section has shown that the value of  $K$  varies with either the square or the cube of the flange thickness for beams loaded with two opposite knife edges.

The effects of the high stresses in the vicinity of the loads must also be considered. For the knife edge loads it

has been shown that the area of the web at its junction with the root radius reaches the yield stress of the steel at relatively low loads. This would affect the bending resistance of the web at the most critical point and thus reduce the loaded edge restraint. However the strain gauges positioned at other web locations have already shown that the extreme fibre stresses are nearly always less than the yield stress for the remainder of the web until very near the failure load. This is verified by the Southwell plot which produces a good straight line near to failure indicating the deflected shape to be sinusoidal.

These factors seem to indicate an elastic buckle of the web, but in the presence of local crushing in the vicinity of the loads and possible flange yield. The elastic buckle could therefore still be a post crushing or post yielding failure, the web buckle occurring only when sufficient yielding and hence reduction in flange restraint is present.

## CHAPTER 5 - YIELD LINE THEORY

### 5.1 Introduction

When a universal beam is subjected to concentrated loads on its flanges in the plane of the web, the web will undergo out of plane deflexions and the flanges will distort. As the load is increased, so the out of plane deflexions will increase until the web reaches its elastic critical load or the section yields in certain regions. The out of plane deflexions could result in the web reaching its yield stress at the outer fibres at a load very much lower than the elastic buckling load, particularly for less slender webbed beams. In this case the resistance to bending of the web, and possibly the flange could be of prime importance in determining the maximum load that a section can sustain.

The theory presented in this chapter is an attempt to provide a simple method of determining the maximum load that a universal beam section can sustain when it has yielded at its outer fibres in certain regions. The resulting expressions for the ultimate load are shown to be dependant on a dimensionless ratio  $\Delta/w_c$ . It is shown that a semi-empirical value for this ratio gives good results when compared with test results of a wide range of universal beams.

## 5.2 Yield Line Method

The method is based on the formation of yield lines due to large deflexions, thus causing a failure mechanism for the beam, consistent with the loading and restraint conditions. The ultimate load is attained when the ultimate moment of resistance in bending is developed along each yield line. If more than one pattern of yield lines satisfies the prescribed conditions, then that which provides the least resistance will be dominant.

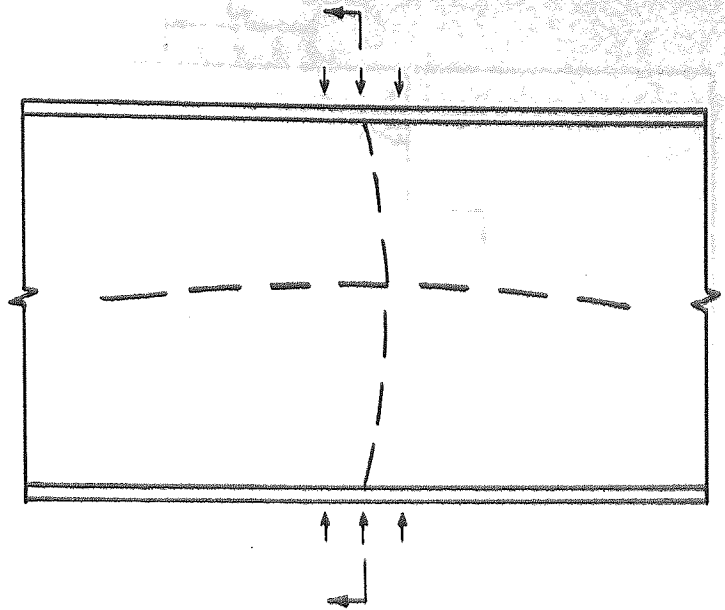
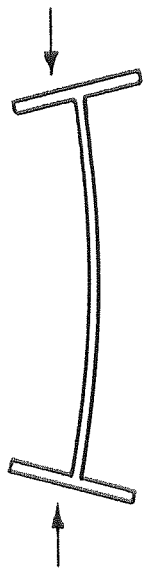
In the following analyses, only the yield line pattern which provides the least resistance is shown. It is possible that in some instances an alternative yield line pattern will give the same result as the one used in the text.

Three possible failure modes are considered for beams with the loading and restraint conditions of Series I to VI and are shown in figure 5.1. The actual deflected shape would be a smooth wave form but for the analyses which follow a simplified shape is assumed.

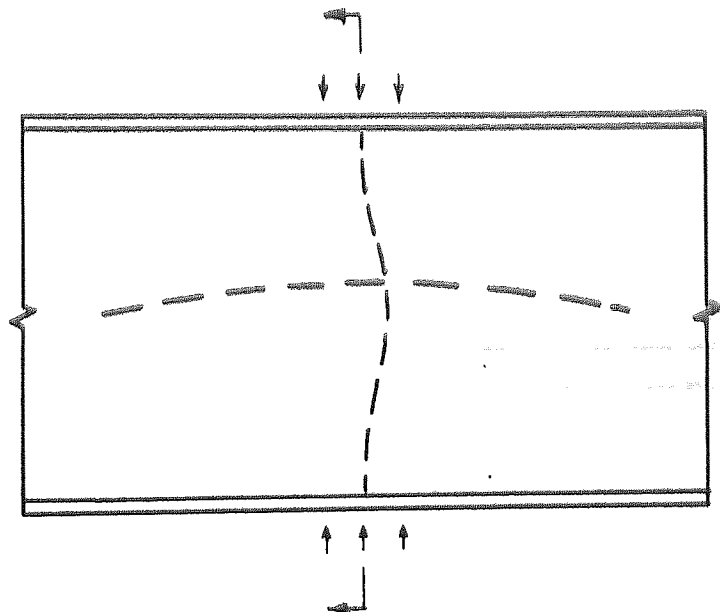
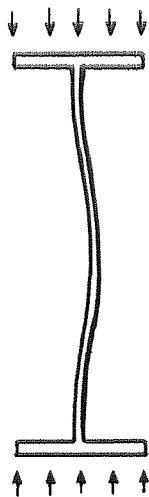
### 5.2.1 Mode 1

The yield line pattern which forms will depend on the length of the applied load  $l_a$ , the overall length of the beam  $L$  and the distance of the applied load from the end of the beam  $l_e$ . The three possible yield line patterns considered, types (i), (ii) and (iii) are shown in figure 5.2. A section drawn through the applied loads will be identical for all three pattern types and is shown in figure

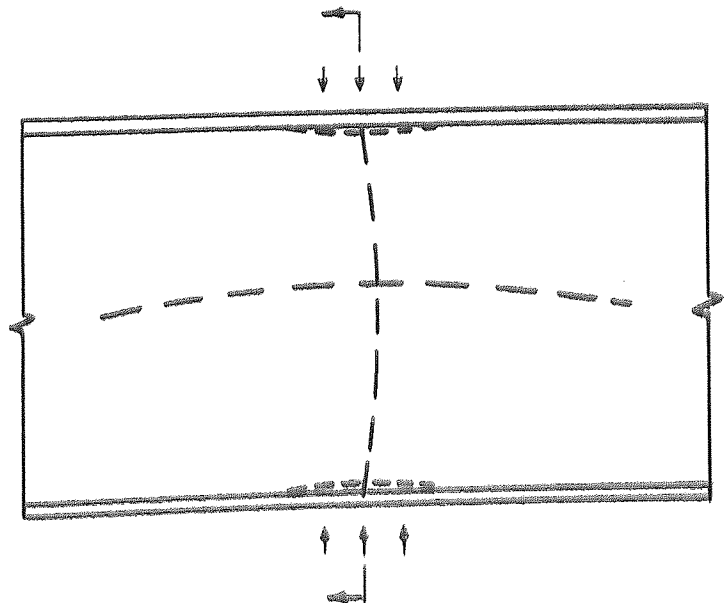
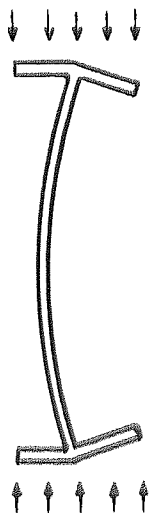




(a) Mode 1



(b) Mode 2



(c) Mode 3

Figure 5.1 Possible failure modes dependent on flange restraint.

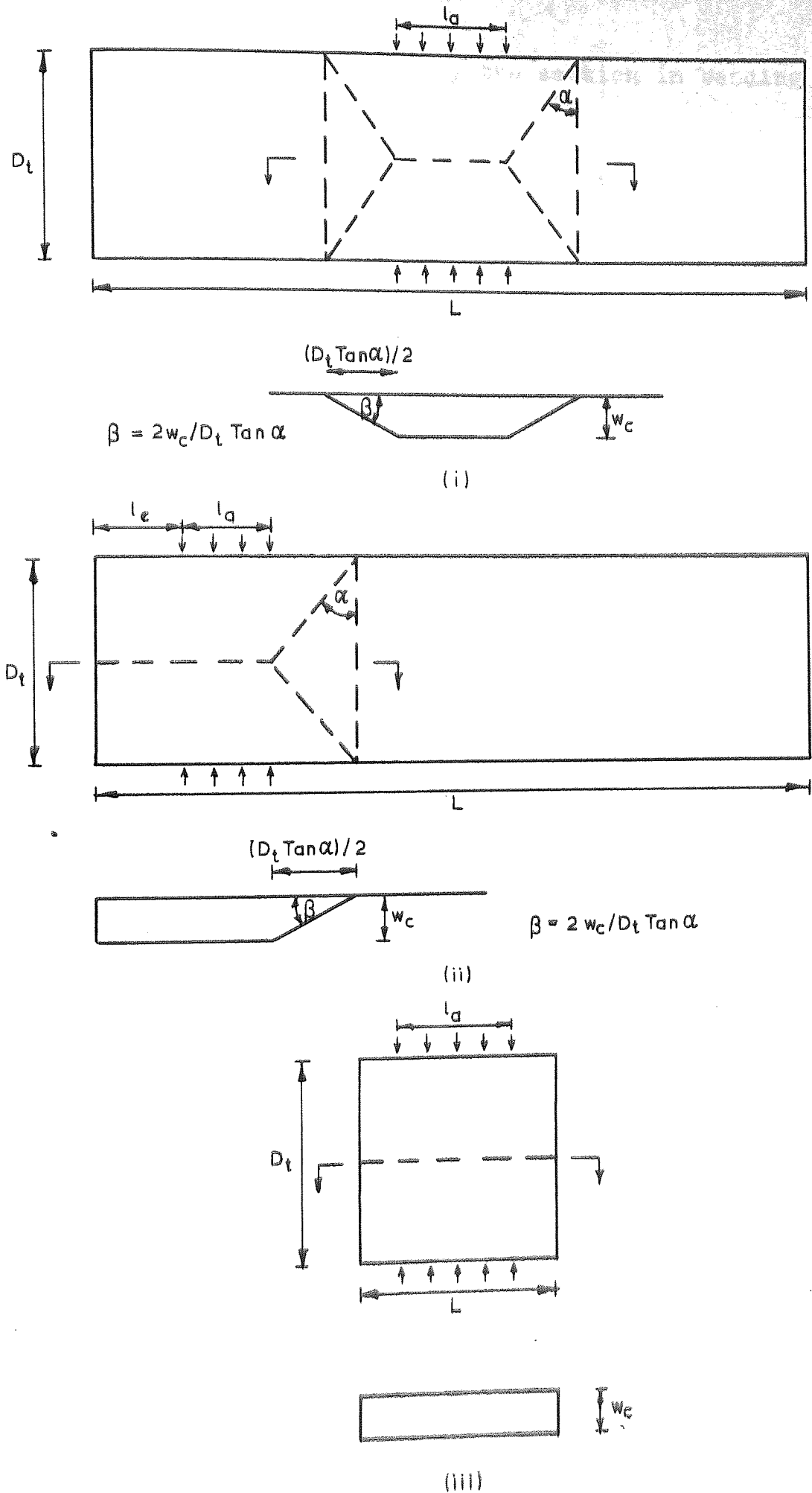


Figure 5.2 Mode I yield line patterns.

5.3. For type (i) the work done by the section in bending along the yield lines is:

$$4 D_t \beta Mw + 2 D_t \tan \alpha \theta Mw + l_a Mw \theta$$

or:

$$Mw ( 4 D_t \beta + 2 D_t \theta \tan \alpha + l_a \theta ) \quad 5.1$$

where Mw is the ultimate moment of resistance in bending per unit length of the web (  $f_{yw} t^2 / 4$  ).

The work done by the applied loads is;

$$2 P \Delta_1 + 2 P e \theta \quad 5.2$$

Equating the work done by the applied loads to the work done by the section in bending:

$$P = \frac{Mw ( 4 D_t \beta + 2 D_t \theta \tan \alpha + l_a \theta )}{2 ( \Delta_1 + 2 w_c e / D_t )} \quad 5.3$$

and hence:

$$P = 2 Mw \left( \frac{2}{\tan \alpha} + \frac{l_a}{D_t} \right) / \left( \frac{\Delta_1}{w_c} + \frac{2 e}{D_t} \right) \quad 5.4$$

$\alpha$  is variable and so the minimum value of P is obtained when  $dP / d\alpha = 0$ :

$$\sec^2 \alpha - 2 \operatorname{cosec}^2 \alpha = 0$$

hence:

$$\tan \alpha = \sqrt{2}$$

and using this value in 5.4:

$$P (i) = 2 Mw \left( 2\sqrt{2} + \frac{l_a}{D_t} \right) / \left( \frac{\Delta_1}{w_c} + \frac{2 e}{D_t} \right) \quad 5.5$$

where P(i) represents the ultimate load for a type (i)

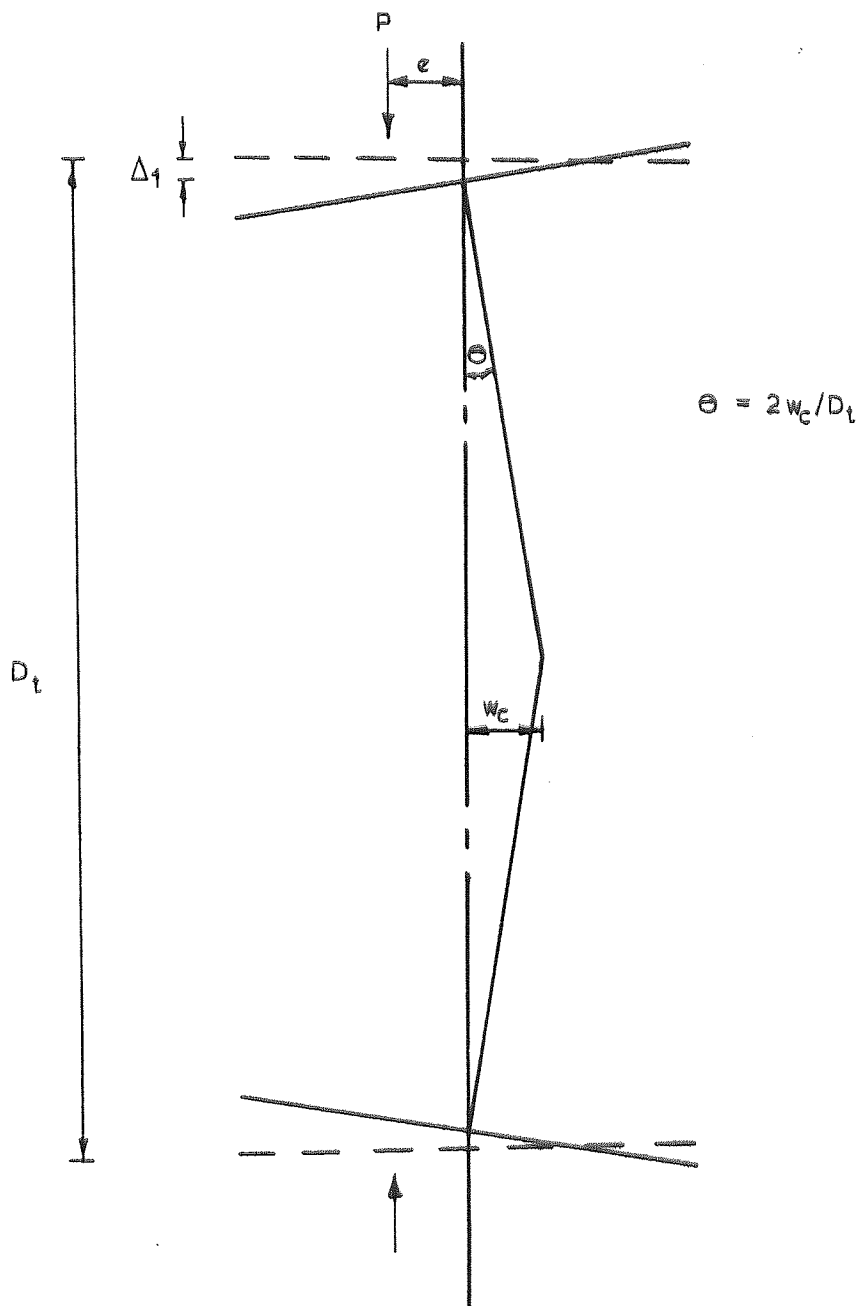


Figure 5.3 Mode I - section through applied loads (diagrammatic).

pattern. Using the same procedure for types (ii) and (iii):

$$P(ii) = 2 Mw \left( \sqrt{2} + \frac{l_a}{D_t} + \frac{l_e}{D_t} \right) / \left( \frac{\Delta_1}{w_c} + \frac{2e}{D_t} \right) \quad 5.6$$

$$\text{and } P(iii) = 2 Mw \left( \frac{L}{D_t} \right) / \left( \frac{\Delta_1}{w_c} + \frac{2e}{D_t} \right) \quad 5.7$$

The conditions of length for each type to occur are:

$$P(ii) \leq P(i) \quad \text{if } l_e / D_t \leq \sqrt{2}$$

$$P(iii) \leq P(i) \quad \text{if } L / D_t \leq 2\sqrt{2} + l_a / D_t \quad 5.8$$

$$P(iii) \leq P(ii) \quad \text{if } L / D_t \leq l_e / D_t + \sqrt{2} + l_a / D_t$$

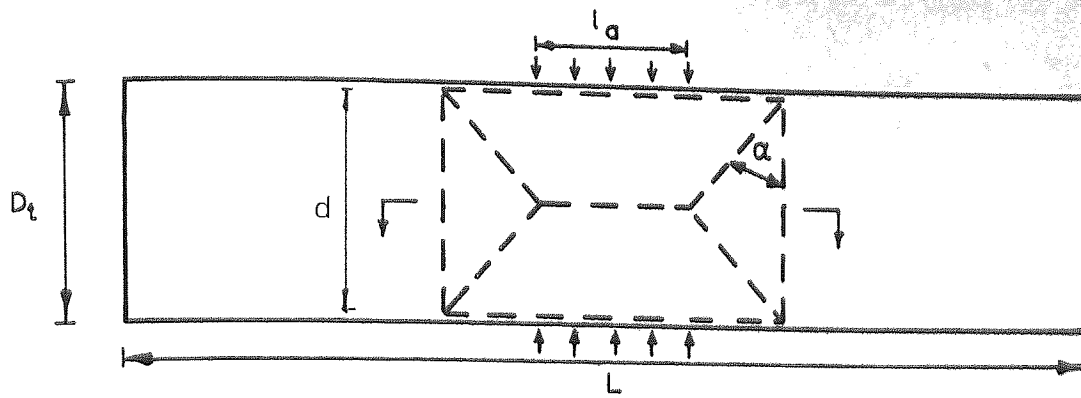
These results are shown graphically in figure 5.4 (for  $e = 0$ ). Referring to figure 5.4, a beam loaded by a point load would be on the line OA or in the region ABCD, the shaded area, depending on the length of the beam. If a beam were loaded at its end, then as the length is increased,  $\lambda$  would be indicated by the line OAB, and if it were loaded at the centre by the line OCD. The shaded area therefore represents a beam loaded by a point load at various distances from the end.

### 5.2.2 Mode 2

The yield line patterns used for a Mode 2 failure are shown in figure 5.5, and the corresponding section drawn through the line of action of the applied loads is shown in figure 5.6. The basic difference in this mode from Mode 1 is the inclusion of yield lines along the web adjacent to the flanges. For a type (i) pattern, the work done by the

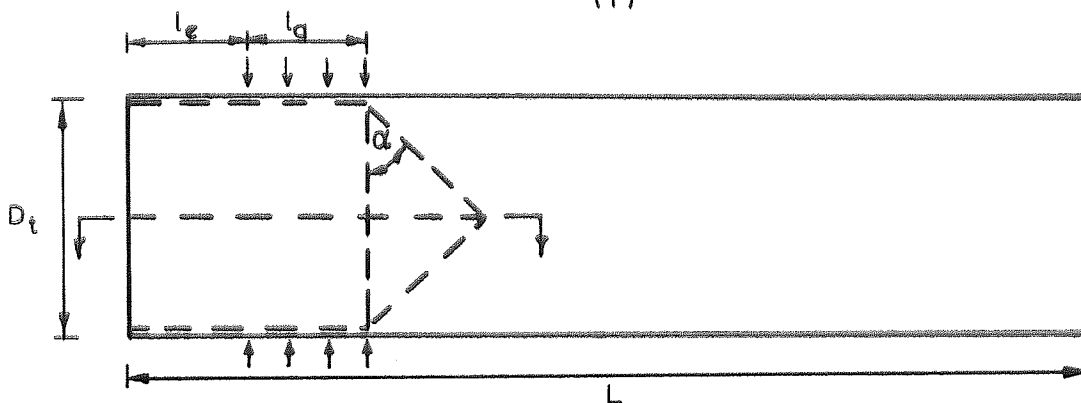






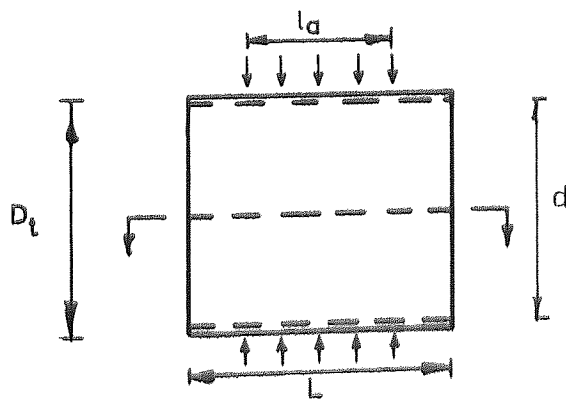
$$\beta = 2w_c / d \tan \alpha$$

(i)



$$\beta = 2w_c / d \tan \alpha$$

(ii)



(iii)

Figure 5.5 Mode 2 yield line patterns.

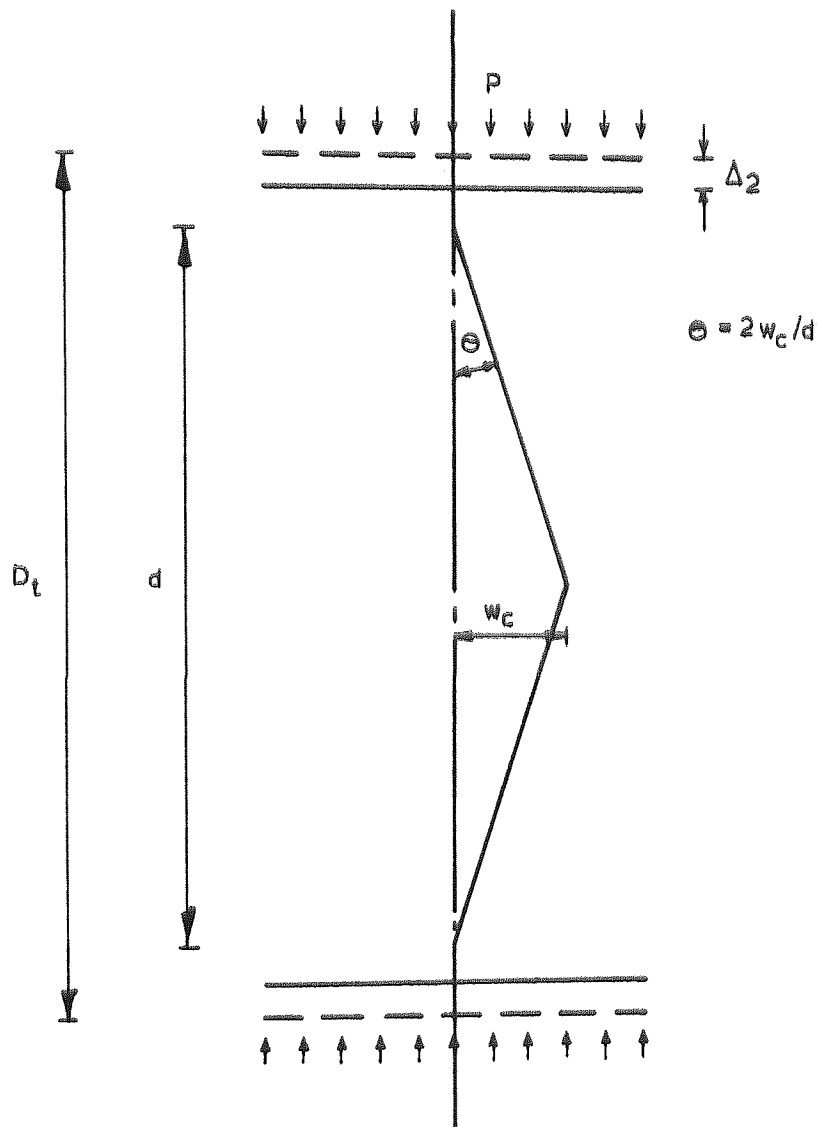


Figure 5.6 Mode 2-section through applied loads (diagrammatic).

section in bending is:

$$4 d M w \beta + 4 d M w \theta \tan \alpha + 4 l_a M w \theta \quad 5.9$$

The work done by the applied loads is  $2 P \Delta_2$  and so by equating the external work to the internal work:

$$P = 4 M w (d \beta + d \theta \tan \alpha + l_a \theta) / \Delta_2 \quad 5.10$$

and hence:

$$P = 4 M w \left( \tan \alpha + \frac{1}{\tan \alpha} + \frac{l_a}{d} \right) \left( \frac{w_c}{\Delta_2} \right) \quad 5.11$$

Minimising  $P$  with respect to  $\alpha$ :

$$\frac{dP}{d\alpha} = 0 = \sec^2 \alpha - \operatorname{cosec}^2 \alpha$$

thus  $\tan \alpha = 1$  and equation 5.11 becomes:

$$P(i) = 4 M w \left( 2 + \frac{l_a}{d} \right) \left( \frac{w_c}{\Delta_2} \right) \quad 5.12$$

and in the same way:

$$P(ii) = 4 M w \left( 1 + \frac{l_a}{d} + \frac{l_e}{d} \right) \left( \frac{w_c}{\Delta_2} \right) \quad 5.13$$

$$P(iii) = 4 M w \left( \frac{L}{d} \right) \left( \frac{w_c}{\Delta_2} \right) \quad 5.14$$

The conditions of length for each failure type to occur are:

$$P(ii) \leq P(i) \quad \text{if} \quad l_e / d \leq 1$$

$$P(iii) \leq P(i) \quad \text{if} \quad L / d \leq 2 + l_a / d \quad 5.15$$

$$P(iii) \leq P(ii) \quad \text{if} \quad L / d \leq l_e / d + 1 + l_a / d$$

These results are shown in figure 5.7 in a similar manner to those previously presented for Mode 1. In this case  $(w_c/\Delta_2)$  is not the same as  $(w_c/\Delta_1)$  for Mode 1.

### 5.2.3 Mode 3

This mode assumes that the flanges yield first followed by a web failure similar to that presented as Mode 1. The three types of flange yield line patterns are shown in figure 5.8 and the common section through the line of action of the applied loads is shown in figure 5.9. If the web remains perpendicular to the flange outside the area formed by the flange yield lines (figure 5.9) then the rotation of the flange will be  $\theta$  at the load point. The flange will rotate at the weakest section which is its junction with the root radius. This rotation  $\theta$  is the same as the rotation of the web at the same location.

For a type (i) yield line pattern, the internal work done by one flange during rotation along the yield lines is:

$$\frac{2 M_f w_c}{D_t} \left( l_a + 4 s_b \tan \bar{\omega} + \frac{2 s_b}{\tan \bar{\omega}} \right) \quad 5.16$$

where  $M_f$  is the ultimate moment of resistance in bending per unit length of the flange  $(T^2 f_y f / 4)$ . For the section to assume the shape shown in figure 5.9 on the line of action of the two forces, the load must be eccentric to the web. Let the load act uniformly on the reduced width  $s_b$ , the distance from the flange edge to the junction of the root and the flange, and let  $P_f$  be the force required to distort the flanges only. Then

$$P = P_f + P \text{ (Mode 1)} \quad 5.17$$

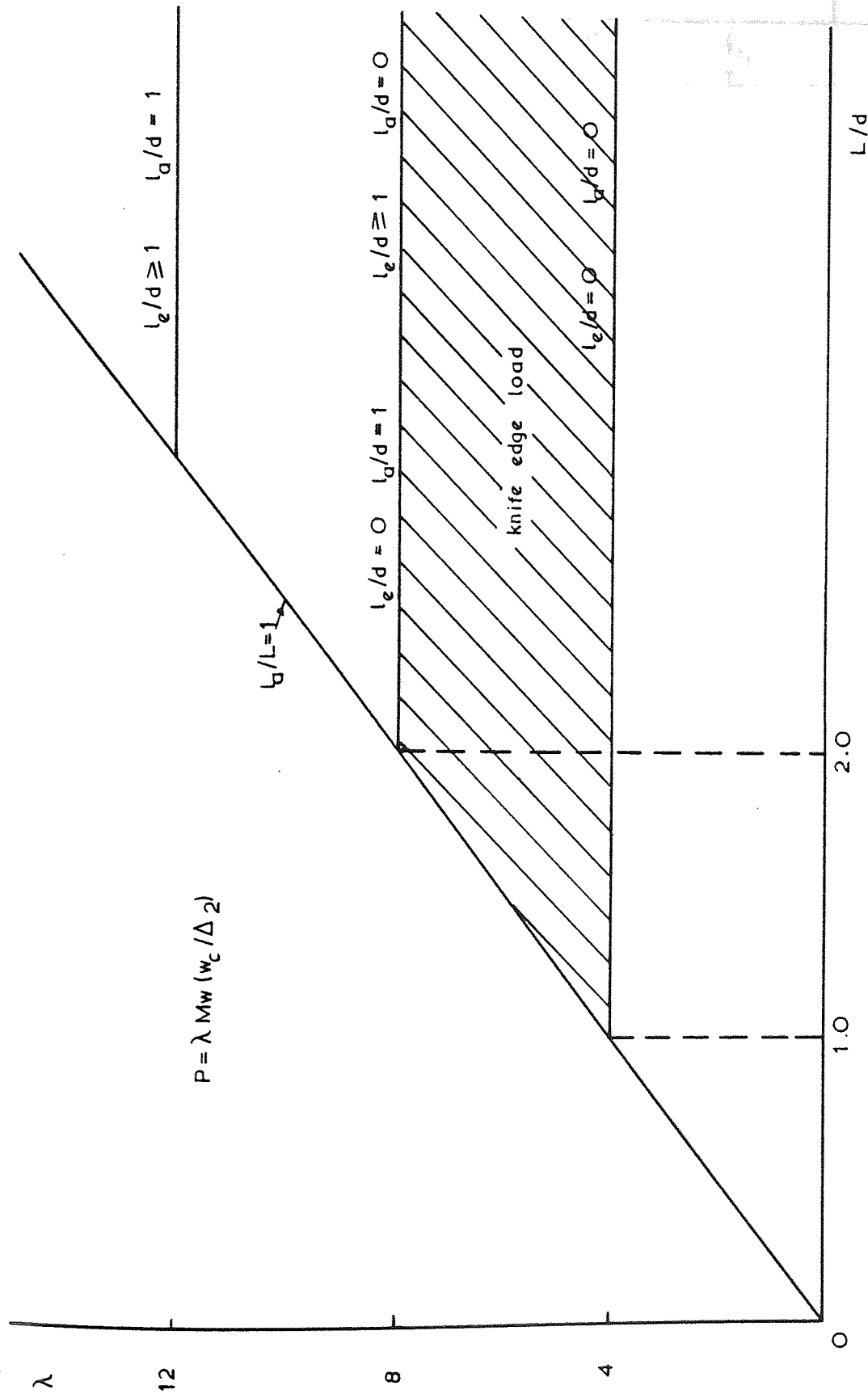


Figure 5.7 Typical results of Mode 2 analysis.



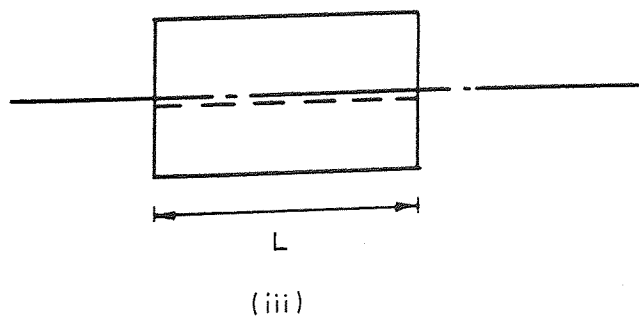
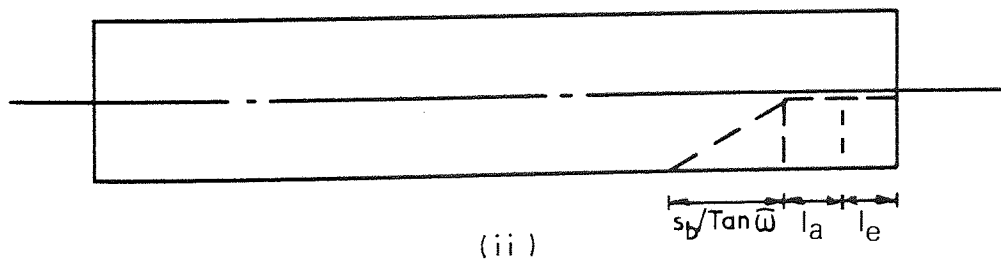
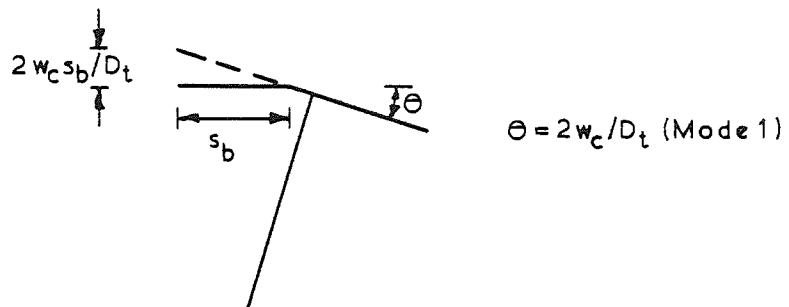
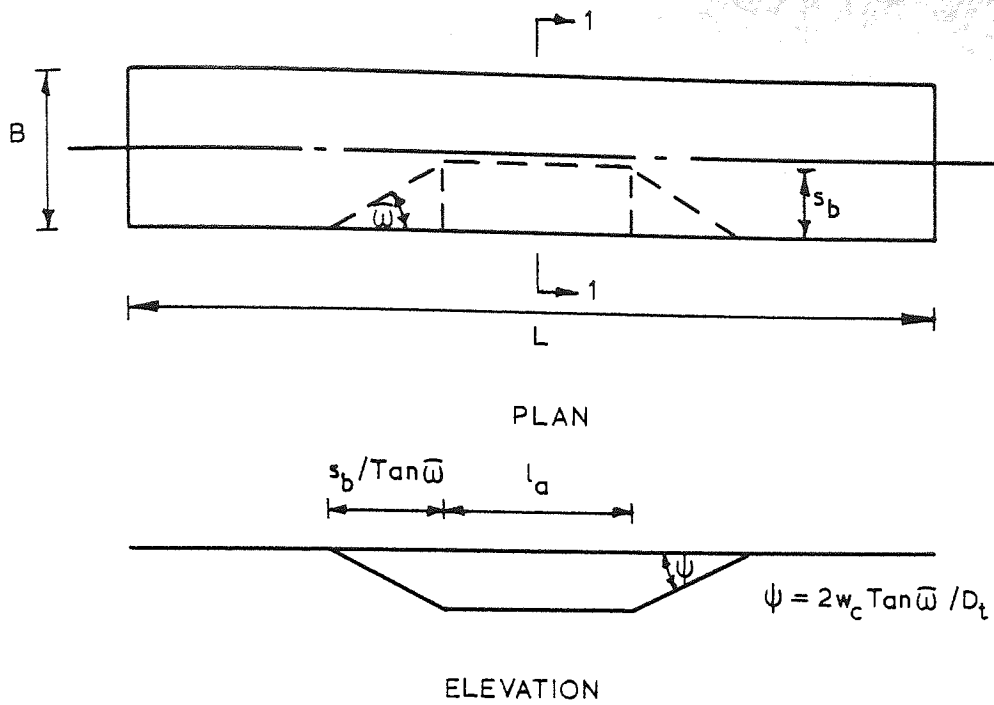


Figure 5.8 Flange yield line patterns.

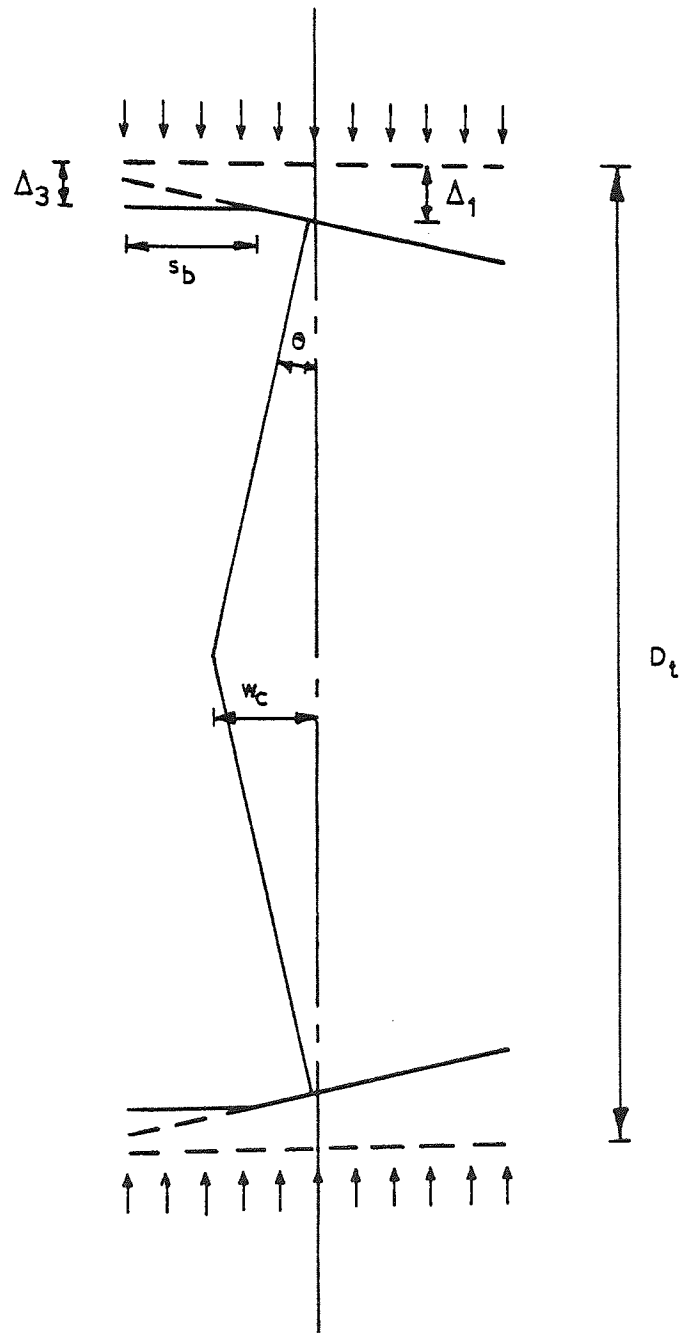


Figure 5.9 Mode 3-Section through applied loads (diagrammatic).

and  $P_f$  can be calculated independantly from the web. The work done by  $P_f$  on the flanges is, assuming  $\theta$  is small:

$$2 P_f e \theta \quad 5.18$$

where

$$e = s_b / 2 \quad \text{and} \quad \theta = 2 w_c / D_t$$

Hence substituting for  $\theta$  and  $e$  and equating the internal work to the external work done:

$$P_f = 2 M_f \left( \frac{l_a}{s_b} + 4 \tan \bar{\omega} + \frac{2}{\tan \bar{\omega}} \right) \quad 5.19$$

For the flange contribution to be a minimum  $P_f$  must be minimised with respect to the arbitrary angle  $\bar{\omega}$ :

$$\frac{d P_f}{d \bar{\omega}} = 0 = 2 \sec^2 \bar{\omega} - \text{Cosec}^2 \bar{\omega} = 0$$

and hence:

$$\tan \bar{\omega} = 1 / \sqrt{2}$$

Using this value for  $\tan \bar{\omega}$  in equation 5.19:

$$P_f = 2 M_f ( 4\sqrt{2} + l_a / s_b ) \quad 5.20$$

If the load is not applied across the whole width of the flange but over a width of  $l_k$  then equation 5.20 becomes:

$$P_f(i) = \frac{4 M_f ( l_a + 4\sqrt{2} s_b )}{( l_k - 2 r - t )} \quad 5.21$$

and for type (ii) and (iii) failure patterns:

$$P_f(ii) = \frac{4 M_f ( l_a + l_e + 2\sqrt{2} s_b )}{( l_k - 2 r - t )} \quad 5.22$$

$$Pf(iii) = \frac{4 M_f L}{(l_k - 2r - t)} \quad 5.23$$

The conditions of length for each to occur are:

$$Pf(ii) \leq Pf(i) \quad \text{if} \quad l_e \leq 2\sqrt{2} s_b$$

$$Pf(iii) \leq Pf(i) \quad \text{if} \quad L \leq 4\sqrt{2} s_b + l_a \quad 5.24$$

$$Pf(iii) \leq Pf(ii) \quad \text{if} \quad L \leq 2\sqrt{2} s_b + l_a + l_e$$

and

$$s_b = (B - 2r - t) / 2 \quad 5.25$$

These results are shown in figure 5.10 and the results of their combination with Mode 1 to produce the Mode 3 failure are shown in figure 5.11.

From the Mode 3 analysis it appears that as  $l_k$  tends to  $(2r + t)$  then the failure load becomes very large. However the failure load due to Mode 2 will then be a minimum and hence the required ultimate load carrying capacity. In other words, the flange failure pattern cannot be formed with zero eccentricity of the applied load, and so other modes should then be considered.

#### 5.2.4 Restraining Effects

##### 5.2.4.1 Flange Restraining Effects

It was assumed in the Mode 1 analysis that due to the nature of the applied load there would be no restraining effect by the flanges on the web. However this can be seen to be an erroneous assumption by considering a very long

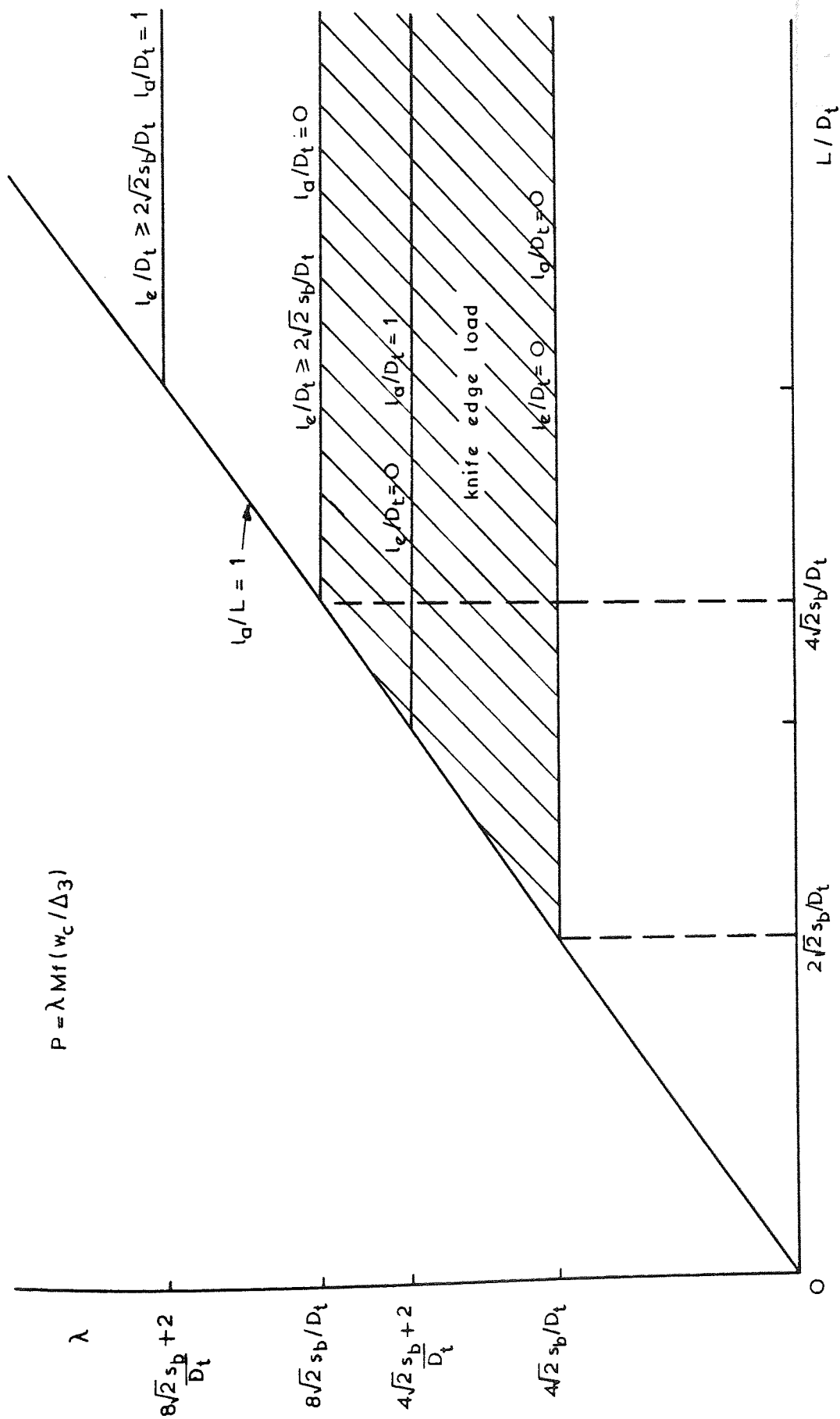


Figure 5.10 Typical results of flange contribution to Mode 3 analysis.

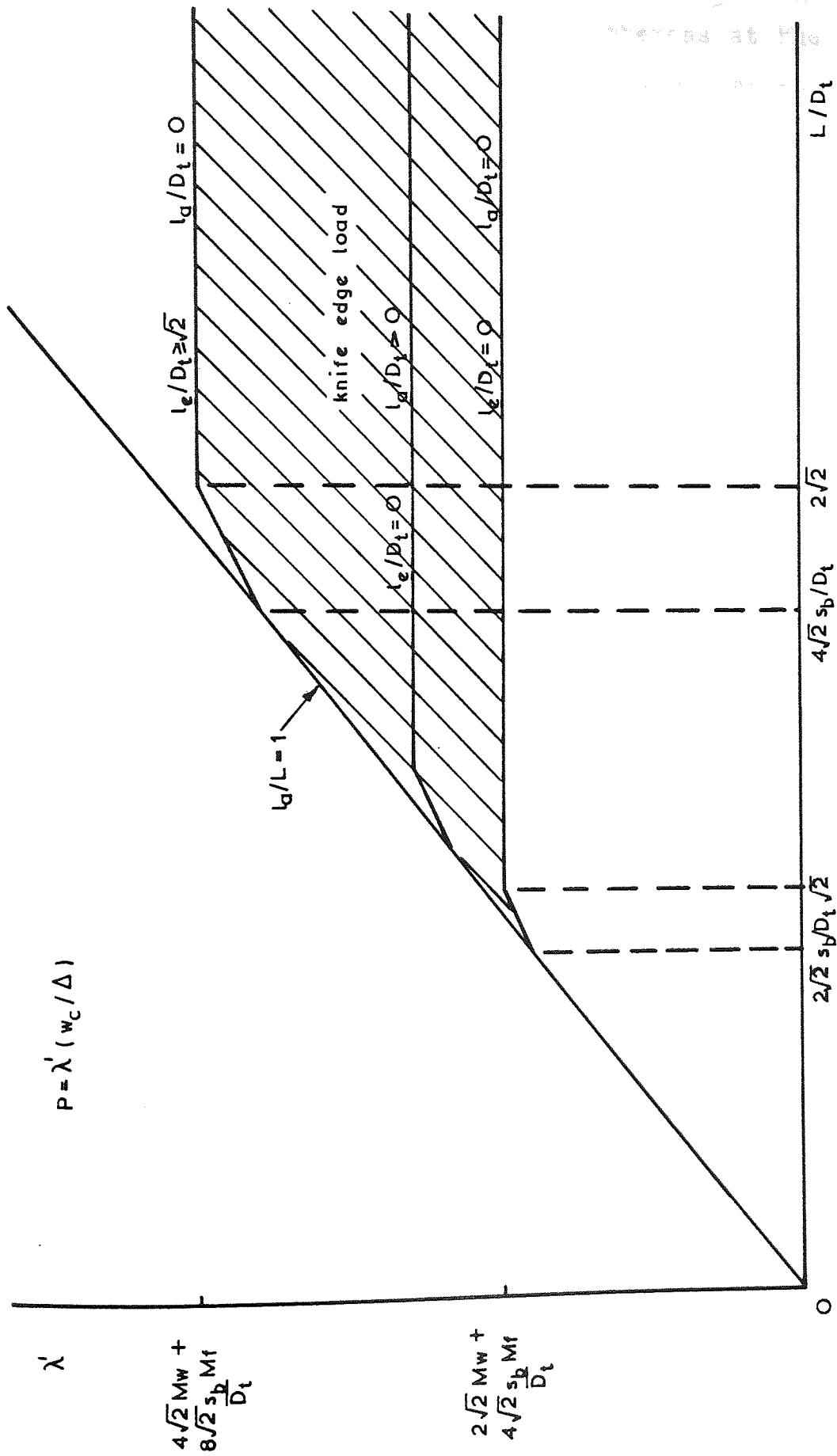


Figure 5.11 Typical results of Mode 3 analysis.



beam, in which case the beam would be unchanged at its ends with the flanges remaining horizontal whereas at the load point they would be inclined at the angle  $\theta$ . To form, there would have to be work done by the flanges and consequently this would be a resistance to the web. The flanges could remain elastic even when the yield line mechanism has formed in the web.

Hence the flanges will provide a restraint, causing the failure load to be somewhere between that of Modes 1 and 2, depending on their physical properties. The Mode 3 failure pattern cannot form as the load cannot go eccentric when applied with ball bearings. The amount of restraint provided will depend on the torsional resistance of the flanges and will probably therefore depend on the quantity  $B T^3$  and the rotation of the beam at its ends and hence the length of the beam.

#### 5.2.4.2 Web Restraining Effects

In a similar way to the restraining effects of the flanges, there must also be restraining effects due to the web away from the area of the yield line pattern. In fact some of the patterns assumed with vertical yield lines in the web may not form unless enough restraint is provided by the web away from the yield line.

This would mean that the results shown in figures 5.4, 5.7 and 5.11 would be slightly erroneous in that the sudden changes in slope would be more likely to be smooth curves. It would also mean that the length to depth ratio ( $L / D_t$  or  $L / d$ ) at which the change in slope occurs in these

figures is also slightly erroneous and is likely to be greater. These factors would depend on the physical properties of the web. This must be considered later when comparing the test results with these graphs as it is likely that the theory will overestimate in the regions of the slope changes.

### 5.3 The $\Delta / w_c$ Ratio

The  $\Delta / w_c$  ratio used for the Mode 2 analysis is different to that used in the Modes 1 and 3 analyses. However if it is assumed that for all modes the rotation of the web  $\theta$  is the same then the ratios  $\Delta_1 / w_c$  and  $\Delta_2 / w_c$  for Modes 1 and 2 respectively can be related in the following way.

Using figures 5.3 and 5.6:

$$\frac{w_{c1}}{w_{c2}} = \frac{D_t}{d} = \frac{D_t - \Delta_1}{d - \Delta_2} \quad 5.26$$

from which:

$$\frac{\Delta_2}{\Delta_1} = \frac{d}{D_t} \quad 5.27$$

and also:

$$w_{c1} / w_{c2} = D_t / d \quad 5.28$$

Hence:

$$\frac{w_{c1}}{w_{c2}} \times \frac{\Delta_2}{\Delta_1} = 1 \quad 5.29$$

and so if the failure pattern for each mode is formed at the

same angle of rotation of the web then the value  $\Delta / w_c$  can be assumed to be the same for all three modes.

### 5.3.1 Empirical Assessment of $\Delta / w_c$

A value for  $\Delta / w_c$  can now be determined from the test results. The beams with predominant bending strains can be seen, from the results of strain gauge recordings presented in Chapter 2, to be those of Series II (tests 4 and 30-32, which were loaded by two opposite ball loads at mid-length and with varying eccentricities). However it was observed that in test 31 there was a tendency for the ball bearing to roll across the flange slightly due to its location over the web. Hence tests 30 and 32 will be used to determine a value of  $\Delta / w_c$ , and the restraint provided by the flanges  $Cr$  (KN) will be included. Equation 5.5 becomes:

$$P = \frac{4\sqrt{2} Mw}{\frac{\Delta}{w} + \frac{2e}{D_t}} + Cr \quad 5.30$$

Substitution of the values of the variables for tests 30 and 32 leads to two simultaneous equations which upon solving give values of:

$$\Delta / w_c = 0.096275$$

$$\text{and } Cr = 0.02 \text{ KN}$$

Obviously  $Cr$  can be neglected.

Using this value of  $\Delta / w_c$  in test 4, for which the eccentricity was zero, then  $P = 237.4 \text{ KN}$  which gives an error of 0.7% when compared to the actual test failure load

of 239.1 KN.

Test 36 used the same beam serial size but was tested by two opposite knife edge loads at mid-length, and using the same value for  $\Delta / w_c$  gives loads of 317.2 KN and 348.6 KN for Modes 2 and 3 respectively. The actual test failure load was 360.2 KN, and failed in the Mode 3 failure pattern.

The lower value of Mode 2 should be taken, in which case the error is 11.9%.

Several assumptions have been made to arrive at a value for  $\Delta / w_c$ , and even then only one beam serial size was utilised. However the suitability of this value can be examined by comparing the test load with the theoretical load obtained by using it for various beam serial sizes.

#### 5.4 Comparison With The Test Results

The theoretical failure loads calculated using the developed theory with the empirical value for  $\Delta / w_c$  are shown for all beams except those in Series II and VII in Table 5.1. Also shown in the same table are the test failure loads and the final retest failure loads, where applicable, and the respective ratios of the theoretical load to these two values. Also shown is which of Modes 2 and 3 gives the lowest theoretical load for beams in Series III to VI.

It can be seen immediately from Table 5.1 that the theoretical load is nearly always less than or equal to the test failure load. It can also be seen that the theoretical load is nearer to the failure load for tests involving beams much longer than the length of the applied load, which in

Test No.	Test Ultimate Load (1)	Final Ultimate Load (2)	Yield Line Analysis	Lowest Mode	Pth Pexp (1)	Pth Pexp (2)
1	62.6	-	36.3	1	.58	-
2	108.8	-	72.7	1	.67	-
3	179.3	-	143.9	1	.80	-
4	239.1	-	224.2	1	.94	-
5	279.0	-	229.1	1	.82	-
6	98.2	-	33.2	1	.34	-
7	127.1	-	61.5	1	.48	-
8	236.9	-	129.8	1	.55	-
9	308.4	-	216.6	1	.70	-
10	298.4	-	248.0	1	.83	-
11	48.0	32.7	30.7	1	.64	.94
12	117.2	43.4	61.1	1	.52	1.41
13	178.4	86.2	122.2	1	.68	1.42
14	159.9	-	183.7	1	1.15	-
15	280.0	-	183.3	1	.65	-
16	54.7	46.1	31.6	1	.58	.69
17	127.7	39.1	62.7	1	.49	1.60
18	236.2	72.7	125.9	1	.53	1.73
19	216.9	166.7	189.1	1	.87	1.13
20	107.3	-	29.2	1	.27	-
21	159.4	-	62.9	1	.39	-
22	255.1	-	125.3	1	.49	-
23	292.8	-	188.8	1	.64	-
24	109.3	-	30.3	1	.28	-
25	173.6	-	60.5	1	.35	-
26	249.5	-	113.2	1	.45	-
27	272.2	-	176.4	1	.65	-
28	218.6	-	73.7	1	.34	-
29	264.6	-	186.4	1	.70	-
33	219.2	-	81.6	2	.37	-
34	323.8	-	163.2	2	.50	-
35	355.2	-	267.8	3	.75	-
36	360.2	-	317.4	2	.88	-
37	210.1	-	89.8	3	.43	-
38	279.0	-	151.2	2	.54	-
39	327.3	-	298.2	3	.91	-
40	344.8	-	314.1	2	.91	-
41	123.8	29.3	53.7	3	.43	1.83
42	175.6	122.8	100.8	3	.57	.82
43	211.0	155.0	161.9	3	.77	1.04
44	215.6	187.1	223.4	3	1.04	1.19
45	215.7	-	73.5	2	.34	-
46	320.2	87.2	147.1	2	.46	1.69
47	371.0	284.0	294.2	2	.79	1.04
48	359.5	338.9	294.2	2	.82	.87
49	150.0	63.0	62.8	3	.42	.81
50	224.7	99.6	130.1	3	.58	1.31

Table 5.1

Test No.	Test Ultimate Load (1)	Final Ultimate Load (2)	Yield Line Analysis	Lowest Mode	Pth Pexp (1)	Pth Pexp (2)
51	260.1	210.8	194.3	3	.75	.92
52	276.2	238.4	257.8	3	.93	1.08
53	159.1	-	60.1	3	.38	-
54	236.5	-	120.1	3	.51	-
55	277.7	-	224.0	3	.81	-
56	306.9	-	287.2	3	.94	-
57	341.1	-	179.5	2	.53	-
58	382.7	-	353.2	2	.92	-
59	398.6	-	353.2	2	.89	-
60	287.4	-	313.2	2	1.09	-
61	268.7	220.7	298.4	3	1.11	1.35
62	241.6	227.6	276.8	3	1.15	1.22
63	219.2	159.0	246.7	3	1.12	1.55
64	193.8	130.0	233.7	3	1.20	1.80
65	156.6	122.6	144.3	3	.92	1.18
66	921.8	792.5	782.7	2	.85	.99
67	277.8	-	297.1	3	1.07	-
68	271.6	-	236.2	2	.87	-
69	219.2	-	195.8	2	.89	-
70	155.6	-	173.4	2	1.11	-
71	450.8	-	367.4	2	.81	-
72	416.0	-	392.8	3	.94	-
73	515.7	-	442.0	3	.86	-
74	784.7	-	472.4	2	.60	-
75	470.8	406.1	399.9	2	.85	.98
76	613.8	480.8	479.9	2	.78	1.00
77	911.8	406.1	479.9	2	.53	1.18
78	452.8	393.3	364.0	2	.80	.92
79	601.9	513.2	468.4	2	.78	.91
80	797.2	587.9	563.4	2	.71	.96
81	1220.7	480.0	545.9	2	.45	1.14
82	1484.8	418.5	557.1	2	.38	1.33
83	348.5	289.0	309.9	2	.89	1.07
84	397.6	348.8	383.3	2	.96	1.10
85	563.0	445.9	468.6	2	.83	1.05
86	827.1	338.8	459.9	2	.56	1.36
87	997.2	384.6	467.4	2	.47	1.21
88	544.1	475.0	374.8	2	.69	.79
89	614.8	512.5	468.4	2	.76	.91
90	774.3	715.0	562.1	2	.72	.79
91	732.4	655.0	562.1	2	.77	.86
92	383.6	375.0	314.0	2	.82	.84
93	402.6	357.5	386.4	2	.96	1.08
94	543.1	420.0	457.4	2	.84	1.09
95	552.1	441.0	466.2	2	.84	1.06

Table 5.1 (cont.)



effect is beams which have the failure pattern remote from the ends of the beam.

This fact can be seen clearly in figures 5.12 and 5.13. Figure 5.12 shows the comparison between the theory and the test results for two beam serial sizes in Series I and III. Figure 5.13 shows the comparison for two beam serial sizes in Series V, which were loaded by two opposite uniformly distributed loads, and also shows the final retest loads for the same beams.

The final retest loads shown in figure 5.13 are much closer to the theoretical loads than the original failure load, particularly for beams in which the failure pattern was not remote from the ends of the beam.

Figure 5.14 shows the comparison between the theory and the test results for each beam serial size or property variation in Series III in which the failure pattern was remote from the end of the beam. All beams were tested by two opposite knife edge loads at their mid-length. Also shown in figure 5.14 is the range in which 67% of the test results lie and is therefore the equivalent of a standard deviation of 16%. The mean value of  $P_{th} / P_{exp}$  for these beams is exactly 1.0. Although many of these results are grouped around 250 - 350 KN, it should be noted that the variation in depth of the sections is from 102 - 466 mm, with similar variations in the other physical properties. It should also be noted that both failure modes were used to derive the theoretical loads.

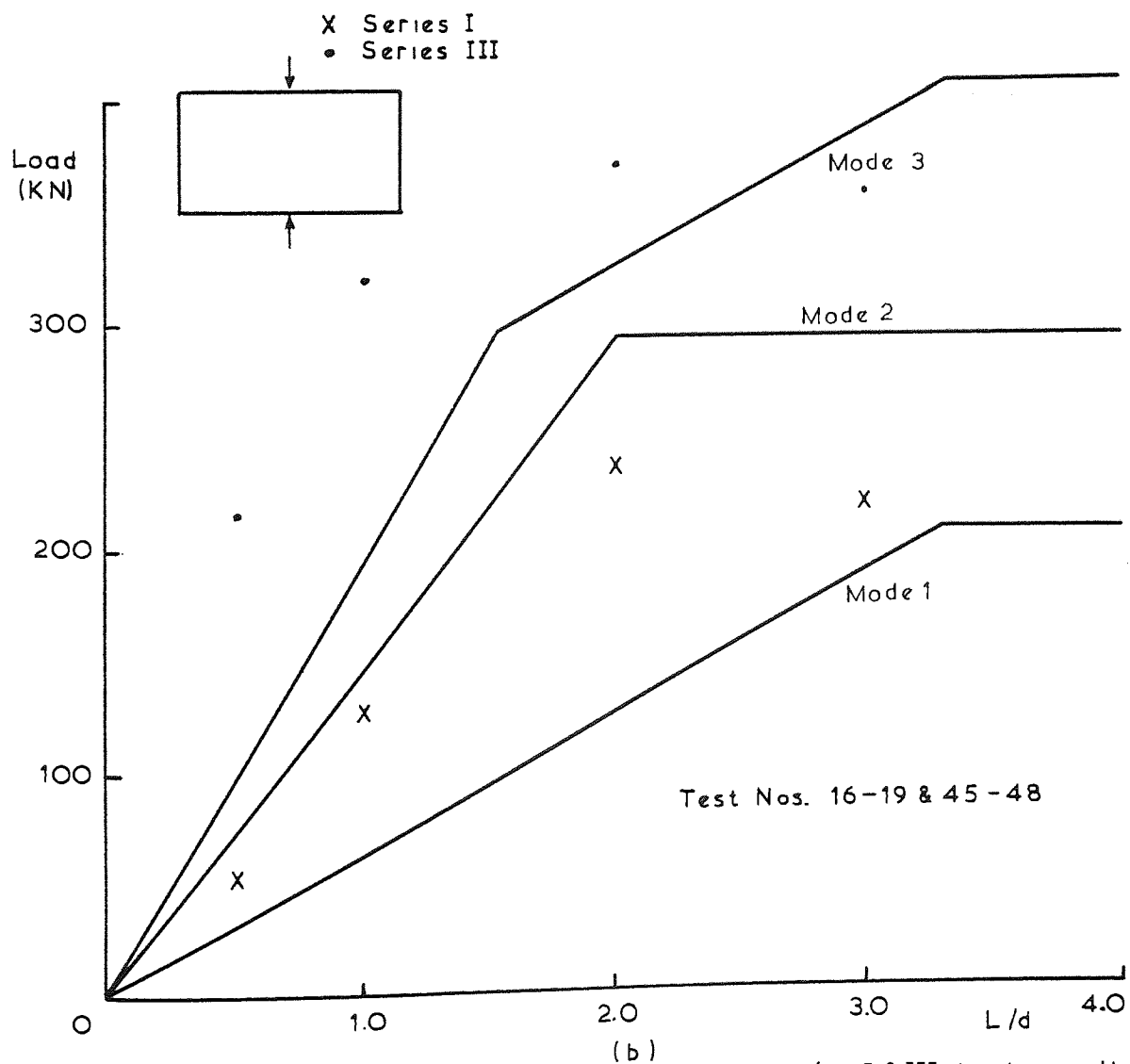
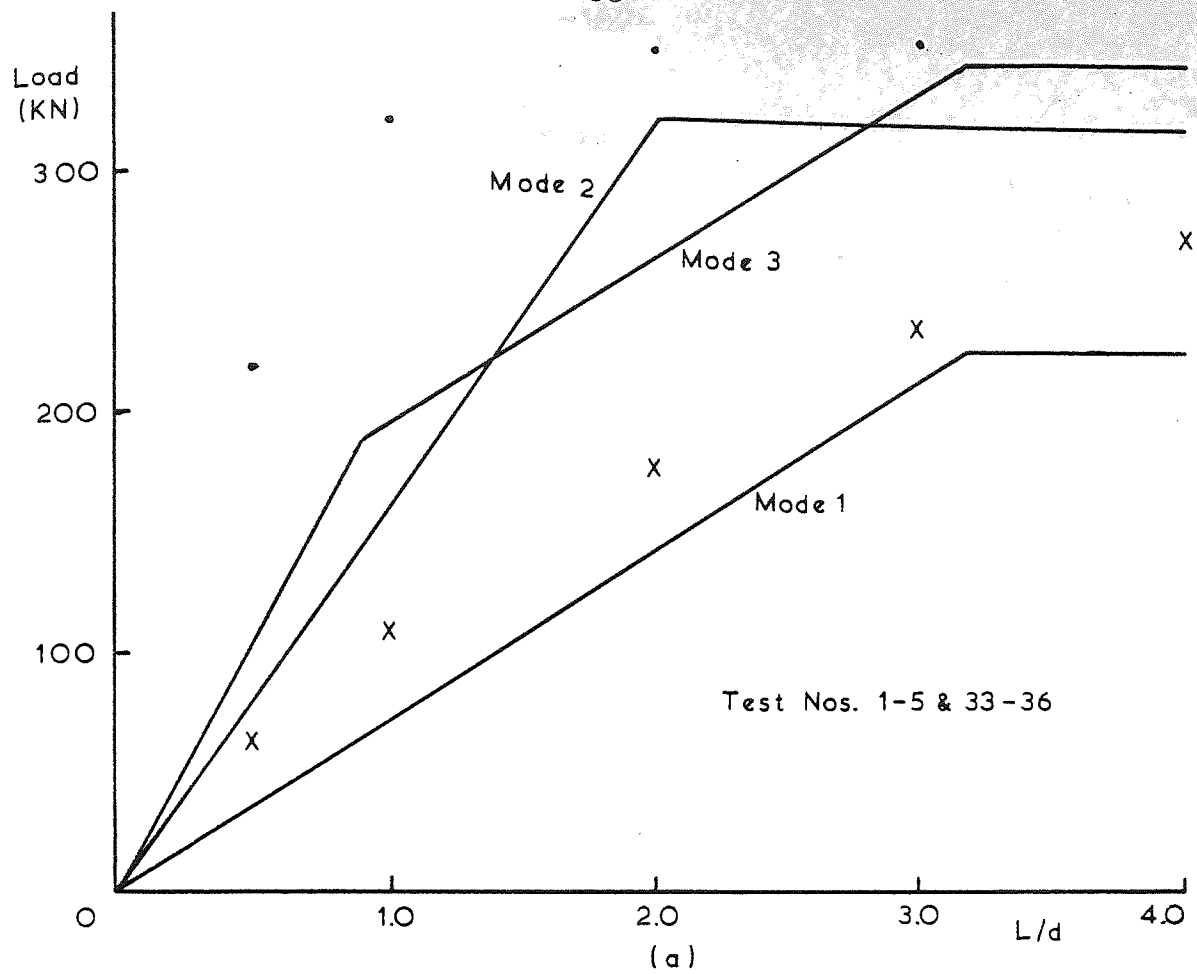


Figure 5.12 Yield line theory compared with Series I & III test results.

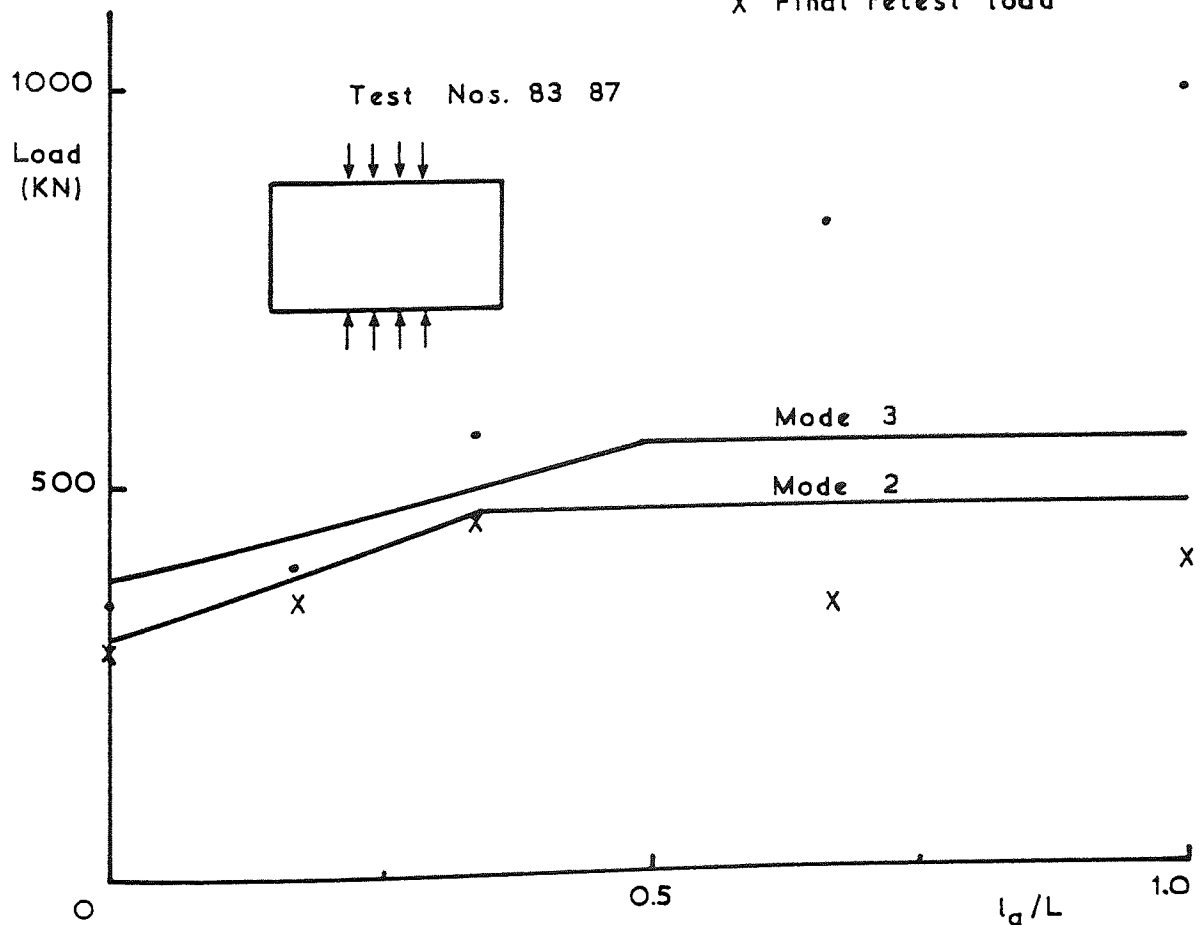
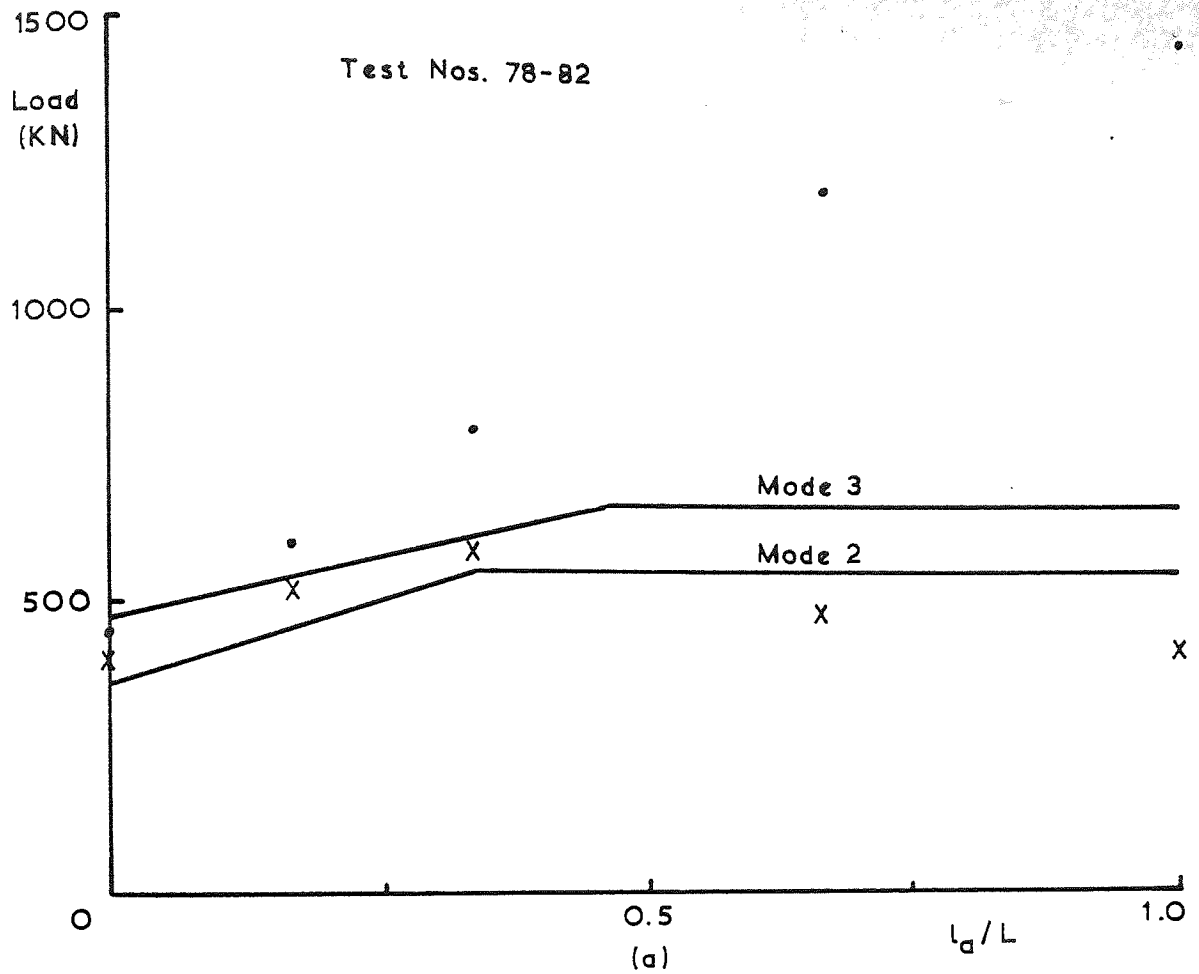


Figure 5.13 Yield line theory compared with Series V test results.

Yield Line Theory Comparison

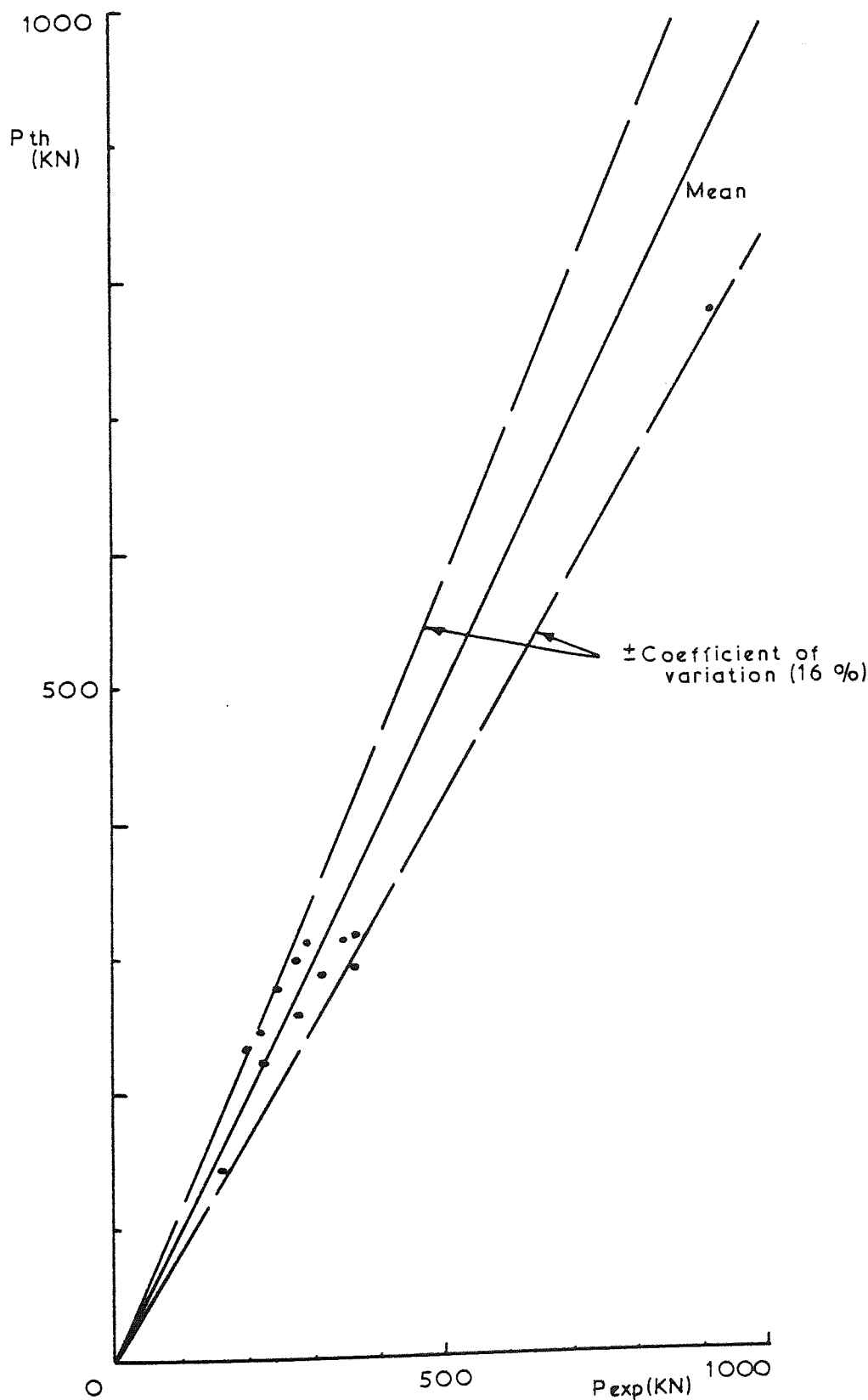


Figure 5.14 Yield line theory compared with test results (failure remote from the end).

### 5.5 Observations and Conclusions from the Comparison

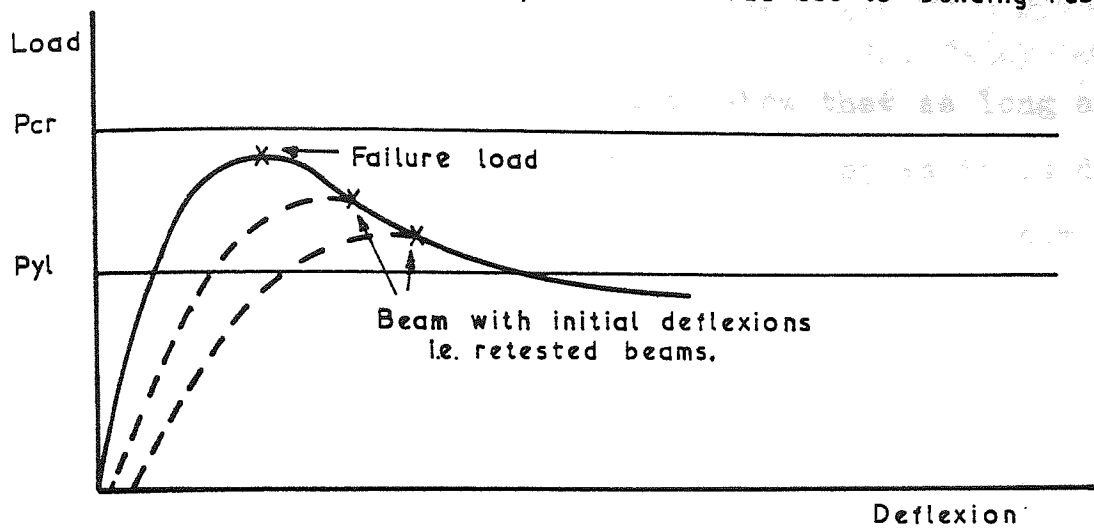
The theory assumes that the rotation of the web  $\theta$  is always small so that  $\tan\theta = \theta$ . When beams were retested, this angle was sometimes too large for this condition to be true, and so the use of the final retest load when comparing with the theoretical loads may not always be justified, hence this comparison must be looked at in general terms.

The axial stiffness of the beam web has been ignored in the development of this yield line theory, and it is therefore possible that the elastic buckling load for the web could theoretically occur either before or after the yield stress is developed due to bending, in which case the method could be either an upper or lower bound solution. With webs with such low slenderness ratios as were tested for this work, it would be more likely to provide the latter as the elastic buckling loads are very high. Thus the load-deflexion curves could be either (a) or (b) in figure 5.15, depending on the magnitude of the deflexions and the onset of yield, whereas that of (c) could be possible for more slender webbed beams. The curves in figure 5.15(a) and (b) are consistent with those produced in Chapter 2 for retested beams, that of (a) for beams with overall web failure and that of (b) for beams with localised failures.

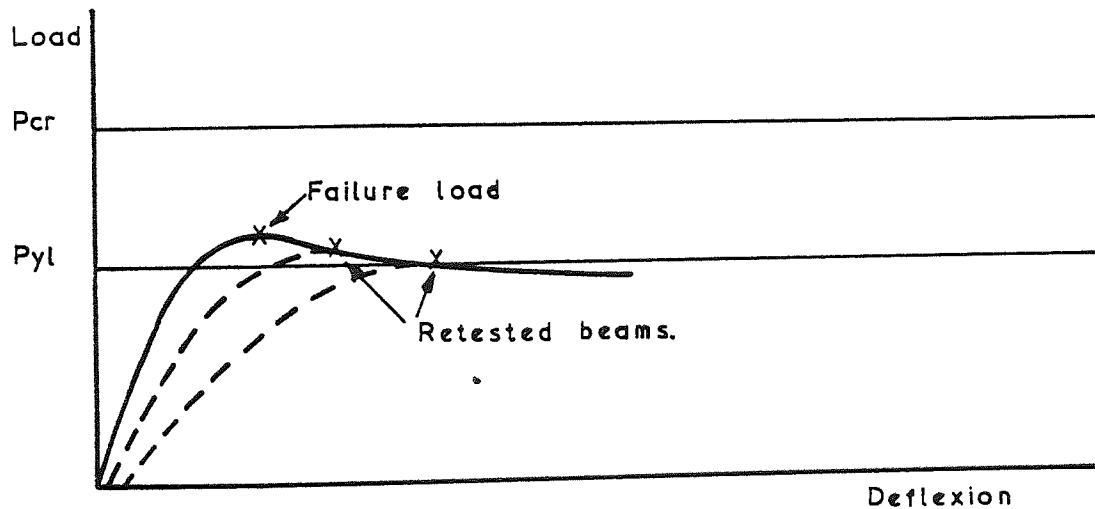
If these assumptions are correct then the values of  $P_{th} / P_{exp}$  obtained in Table 5.1 are consistent. However the variation between localised failure pattern results and overall failure pattern results could simply be due to the ratio  $\Delta / w_c$ . This value may be different for various types

$P_{cr}$  : Theoretical elastic buckling load.

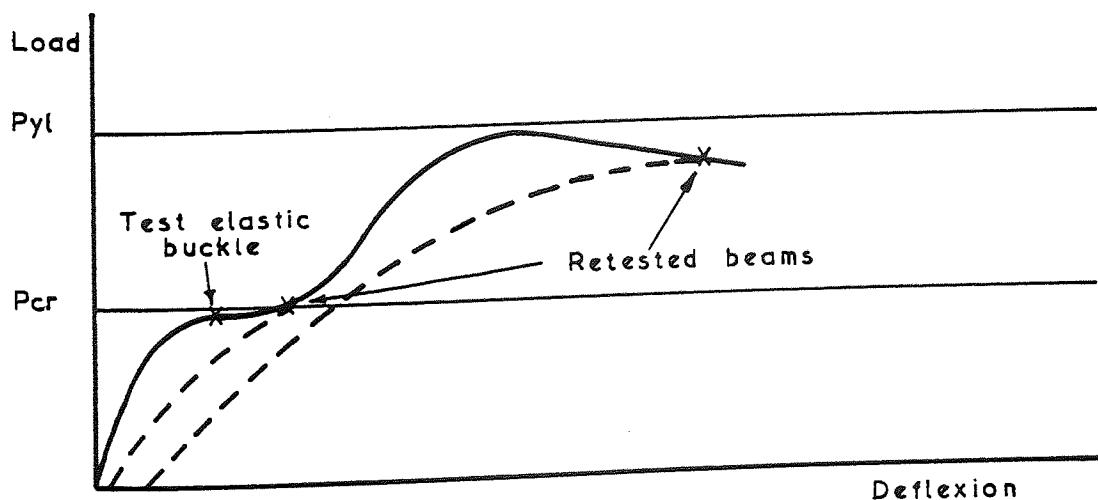
$P_{yl}$  : Maximum load due to bending resistance.



(a)



(b)



(c)

Figure 5.15



of failure.

However the method does seem to show that as long as the beam is approximately three times as long as it is deep, then the maximum load that it can sustain can be determined without consideration of its depth.

As mentioned earlier in this chapter, restraining effects of the flanges and the web away from the yielded region mean that comparison between this theory and the test results can only be considered in detail for long beams i.e. beams which are longer than the loaded length and have a portion of their length virtually unaffected by the applied loads.

## CHAPTER 6 - LOCAL CRUSHING AND EMPIRICAL ASSESSMENT OF THE TEST RESULTS

### 6.1 Introduction

It is possible that some beams when subjected to concentrated loads on the flanges yield at the junction of the web and the root fillets in the vicinity of the applied loads thus causing overall failure or initiating overall failure of the beam in another form. For example, the local yielding could reduce the restraint at the loaded edges thus initiating an elastic buckle of the web. Alternatively the local crushing could be accompanied by a yield line pattern in the web.

Most previous considerations of local crushing have assumed failure of the beam when the yield stress is attained at the web junction with the root, and have made no allowance for any flange strength or web resistance in the unyielded area. This chapter will firstly consider local crushing with some allowance made for these factors.

The second part of this chapter will examine the experimental results presented in Chapter 2 to see if there are any empirical relationships between them.

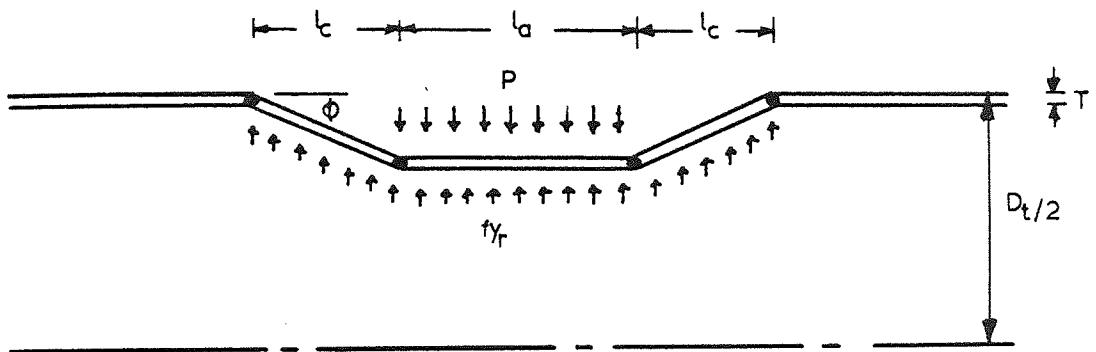
### 6.2 Local Crushing Theory

Consider the local crushing failure and flange yielding mechanism shown in figure 6.1. The load  $P$  has moved through a distance  $\Delta$  thus causing the web to yield at its junction with the root along a length of  $l_a + 2 l_c$ . The rotation in

location of the plastic hinges;

is only; assuming the

the plastic hinge is



● indicates plastic hinge in flange

Figure 6.1

the flanges has caused the formation of the plastic hinges.

Considering half of the beam depth only; equating the work done by the load in moving a distance  $\Delta$  to the work done by the web and the flange:

$$P \Delta = 2 l_c f_{y_r} \frac{\Delta}{2} t + f_{y_r} l_a \Delta t + 4 M_p \phi \quad 6.1$$

in which:

$$M_p = B T^2 f_{y_f} / 4$$

the plastic moment of resistance of the flange.

Assuming small angles and deflexions:

$$\phi = \tan \phi = \Delta / l_c$$

The work done due to the axial force in the flanges will be negligible due to the small angles and deflexions.

Equation 6.1 can thus be written:

$$P = f_{y_r} t (l_a + l_c) + f_{y_r} T^2 B / l_c \quad 6.2$$

The only variable in this equation is  $l_c$  and so the load  $P$  will be a minimum when its differential with respect to  $l_c$  is equal to zero. Thus:

$$\frac{dP}{dl_c} = 0 = f_{y_r} t - \frac{B T^2 f_{y_f}}{l_c^2}$$

and rearranging:

$$l_c = T \sqrt{B f_{y_f} / t f_{y_r}} \quad 6.3$$

and so using this value for  $l_c$  in equation 6.2:

$$P = 2 T \sqrt{B t f_{y_f} f_{y_r}} + f_{y_r} l_a t \quad 6.4$$

This assumes that the load is applied sufficiently

remote from the end of the beam for the mechanism to form.  
For a long beam loaded at the end:

$$P = T \sqrt{B t f_y f_y} + f_y l_a t \quad 6.5$$

This load is therefore irrespective of the depth of the beam, which is consistent with the findings of Chapter 5 and also the work of Winter and Pian (32) and Delesques (33).

### 6.3 Suitability of the Crushing Theory

To examine the suitability of equation 6.4, the ultimate load  $P$  from the tests can be plotted graphically against the term  $2 T \sqrt{B t f_y f_y}$  for all sufficiently long beams loaded by two opposite knife edge loads. This will then encompass a whole range of beam serial sizes with varying physical properties. The long beams loaded by two opposite knife edge loads at mid-length (Series III) are also considered to be the most likely to crush in the suggested manner. In this case the term  $f_y l_a t$  in equation 6.4 is zero since  $l_a$  is zero.

Figure 6.2 shows the variation of the ultimate test load with the term  $2 T \sqrt{B t f_y f_y}$  for all beams in Series III which had an aspect ratio  $L/d$  of greater than or equal to 2.5. It can be seen that the test results are consistently greater than the line representing equation 6.4 with  $l_a = 0$ .

This discrepancy could represent the load required (say  $P_p$ ) to form a post crushing failure of the web, as the failure pattern shown in figure 6.1 is not sufficient for an overall failure of the beam.

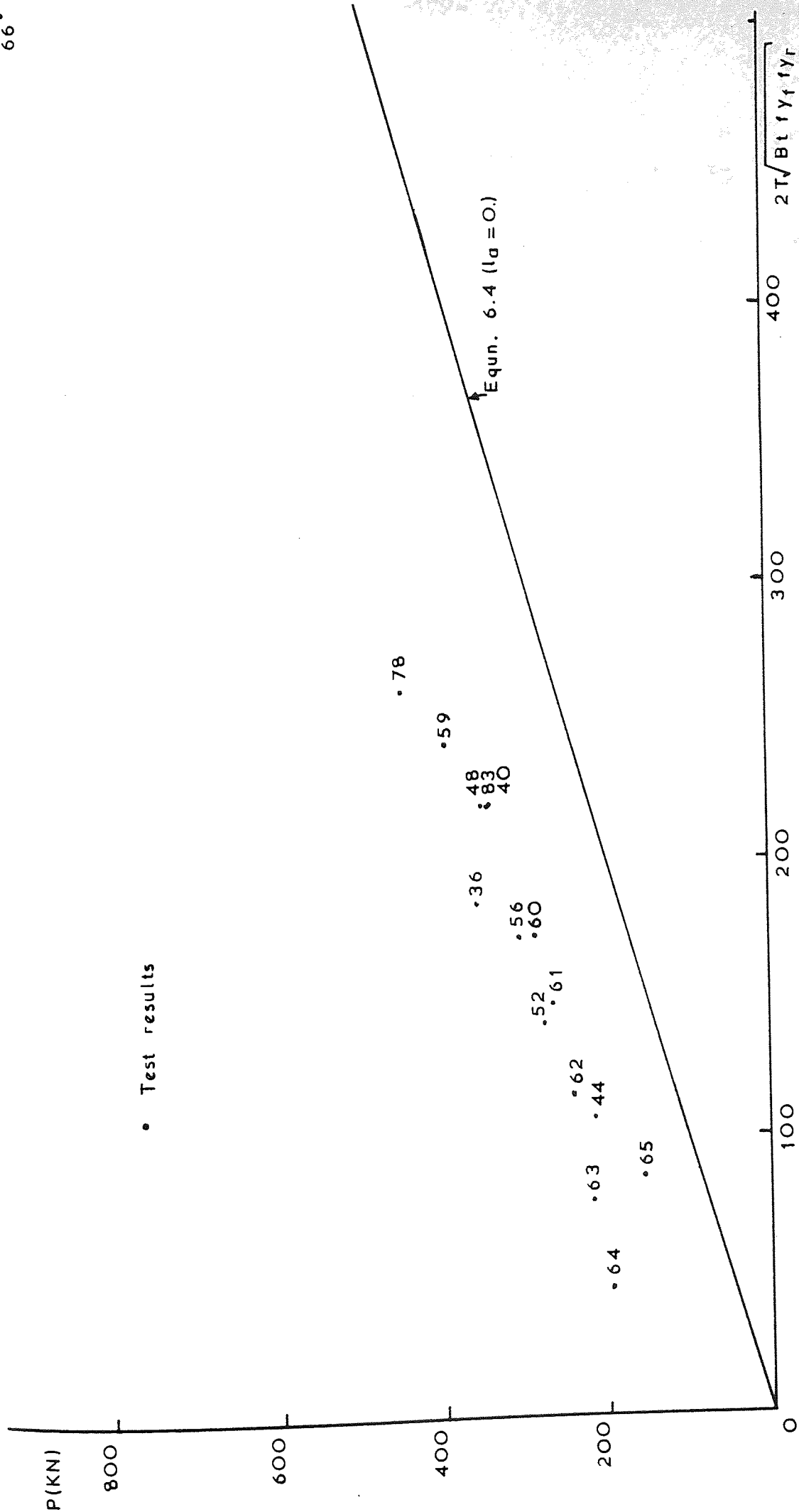


Figure 6.2



Thus equation 6.4 becomes:

$$P = 2 T \sqrt{B t f_y f_{y_r}} + f_{y_r} l_a t + P_p \quad 6.6$$

From figure 6.2 it can be seen that  $P_p$  varies between tests.

It is anticipated that  $P_p$  will vary with  $(\pi^2 D / D_t)$ , the elastic plate buckling term or  $(f_{y_w} t^2 / 4)$ , the moment of resistance per unit length for the web. Both these terms have been used previously in Chapters 4 and 5 respectively. These factors can be investigated immediately by plotting  $P_{exp} - 2 T \sqrt{B t f_y f_{y_r}}$  against each in turn for the tests used in figure 6.2.

Figure 6.3 shows that  $P_p$  would be more likely to vary with  $(t^2 f_{y_w})$  than  $(\pi^2 D / D_t)$  as the respective coefficient of variation from the mean are 13.4% and 32.1%. Utilising the mean slope from figure 6.3(a), which is 9.33, the following results show the comparison with the experimental results from this work and that of Winter and Pian (32).

Author		Winter and Pian	
Test No.	P <sub>th</sub> / P <sub>exp</sub>	Test No.	P <sub>th</sub> / P <sub>exp</sub>
36	.91	2	.97
40	1.04	4	1.04
44	1.06	9	1.07
48	.97	9	1.16
52	.98	10	1.16
56	.94	11	1.08
59	1.00	13	1.11
60	1.09	14	1.20
61	1.10	15	1.11
62	1.10	Mean 1.10	
63	1.02		
64	.99		
78	.94		
83	1.02		
65	1.02	Coefficient of variation = 12.7%	
66	.92		
Coefficient of variation = 6.2%		Coefficient of variation = 12.7%	

Table 6.1

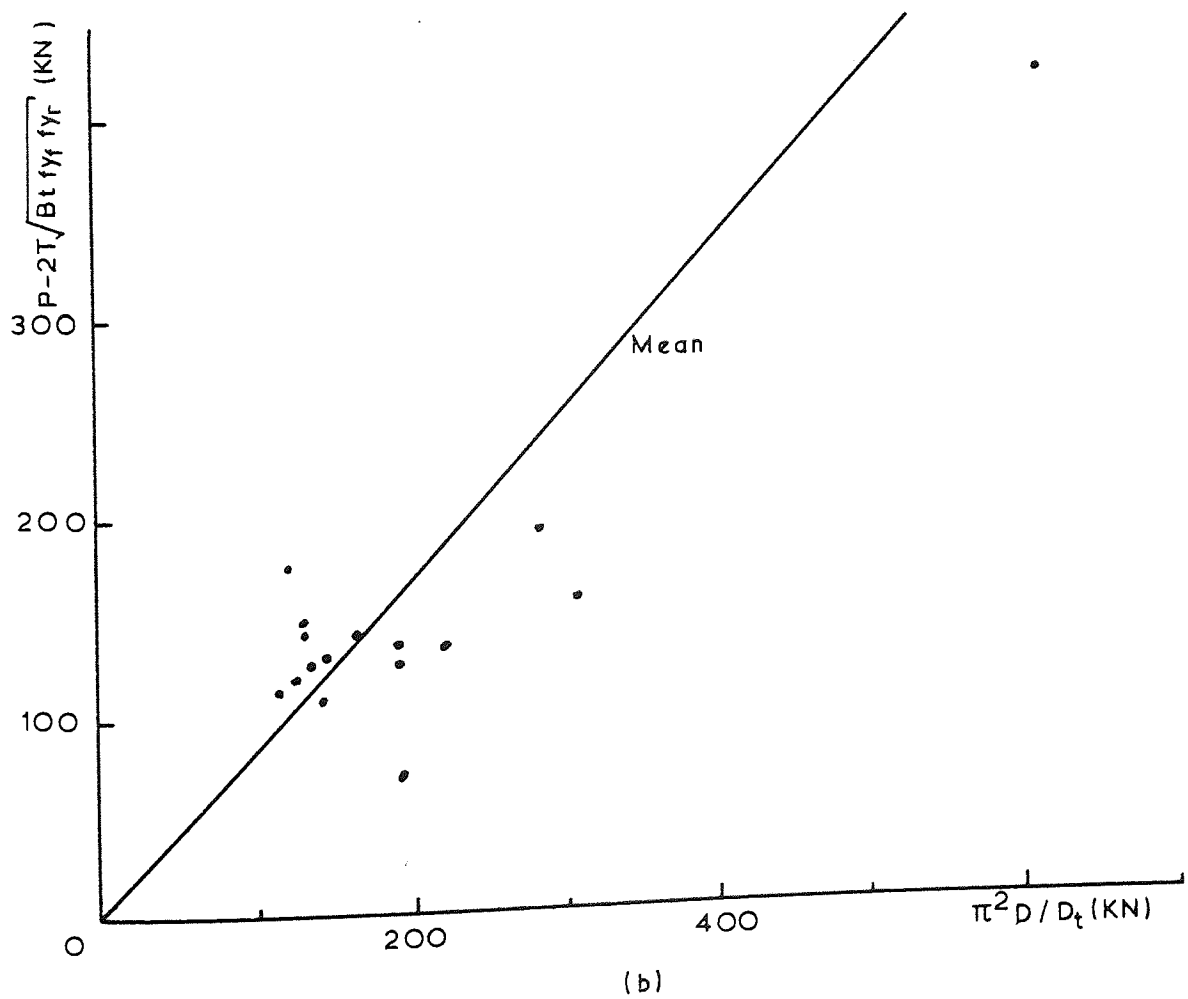
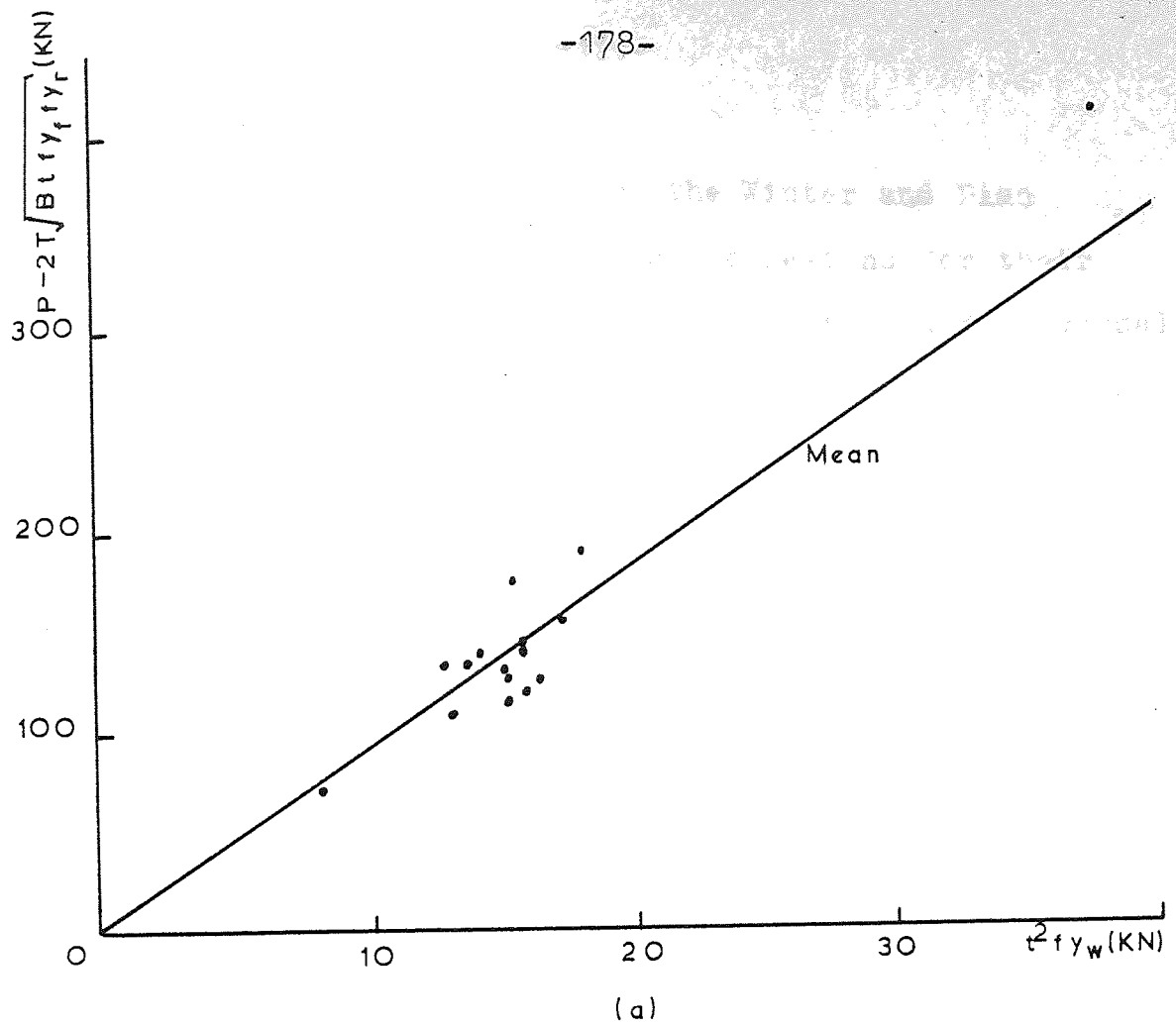


Figure 6.3

The theory overestimates for the Winter and Pian results. However the flange to web connexions for their cold formed sections were not very substantial and universal beams which were used for the author's tests have a radiused root fillet at the junction of the flange and web.

If the mechanism shown in figure 6.1 had been incorrect and instead the stress at the root radius had been assumed to vary linearly between the yield stress at the load point and zero at the outermost hinges, then the variables would have remained unchanged but equation 6.6 would have been:

$$P = 2.121 T \sqrt{B t f_{y_f} f_{y_r}} + f_{y_r} l_a t + P_p$$

This shows that for long beams loaded by two opposite knife edge loads ( $l_a = 0$ ), the general expression is:

$$P = c_1 T \sqrt{B t f_{y_f} f_{y_r}} + c_2 t^2 f_{y_w}$$

where  $c_1$  and  $c_2$  are constants dependent on the distribution of the yield stress in the mechanism. Using the least square method for the test results used previously, then:

Author		Winter and Pian	
Test No.	Pth / Pexp	Test No.	Pth / Pexp
36	.93	2	.95
40	1.08	4	1.02
44	1.05	9	1.02
48	1.02	9	1.10
52	.99	10	1.11
56	.98	11	1.04
59	1.04	13	1.05
60	1.11	14	1.14
61	1.10	15	1.05
62	1.08		Mean 1.05
63	.97		
64	.91		
78	.98		
83	1.06		
65	1.04		
66	.96		
Coefficient of variation = 6.1%		Coefficient of variation = 8.0%	

Table 6.2

where:

$$c_1 = 2.339 \quad \text{and} \quad c_2 = 7.845$$

as determined from the authors results only. Using these values, it can be seen from Table 6.2 that the accuracy of the author's results remains almost the same, but that the coefficient of variation is reduced for the results of Winter and Pian.

The Series III results were used for the determination of  $P_p$ , as for the longer beams there is more likely to be sufficient restraint provided away from the mechanism for all the necessary plastic hinges to form in the flanges. For beams with insufficient restraint away from the mechanism such as short lengths loaded by two opposite knife edge loads and long beams loaded by relatively long lengths of uniformly distributed loads, the plastic hinges will not form and the flange will deform in an elastic manner.

Equation 6.6 can also be written:

$$P = 2 T \sqrt{B t f_{y_f} f_{y_r}} + l_a f_{y_r} t + 8 (f_{y_w} t^2 / 4) \quad 4.67 \quad \dots\dots 6.7$$

for long beams loaded by knife edge loads, the last term now being consistent with the work of Chapter 5. Using the appropriate mechanism for the web for short beams or beams loaded with a relatively long uniformly distributed load:

$$P = L f_{y_r} t + 4 (f_{y_w} t^2 / 4) \frac{L}{d} \quad 4.67 \quad 6.8$$

Using these two limits, the crushing theory can now be compared with the rest of the test results.

Figure 6.4 shows the comparison with the Series III test results and figure 6.5 the comparison with the Series V

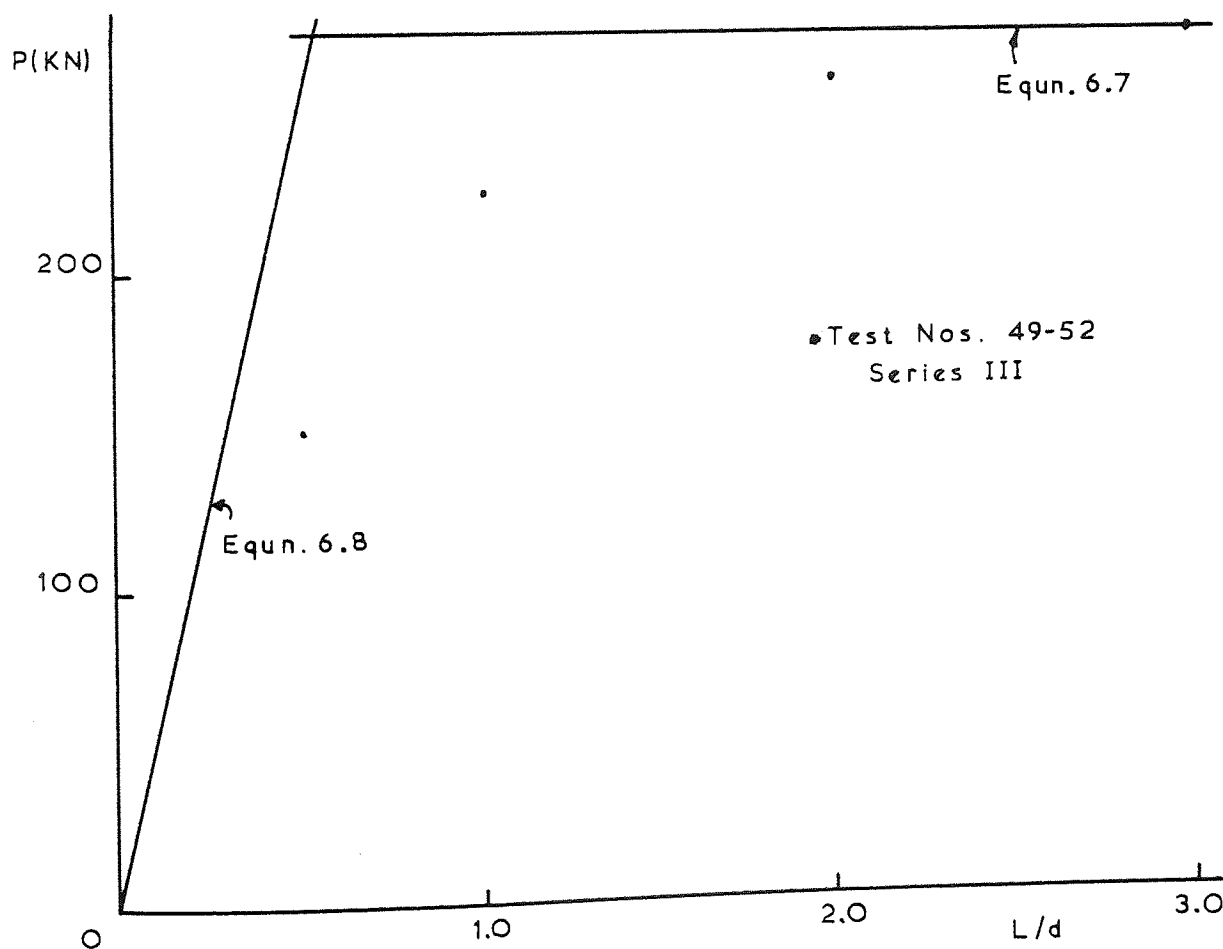
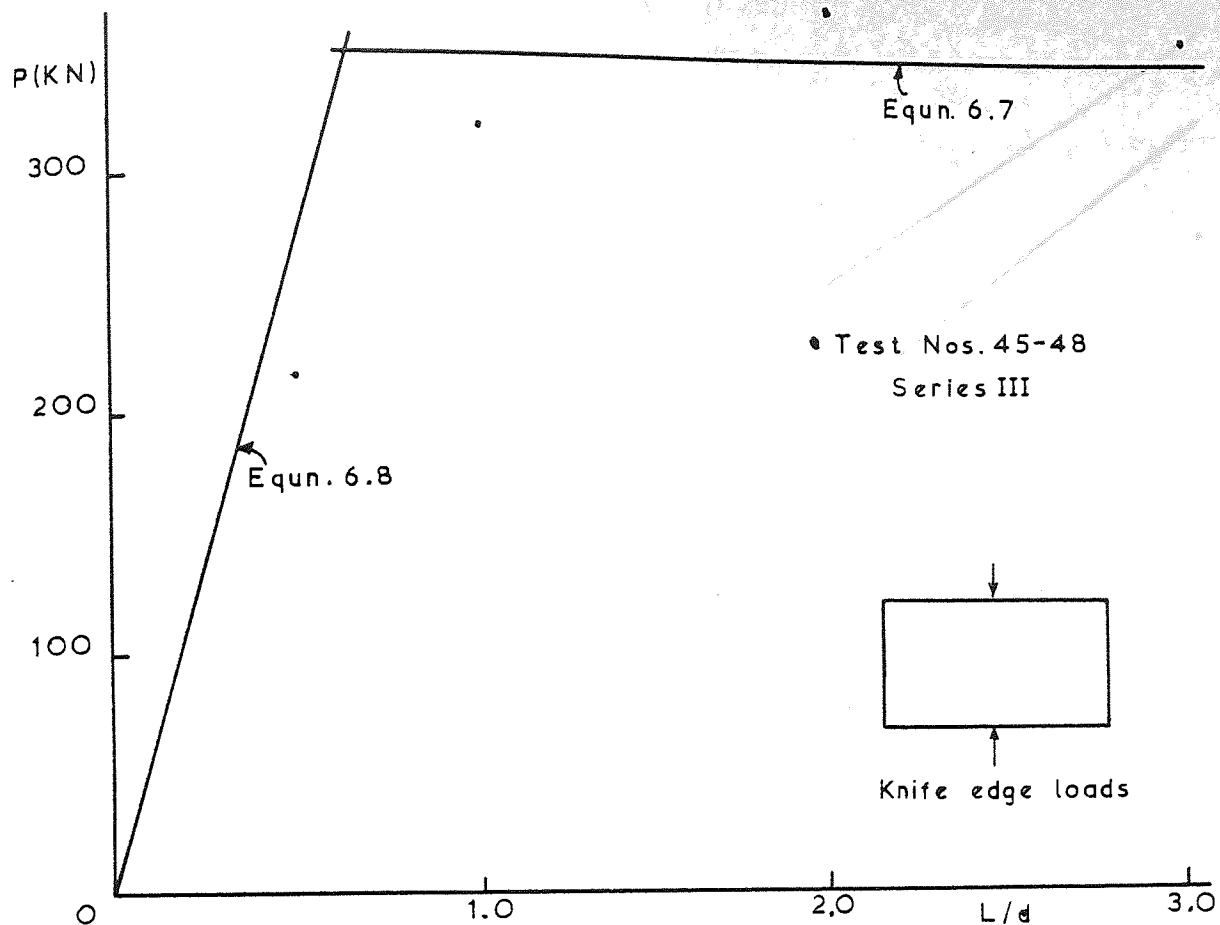


Figure 6.4 Typical comparison of Local Crushing theory and Series III test results.

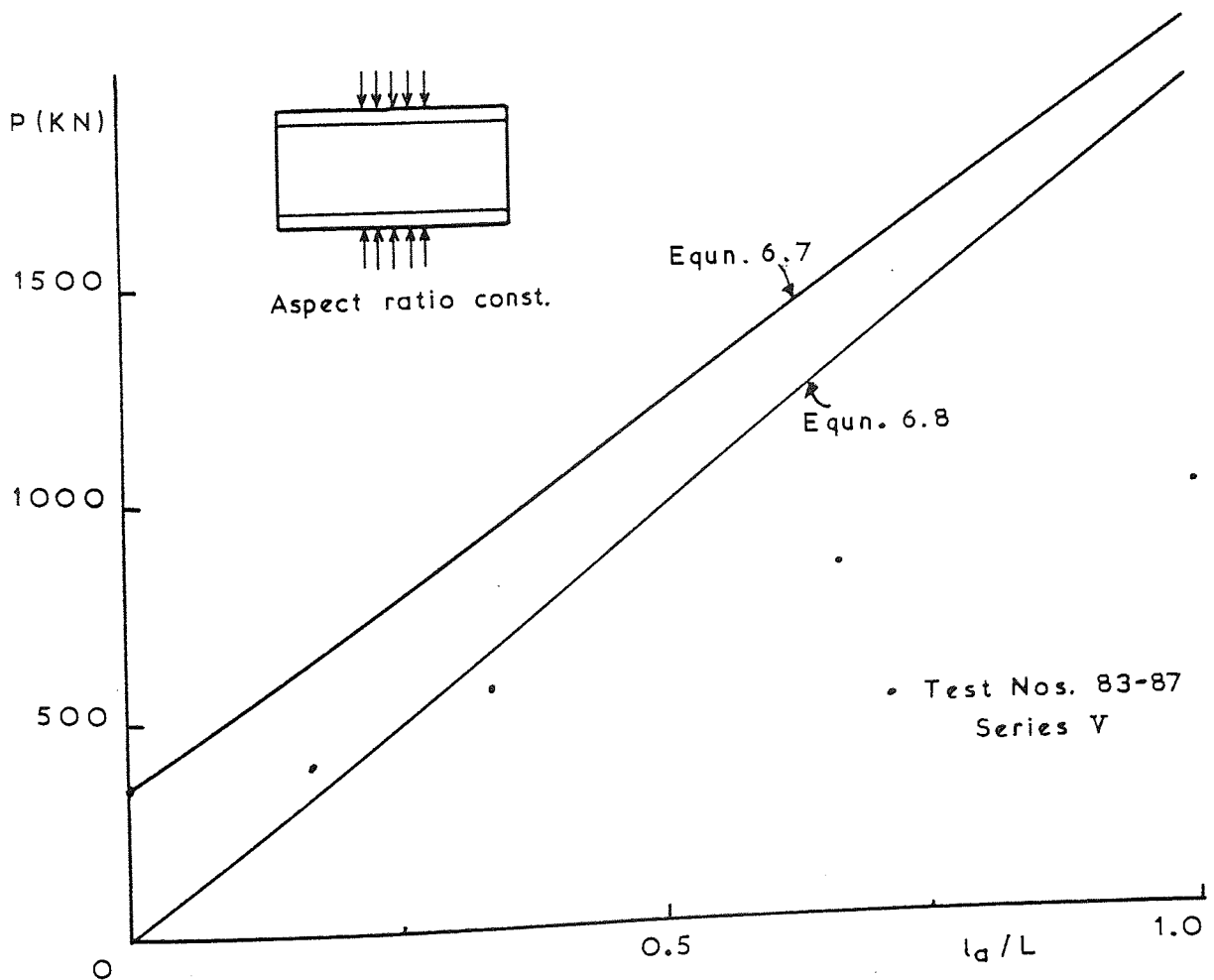
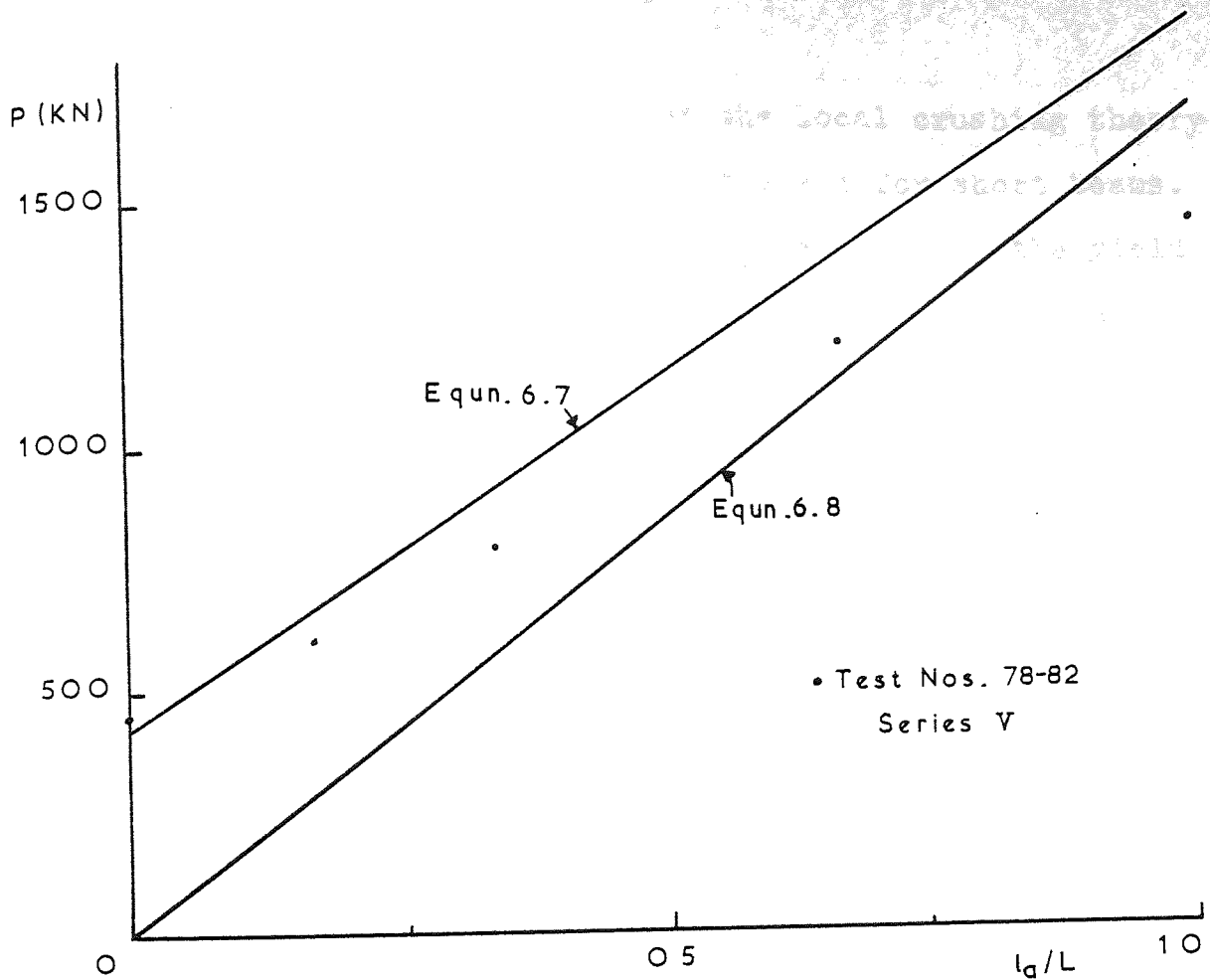


Figure 6.5 Typical comparison of Local Crushing theory and Series V test results.



test results. It can be seen that the local crushing theory overestimates for long bearing lengths and for short beams. This is similar to the comparison in Chapter 5 of the yield line theory with the test results. Comparison with the Series VI test results would merely show that the failure load does not always vary with the length of the uniformly distributed load as indicated by the crushing theory. However this could well be due to the beams failing in another mode, such as elastic or elasto-plastic buckling.

The method does show however that for long beams loaded with two opposite knife edge loads, the failure load can be predicted without considering the depth of the beam.

#### 6.4 Empirical Assessment of the Test Results

Some of the series will now be investigated empirically to see if there are any relationships to be observed between the test failure loads and the individual beam properties.

##### 6.4.1 Series III

It was illustrated in Chapter 2, for beams in Series III, the manner in which the load carrying capacity of a beam subjected to two opposite knife edge loads at mid-length varies with the increase in length or  $L/d$  ratio. It was shown that there would be very little increase in the ultimate load after an aspect ratio of approximately 3.0. Table 6.3 shows the proportion of the ultimate load at an  $L/d$  ratio of 3.0 that each smaller ratio sustained in the tests.

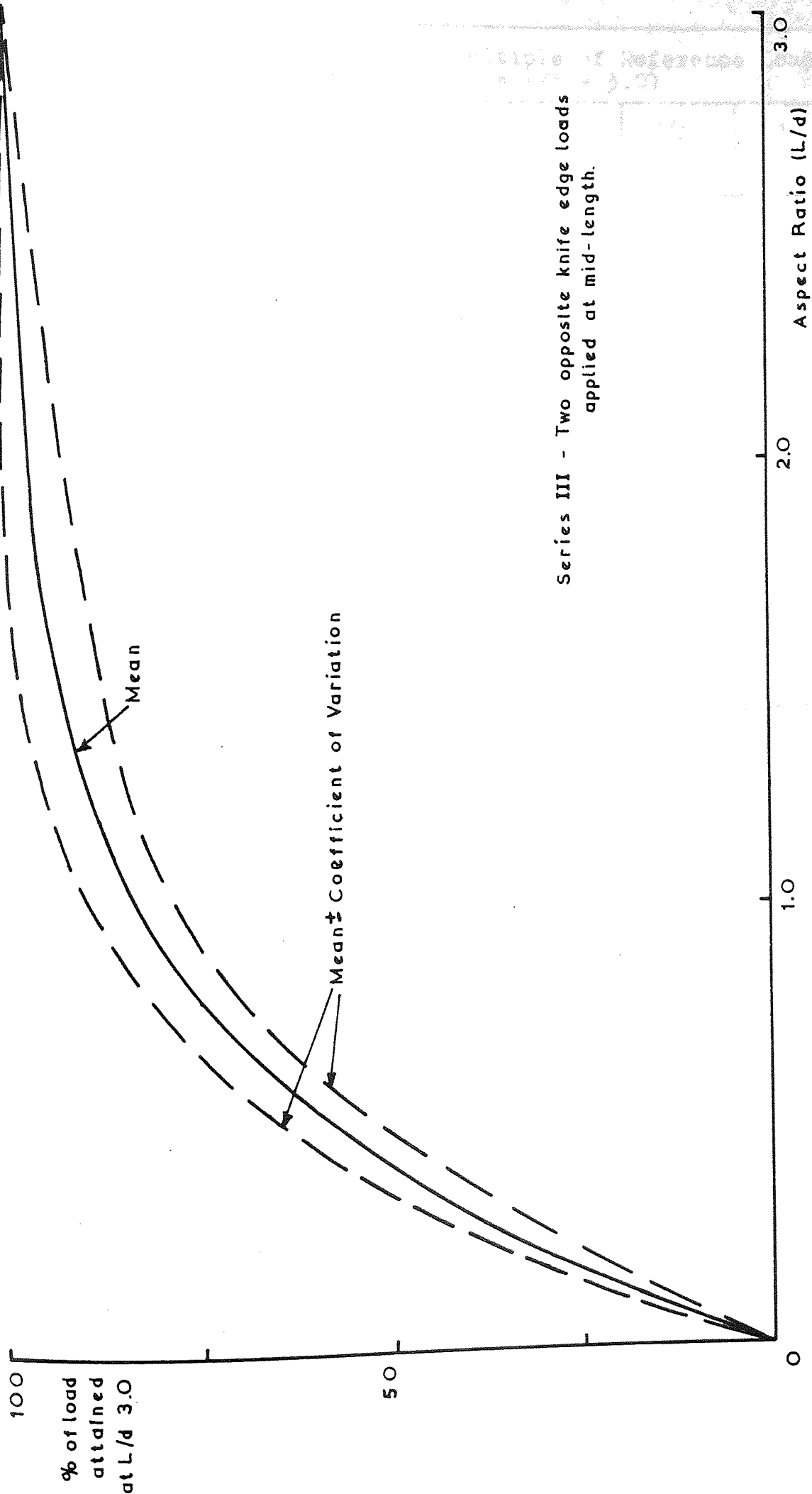
% of Load Attained at L/d Ratio of 3.0			
L/d Ratio Test Nos.	0.5	1.0	2.0
33 - 36	60.8	90.8	98.6
37 - 40	60.9	80.9	94.9
41 - 44	57.4	81.4	97.9
45 - 48	60.0	89.1	103.2
49 - 52	54.2	81.4	94.2
53 - 56	51.8	77.1	90.5
57 - 59	--	85.7	96.1
Mean	57.5	83.7	96.5
Coefficient of variation (%)	6.7	5.5	4.0

Table 6.3

These results are shown graphically in figure 6.6. Thus if an empirical method were devised for determining the load carrying capacity of a long beam such as the load dispersion method or the yield line method, then the variation for smaller lengths can be predicted to the accuracies shown above. For the load dispersion method, this variation could be incorporated in the angle of dispersion.

#### 6.4.2 Series V and VI

The empirical assessment of the loads attained for beams in Series III can now be repeated for the Series V and VI test results, using the same test load as reference (long beam loaded by two opposite knife edges at mid-length), for various beam serial sizes in the following way, shown in Tables 6.4 and 6.5 respectively:



Series III - Two opposite knife edge loads applied at mid-length.

Figure 6.6

Load attained as Multiple of Reference Load (Knife edges, $L/d = 3.0$ )				
$l_a/L$ Ratio	1/6	1/3	2/3	1
Test Nos.				
60, 72 - 74	1.45	1.79	2.73	--
40, 75 - 77	1.37	1.78	2.64	--
78 - 82	1.33	1.74	2.70	3.28
83 - 87	1.14	1.62	2.37	2.86
Mean	1.32	1.73	2.61	3.07
Coefficient of variation (%)	10.2	4.2	6.2	

Table 6.4 Series V

Load attained as Multiple of Reference Load (Knife edges, $L/d = 3.0$ )				
$L/d$ Ratio	2.0	4.0		5.0
$l_a/L$ Ratio	0.5	0.5	1.0	1.0
Test Nos.				
88 - 91	1.20	1.36	1.71	1.62
92 - 95	1.10	1.16	1.56	1.58
Mean	1.15	1.26	1.63	1.60

Table 6.5 Series VI

The variation between the comparable results in Tables 6.3, 6.4 and 6.5 are quite small. Thus if the test failure load could be predicted for one type of test, then the failure load for a different test could be predicted to the accuracies shown.

Beam reference N (254 x 146 x 43Kg/m) test results, test numbers 78 - 82 and 88 - 91, are shown in figure 6.7. Also shown is the line representing  $f_y L t$ , which can be seen to be significant. It appears that the beam fails when the yield stress is attained at the junction of the web and the root along the whole length, unless the load is applied

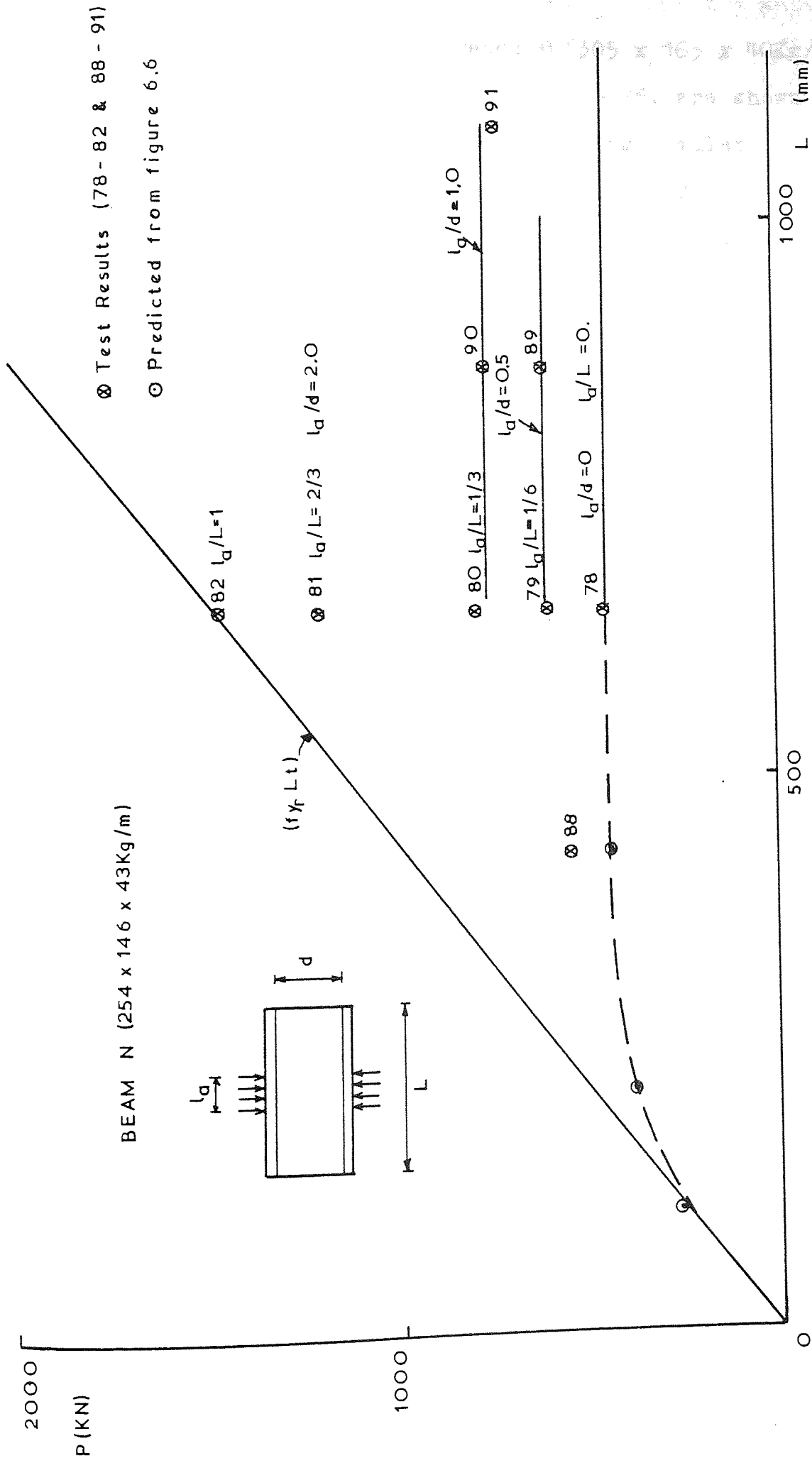


Figure 6.7 Variation of failure loads for beam N with beam length, showing the effects of the applied load length.

remote from the ends. Beam reference M (305 x 165 x 40Kg/m) test results, test numbers 83 - 87 and 92 - 95, are shown in a similar way in figure 6.8. Although having similar empirical relationships between the ultimate loads as shown in Tables 6.4 and 6.5, this beam has no apparent relationship with the line  $f_y L t$ , although all the results fall below the line.

### 6.5 Conclusions

The observations from the two previous sections, 6.4.1 and 6.4.2, indicate an overall relationship between the test results as shown in figure 6.9, for the wide range of beam sizes included in this work. Further, in figure 6.9, the straight line from the origin representing  $l_a/L = 1$  is sometimes equal to the quantity  $f_y L t$ , and it is possible that at other times this line is related to  $f_y L t$  indirectly. It has been shown that the load for various  $l_a/d$  and  $L/d$  ratios are related even though some beams having the same section showed different failure patterns.

Considering figure 6.9, and in particular the aspect ratio ( $L/d$ ) 3.0, the load at any point between the lines  $l_a/L = 1$  and  $l_a/L = 0$  is approximately:

$$P = P_0 + \frac{l_a}{L} (P_1 - P_0) \quad 6.9$$

where  $P_0$  is the load at  $l_a/L = 0$   
and  $P_1$  is the load at  $l_a/L = 1$

It was shown in the previous section that  $P_0$  is related to  $P_1$  at an aspect ratio of 3.0, thus:



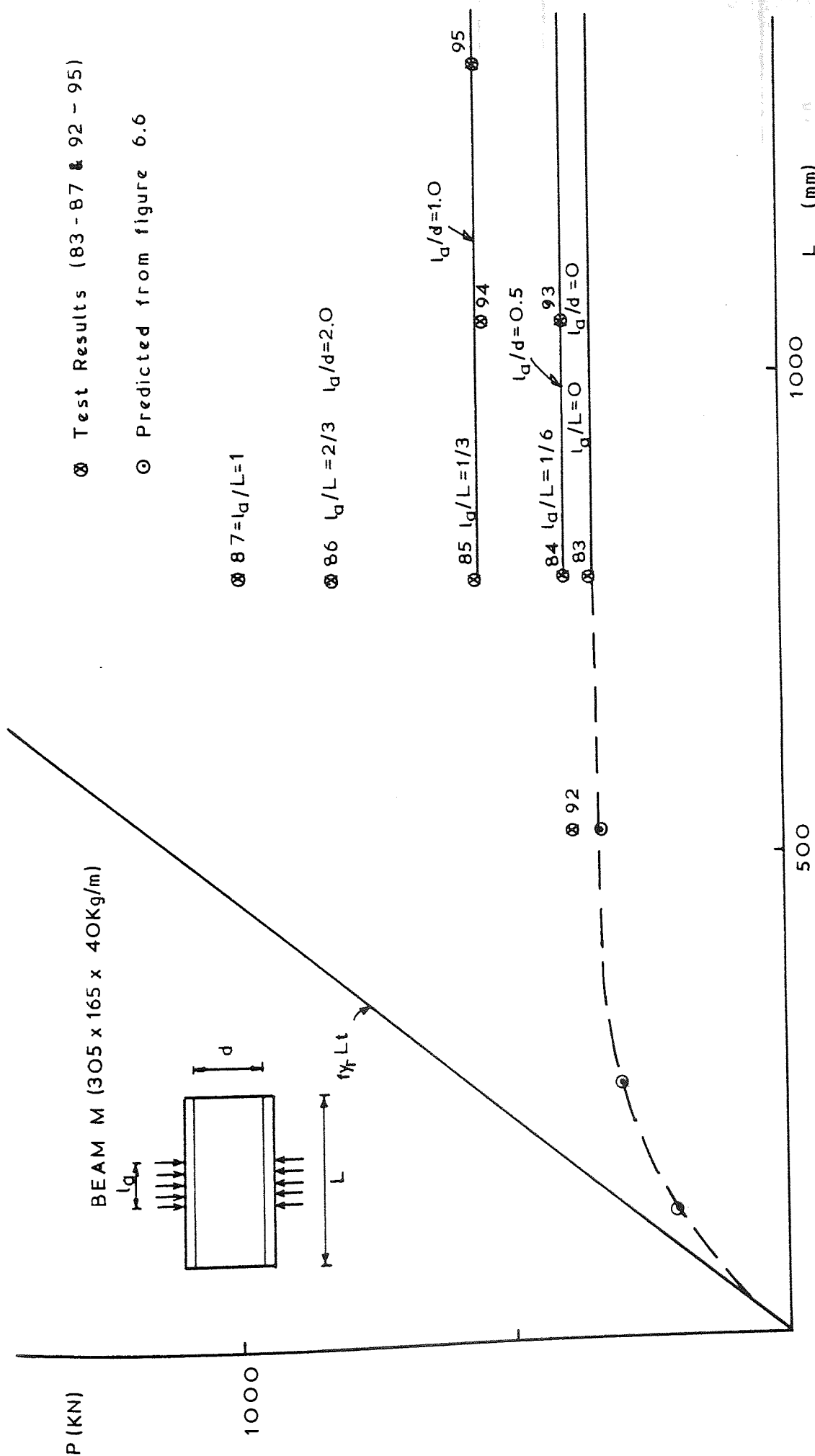


Figure 6.8 Variation of failure loads for beam M with beam length, showing the effects of the applied load length.

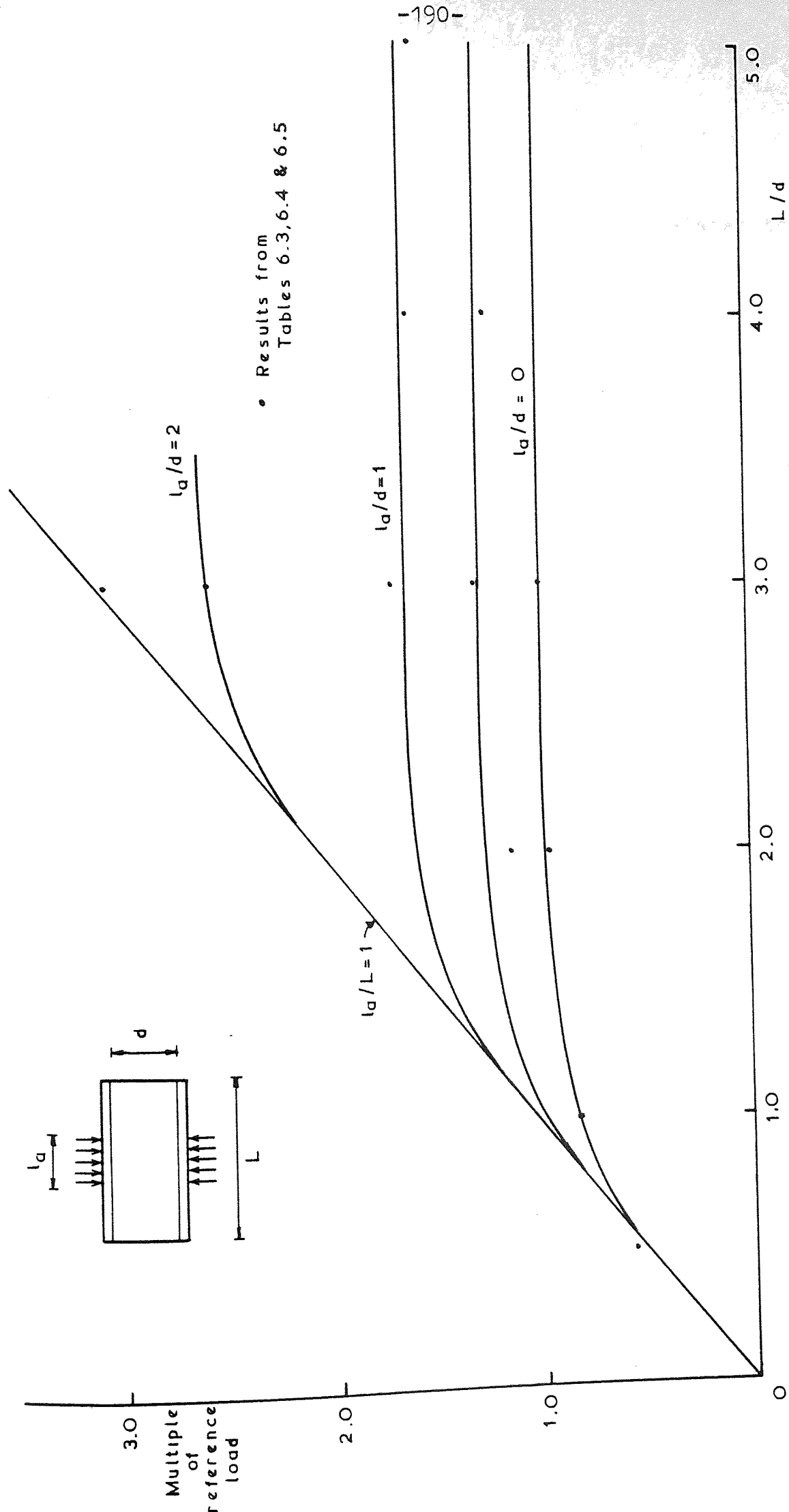


Figure 6.9 General trend of beam failure loads indicated by the empirical relationships.

$$P = P_0 + \frac{l_a}{L} (k_3 P_0 - P_0)$$

where  $k_3$  is some parameter which appears to be related to the aspect ratio ( $L/d$ ). Thus:

$$\frac{P}{P_0} = 1 + \frac{l_a}{L} (k_3 - 1) \quad 6.10$$

Assuming that these empirical relationships would be apparent for other aspect ratios, then in general:

$$\frac{P}{P_0} = 1 + \frac{l_a}{L} (k - 1) \quad 6.11$$

where  $k = f(L/d)$ .

This equation shows the ultimate load for a universal beam subjected to a length of loading applied across the flange to be the sum of two quantities. One quantity is irrespective of the depth of the section and the length of the load, the other quantity being dependent on both.

The crushing theory developed in the first part of this chapter conforms to these findings. The load carrying capacity could be determined with no consideration of the depth of the section for knife edge loads applied remote from the beam end. However the method was inaccurate for applied loads of some length, which may be due to the fact that the appropriate formula (equation 6.8) does not have a form similar to that of equation 6.11.

## CHAPTER 7 - CONCLUSIONS AND SUGGESTIONS FOR FURTHER RESEARCH

### 7.1 Introduction

It was shown earlier in this work that several authors have conducted tests on various types of steel beams but have had difficulty in establishing the exact mode of failure or isolating the effects which led to their eventual failure. Several authors assumed a mode of failure such as crushing of the web under the load or web buckling to establish a theoretical approach to suit the test results. Consequently several different theories and design guides can be found in various texts.

As similar difficulties in determining the cause of failure were likely to be experienced in this work, it was concluded that a different approach was required. It was decided therefore to examine several different theoretical approaches, each based on a predetermined mode of failure and satisfying the loading and restraint conditions imposed in the laboratory tests. Each theory was developed to a stage at which the significant variables affecting the beam load carrying capacities could be ascertained. Each theoretical approach could then be compared with the results of tests on various beam section sizes to see which, if any, compared favourably.

## 7.2 Conclusions from the Test Results

Observations made during the tests showed that every beam tested had large out of plane deflexions in the web at failure. Even though some beams had areas of very high direct stresses, the applied load was maintained until the web deflexions became significant. The rate of increase of the web deflexions varied between tests, in some tests they were small until failure when they increased suddenly and in other tests they were apparent at low loads and increased until failure.

The degree of yielding also varied between tests, the areas in which high stresses could be detected were:

1. The flange in the vicinity of the applied load. These high stresses were due to bending and large rotations, although high direct stresses will also be inherent due to the method of loading. The large rotations of the flange for some beams would have allowed the web to deflect considerably.
2. The web at its junction with the root in the vicinity of the applied load. These high stresses were due to both bending and direct stresses. These high stresses would have allowed the deflexions of the remainder of the web to increase.
3. The web at or near to the beam mid-depth. The large stresses induced at this location were direct and bending stresses. In some tests the bending stresses were predominant prior to failure and in other tests they were negligible prior to failure but increased dramatically when the beam failed.

Each of these regions of high stresses would have an influence on the beam load carrying capacity. However high stresses at one location could have been induced due to high stresses at another. For instance high bending stresses at the web mid-depth could have been due to high bending stresses and hence rotations at the web root.

The Southwell plot for beams in Series I (for lengths up to  $L/d = 2.0$ ) gave a very good straight line indicating an elastic buckle at a load almost identical to the maximum load attained in the tests. Hence it is possible that the beam buckled elastically and that high bending stresses at the web mid-depth were induced very near to failure and had little effect on the maximum load attained during the tests. For the long beams in Series I the Southwell plot gave a good straight line also, but indicated an elastic buckling load of slightly greater magnitude than the maximum load attained. It is probable that in this case the yielding at the web root permitted large rotations, hence increasing the web deflexions at the mid-depth, this in turn causing yielding at a lower load than the elastic buckling load and thus causing premature failure of the beam.

The Southwell plot for beams in other series did not give satisfactory straight lines, and so any results deduced from the plot would be erroneous. The incidence of yielding for beams which had loads spread across the flanges was greater than for beams loaded by concentrated point loads. For these beams yielding also sometimes occurred in the flanges. As yielding occurred at so many different locations for different tests, no definite conclusions as to the mode of failure can be determined from the test results



except for beams in Series I and II which were loaded by concentrated point loads. However, for beams loaded by uniformly distributed loads there was less yielding at all locations in the section.

The retest loads showed that beams loaded by uniformly distributed loads were more likely to take considerably less load in a retest than was attained in the initial test. This tends to indicate a stability criterion resulting in a highly deformed shape.

The effects of bending and shear as included for tests in Series VII are shown to have little effect on the failure load for a beam with a span to depth ratio ( $s/d$ ) of up to 5.0. However this was ascertained for one beam serial size only, consequently for other serial sizes the effects may be different.

### 7.3 Conclusions from the Comparisons of Individual Theories with the Test Results

In this work the emphasis has been placed on determining the main criteria affecting failure and the mode of failure rather than developing an accurate analytical method for determining the failure load of a universal beam. It is thought that once the cause of failure can be determined with sufficient accuracy, then an analytical analysis can be investigated in greater detail and compared with relevant test results. Nevertheless the theories developed here have been shown to be quite feasible in some instances.

The three different theories which have been considered

here have all shown reason to be relevant within certain loading and restraint conditions. Although the theories contain certain empirical constants, the comparisons show the variables to be relevant in some instances. Each of the three theories represent a particular mode of failure, each dependent on certain failure criteria being more relevant than others. The predominant criterion for each mode of failure is:

1. Elastic buckling theory - stability of the web.
2. Yield line theory - ultimate moment of resistance due to bending for the web and the flanges.
3. Local crushing theory - the maximum predominantly direct stress system attainable at the web root, accompanied by out of plane deflexions of the web and flange bending.

The comparison of each individual theory indicates that each one could be relevant for certain loading and restraint conditions. The yield line theory and the crushing theory have certain similarities which enable them to be considered together. Both these theories indicate similar variables, each showing that for long beams the depth of the section has little or no effect on the failure load. Both show reasonable agreement with the test results for long beams loaded by knife edge loads but vary quite considerably with the test results for other loading conditions.

However by considering the empirical relationships between failure loads as in Chapter 6, it was shown that this would be expected. This showed that for knife edge loads (long beam lengths) the beam depth is not relevant in determining the failure load but, when the loads are uniformly distributed the depth of the section is relevant.

The comparison of the Series I test results with the elastic buckling theory (figure 4.15) show very good agreement and confirm the indications shown by the recordings made during the tests. The comparison shows that for length to depth ratios ( $L/d$ ) of up to 2.0 the beams failed at the elastic buckling load and that for length to depth ratios of greater than 2.0 they generally failed below the elastic buckling load. However the indications from the previous section showed that this would be so, due to the high bending stresses in the web and the local crushing at the load application point. The flange resistance to rotation is also likely to have an effect for long lengths.

Thus if the Series I test beams did buckle elastically then the retest loads attained show that the post-buckling strength is lower. Hence if a beam develops high bending stresses before it has buckled elastically, then it will fail at a lower load than the elastic buckling load. This is confirmed by beams tested in Series II which were tested with eccentric concentrated point loads. The Southwell plot using deflexions when the beam is still elastic in the web (at the mid-depth) indicates a test critical load, which is never attained due to the effects of subsequent yielding at the extreme fibres of the web.

Thus it appears that for the beams utilised in this work, the elastic buckling load is an upper bound, and is the load carrying capacity for a beam with ideally elastic properties. The non-linear effects of the stress-strain relationship reduce the load carrying capacity. The effects of any initial eccentricity in the web would also reduce the load carrying capacity.

For beams other than those in Series I and II, as well as the effects of yielding at the web extreme fibres due to bending, the effects of the loading conditions and the restraint which the application of the load itself provides will also affect the buckling load. Consider first the beam most likely to fail due to elastic buckling, a short beam in Series III (two opposite knife edge loads) or a beam loaded by long uniformly distributed load in Series V or VI. Some of these tests showed no signs of yielding at the extreme fibres of the web or at the web root up until the very sudden failure. However as can be seen in figures 4.16 and 4.18 these beams did not have the equivalent of fully restrained loaded edges. Even if the stresses due to bending in the web are accounted for by using the Perry formula (as incorporated in the BS 449 design in Chapter 3), the restraint is still not the equivalent of full restraint. Thus in this case, beams which fail in quite an obvious elastic buckling manner must fall short of the fully restrained edge conditions due to another factor.

This further factor can be detected by examining the deformed shapes of the relevant test beams after the first loading cycle. It can be seen that the flanges do not remain exactly perpendicular to the original web position, so that the web and sometimes the flanges rotate at their junction with the root. It was shown earlier in the work that for some tests the flange rotated and lifted off one side of the applied load which in fact means that the condition for the web to act as a clamped plate is not observed as its slope at the loaded edges does not remain zero. This is due to torsion in the flanges.

There is one further effect which must also be considered. That is the high stresses which are induced in the web at its junction with the root, due to the high concentration of the load. This would also reduce the restraint provided.

Hence by considering all these factors, only a beam with thick flanges and a slender web loaded across the flanges would be expected to fail as a fixed ended strut. Test beam 33 would be most likely to satisfy these conditions, and in fact its equivalent plate buckling coefficient is ( $K_1$ ) 3.87 which compares with 4.0 for a fixed ended strut.

The failure loads for other beams would be expected to be an elasto-plastic buckling load depending on the non linear consideration of the stress-strain relationship. Hence the value of the coefficient of restraint  $R$  referred to in Chapter 4 would be likely to vary with the properties of the section but not in a direct way. The non linear effects of the stress-strain relationship would affect both the restraint at the loaded edges and also the stresses at the extreme fibres of the web.

If these hypotheses are correct then the conclusions from Chapters 5 and 6 conform. Both chapters deduced that for certain loading conditions, the load carrying capacity of a rolled steel beam could be determined without considering the depth of the beam. Both methods show that when loading conditions produce considerable yielding at the load point or at the extreme fibres of the web due to bending the load carrying capacity can be determined by considering the ultimate strength of the section.

The yield line theory seems to give more consistent results when compared with the results of the tests. For the case when long beams are loaded by knife edge loads the crushing theory gives a coefficient of variation of 6% compared to 16% for the yield line theory. However the empirical constant for the yield line theory was determined from a different failure mode and yet gave a mean value of  $P_{th} / P_{exp}$  of 1.0 whereas the empirical constant for the crushing theory was determined from the test results considered. Also the yield line theoretical loads show some correlation with the retest loads for beams which almost certainly failed in the initial test due to web instability. The yield line theory also considers the rotation of the flanges in deriving the theoretical failure loads which is consistent with the observations from the test results. It is also possible that neither of these two approaches is correct but as each has the main variables involved, a satisfactory approximation has been found.

#### 7.4 Summary

The complexity of the problem and the various factors which influence the load carrying capacity of a universal beam or joist illustrate why the various design guides in use at the present time are only effective when beams have certain loading conditions. It has been shown that an approach such as the BS 449 design guide, which uses the Perry formula includes the effects of large stresses at the extreme fibres of the web at the mid-depth but overestimates the restraint provided by a load applied across the flange.



this is due to the high stresses imposed in both the flange and the web in the vicinity of the applied load thus permitting rotation of the flange and the web.

It has been shown that if a beam is loaded in such a way that the stresses are kept within the elastic range, then the failure load can be determined by elastic instability analysis, providing the degree of restraint present can be determined. However when a beam is loaded in a manner such that there is a high incidence of yielding then the failure load can be determined with reasonable accuracy without considering the depth of the beam i.e. by assessing the ultimate strength of the section.

It has proved impossible to determine the effective or equivalent restraint which a beam will have on its loaded edges due to its physical properties and the type of loading imposed. This is due to the non-linear stress-strain effects which would have a very complicated effect.

It was shown that if the design of a beam against local failure is based on the large deflexion yield line analysis, then the design will always be conservative, even if the beam has initial deformations. The only instance when this would not be so is when beams with excessively large deflexions are considered, in which case any method of analysis would be incorrect.

The yield line analysis method incorporates an empirical constant, which although suitable for the range of beams considered in this work may vary for other section sizes or beam types.

## 7.5 Suggestions for Further Research

Primarily any further work in this field should develop the state of knowledge. As the present work does not consider bending and shear stresses in great detail, it is thought that as this is the simplest form of loading to analyse, the theoretical work advanced here should be continued for direct stresses only. This would then determine whether the hypotheses proffered in this work as to the mode of failure are correct.

To this end it is thought that the next stage in the advancement of this work should be the inclusion of the non-linear stress-strain effects in the stability analysis. As the stability analysis for elastic beams subjected to concentrated loads has been shown in this report to be quite complex it seems probable that to include non-linear effects would necessitate the use of analysis by the finite element method. Alternatively the elastic analysis method developed here could possibly be used by incorporating reduction coefficients for the plate buckling coefficients, either theoretically or empirically based.

Further more detailed study of the yield line method is also required with special consideration of the empirical constant.

The effects of bending and shear were only considered in this work for one beam serial size and were not analysed in any great detail. Further work should be carried out to determine if bending and shear have such slight influence for other beam serial sizes and modes of failure.



In practice beams are often supported on 'stiff bearings'. This work has shown that a load previously considered to provide full restraint to a beam does not in fact do so. The effects of stiff bearings, seating angles etc. should also be considered in more detail.

The effects of multiple loads acting on universal beams or joists should also be considered at some further stage.

24th. October 1942

House 2. "University"

Engineering and

British Standards

Building

British Standards

Building

"Annexes"

British Standards

course of

University

University

University

University

University

University

University

University

University

University

University

University

University

REFERENCES

1. Hrennikoff A. "Lessons of the Collapse of the Vancouver 2nd. Narrows Bridge". Trans., A.S.C.E., 1961.
2. "Report by H.M. Factory Inspectorate on the Collapse of Falsework for the Viaduct over the River Loddon on 24th. October 1972". Published 1973.
3. Holmes M. "Universal Beams as Runway Beams". Civil Engineering and Public Works Review, 1964 (May).
4. British Standard 449 "The Use of Structural Steel in Building". April 1932.
- 4(a). British Standard 449 "The Use of Structural Steel in Building - Part 2 (Metric Units)". 1969. and "Amendment Slip No. 5". Published 31st. July 1975.
5. British Standard Code of Practice for Falsework. (in course of preparation), Draft published 1975.
6. Glanville First Report, Steel Structures Research Committee. H.M.S.O. 1931.
7. Pippard A.J.S. and Baker J.F. "The Analysis of Engineering Structures". Edward Arnold & Co. 1943.
8. Bryan G.H. "On the Stability of a Plane Plate Under Thrusts in its Own Plane with Application to the Buckling of the Sides of a Ship". Proc. London Math. Soc., 1891.
9. Stowell E.Z. and Houbolt J.C. "Critical Stress of Plate Columns". N.A.C.A., T.N. 2163, 1950.
10. Weinowsky-Krieger S. "Stability of a Rectangular Plate with Free Loaded Edges". Ingenieur Archiv., Vol. 19, 1951.



11. Timoshenko S. "Theory of Elastic Stability": McGraw Hill Co., 1937.
12. Bleich F. "Buckling Strength of Metal Structures". McGraw Hill Co., 1952.
13. Stowell E.Z. & Others "Buckling Stresses for Flat Plates and Sections". Trans., A.S.C.E., Vol. 117, 1952.
14. Gerard G. and Becker H. "Handbook of Structural Stability - Part 1 - Buckling of Flat Plates". N.A.C.A., T.N. 3781.
15. Leggett D.M.A. "The Effect of Two Isolated Forces on the Stability of a Flat Rectangular Plate". Proc. Camb. Phil. Soc., Vol. 33, 1937.
16. Yamaki N. "Buckling of a Rectangular Plate under Locally Distributed Forces Applied on Two Opposite Edges". Rep. Inst. High Speed Mech., Tohoku Univ., Vol. 3 (1953) and Vol. 4 (1954).
17. Zetlin L. "Elastic Instability of Flat Plates Subjected to Partial Edge Loads". Proc. A.S.C.E., Eng. Mech. Div., Vol. 81, 1955.
18. Alfutov N.A. and Balabukh L.I. "Energy Criterion of the Stability of Elastic Bodies which does not require the Initial Stress-Strain State". Prikladnaya Matematika I Mekhanika, Vol. 32, 1968.
19. Alfutov N.A. and Balabukh L.I. "On the Possibility of Solving Plate Stability Problems without a Preliminary Determination of the Initial State of Stress". Prikladnaya Matematika I Mekhanika, Vol. 31 1967.

20. Khan M.Z. and Walker A.C. "Buckling of Plates Subjected to Localised Edge Loading". Structural Engineer, June 1972.
21. Kapur K. and Hartz B.J. "Stability of Plates using the Finite Element Method". Proc., A.S.C.E. Eng. Mech. Div., 1966.
22. White R.N. and Cottingham W.S. "Stability of Plates under Partial Edge Loading". Proc., A.S.C.E., Eng. Mech. Div., Vol. 88, 1962.
23. Rockey K.C. and Bagchi D.K. "Buckling of Plate Girder Webs under Partial Edge Loads". Int. Journ. Mech. Sci., Vol. 12, 1970.
24. Ilyushin A.A. "The Elasto-plastic Stability of Plates". N.A.C.A., T.M. 1188.
25. Ilyushin A.A. "Ustoichivost Plastinok i Obolochek za Predelom Uprugosti". Prikladnaya Matematika i Mekhanika, No. 5, 1944. (Also available as N.A.C.A., T.M. 1116).
26. Gerard G. "Secant Modulus Method for Determining Plate Instability Above the Proportional Limit". Journ. Aero. Sci., Vol. 13, 1946.
27. Stowell E.Z. "A Unified Theory of Plastic Buckling of Columns and Plates". N.A.C.A., T.N. 1556, Rep. 898, 1948.
28. Moore H.F. "The Strength of I-Beams in Flexure". Univ. of Illinois, Eng. Exp. Stat., Bulletin No. 68, Sept. 1913.
29. Moore H.F. and Wilson W.M. "The Strength of Webs of I-Beams and Girders". Univ. of Illinois, Eng. Exp. Stat., Bulletin No. 86, May 1916.



30. Lyse I. and Godfrey H.J. "Investigation of Web Buckling in Steel Beams". Trans., A.S.C.E., Paper No. 1907, 1934.
31. Wastlund G. and Bergman S.G.A. "Buckling of Webs in Deep Steel I-Beams". Pubs. Intern. Assoc. Bridge and Struct. Eng., Vol. 8, 1947.
32. Winter G. and Pian R.H.J. "Crushing Strength of Thin Steel Webs". Cornell Univ. Eng. Exp. Stat., Bulletin 35, Part 1, April 1946.
33. Delesques R. "Ultimate Strength of Webs of Beams without Intermediate Stiffeners ". Construction Metalique, No. 2, P. 547, 1974.
34. Bergfelt A. "Studies and Tests on Slender Plate Girders without Stiffener Strength and Local Web Crippling". Work Commission Report, A.I.P.C., Vol. 11, 1971.
35. Bergfelt A. and Hovik J. "Thin Walled Deep Beams under Static Loads". Final Report 8th. Congress A.I.P.C., New York, 1968.
36. Frocht M.M. "Photoelasticity". Vol. III, John Wiley and Sons Inc., 1948.
37. Coker E.G. and Filon L.N.P. "A Treatise on Photo-elasticity". 2nd. Edition rev. by H.T. Jessop, C.U.P. 1957.
38. Voorn W.J.M. "De Plooisterkte van Onverstijfde I-Profielen bij Geconcentreerde Lasten". BI - 71 - 10 T.N.O. I.B.B.C., March 1971, (Dutch Report).
39. BS 4360, "British Standard Specification for Weldable Structural Steels". 1972.

40. Shedd T.C. "Structural Design in Steel". John Wiley and Sons Inc., 1934.
41. Majid K.I. "Non-linear Structures". Butterworth and Co. Ltd., 1972.
42. Southwell R.V. "On the Analysis of Experimental Observations in Problems of Elastic Stability". Proc. of the Royal Soc., 1932, Vol. 135, Series A.
43. Horton W.H. and Cundari F.L. "On the Applicability of the Southwell Plot to the Interpretation of Test Data from Instability Studies of Shell Bodies". Proc. A.I.A.A. / A.S.M.E. 8th Structs., Struct. Dyn. and Matls. Conf., Calif. (A.I.A.A. New York 1967).
44. Roorda J. "Some Thoughts on the Southwell Plot". Journ., E.M.D., A.S.C.E., 1967, Vol. 93, EM6.

## Ground Deflection

As the complete analysis

the tests

gauge or mechanical

and nuclear strain gauges

indicate the strain

distance is

4/2.

## APPENDIX A.1: Table A.1:

at the base

depth of the web

deflection gauge;

the line of action of the

deflection gauge; located

average of the

web position.

It is likely that for gauges

strains, that the gauge has ceased to

This should be considered when

for some readings or or near the

indicated in Table A.1



### A.1 Strain and Deflexion Recordings

Table A.1 contains the complete set of strain and deflexion recordings for all the tests which utilised electrical resistance strain gauges or mechanical deflexion gauges.

All strain gauge reference numbers are in accordance with figure 2.4. The number in brackets after the strain gauge reference number for tests 98 - 100 is the distance in millimetres from the beam mid-length to the strain gauge position when the spacing of gauges is not  $d/4$ .

The following abbreviations are used in Table A.1:

C.D.G. - Central deflexion gauge; located at the beam mid-length at the mid-depth of the web.

L.P.D.G. - Load point deflexion gauge; located at the web mid-depth along the line of action of the applied loads.

V.D.G. - Vertical deflexion gauge; located under the bottom flange at the beam mid-span (average of two gauges located each side of the web position).

R - Retest.

It is likely that for gauges which show very high strains, that the gauge has ceased to function correctly. This should be considered when utilising these results.

For some readings at or near the failure load it is indicated in Table A.1 that the readings cannot be

guaranteed. There are two reasons why:

1. The instability of the test beam and consequent fluctuation of the gauges at the applied load.
2. The actual load applied (when readings are indicated at failure) is variable due to the nature of hydraulic testing machines.

Thus readings indicated by a \* are only intended as a guide to the overall beam behaviour rather than accurate recording of the state of stress.

Strains  $\times 10^6$  and Deflexions (mm).

Test No. 3

Gauge Ref.	Load (KN)	20	40	60	80	100	120	140	160	180
1		-106	-216	-353	-510	-769	-1033	-1486	-2125	-1974
2		-39	-63	-60	-32	56	252	624	1230	1800
3		-81	-170	-279	-410	-592	-858	-1266	-1862	-1752
4		-20	-20	4	52	156	354	711	1284	1616
5		-49	-101	-170	-255	-378	-571	-887	-1388	-1367
6		12	34	77	136	236	404	687	1143	1191
7		-25	-58	-100	-153	-235	-368	-597	-994	-939
8		17	44	86	136	216	337	536	863	834
9		-13	-27	-50	-81	-133	-220	-382	-678	-519
10		16	49	93	141	213	316	482	766	692
C.D.G.		.09	.33	.69	1.11	1.81	2.92	4.70	7.55	

Table A.1



Strains  $\times 10^6$  and Deflexions (mm).

Test No. 4

Load (KN)	20	40	60	80	100	120	140	160	180	200	220	240
Gauge Ref.												
1	-90	-179	-274	-377	-504	-653	-828	-1081	-1512	-2136	-2929	-4717
2	-47	-87	-125	-152	-155	-136	-81	60	404	995	1796	3310
3	-63	-129	-198	-274	-373	-491	-636	-855	-1245	-1844	-2643	-4471
4	-21	-38	-53	-58	-42	-6	60	206	531	1085	1860	3457
5	-30	-60	-95	-135	-193	-266	-362	-519	-830	-1354	-2119	-3768
6	-1	5	14	30	61	109	179	307	575	1038	1733	3204
7	-14	-28	-46	-67	-102	-148	-211	-318	-548	-969	-1641	-3110
8	13	26	40	60	90	131	186	283	481	833	1413	2749
9	-7	-16	-25	-39	-63	-94	-136	-211	-376	-692	-1241	-2518
10	12	25	37	54	78	111	154	227	376	647	1110	2254
11	-5	-11	-19	-28	-45	-67	-98	-151	-271	-499	-914	-1989
12	9	20	29	42	61	87	120	177	294	503	860	1745
13	-1	-20	-5	-11	-21	-36	-57	-91	-169	-309	-554	-1260
14	8	20	29	43	61	85	116	169	276	474	816	1674
O.D.G.	.05	.19	.33	.51	.82	1.21	1.74	2.68	4.39	7.42	12.61	18.74

Table A.1 (cont.)

Strains  $\times 10^6$  and Deflexions (mm).

Gauge Ref.	Load (KN)	Test No. 5										*Fail
		20	40	80	120	160	180	200	220	240	260	
1	-64	-150	-332	-547	-851	-1092	-1446	-1946	-2512	-3220	-5660	
2	-56	-98	-168	-187	-102	39	317	787	1352	2074	4172	
3	-29	-78	-183	-315	-516	-685	-941	-1322	-1768	-2330	-3753	
4	-26	-49	-84	-77	15	149	404	832	1363	2071	4017	
5	0	-26	-90	-181	-341	-488	-730	-1122	-1628	-2334	-4440	
6	-8	-6	4	41	138	248	441	768	1199	1829	3690	
7	4	-7	-34	-80	-175	-268	-431	-720	-1126	-1754	-3589	
8	2	13	33	71	146	221	351	576	896	1418	3053	
9	14	8	-5	-31	-92	-153	-264	-467	-775	-1289	-2805	
10	9	19	42	78	141	203	307	490	753	1201	2630	
11	13	8	0	-19	-63	-108	-188	-335	-558	-952	-2200	
12	15	23	42	70	120	168	248	387	589	934	2070	
13	14	10	2	-13	-49	-84	-147	-259	-426	-723	-1733	
14	12	19	34	57	98	137	203	318	481	755	1649	
15	13	9	3	-8	-36	-65	-114	-199	-318	-519	-1193	
16	0	5	17	33	65	98	150	243	372	584	1238	
17	13	10	6	-2	-25	-48	-85	-145	-219	-327	-626	
18	8	12	20	36	64	92	139	224	347	553	1191	
C.D.G.	.00	.07	.34	.81	1.69	2.52	3.91	6.23	9.31	13.11	20.81	

\* Readings cannot be guaranteed.

Table A.1 (cont.)

# Strains $\times 10^6$ and Deflexions (mm).

Test No. 6

Load (KN)	10	20	30	40	50	60	70	80	*90
Gauge Ref.									
1	-65	-133	-204	-279	-365	-471	-605	-799	-1128
2	-55	-127	-197	-258	-304	-334	-336	-266	-75
C.D.G.	.00	.00	.01	.04	.09	.17	.30	.56	1.05

Test No. 7

Load (KN)	10	20	30	40	50	60	70	80	90	100	110	120
Gauge Ref.												
1	-73	-154	-244	-330	-417	-517	-622	-752	-901	-1089	-1335	-1686
2	-32	-61	-86	-110	-133	-144	-146	-129	-81	6	158	430
C.D.G.	.04	.10	.18	.27	.34	.45	.56	.71	.93	1.22	1.68	2.38

Test No. 8

Load (KN)	20	40	60	80	100	120	140	160	180	200	220
Gauge Ref.											
1	-134	-269	-400	-532	-663	-813	-973	-1120	-1228	-1582	-1746
2	-71	-144	-218	-295	-347	-393	-419	-422	-388	-296	-216
C.D.G.	.00	.04	.08	.11	.18	.27	.41	.58	.79	1.15	1.69

Table A.1 (Cont.)



Strains  $\times 10^6$  and Deflexions (mm).

Test No. 9

Load (KN) 40 80 120 160 200 240 280

Gauge Ref.

1 -226 -466 -717 -969 -1249 -1532 -1915  
2 -151 -295 -397 -475 -516 -498 -323

C.D.G.

.02 .10 .25 .46 .69 1.07 1.95

Test No. 10

Load (KN) 20 40 60 80 100 120 140 160 200 240 280

Gauge Ref.

1 -96 -208 -318 -434 -546 -657 -782 -917 -1208 -1572 -2311  
2 -77 -168 -252 -332 -406 -477 -543 -587 -647 -578 -112

C.D.G.

.04 .09 .14 .19 .24 .30 .37 .48 .77 1.28 1.75

Test No. 11

Load (KN) 10 20 30 40 45 \*Fail 10 \*R 1 10 \*R 2

Gauge Ref.

1 -110 -254 -440 -770 -1398  
2 -3 15 67 258 790

C.D.G.

.14 .40 .80 1.67 3.65 8.37 - 10.72 5.57 13.22

\* Reading cannot be guaranteed.

Table A.1 (cont.)

Strains x  $10^6$  and Deflexions (mm).

		Test No. 12											
Load (kN)	Gauge Ref.	10	20	30	40	50	60	70	80	90	100	110	*Fail
1		-57	-114	-175	-238	-301	-367	-448	-546	-681	-861	-1168	
2		-51	-99	-146	-198	-245	-285	-308	-284	-228	-106	121	
C.D.G.		.00	.00	.03	.08	.13	.20	.32	.54	.87	1.36	2.18	3.45

		Test No. 13										
Load (KN)		20	40	60	80	100	120	140	160	*Fail	10	*R 1
Gauge Ref.												
1		-145	-293	-443	-595	-786	-1019	-1315	-1776			
2		-51	-98	-138	-142	-105	-16	169	559			
C.D.G.		.02	.13	.26	.46	.76	1.18	1.89	3.25	8.07	13.36	22.07

		Test No. 14									
Load (KN)	Gauge Ref.	20	40	60	80	100	120	140	*Fail		
1		-105	-218	-334	-437	-560	-717	-968			
2		-77	-153	-231	-286	-324	-323	-197			
C.D.G.		0	0	0	.03	.15	.43	1.23	5.23	2.02	

\* Reading cannot be guaranteed

Table A.1 (cont.)

Strains x 10<sup>6</sup> and Deflexions (mm)

		Test No. 15										
Load (kN)	Gauge Ref.	20	40	60	80	100	140	180	200	220	240	260
-96	1	-196	-303	-391	-474	-659	-841	-914	-1000	-1077	-1124	
-99	2	-180	-273	-360	-450	-615	-763	-824	-874	-905	-944	
.18	C.D.G.	.23	.27	.32	.36	.45	.53	.57	.59	.61	.71	

		Test No. 16		
Load (KN)	Gauge Ref.	10	20	50
-97	1	-198	-399	-697
-13	2	-22	62	244
.09	C.D.G.	.24	.73	1.57
				3.64
				6.65

Gauge Ref.

		Test No. 17				
Load (KN)	Gauge Ref.	20	40	60	80	100
-139	1	-277	-428	-616	-908	-1120
-59	2	-89	-119	-96	18	173
.28	C.D.G.	.46	.68	1.02	1.64	2.18
						3.26
						6.10
						2.82

		Test No. 17				
Load (KN)	Gauge Ref.	20	40	60	80	100
-139	1	-277	-428	-616	-908	-1120
-59	2	-89	-119	-96	18	173
.28	C.D.G.	.46	.68	1.02	1.64	2.18
						3.26
						6.10
						2.82

Gauge Ref.

		Test No. 17				
Load (KN)	Gauge Ref.	20	40	60	80	100
-139	1	-277	-428	-616	-908	-1120
-59	2	-89	-119	-96	18	173
.28	C.D.G.	.46	.68	1.02	1.64	2.18
						3.26
						6.10
						2.82

\* Reading cannot be guaranteed

Table A.1 (cont.)



Strains  $\times 10^6$  and Deflexions (mm)

Test No. 18

Load (KN)	20	40	60	80	100	120	140	160	180	200
Gauge Ref.										
1	-80	-165	-246	-331	-432	-546	-668	-814	-1029	-1477
2	-101	-189	-276	-353	-420	-480	-512	-517	-429	-112
C.D.G.	0	0	0	0	0	0	.12	.33	.73	1.75

Test No. 19

Load (KN)	20	40	60	80	100	120	140	160	180	200	10	R 1
Gauge Ref.												
1	-127	-239	-366	-513	-681	-883	-1114	-1402	-1741	-2133		
2	-48	-89	-120	-139	-132	-88	-3	144	366	674		
C.D.G.	.19	.30	.45	.63	.87	1.21	1.65	2.27	3.09	4.24	7.40	16.77

Test No. 20

Load (KN)	10	20	30	40	50	60	70	80	90	100
Gauge Ref.										
1	-108	-221	-326	-426	-528	-628	-730	-836	-1037	-1471
2	-34	-74	-128	-168	-225	-272	-315	-436	-279	15
C.D.G.	.07	.18	.22	.27	.31	.35	.40	.48	.73	1.45

Table A.1 (cont.)

Strains  $\times 10^6$  and Deflexions (mm)

Test No. 21

Load (KN)	20	40	60	80	100	120	140
Gauge Ref.							
1	-119	-239	-379	-520	-696	-948	-1365
2	-91	-187	-274	-332	-349	-288	-46
C.D.G.	.13	.18	.26	.38	.58	.93	1.69

Test No. 22

Load (KN)	20	40	60	80	100	120	140	160	180	200	220
Gauge Ref.											
1	-93	-203	-303	-402	-494	-574	-668	-748	-827	-923	-1050
2	-100	-210	-317	-420	-510	-592	-676	-745	-797	-823	-783
C.D.G.	.02	.02	-.01	-.05	-.08	-.10	-.12	-.11	-.10	-.03	.25

Test No. 23

Load (KN)	40	80	120	160	200	220	240	260	280
Gauge Ref.									
1	-235	-471	-693	-900	-1113	-1224	-1324	-1457	-1732
2	-161	-331	-492	-622	-738	-788	-810	-811	-624
C.D.G.	.18	.28	.40	.54	.69	.78	.90	1.12	1.80

Table A.1 (cont.)

Strains  $\times 10^6$  and Deflexions (mm)

Test No. 24

Load (KN)	10	20	30	40	50	60	70	80	90	100
Gauge Ref.										
1	-125	-234	-347	-461	-575	-685	-829	-991	-1214	-1532
2	-58	-117	-181	-244	-299	-327	-360	-364	-306	-127
C.D.G.	.07	.14	.18	.22	.27	.33	.40	.51	.70	1.01

Test No. 25

Load (KN)	20	40	60	80	100	120	140	160
Gauge Ref.								
1	-171	-329	-501	-676	-863	-1066	-1309	-1685
2	-105	-220	-329	-420	-468	-455	-390	-150
C.D.G.	.10	.12	.15	.20	.32	.48	.73	1.27

Test No. 26

Load (KN)	20	40	60	80	100	120	140	160	180	200	220	240
Gauge Ref.												
1	-150	-283	-417	-546	-671	-769	-866	-963	-1064	-1124	-1244	-1586
2	-127	-250	-376	-494	-614	-712	-803	-893	-989	-1015	-1011	-892
C.D.G.	0	.03	.03	.03	.02	.02	.02	.04	.07	.15	.36	1.05

Table A.1 (cont.)

Strains  $\times 10^6$  and Deflexions (mm)

Test No. 27

Load (KN)	40	80	120	160	200	220	240	260
Gauge Ref.								
1	-283	-545	-826	-1111	-1403	-1562	-1742	-2003
2	-173	-351	-535	-719	-803	-785	-729	-562
C.D.G.	.18	.32	.39	.45	.59	.74	1.00	2.57

Test No. 28

Load (KN)	20	40	60	80	100	120	140	160	180	*Fail
Gauge Ref.										
1	-124	-245	-354	-445	-530	-631	-753	-884	-1049	-1309
2	-65	-132	-217	-312	-401	-471	-532	-558	-520	-374
C.D.G.	.09	.13	.15	.12	.12	.15	.18	.26	.46	.98

Test No. 29

Load (KN)	40	80	120	160	200	220	240	*Fail
Gauge Ref.								
1	-222	-451	-684	-969	-1275	-1461	-1658	
2	-118	-236	-335	-393	-385	-334	-242	
C.D.G.	.18	.37	.59	.90	1.32	1.63	2.05	2.80

\* Reading cannot be guaranteed

Table A.1 (cont.)

Strains x 10<sup>6</sup> and Deflexions (mm)

Gauge Ref.	Load (KN)	Test No. 30											
		40	80	120	160	200	240	260	280	300	320	340	360
1	-214	-307	-429	-573	-752	-1006	-1210	-1409	-1760	-2126	-2595	-3063	
2	-171	-205	-216	-199	-136	1	59	182	238	563	1053	1536	
3	-196	-269	-370	-491	-646	-872	-1061	-1245	-1583	-1936	-2409	-2937	
4	-138	-148	-136	-103	-32	100	148	256	293	579	1029	1522	
5	-173	-218	-286	-370	-480	-646	-802	-949	-1246	-1552	-1991	-2506	
6	-102	-82	-42	12	94	225	263	356	365	603	996	1461	
7	-157	-190	-237	-296	-371	-488	-612	-723	-976	-1219	-1592	-2057	
8	-86	-56	-11	44	116	223	245	312	288	464	777	1176	
9	-150	-177	-215	-259	-317	-404	-508	-595	-816	-1002	-1297	-1688	
10	-88	-60	-22	20	77	157	160	205	150	273	505	813	
11	-143	+164	-192	-224	-265	-327	-414	-480	-669	-799	-995	-1264	
12	-93	-70	-39	-4	37	99	90	120	46	136	311	540	
13	-139	-150	-170	-193	-221	-263	-336	-383	-551	-631	-733	-868	
14	-95	-74	-45	-13	24	79	65	92	16	100	271	498	
C.D.G.	.10	.35	.73	1.20	1.91	2.91	3.57	4.37	5.37	7.02	9.72	13.17	

Table A.1 (cont.)

(cont.)



# Strains $\times 10^6$ and Deflexions (mm)

Test No. 31

Load (KN)	10	20	30	40	50	60	70	80	90	100	110	*120
Gauge Ref.												
1	-133	-329	-510	-715	-932	-1153	-1383	-1614	-1860	-2149	-2462	-3240
2	86	226	367	532	712	902	1108	1319	1548	1816	2111	2800
3	-126	-311	-488	-690	-907	-1130	-1368	-1610	-1873	-2186	-2547	-3409
4	90	228	365	524	697	881	1080	1286	1513	1781	2088	2779
5	-97	-245	-388	-558	-746	-947	-1164	-1393	-1646	-1954	-2320	-3132
6	87	218	347	495	657	831	1025	1231	1463	1748	2084	2717
7	-75	-190	-303	-441	-597	-767	-960	-1165	-1402	-1694	-2052	-2800
8	71	176	278	396	528	671	835	1014	1224	1489	1816	2466
9	-56	-141	-227	-332	-451	-583	-738	-909	-1112	-1369	-1693	-2319
10	54	135	214	306	409	522	653	798	971	1196	1482	2044
11	-41	-103	-164	-239	-323	-416	-527	-652	-805	-1007	-1276	-1784
12	42	106	169	241	322	410	510	621	753	925	1146	1573
13	-26	-67	-105	-150	-200	-254	-316	-386	-475	-598	-772	-1117
14	39	98	155	221	297	380	474	578	702	864	1073	1475
C.D.G.	.59	1.52	2.40	3.45	4.55	5.71	7.03	8.49	10.16	12.21	14.84	20.30

\* Readings cannot be guaranteed

Table A.1 (cont.)



Strains  $\times 10^6$  and Deflexions (mm)

Test No. 32

Gauge Ref.	Load (KN)	10	20	30	40	50	60	70	80	90	100	*110
1		-152	-390	-623	-841	-1045	-1240	-1468	-1685	-1927	-2180	-2475
2		112	304	499	689	870	1044	1254	1458	1686	1924	2212
3		-147	-383	-620	-847	-1061	-1267	-1509	-1740	-2001	-2280	-2662
4		112	301	497	689	873	1053	1269	1480	1718	1974	2309
5		-120	-318	-524	-727	-928	-1124	-1360	-1591	-1854	-2143	-2570
6		105	284	467	647	825	1001	1217	1433	1683	1956	2344
7		-96	-255	-422	-594	-769	-946	-1165	-1386	-1644	-1934	-2389
8		86	230	380	531	681	834	1025	1222	1458	1723	2144
9		-73	-192	-318	-450	-586	-729	-908	-1094	-1320	-1579	-1984
10		66	178	296	415	535	658	817	983	1189	1427	1814
11		-56	-145	-239	-337	-439	-547	-688	-838	-1025	-1245	-1599
12		52	136	226	316	408	503	624	752	911	1098	1405
13		-42	-107	-173	-238	-304	-375	-466	-567	-695	-850	-1106
14		41	114	194	276	360	448	561	682	834	1013	1314
C.D.G.		.72	1.87	3.15	4.24	5.36	6.44	8.01	9.56	11.22	13.42	16.72

\* Readings cannot be guaranteed

Table A.1 (cont.)

# Strains $\times 10^6$ and Deflexions (mm)

Test No. 34

Load (KN)	50	75	100	125	150	175	200	225	250	275	300
Gauge Ref.											
1	-129	-212	-296	-364	-450	-550	-671	-749	-841	-923	-1257
2	-222	-338	-456	-556	-678	-767	-809	-888	-999	-1059	-1005
3	-77	-126	-179	-220	-276	-347	-439	-495	-567	-632	-925
4	-150	-223	-301	-366	-445	-496	-504	-553	-640	-682	-635
5	-9	-17	-34	-46	-63	-99	-154	-181	-230	-273	-516
6	-66	-91	-123	-148	-179	-185	-155	-171	-226	-246	-177
C.D.G.	.97	1.69	1.92	1.95	1.99	1.97	2.02	2.01	2.05	2.46	2.63

Test No. 35

Load (KN)	40	80	120	160	200	220	240	260	280	300	320	340
Gauge Ref.												
1	-56	-206	-357	-525	-695	-796	-896	-1035	-1210	-1574	-1906	-2409
2	-256	-404	-540	-667	-737	-757	-755	-715	-622	-365	-49	453
3	0	-95	-198	-303	-428	-507	-588	-705	-855	-1167	-1471	-1933
4				Gauge Broken								
5	57	27	-1	-40	-97	-136	-182	-251	-342	-544	-760	-1116
6	-127	-163	-190	-210	-211	-202	-187	-152	-88	68	250	548
7	71	73	75	75	57	42	20	-12	-58	-165	-293	-515
8	-69	-74	-71	-62	-47	-35	-21	2	42	133	231	394
9	82	106	132	157	164	164	157	143	124	75	7	-113
10	-26	-7	18	50	78	95	107	129	157	218	282	394
C.D.G.	-1.25	-1.67	-1.78	-1.80	-1.74	-1.48	-1.23	-.83	.07	.25	.25	-

Table A.1 (cont.)

Strains x 10<sup>6</sup> and Deflexions (mm)

		Test No. 36											
		40	80	120	160	200	240	260	280	300	320	340	*360
Gauge Ref.	Load (KN)	-111	-261	-406	-562	-725	-945	-1049	-1249	-1550	-2009	-2753	-4573
		-206	-332	-448	-553	-634	-670	-643	-545	-325	124	879	2489
		-61	-166	-264	-376	-498	-671	-758	-927	-1188	-1603	-2310	-4133
		-154	-229	-296	-355	-396	-396	-359	-258	-55	348	1021	2593
		0	-38	-72	-118	-176	-275	-331	-441	-620	-927	-1522	-2982
		-84	-102	-115	-125	-125	-105	-75	-2	134	408	883	2176
		26	17	11	-1	-24	-72	-102	-163	-264	-447	-870	-2065
		-61	-60	-56	-48	-38	-17	3	47	126	293	591	1551
		24	22	26	24	7	-7	-22	-54	-105	-196	-454	-1285
		-43	-40	-32	-23	-15	0	13	39	85	189	369	999
		15	17	23	25	23	11	3	-13	-40	-79	-222	-707
		-32	-28	-20	-14	-6	3	13	31	61	137	254	656
		24	32	44	53	57	54	51	44	36	36	-9	-121
		-10	-4	7	17	27	39	48	63	92	162	268	652
C.D.G.		-28	-23	-19	-12	.01	.32	.53	1.01	1.86	3.50	5.14	11.22

\* Readings cannot be guaranteed

Table A.1 (cont.)

Strains x 10<sup>6</sup> and Deflexions (mm)

Test No. 37

Load (KN) 20 40 60 80 100 120 140 160 180 \*Fail

Gauge Ref.

1 -237 -375 -505 -626 -745 -867 -989 -1099 -1179 -1217  
2 -36 -164 -294 -431 -556 -691 -832 -956 -1060 -960

C.D.G.

.37 .38 .38 .38 .38 .38 .40 .45 .52 .78

Test No. 38

Load (KN) 40 80 120 160 200 220 240 260

Gauge Ref.

1 -339 -596 -837 -1060 -1260 -1332 -1341 -1505  
2 -90 -274 -450 -631 -782 -829 -831 -821

C.D.G.

.45 .54 .64 .79 .94 .99 1.03 1.07

Test No. 39

Load (KN) 40 80 120 160 200 220 240 260 300 320

Gauge Ref.

1 -204 -422 -627 -842 -1035 -1128 -1207 -1295 -1377 -1334  
2 -194 -386 -567 -735 -865 -930 -967 -995 -963 -900

C.D.G.

.04 .04 .05 .05 .05 .06 .07 .06 .09 .36

\* Readings cannot be guaranteed

Table A.1 (cont.)

# Strains $\times 10^6$ and Deflexions (mm)

Test No. 40

Load (KN)	40	80	120	160	200	240	280	320
Gauge Ref.								
1	-55	-229	-416	-610	-796	-987	-1203	-1409
2	-322	-542	-738	-921	-1051	-1149	-1180	-1157
C.D.G.	.36	.40	.41	.41	.39	.35	.27	.12

Test No. 41

Load (KN)	10	20	30	40	50	60	70	80	90	100	110	120
Gauge Ref.												
1	-208	-308	-401	-505	-596	-702	-824	-949	-1103	-1291	-1541	-2001
2	92	74	51	28	12	-7	-15	-4	22	88	220	571
C.D.G.	.76	.88	.96	1.02	1.10	1.18	1.23	1.35	1.52	1.77	2.15	2.97

Test No. 42

Load (KN)	20	40	60	80	100	120	140	160
Gauge Ref.								
1	-283	-429	-573	-717	-850	-999	-1223	-1610
2	85	28	-36	-87	-120	-139	-90	123
C.D.G.	.90	1.05	1.15	1.26	1.40	1.63	2.10	2.93

Tabl A.1 (cont.)

Strains  $\times 10^6$  and Deflexions (mm)

Test No. 43

Load (KN) 40 80 120 160 200

Gauge Ref.

1 -230 -461 -667 -933 -1786  
2 -123 -251 -319 -304 237

C.D.G. .19 .32 .45 .79 2.75

Test No. 44

Load (KN) 40 80 120 160 180 200

Gauge Ref.

1 -255 -496 -745 -1065 -1340 -1820  
2 -143 -243 -298 -223 -100 216

C.D.G. .21 .41 .72 1.32 1.90 3.12 9.00 5.35 11.10 9.24 13.10 16.30

Test No. 45

Load (KN) 20 40 60 80 100 120 140 160 180 200

Gauge Ref.

1 -107 -232 -352 -472 -593 -719 -849 -996 -1158 -1496  
2 -122 -235 -346 -456 -562 -666 -756 -830 -859 -663

C.D.G. -.01 0 -.02 -.05 -.08 -.07 -.04 .01 .10 .48

\* Readings cannot be guaranteed

Table A.1 (cont.)



Strains x 10<sup>6</sup> and Deflexions (mm)

Test No. 46

Load (KN)	40	80	120	160	200	220	240	260	280	300
Gauge Ref.										
1	-309	-524	-713	-923	-1124	-1227	-1341	-1452	-1545	-1675
2	-50	-202	-348	-491	-605	-634	-642	-596	-498	-299

Test No. 47

Load (KN)	40	80	120	160	200	240	280	320	360
Gauge Ref.									
1	-152	-312	-437	-645	-795	-911	-966	-998	-1223
2	-195	-370	-498	-697	-849	-991	-1125	-1191	-1020
C.D.G.	-.11	-.14	-.16	-.20	-.22	-.25	-.33	-.36	.27

Test No. 48

Load (KN)	40	80	120	160	200	240	280	320	340	*Fail	R 1	R 2
Gauge Ref.												
1	-165	-338	-519	-694	-886	-1070	-1268	-1517	-1734			
2	-182	-342	-488	-611	-716	-802	-843	-756	-528			
C.D.G.	-.07	-.08	-.02	.05	.20	.34	.58	1.10	1.73	5.00	8.90	10.85

\* Readings cannot be guaranteed

Table A.1 (cont.)

Strains  $\times 10^6$  and Deflexions (mm)

Test No. 49

Load (KN)	20	40	60	80	100	110	120	130	140
Gauge Ref.									
1	-144	-274	-421	-564	-715	-800	-900	-1036	-1279
2	-162	-321	-473	-620	-761	-811	-843	-808	-637
C.D.G.	-.14	-.19	-.20	-.19	-.15	-.11	-.03	.13	.48

Test No. 50

Load (KN)	20	40	60	80	100	120	140	160	180	200	220
Gauge Ref.											
1	-120	-249	-388	-515	-646	-764	-874	-998	-1138	-1359	
2	-50	-141	-235	-319	-403	-470	-511	-533	-505	-397	
C.D.G.	.45	.45	.48	.51	.52	.55	.59	.70	.87	1.26	2.55

Test No. 51

Load (KN)	20	40	60	80	100	120	140	160	180	200	220	240
Gauge Ref.												
1	-247	-373	-500	-620	-730	-844	-925	-983	-1054	-1094	-1173	-1311
2	43	-44	-135	-221	-296	-377	-461	-535	-583	-625	-676	-712
C.D.G.	.52	.56	.60	.65	.69	.74	.77	.81	.89	.99	1.15	1.61

Table A.1 (cont.)

Strains  $\times 10^6$  and Deflexions (mm)

Test No. 52

Load (KN)	40	80	120	160	200	240	260	20	R 1	20	R 2	R 3
Gauge Ref.												
1	-398	-624	-804	-965	-1070	-1151	-1223					
2	-26	-226	-396	-553	-688	-815	-918					
C.D.G.	.51	.53	.58	.72	1.03	1.40	1.96	5.06	7.44	6.25	9.10	10.05

Test No. 53

Load (KN)	20	40	60	80	100	120	140
Gauge Ref.							
1	-180	-366	-551	-740	-952	-1120	-1200
2	-168	-335	-501	-661	-818	-910	-985
C.D.G.	-.03	0	.03	.04	.06	.10	.06

Test No. 54

Load (KN)	20	40	60	80	100	120	140	160	180	200	220
Gauge Ref.											
1	-229	-379	-519	-654	-794	-916	-1031	-1097	-1095	-1048	
2	-21	-133	-246	-362	-484	-600	-707	-783	-823	-831	
C.D.G.	.30	.37	.40	.42	.46	.49	.53	.65	.77	.89	1.09

Table A.1 (cont.)

(cont.)

Strains  $\times 10^6$  and Deflexions (mm)

Test No. 55

Load (KN) 40 80 120 160 200 220 240 260 \*Fail

Gauge Ref.

1 -200 -465 -728 -965 -1164 -1256 -1316 -1337  
2 -291 -538 -743 -876 -949 -960 -933 -901

C.D.G. -.09 -.11 -.12 -.11 -.07 -.06 .01 .15 .57

Test No. 56

Load (KN) 40 80 120 160 200 220 240 260 280 300

Gauge Ref.

1 -417 -663 -892 -1031 -1128 -1175 -1207 -1267 -1421  
2 -93 -316 -542 -764 -947 -1014 -1051 -1092 -1188

C.D.G. -.21 -.20 -.21 -.27 -.30 -.32 -.33 -.30 -.08 1.75

Test No. 57

Load (KN) 40 80 120 160 200 220 240 260 280 300

Gauge Ref.

1 -262 -453 -640 -841 -995 -1047 -1063 -1085 -1156  
2 -128 -307 -482 -661 -827 -906 -960 -993 -1056

C.D.G. .16 .16 .18 .26 .29 .31 .32 .35 .39 .46

\* Readings cannot be guaranteed

Table A.1 (cont.)

Strains  $\times 10^6$  and Deflexions (mm)

Test No. 58

Load (KN)	40	80	120	160	200	240	260	280	300	320	340	360
Gauge Ref.												
1	-290	-488	-677	-875	-1066	-1217	-1258	-1293	-1341	-1406	-1504	
2	-73	-241	-394	-540	-667	-748	-766	-785	-839	-959	-1076	
C.D.G.	.20	.28	.39	.55	.72	.87	.94	1.01	1.10	1.24	1.45	1.90

Test No. 59

Load (KN)	40	80	120	160	200	240	280	320	360	*380
-----------	----	----	-----	-----	-----	-----	-----	-----	-----	------

Gauge Ref.

1	-105	-276	-454	-616	-764	-874	-970	-1042	-1092	-1325
2	-265	-442	-626	-799	-958	-1075	-1135	-1115	-1186	-1122
C.D.G.	.25	.29	.37	.45	.52	.59	.66	.81	1.04	2.00

Test No. 60

Load (KN)	40	80	120	140	160	180	200	220	240	260	*280
-----------	----	----	-----	-----	-----	-----	-----	-----	-----	-----	------

Gauge Ref.

C.D.G.	.33	.54	.82	.97	1.15	1.35	1.65	2.19	3.00	4.50	6.50
--------	-----	-----	-----	-----	------	------	------	------	------	------	------

\* Readings cannot be guaranteed

Table A.1 (cont.)

Strains x 10<sup>6</sup> and Deflexions (mm)

Gauge Ref.	Load (KN)	Test No. 61							
		40	80	120	160	200	220	240	260
1	-82	-221	-372	-568	-834	-1065	-1527	-2503	
2	-257	-374	-483	-522	-458	-317	53	941	
3	-45	-140	-248	-410	-657	-884	-1336	-2261	
4	-187	-247	-316	-336	-265	-137	221	1077	
5	-245	-327	-393	-433	-601	-771	-1117	-1873	
6	40	30	19	36	119	236	511	1153	
7	-100	-137	-141	-173	-248	-346	-568	-1087	
8	78	87	95	118	187	270	454	876	
9	-199	-235	-259	-244	-311	-379	-514	-842	
10	-159	-164	-156	-127	-79	-23	86	368	
11	-177	-205	-202	-208	-227	-269	-374	-569	
12	33	43	53	69	111	154	245	459	
13	53	63	68	64	48	29	-15	-86	
14	11	25	37	57	95	142	234	458	
21	-543	-898	-1298	-3883	-11826	-10822	-4365	-4738	
22	-902	-1514	-2799	-9110	-27064	32700	-15684	-13339	
27	-733	-1109	-1916	-7434	-22675	32700	-25185	-17683	
28	-743	-1238	-1963	-7761	-25321	-23412	-11252	-9419	
C.D.G.	0	0	.06	.31	1.02	1.85	3.66	7.76	

Table A.1 (cont.)



# Strains $\times 10^6$ and Deflexions (mm)

Test No. 62

Load (KN)	40	80	115	140	160	180	200	210	220	230	240	20
Gauge Ref.												
1	-100	-229	-351	-466	-583	-737	-1020	-1280	-1651	-2176	-3435	-3370
2	-160	-282	-367	-397	-396	-345	-183	19	348	858	1827	2394
3	-51	-135	-222	-314	-414	-552	-807	-1043	-1390	-1894	-3141	-3522
4	-101	-175	-224	-236	-225	-173	-13	177	482	960	1866	2127
5	0	-26	-63	-110	-167	-252	-416	-579	-829	-1229	-2054	-1768
6	-31	-45	-47	-33	-8	48	189	335	560	907	1579	1321
7	15	11	0	-20	-48	-94	-186	-282	-434	-693	-1258	-960
8	0	7	21	42	69	118	221	321	468	692	1142	855
9	15	16	12	2	-12	-38	-92	-147	-236	-387	-729	-497
10	9	21	29	48	68	105	176	240	332	475	760	565
11	12	14	13	7	-1	-18	-51	-84	-134	-215	-386	-262
12	16	28	15	33	51	81	133	180	245	346	548	414
13	38	54	64	69	67	66	58	46	32	19	23	38
14	21	37	26	44	60	89	136	179	241	344	565	427
C.D.G.	-0.33	-0.31	-0.23	-0.06	0.20	0.66	1.60	2.60	4.10	6.40	11.50	7.66
Load (KN)	R 1	20	R 2	20	R 3							

Gauge Ref.

C.D.G. 17.50 10.52 20.02 11.49 21.29

Table A.1 (cont.)

Strains x 10<sup>6</sup> and Deflexions (mm)

Test No. 63

Load (KN)	20	40	60	80	100	120	140	160	180	*200	*Fail
Gauge Ref.											
1	-173	-262	-340	-418	-480	-534	-594	-660	-690	-361	2181
2	40	-4	-57	-107	-161	-222	-288	-373	-514	-1051	-4047
3	-146	-200	-253	-310	-351	-405	-432	-467	-464	-122	2255
4	63	38	5	-25	-63	-111	-162	-223	-331	-784	-3727
5	-93	-113	-135	-159	-172	-197	-191	-185	-142	127	1881
6	70	71	64	56	41	20	1	-19	-65	-338	-2540
7	-59	-68	-73	-78	-80	-75	-72	-58	-14	149	1253
8	61	67	68	71	69	64	62	62	41	-97	-1593
9	-33	-29	-32	-39	-38	-58	-33	-18	5	108	762
10	36	43	47	51	49	48	46	45	39	-33	-910
11	-24	-25	-25	-25	-23	-21	-16	-7	8	67	513
12	26	29	33	36	38	37	39	39	35	-3	-390
13	-7	-6	-3	-1	0	8	11	19	35	77	519
14	19	24	28	31	33	35	36	39	41	26	58
C.D.G.	-.73	-.90	-.96	-1.01	-1.01	-.99	-.96	-.86	-.50	.80	

\* Readings cannot be guaranteed

Table A.1 (cont.)

Strains x 10<sup>6</sup> and Deflexions (mm)

		Test No. 64									
		Load (KN)	20	40	60	80	100	120	140	160	*180
Gauge Ref.											
1	64.001		-130	-203	-264	-312	-339	-357	-342	-124	-693
2	64.002		-1	-66	-139	-220	-322	-453	-637	-1036	-1942
3	64.003		-105	-152	-187	-214	-224	-216	-172	57	818
4	64.004		20	-20	-71	-134	-209	-310	-450	-781	-1613
5	64.005		-68	-81	-87	-88	-75	-42	22	220	781
6	64.006		584	571	551	520	480	429	362	158	-473
7	64.007		-30	-29	-26	-17	0	29	76	203	532
8	64.008		31	30	23	11	-8	-30	-62	-172	-564
9	64.009		-23	-22	-17	-10	1	20	53	126	327
10	64.010		23	23	21	15	9	-2	-14	-70	-284
11	64.011		-10	-7	-4	0	8	20	38	83	207
12	64.012		11	12	10	7	2	-3	-9	-37	-133
13	64.013		-8	-5	-2	1	7	16	31	61	165
14	64.014		13	15	15	14	12	11	11	4	-5
C.D.G.			-84	-89	-86	-77	-57	-28	24	1.75	5.75

		Test No. 66								
Load (KN)		10	20	30	40	50	60	70	80	90
Gauge Ref.										
1		-136	-278	-410	-543	-664	-784	-884	-967	-1065
2		-147	-302	-439	-570	-686	-789	-892	-1011	-1155
C.D.G.		.20	.30	.39	.42	.44	.48	.59	.84	1.84

\*Readings cannot be guaranteed

Table A.1 (cont.)

Strains  $\times 10^6$  and Deflexions (mm)

Gauge Ref.	Load (KN)	Test No. 67				
		40	80	120	160	200
1		-71	-136	-216	-318	-480
2		27	43	65	104	193
3		-146	-291	-458	-653	-916
4		-11	-33	-41	-15	98
5		-202	-403	-631	-885	-1200
6		-48	-107	-146	-138	-6
7		-145	-290	-458	-655	-945
8		-11	-37	-48	-24	81
9		-73	-139	-220	-326	-506
10		23	33	51	88	178
11		-29	-49	-77	-121	-213
12		38	60	85	119	187
13		2	15	22	18	-17
14		56	91	128	167	229
C.D.G.		.24	.37	.54	.79	1.26
L.P.D.G.		.42	.69	1.00	1.41	1.85

1.43

3.76

Table A.1 (cont.)

Strains  $\times 10^6$  and Deflexions (mm)

		Test No. 68						
Load (KN)		40	80	120	160	200	240	260
Gauge Ref.	1	-1	0	-1	-7	-28	-101	-223
	2	8	18	26	36	56	118	223
	3	-11	-20	-36	-57	-104	-247	-466
	4	8	17	25	39	68	175	354
	5	-43	-86	-137	-197	-298	-559	-921
	6	-6	-12	-14	-7	30	212	522
	7	-111	-225	-348	-476	-656	-1042	-1528
	8	-53	-105	-148	-173	-137	138	635
	9	-161	-328	-503	-683	-909	-1381	-1975
	10	-96	-191	-273	-333	-309	8	597
	11	-105	-217	-341	-478	-696	-1291	-1933
	12	-53	-107	-155	-187	-175	78	605
	13	-47	-97	-163	-248	-416	-850	-1480
	14	-3	-7	-8	-4	33	298	813
C.D.G.		.14	.24	.34	.41	.47	.78	1.43
L.P.D.G.		.15	.28	.45	.63	1.00	2.24	5.45

Table A.1 (cont.)

Strains  $\times 10^6$  and Deflexions (mm)

Gauge Ref.	Load (KN)	Test No. 69									
		20	40	60	80	100	120	140	160	180	200
1		31	39	44	47	49	50	49	45	36	18
2		31	31	30	32	33	42	38	39	47	63
3		38	48	55	60	61	63	59	52	37	6
4		30	27	29	32	34	38	40	43	53	77
5		31	40	44	46	44	39	30	15	-12	-74
6		29	23	23	25	28	32	35	40	61	105
7		27	24	13	0	-16	-35	-58	-89	-142	-259
8		14	-1	-11	-18	-23	-23	-20	-4	37	133
9		-8	-45	-93	-141	-192	-243	-292	-348	-442	-634
10		-17	-63	-103	-139	-169	-188	-194	-173	-106	56
11		-43	-117	-203	-287	-376	-472	-573	-696	-873	-1185
12		-50	-128	-202	-270	-332	-389	-434	-456	-421	-246
13		-56	-144	-245	-346	-461	-599	-765	-984	-1273	-1760
14		-74	-163	-250	-330	-414	-506	-601	-686	-704	-563
C.D.G.		- .14	- .21	- .27	- .31	- .33	- .34	- .42	- .42	- .39	- .29
L.P.D.G.		- .07	- .12	- .11	- .12	- .09	- .05	.03	.21	.54	1.30

Table A.1 (cont.)



Strains  $\times 10^6$  and Deflexions (mm)

Gauge Ref.	Load (KN)	Test No. 70							
		20	40	60	80	100	120	140	*150
1	74	74	78	80	83	81	61	51	6
2	-57	-59	-53	-48	-42	-35	-30	-7	2
3	95	98	106	112	118	119	100	88	8
4	-68	-70	-63	-56	-47	-37	-27	2	-3
5	116	123	133	141	149	149	121	90	-79
6	-83	-83	-73	-64	-51	-35	-11	35	40
7	130	133	139	143	145	133	64	-37	-376
8	-101	-104	-95	-86	-72	-48	5	105	236
9	115	93	74	49	19	-37	-222	-490	-1071
10	-140	-159	-171	-180	-180	-154	-26	190	730
11	52	-38	-127	-224	-335	-493	-866	-1344	-2555
12	-221	-306	-381	-449	-507	-512	-323	73	1607
13	-11	-176	-339	-514	-713	-974	-1521	-2158	-3556
14	-289	-439	-575	-702	-814	-850	-577	67	3175
L.P.D.G.	0	-0.08	-0.08	-0.05	.05	.39	1.72	3.52	-

\* Readings cannot be guaranteed

Table A.1 (cont.)

Strains x 10<sup>6</sup> and Deflexions (mm)

Test No. 71

Load (KN)	40	80	120	160	200	240	280	320	360	400	420	440
Gauge Ref.												
1	-97	-218	-340	-459	-580	-698	-804	-891	-864	-378	495	1311
2	-137	-250	-371	-490	-617	-748	-888	-1046	-1267	-1868	-2644	-3303
3	-45	-125	-205	-292	-382	-461	-534	-616	-589	121	534	353
4	-112	-192	-275	-358	-452	-545	-648	-765	-937	-1463	-2205	-2932
5	-6	-27	-52	-77	-109	-141	-167	-181	-136	96	503	998
6	-50	-64	-88	-113	-151	-186	-230	-281	-359	-673	-1230	-1874
7	20	28	31	31	22	13	7	8	42	151	335	598
8	-13	-9	-11	-10	-15	-19	-29	-40	-63	-198	-494	-926
9	26	38	46	53	52	52	50	55	82	133	216	355
10	0	16	23	32	29	28	24	21	20	-19	-136	-343
11	22	34	43	53	54	55	55	62	87	119	171	258
12	6	24	35	44	41	42	39	36	42	35	-6	-84
13	25	41	54	68	75	81	85	99	127	159	212	303
14	14	38	55	69	70	73	74	77	87	94	91	91
O.D.G.	.10	.10	.11	.11	.11	.14	.21	.34	.70	2.35	4.85	7.85

Table A.1 (cont.)

# Strains $\times 10^6$ and Deflexions (mm)

Test No. 72

Load (KN)	40	80	120	160	200	240	280	320	340	360	380	400
Gauge Ref.												
1	-69	-191	-322	-466	-615	-785	-971	-1212	-1366	-1558	-1818	-2353
2	-97	-172	-240	-302	-350	-385	-389	-352	-299	-202	-14	518
3	-72	-198	-330	-465	-598	-746	-901	-1096	-1219	-1370	-1579	-2028
4	-88	-156	-214	-262	-293	-308	-295	-239	-181	-84	84	530
5	-19	-91	-159	-232	-305	-384	-470	-583	-658	-753	-887	-1215
6	-53	-77	-97	-109	-109	-100	-68	-16	26	92	197	459
7	17	-3	-34	-62	-88	-120	-152	-200	-236	-282	-353	-540
8	-20	-16	-3	-11	-2	14	38	70	91	122	168	282
9	37	33	20	16	8	0	-7	-22	-35	-51	-77	-158
10	-14	-7	-4	0	10	21	38	54	63	76	94	139
11	41	51	43	44	47	48	51	52	48	45	36	13
12	0	7	9	29	19	27	39	49	53	61	69	93
13	39	51	61	71	81	92	105	115	120	127	137	146
14	0	14	31	27	38	68	66	79	85	95	106	135
C.D.G.	.15	.21	.30	.41	.53	.70	.91	1.25	1.48	1.83	2.43	3.81

Table A.1 (cont.)

Strains  $\times 10^6$  and Deflexions (mm)

Test No. 73

Load (KN)	80	120	160	200	240	280	320	360	400	440	480	*Fail
Gauge Ref.												
1	-44	-60	-74	-87	-95	-96	-91	-69	-22	71	304	2212
2	-87	-142	-205	-275	-356	-448	-562	-708	-882	-1104	-1480	-4156
3	-90	-126	-159	-191	-217	-238	-249	-240	-203	-119	93	2001
4	-174	-256	-341	-432	-532	-640	-766	-916	-1082	-1288	-1623	-4250
5	-115	-163	-204	-240	-270	-293	-304	-295	-262	-191	-22	1499
6	-223	-318	-408	-498	-593	-691	-797	-913	-1037	-1189	-1439	-3353
7	-39	-59	-76	-89	-98	-103	-101	-88	-63	-17	83	922
8	-147	-202	-255	-304	-355	-408	-465	-531	-601	-690	-841	-1889
9	19	20	23	26	31	37	47	60	78	103	154	557
10	-68	-88	-106	-124	-141	-160	-181	-206	-234	-271	-339	-925
11	37	47	56	62	71	80	90	101	113	127	152	346
12	-25	-26	-28	-28	-29	-30	-32	-35	-38	-46	-63	-284
13	56	74	90	104	120	135	151	167	182	198	222	393
14	10	23	36	50	62	74	89	102	116	128	144	176
C.D.G.	-.25	-.25	-.22	-.16	-.09	0	.12	.32	.58	.97	1.68	-

\* Readings cannot be guaranteed

Table A.1 (cont.)

Strains x 10<sup>6</sup> and Deflexions (mm)

Test No. 74

Load (KN)	80	160	240	320	400	480	560	600	640	680	720	760
Gauge Ref.												
1	-106	-243	-379	-525	-686	-870	-1087	-1218	-1364	-1533	-1736	-2030
2	-10	-34	-59	-72	-68	-37	31	89	165	266	406	639
3	-150	-315	-471	-632	-808	-1007	-1240	-1381	-1534	-1708	-1917	-2198
4	-31	-66	-94	-105	-96	-55	28	96	184	298	459	728
5	-205	-386	-547	-710	-886	-1085	-1318	-1456	-1606	-1777	-1982	-2240
6	-73	-122	-155	-170	-162	-127	-50	11	93	201	355	625
7	-215	-374	-511	-649	-796	-964	-1160	-1278	-1407	-1557	-1742	-2020
8	-89	-135	-164	-178	-179	-158	-107	-64	-7	70	187	401
9	-141	-237	-322	-408	-500	-608	-734	-810	-895	-996	-1126	-1343
10	-53	-74	-88	-95	-95	-84	-58	-36	-5	35	99	221
11	-49	-80	-110	-140	-176	-216	-267	-297	-338	-378	-443	-556
12	0	7	13	22	32	47	66	81	99	121	154	-214
13	17	33	47	58	67	74	78	78	76	71	57	19
14	43	78	106	135	163	192	223	241	261	283	310	355
C.D.G.	.34	.61	.80	1.00	1.22	1.49	1.86	2.08	2.35	2.67	3.09	3.71

Table A.1 (cont.)

# Strains $\times 10^6$ and Deflexions (mm)

Test No. 75

Load (KN)	80	160	240	280	320	360	400	440	*Fail	50	R 1	R 2
-----------	----	-----	-----	-----	-----	-----	-----	-----	-------	----	-----	-----

Gauge Ref.

1	-402	-684	-986	-1133	-1261	-1379	-1452	-1444				
2	-226	-500	-781	-919	-1050	-1156	-1256	-1383				

C.D.G.

	.19	.23	.27	.28	.30	.32	.39	.52	1.75	1.06	2.80	4.20
--	-----	-----	-----	-----	-----	-----	-----	-----	------	------	------	------

Load (KN)	80	160	240	320	360	400	440	480	520	560	600	*Fail
-----------	----	-----	-----	-----	-----	-----	-----	-----	-----	-----	-----	-------

Gauge Ref.

1	-238	-519	-769	-1008	-1156	-1283	-1425	-1587	-1765	-1848	-2147	-2162
2	-191	-371	-531	-692	-767	-835	-902	-951	-994	-994	-947	-9505

C.D.G.

	-.58	-.56	-.55	-.56	-.56	-.55	-.54	-.53	-.47	-.40	-.16	1.84
--	------	------	------	------	------	------	------	------	------	------	------	------

Test No. 77

Load (KN)	80	160	240	320	400	480	560	640	720	800	880	*Fail
-----------	----	-----	-----	-----	-----	-----	-----	-----	-----	-----	-----	-------

Gauge Ref.

1	16	-11	-53	-106	-162	-220	-287	-362	-449	-565	-756	
2	-97	-119	-161	-197	-248	-290	-342	-391	-441	-490	-511	

C.D.G.

	-.04	-.07	-.10	-.14	-.15	-.16	-.16	-.16	-.15	-.12	.04	2.86
--	------	------	------	------	------	------	------	------	------	------	-----	------

\* Readings cannot be guaranteed

Table A.1 (cont.)



# Strains $\times 10^6$ and Deflexions (mm)

Test No. 78

Load (KN)	100	150	200	250	300	350	400	*Fail	50	*R 1	*R 2	*R 3
-----------	-----	-----	-----	-----	-----	-----	-----	-------	----	------	------	------

Gauge Ref.

1	-152	-313	-470	-624	-757	-895	-1071					
2	-643	-872	-1092	-1290	-1408	-1459	-1429					

C.D.G.

	.31	.33	.36	.39	.42	.51	.74	5.04	5.80	10.00	12.00	12.50
--	-----	-----	-----	-----	-----	-----	-----	------	------	-------	-------	-------

Test No. 79

Load (KN)	50	100	150	200	250	300	350	400	450	500	550	600
-----------	----	-----	-----	-----	-----	-----	-----	-----	-----	-----	-----	-----

Gauge Ref.

1	-150	-309	-478	-640	-792	-946	-1107	-1231	-1272	-1242	-1272	-1262
2	-216	-402	-569	-745	-917	-1093	-1267	-1427	-1540	-1571	-1555	-1505

C.D.G.

	-.03	-.10	-.13	-.15	-.18	-.20	-.21	-.21	-.18	-.16	-.07	1.15
--	------	------	------	------	------	------	------	------	------	------	------	------

Test No. 80

Load (KN)	100	200	300	400	450	500	550	600	650	700	750	*Fail
-----------	-----	-----	-----	-----	-----	-----	-----	-----	-----	-----	-----	-------

Gauge Ref.

1	-185	-432	-668	-883	-998	-1107	-1224	-1365	-1461	-1507	-1586	-1774
2	-236	-470	-709	-941	-1057	-1174	-1291	-1430	-1506	-1571	-1450	-1341

C.D.G.

	-.41	-.30	-.25	-.24	-.24	-.24	-.24	-.24	-.23	-.20	-.07	.65
--	------	------	------	------	------	------	------	------	------	------	------	-----

\* Readings cannot be guaranteed

Table A.1 (cont.)

# Strains x 10<sup>6</sup> and Deflexions (mm)

Test No. 81

Load (KN)	100	200	300	400	500	600	700	800	900	1000	1100	1200*
Gauge Ref.												
1	-268	-369	-475	-574	-681	-793	-909	-1019	-1163	-1335	-1457	-1535
2	5	-89	-185	-284	-385	-494	-605	-733	-905	-1078	-1301	-1597
C.D.G.	-.26	-.20	-.17	-.16	-.15	-.12	-.08	-.03	.13	.15	.17	.34

Test No. 82

Load (KN)	200	400	600	700	800	900	1000	1100	1200	1300	1400	1450
Gauge Ref.												
1	-16	-109	-224	-286	-351	-417	-485	-551	-621	-681	-738	-687
2	-232	-363	-511	-593	-681	-778	-876	-980	-1101	-1240	-1451	-1602
C.D.G.	.16	.22	.24	.25	.25	.26	.28	.29	.30	.32	.32	.29

Test No. 83

Load (KN)	50	100	150	200	250	300	*Fail	50	*R 1	50	*R 2	*R 3
Gauge Ref.												
1	-205	-417	-631	-831	-1020	-1248						
2	-218	-431	-609	-747	-853	-893						
C.D.G.	-.03	-.04	-.02	.05	.10	.19	7.46	5.05	9.50	5.20	10.40	12.00

\* Readings cannot be guaranteed

Table A.1 (cont.)

Strains  $\times 10^6$  and Deflexions (mm)

Test No. 84

Load (KN)	50	100	150	200	250	300	350
Gauge Ref.							
1	-405	-620	-855	-1127	-1372	-1650	-2035
2	22	-114	-230	-320	-414	-481	-433
C.D.G.	-.10	-.14	-.30	-.45	-.42	-.28	.04

Test No. 85

Load (KN)	50	100	150	200	250	300	350	400	450	500	*550
Gauge Ref.											
1	-284	-421	-555	-691	-835	-985	-1146	-1311	-1507	-1742	-2211
2	54	-29	-111	-190	-269	-340	-405	-455	-489	-487	-192
C.D.G.	-.05	.05	.12	.18	.24	.31	.38	.46	.58	.76	1.35

Test No. 86

Load (KN)	100	200	300	400	450	500	550	600	650	700	750	*800
Gauge Ref.												
1	22	-38	-101	-148	-169	-181	-189	-188	-173	-118	-30	-28
2	-230	-395	-543	-723	-816	-930	-1023	-1149	-1279	-1435	-1642	-1720
C.D.G.	.05	.23	.38	.53	.61	.71	.80	.92	1.05	1.22	1.48	1.95

\* Readings cannot be guaranteed

# Strains x 10<sup>6</sup> and Deflexions (mm)

Test No. 87

Load (KN)	100	200	300	400	500	600	700	800	850	900	950	*Fail
Gauge Ref.												
1	260	235	205	179	144	119	107	114	133	172	255	617
2	-363	-475	-580	-686	-817	-957	-1128	-1324	-1438	-1579	-1777	-2463
C.D.G.	1.22	1.43	1.61	1.75	1.90	2.06	2.30	2.55	2.70	2.88	3.14	4.80

Test No. 88

Load (KN)	50	100	150	200	250	300	350	400	450	500	
Gauge Ref.											
1	-333	-510	-702	-886	-1099	-1284	-1448	-1520	-1566	-1539	
2	-26	-195	-347	-516	-655	-809	-941	-1068	-1126	-1155	
C.D.G.	-.05	.01	.09	.19	.34	.39	.39	.40	.43	.43	

Test No. 89

Load (KN)	50	100	150	200	250	300	350	400	450	500	550	*600
Gauge Ref.												
1	-195	-364	-524	-687	-853	-1013	-1141	-1256	-1280	-1329	-1315	-1368
2	-187	-360	-541	-717	-875	-1059	-1244	-1405	-1489	-1521	-1562	-1555
C.D.G.	-.16	-.21	-.24	-.28	-.30	-.31	-.31	-.31	-.31	-.30	-.27	.16

\* Readings cannot be guaranteed

Table A.1 (cont.)

# Strains $\times 10^6$ and Deflexions (mm)

Load (KN)	Gauge Ref.	Test No. 90											*Fail
		100	200	300	350	400	450	500	550	600	650	700	
1	-187	-413	-634	-725	-825	-921	-1021	-1108	-1194	-1264	-1267	-1245	
2	-288	-560	-811	-935	-1060	-1186	-1316	-1451	-1608	-1782	-1868	-1937	
C.D.G.	-.19	-.23	-.25	-.25	-.24	-.23	-.22	-.21	-.18	-.13	-.05	.21	

Load (KN)	Gauge Ref.	Test No. 91											
		100	200	250	300	350	400	450	500	550	600	650	700
	1	-165	-383	-490	-600	-705	-812	-907	-1014	-1117	-1212	-1299	-1308
	2	-376	-608	-728	-851	-982	-1102	-1229	-1353	-1489	-1635	-1807	-2387
	C.D.G.	-.07	-.11	-.12	-.12	-.11	-.10	-.09	-.07	-.05	-.03	.01	.35

Load (KN)	Gauge Ref.	Test No. 92								1.13
		50	100	150	200	250	300	350		
	1	-486	-716	-940	-1177	-1445	-1747	-2208		
	2	104	-54	-192	-310	-406	-427	-284		
C.D.G.		-0.16	-0.01	0.10	0.22	0.39	0.64	1.13		

\* Readings cannot be guaranteed

Strains  $\times 10^6$  and Deflexions (mm)

		Test No. 93							
Load (KN)		50	100	150	200	250	300	350	*Fail

Gauge Ref.

1	-309	-510	-712	-930	-1148	-1384	-1682	
2	-311	-177	-317	-454	-585	-688	-701	

C.D.G.

	.11	.19	.29	.38	.48	.59	.84	4.20
--	-----	-----	-----	-----	-----	-----	-----	------

Test No. 94

Load (KN)	50	100	150	200	250	300	350	400	450	500
-----------	----	-----	-----	-----	-----	-----	-----	-----	-----	-----

Gauge Ref.

1	129	55	-16	-79	-133	-175	-201	-200	-157	-7
2	-368	-509	-646	-812	-972	-1143	-1329	-1552	-1813	-2172

C.D.G.

	.08	.07	.07	.09	.13	.19	.28	.41	.59	.94
--	-----	-----	-----	-----	-----	-----	-----	-----	-----	-----

Test No. 95

Load (KN)	50	100	150	200	250	300	350	400	450	500	*550
-----------	----	-----	-----	-----	-----	-----	-----	-----	-----	-----	------

Gauge Ref.

1	-320	-470	-610	-764	-911	-1070	-1363	-1439	-1671	-1970	-3340
2	109	38	-30	-96	-153	-206	-245	-258	-246	-160	540

C.D.G.

	-.31	-.21	-.14	-.06	.01	.09	.19	.31	.48	.77	2.00
--	------	------	------	------	-----	-----	-----	-----	-----	-----	------

\*Readings cannot be guaranteed

Table A.1 (cont.)



Strains  $\times 10^6$  and Deflexions (mm)

Test No. 96

Load (KN)	40	80	120	160	200	240	280	300	20	R 1	R 2	R 3
Gauge Ref.												
1	-44	-156	-271	-404	-571	-822	-1114	-1387				
2	-128	-178	-220	-238	-217	-107	27	227				
3	-56	-156	-261	-384	-544	-796	-1078	-1371				
4	-100	-131	-157	-161	-130	-19	125	342				
5	-53	-127	-205	-297	-422	-615	-828	-1060				
6	-89	-102	-111	-105	-73	27	158	344				
7	-43	-91	-137	-194	-272	-396	-529	-680				
8	-47	-44	-40	-26	1	77	170	296				
9	-31	-56	-78	-108	-154	-233	-316	-414				
10	-21	-10	1	17	43	101	167	251				
11	-23	-32	-39	-52	-75	-122	-165	-220				
12	-16	-4	6	21	43	88	136	198				
13	-12	-9	-2	-3	-10	-34	-49	-69				
14	-12	3	19	36	61	105	155	218				
21	-5	-146	-290	-457	-663	-960	-1274	-1552				
22	-648	-1003	-1318	-1471	-2561	-10735	-19964	-24437				
23	-42	-384	-718	-1133	-2746	-21715	-31033	32700				
24	-287	-421	-547	-636	-656	-572	-519	-376				
25	-82	-157	-230	-303	-379	-468	-562	-616				
26	-20	-30	-39	-47	-52	-44	-38	-31				
27	-100	-111	-113	-94	-41	77	229	437				
28	43	31	9	-30	-104	-243	-421	-639				
29	165	186	210	225	240	233	236	203				
30	-182	-205	-228	-242	-244	-185	-140	-51				
31	64	37	9	-37	-117	-274	-439	-663				
32	-128	-143	-155	-148	-113	12	158	385				
33	-181	-290	-396	-500	-610	-729	-850	-928				
34	0	-37	-76	-114	-150	-176	-200	-194				
35	-403	-578	-730	-854	-943	-941	-967	-958				
36	-15	-192	-379	-579	-804	-1058	-1340	-1536				
C.D.G.	.25	.29	.37	.52	.83	1.46	2.27	3.38	2.38	6.70	7.35	8.10
V.D.G.	.38	.47	.54	.60	.67	.77	.84	.91				

Table A.1 (cont.)

Strains  $\times 10^6$  and Deflexions (mm)

Test No. 97

Load (KN)	40	80	120	160	200	240	280	300	20	R 1	R 2	R 3
Gauge Ref.												
1	-95	-140	-178	-195	-171	-95	112	334				
2	-15	-99	-183	-292	-439	-640	-995	-1275				
3	-93	-121	-142	-144	-110	-28	184	412				
4	21	-34	-92	-174	-293	-456	-761	-1029				
5	-70	-78	-81	-69	-30	42	220	394				
6	46	15	-17	-71	-153	-265	-483	-691				
7	-62	-70	-75	-69	-41	8	132	253				
8	33	-1	-37	-89	-162	-253	-408	-546				
9	-67	-86	-101	-108	-99	-73	5	85				
10	13	-31	-77	-135	-209	-290	-414	-508				
11	-47	-47	-49	-44	-27	0	65	126				
12	23	-7	-38	-80	-133	-191	-276	-339				
13	-17	-4	7	26	58	95	168	234				
14	36	25	12	-8	-38	-71	-111	-132				
21	-682	-1067	-1372	-1592	-2290	-12246	-25619	-16423				
22	41	-264	-565	-1019	-1847	-10581	-26498	-15288				
23	-261	-390	-506	-597	-619	-573	-398	-169				
24	34	-86	-203	-355	-559	-837	-1275	-1647				
25	11	0	-9	-11	-2	16	62	106				
26	-53	-105	-157	-218	-288	-368	-478	-536				
27			Gauge	Broken								
28	-98	-121	-140	-154	-144	-105	14	155				
29	-98	-108	-117	-118	-102	-60	60	176				
30	128	136	144	141	124	80	-38	-154				
31	-84	-98	-108	-109	-91	-47	78	197				
32	84	72	60	35	-5	-68	-195	-307				
33	-52	-98	-137	-173	-202	-232	-265	-274				
34	-57	-147	-233	-330	-433	-522	-606	-650				
35	-122	-292	-441	-598	-760	-937	-1149	-1226				
36	-152	-312	-459	-610	-752	-859	-932	-970				
C.D.G.	-70	-73	-71	-77	-52	-07	.04	2.93	3.00	7.25	7.85	8.75
V.D.G.	.42	.53	.63	.72	.82	.93	1.05	1.12				

Table A.1 (cont.)

Strains x 10 <sup>6</sup> and Deflexions (mm)		Test No. 98							*Fail	
Gauge Ref.	Load (KN)	40	80	120	160	200	240	280	320	360
1		-43	-104	-166	-228	-287	-345	-402	-461	-530
2	(100)	-83	-150	-216	-278	-343	-405	-468	-524	-578
3	(100)	-22	-53	-86	-117	-148	-180	-212	-244	-281
4	(100)	-56	-100	-143	-187	-232	-280	-327	-370	-406
5	(200)	6	5	4	4	5	5	5	7	16
6	(200)	-24	-43	-64	-84	-107	-132	-162	-195	-231
7	(464)	-13	-19	-20	-23	-29	-38	-44	-49	-51
8	(464)	3	4	0	0	0	2	3	5	4
9	(564)	-39	-71	-96	-120	-146	-174	-197	-216	-234
10	(564)	-12	-26	-43	-58	-68	-70	-70	-59	-49
11	(664)	-46	-89	-125	-163	-205	-252	-299	-353	-409
12	(664)	-28	-58	-91	-122	-152	-175	-201	-224	-250
13	(764)	-20	-36	-53	-70	-95	-125	-159	-200	-245
14	(764)	-10	-24	-39	-56	-73	-87	-105	-119	-138
15	(842)	-10	-19	-25	-32	-43	-57	-74	-93	-114
16	(842)	-3	-6	-11	-14	-20	-17	-21	-19	-18
23		-95	-208	-324	-439	-554	-664	-767	-876	-1012
24		-136	-246	-349	-449	-548	-642	-724	-794	-847
25		-32	-73	-112	-153	-190	-227	-261	-290	-313
26		-42	-83	-123	-160	-201	-239	-281	-326	-383
27		-29	-59	-87	-110	-136	-167	-194	-210	-242
28		-14	-39	-65	-84	-111	-140	-180	-218	-275
29		12	14	13	13	15	19	22	29	37
30		-18	-25	-32	-37	-47	-53	-64	-75	-88
31		-11	-28	-44	-60	-77	-94	-113	-131	-149
32		-16	-30	-45	-60	-74	-83	-96	-106	-120
33		-95	-175	-247	-321	-405	-496	-595	-706	-820
34		-51	-110	-175	-239	-301	-359	-422	-486	-546
35		-243	-438	-618	-821	-1043	-1230	-1406	-1492	-1597
36		-148	-331	-525	-744	-975	-1155	-1271	-1347	-1334
C.D.G.		-.11	-.06	1.03	1.06	1.07	.08	.17	.21	.57
V.D.G.		.45	.87	1.15	1.52	1.86	2.24	2.60	3.03	3.44

\* Readings cannot be guaranteed

Table A.1 (cont.)

Load (KN)		Strains $\times 10^6$ and Deflexions (mm)					
Gauge Ref.		Test No. 99					
		40	80	120	160	200	240
							*Fail
1	(100)	-130	-246	-354	-457	-571	-703
2	(100)	111	201	269	323	412	550
3	(100)	-180	-343	-478	-612	-767	-964
4	(200)	85	150	195	236	295	398
5	(200)	-148	-272	-366	-453	-561	-712
6	(200)	51	110	149	177	229	302
7	(675)	-45	-78	-106	-131	-161	-195
8	(675)	38	69	92	117	145	182
9	(775)	-50	-97	-137	-178	-224	-274
10	(775)	21	33	40	48	59	78
11	(875)	-64	-126	-180	-236	-296	-362
12	(875)	-20	-22	-40	-53	-63	-64
13	(975)	-41	-79	-112	-144	-179	-219
14	(975)	-8	-2	-10	-14	-15	-10
15	(1053)	-32	-52	-76	-88	-108	-128
16	(1053)	-9	9	8	12	21	36
23		-274	-544	-796	-1057	-1345	-1674
24		186	352	493	625	804	1056
25		-49	-94	-129	-162	-198	-237
26		26	42	48	40	52	87
27		15	24	33	40	54	85
28		-72	-133	-187	-252	-313	-385
29		-14	-29	-42	-51	-63	-79
30		-2	11	16	21	28	39
31		-39	-80	-117	-153	-193	-240
32		2	18	20	26	36	53
33		-85	-164	-236	-306	-378	-451
34		-60	-112	-176	-241	-306	-365
35		-146	-302	-444	-589	-734	-872
36		-153	-358	-576	-805	-1038	-1269
C.D.G.		1.25	1.93	2.75	3.58	4.20	5.26
V.D.G.		1.81	1.32	1.72	2.11	2.62	3.07

\* Readings cannot be guaranteed

Table A.1 (cont.)

## A.2 Elastic Analysis Details

In Chapter 4, the analysis for a rectangular plate restrained along the two opposite loaded edges and free along the unloaded edges was presented. It was shown that the value of K, the elastic plate buckling coefficient, is dependent on the value of the wave length ratio  $\alpha = A / m$ . The resultant expression for K can then be differentiated with respect to  $\alpha$  to arrive at a minimum value, given the loading and boundary conditions. Equation 4.18 gave the following expression for K:

$$K = \frac{\left( \frac{\pi \rho}{\alpha} + \frac{\sin \pi \rho}{\alpha} \right) \left( \alpha^2 R_1 + 2 + \frac{R_2}{\alpha^2} \right) - 4(1-\nu) \frac{\sin \pi \rho}{\alpha}}{\frac{\alpha^2}{\beta} \left( \frac{\beta \pi}{\alpha} + \frac{\sin \beta \pi}{\alpha} \right) - \frac{\rho}{\beta \alpha} \frac{\sin \beta \pi}{\rho} \frac{[3R_3(1+Z) - R_4(1-Z)]}{(3\rho^2 + 2 + 3/\rho^2)}}$$

.....A.1

or:

$$K = \frac{\text{Numerator}}{\text{Denominator}} \quad \text{A.2}$$

then:

$$\begin{aligned} \frac{dK}{d\alpha} &= (\text{Denominator}) \times \frac{d}{d\alpha} (\text{Numerator}) \\ &\quad - (\text{Numerator}) \times \frac{d}{d\alpha} (\text{Denominator}) = 0 \end{aligned}$$

.....A.3

this results in an expression for the left hand side of A.3 of:

$$\begin{aligned}
 & (\text{Denominator}) \times \left\{ 2 \left( \frac{\pi \rho}{\alpha} + \frac{\sin \pi \rho}{\alpha} \right) (R_1 \alpha - R_2 / \alpha^3) \right. \\
 & \quad \left. + 4 (1-v) \frac{\pi \rho}{\alpha^2} \frac{\cos \pi \rho}{\alpha} - \left( 1 + \frac{\cos \pi \rho}{\alpha} \right) \frac{\pi \rho}{\alpha^2} (R_1 \alpha^2 + 2 + R_2 / \alpha^2) \right\} \\
 & - (\text{Numerator}) \times \left\{ \frac{2\alpha}{\beta} \left( \frac{\pi \beta}{\alpha} + \frac{\sin \pi \beta}{\alpha} \right) - \pi \left( 1 + \frac{\cos \pi \beta}{\alpha} \right) \right. \\
 & \quad \left. - \left[ \frac{\frac{\rho}{\alpha \beta} \frac{\sin \pi \beta}{\rho}}{(3 \rho^2 + 2 + 3 / \rho^2)} \right] \times \right. \\
 & \quad \left[ \frac{(3 R_3 + R_4) \left( \left( 1 - 3 \left( \frac{\rho}{\alpha} \right)^2 \right) \frac{\sin \pi \rho}{\alpha} - \frac{\pi \rho}{\alpha} \left( 1 - \left( \frac{\rho}{\alpha} \right)^2 \right) \frac{\cos \pi \rho}{\alpha} \right)}{\pi \rho (1 - (\rho / \alpha)^2)^2} \right. \\
 & \quad \left. \left. - \frac{1}{\alpha} \left( 3 R_3 (1 + Z) - R_4 (1 - Z) \right) \right] \right\} \dots A.4
 \end{aligned}$$

where:

$$Z = \frac{\alpha}{\pi \rho} \left( \frac{1}{1 - (\rho / \alpha)^2} \right) \frac{\sin \pi \rho}{\alpha} \quad A.5$$

Obviously the value of  $\alpha$  for expression A.4 to be equal to zero can only be determined practically either by a graphical method or by a computer analysis. The author chose the latter, the flow diagram for which is shown in figures A.1 and A.2. The main process involves an iteration technique.

In the computer program the value of  $\alpha$  is increased in large steps until expression A.4 changes sign, and then increased in smaller steps from the last value before the



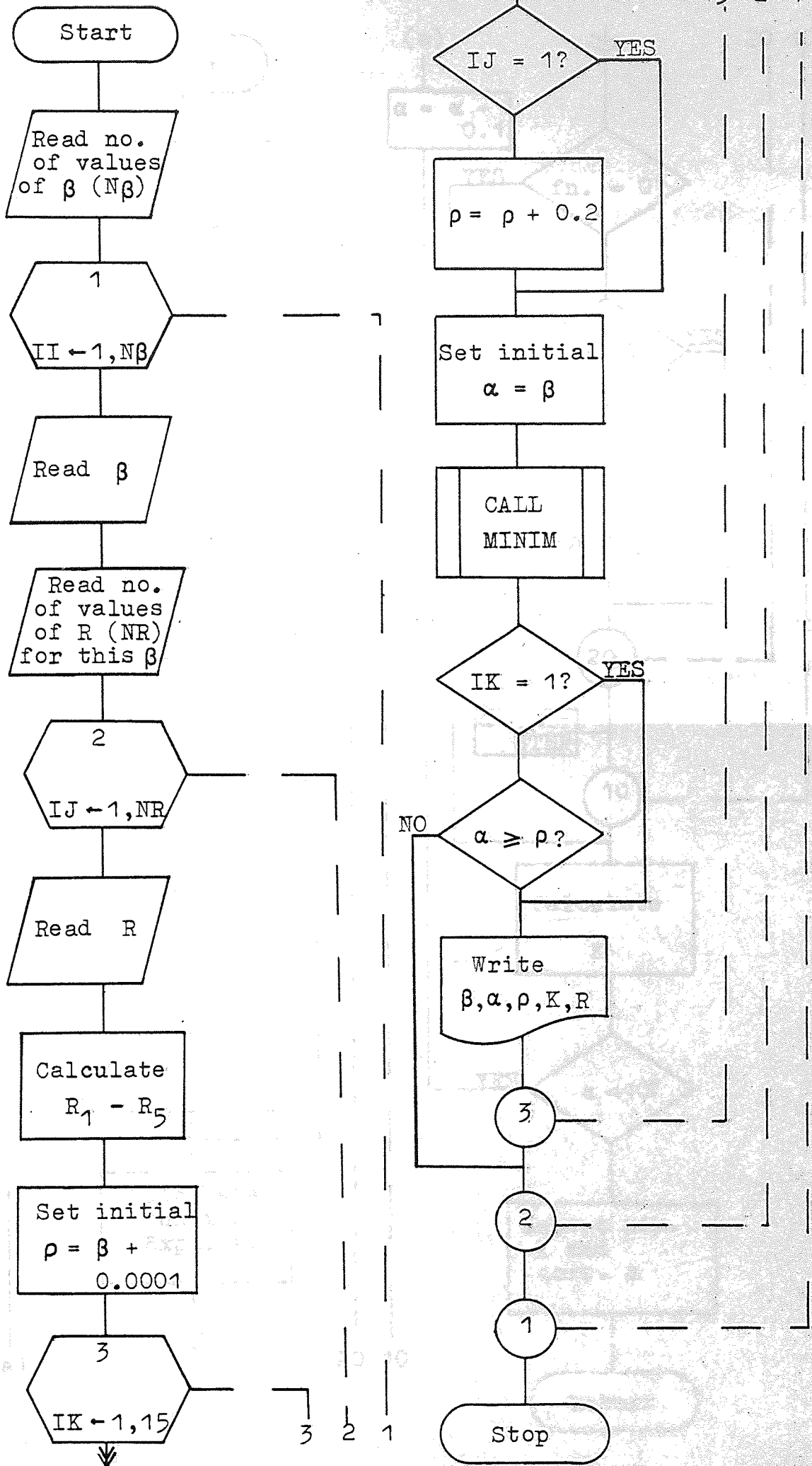


Figure A.1 Main Program

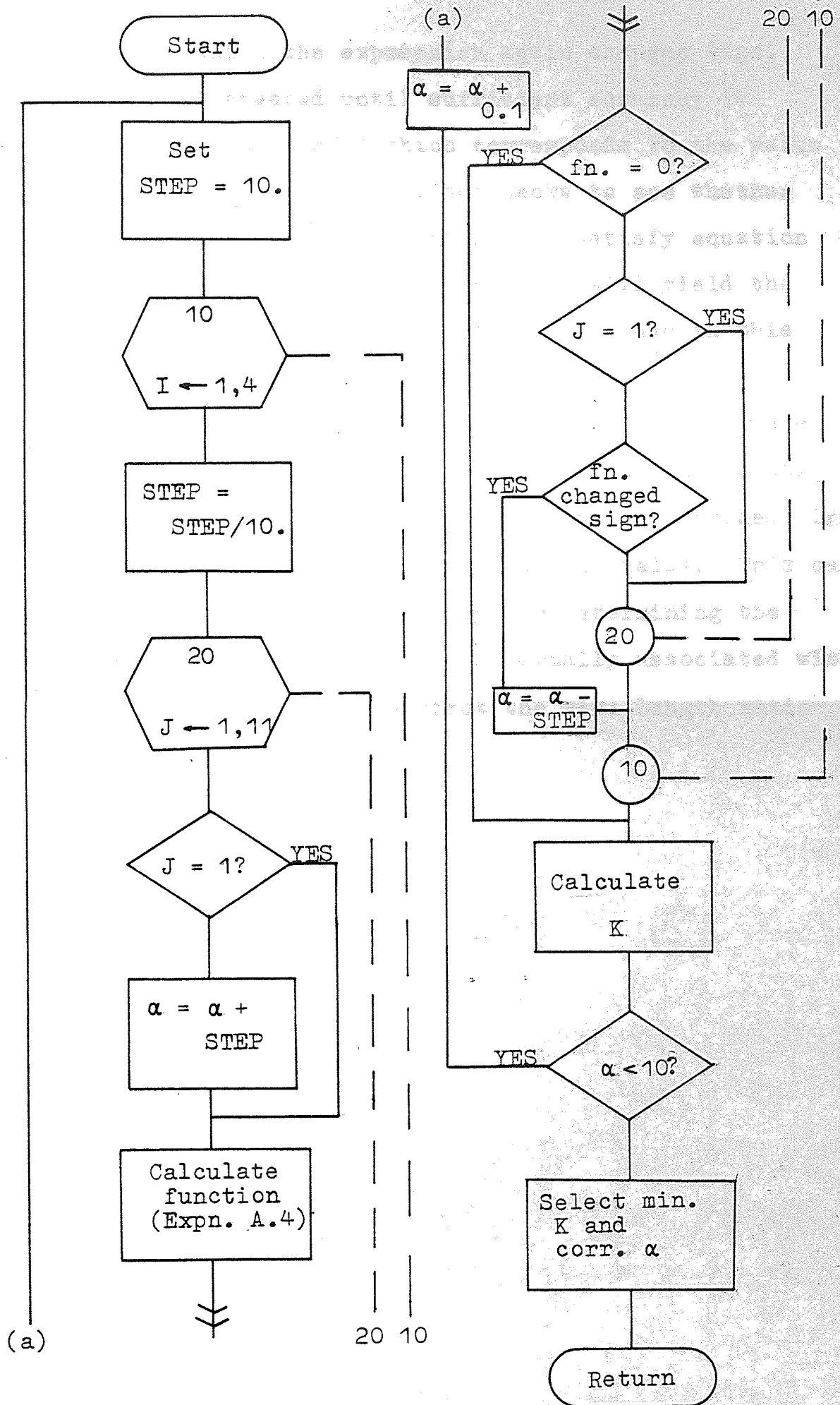


Figure A.2 Subroutine MINIM.

change of sign until the expression again changes sign. This process is repeated until sufficient accuracy is obtained for the value of  $K$  which corresponds to the value of  $\alpha$  determined. The program also checks to see whether there is a further value of  $\alpha$  which will satisfy equation A.3 and if there is selects the one which will yield the lowest value of  $K$ . The results obtained for use in this work are shown in Table A.2.

The value of the wave length ratio  $\alpha$  for small plate lengths was taken as approximately the loaded length ratio  $\beta ( = C / m ) + 11.0$ ; if expression A.4 had not changed sign at any of the increments leading up to this value. This can be seen to give sufficient accuracy for determining the value of  $K$ , as the values are those normally associated with a strut. In actual fact for a strut the wave length ratio would be infinitely large.

Aspect	Buckling	Wave	Aspect	Buckling	Wave	Aspect	Buckling	Wave
Ratio	Coefficient	Length	Ratio	Coefficient	Length	Ratio	Coefficient	Length
l/m	K	Ratio	l/m	K	Ratio	l/m	K	Ratio
		A/m			A/m			A/m

Loaded length ratio = C/m = 0.05

Restraint coefficient = 0.0			Restraint coefficient = 0.4			Restraint coefficient = 1.0		
0.05	0.050	11.160	0.05	0.063	11.160	0.05	0.091	11.160
0.25	0.251	11.290	0.25	0.316	11.291	0.05	0.454	11.291
0.45	0.452	11.351	0.45	0.570	11.352	0.45	0.817	11.352
0.65	0.653	11.407	0.65	0.823	11.408	0.65	1.180	11.408
0.85	0.853	11.454	0.85	1.074	11.457	0.85	1.542	11.458
1.05	1.051	11.483	1.05	1.324	11.490	1.05	1.897	4.478
1.25	1.236	3.890	1.25	1.545	3.140	1.25	2.158	2.319
1.45	1.377	2.787	1.45	1.693	2.393	1.45	2.295	1.932
1.65	1.476	2.445	1.65	1.786	2.164	1.65	2.367	1.839
1.85	1.546	2.324	1.85	1.850	2.103	1.85	2.394	-
2.05	1.601	2.300	2.05	1.879	-			
2.25	1.615	-						

Restraint coefficient = 2.0			Restraint coefficient = 5.0			Restraint coefficient = $\infty$		
0.05	0.122	11.160	0.05	0.159	11.160	0.05	0.200	11.160
0.25	0.609	11.364	0.25	0.795	11.365	0.25	1.001	11.363
0.45	1.096	11.351	0.45	1.431	11.351	0.45	1.803	11.350
0.65	1.582	11.408	0.65	2.067	11.407	0.65	2.604	11.406
0.85	2.067	11.457	0.85	2.700	11.456	0.85	3.401	11.454
1.05	2.527	3.021	1.05	3.264	2.310	1.05	4.048	1.880
1.25	2.800	1.896	1.25	3.510	1.619	1.25	4.226	1.437
1.45	2.901	1.667	1.45	3.560	1.509	1.45	4.228	-
1.65	2.938	-	1.65	3.565	-			

Table A.2

Aspect	Buckling	Wave	Aspect	Buckling	Wave	Aspect	Buckling	Wave
Ratio	Coefficient	Length	Ratio	Coefficient	Length	Ratio	Coefficient	Length
$l/m$	K	Ratio	$l/m$	K	Ratio	$l/m$	K	Ratio
		A/m			A/m			A/m

Loaded length ratio =  $C/m = 0.1$

Restraint coefficient = 0.0			Restraint coefficient = 0.4			Restraint coefficient = 1.0		
0.10	0.100	11.210	0.10	0.127	11.210	0.10	0.182	11.210
0.30	0.301	11.210	0.30	0.380	11.210	0.30	0.545	11.210
0.50	0.502	11.366	0.50	0.633	11.367	0.50	0.908	11.367
0.70	0.703	11.421	0.70	0.886	11.422	0.70	1.271	11.423
0.90	0.902	11.466	0.90	1.137	11.469	0.90	1.632	11.469
1.10	1.100	11.422	1.10	1.385	6.154	1.10	1.975	3.405
1.30	1.277	3.469	1.30	1.590	2.864	1.30	2.204	2.178
1.50	1.406	2.675	1.50	1.722	2.317	1.50	2.320	1.898
1.70	1.497	2.407	1.70	1.806	2.143	1.70	2.385	1.839
1.90	1.562	2.315	1.90	1.866	2.105	1.90	2.339	-
2.10	1.615	2.306	2.10	1.882	-			
2.30	1.618	-						

Restraint coefficient = 2.0			Restraint coefficient = 5.0			Restraint coefficient = $\infty$		
0.10	0.243	11.210	0.10	0.318	11.210	0.10	0.400	11.210
0.30	0.730	11.210	0.30	0.954	11.210	0.30	1.202	11.210
0.50	1.218	11.367	0.50	1.590	11.360	0.50	2.003	11.365
0.70	1.704	11.427	0.70	2.225	11.421	0.70	2.803	11.420
0.90	2.188	11.469	0.90	2.857	11.467	0.90	3.598	5.434
1.10	2.617	2.526	1.10	3.359	2.017	1.10	4.135	1.690
1.30	2.839	1.814	1.30	3.538	1.573	1.30	4.239	-
1.50	2.920	1.666	1.50	3.574	-			
1.70	2.945	-						

Table A.2 (cont.)



Aspect	Buckling	Wave	Aspect	Buckling	Wave
Ratio	Coefficient	Length	Ratio	Coefficient	Length
l/m	K	Ratio	l/m	K	Ratio
		A/m			A/m

Loaded length ratio =  $C/m = 0.25$

Restraint coefficient = 0.0					
Aspect	Buckling	Wave	Aspect	Buckling	Wave
Ratio	Coefficient	Length	Ratio	Coefficient	Length
l/m	K	Ratio	l/m	K	Ratio
		A/m			A/m
0.25	0.251	11.360	0.25	0.316	11.360
0.45	0.452	11.360	0.45	0.570	11.360
0.65	0.653	11.360	0.65	0.822	11.360
0.85	0.852	11.464	0.85	1.074	11.466
1.05	1.051	11.502	1.05	1.324	11.505
1.25	1.239	4.088	1.25	1.548	3.265
1.45	1.384	2.865	1.45	1.704	2.455
1.65	1.486	2.493	1.65	1.802	2.204
1.85	1.559	2.358	1.85	1.869	2.133
2.05	1.615	2.325	2.05	1.906	-
2.25	1.636	-			

Restraint coefficient = 1.0					
Aspect	Buckling	Wave	Aspect	Buckling	Wave
Ratio	Coefficient	Length	Ratio	Coefficient	Length
l/m	K	Ratio	l/m	K	Ratio
		A/m			A/m
0.25	0.454	11.360	0.25	0.454	11.360
0.45	0.817	11.360	0.45	0.817	11.360
0.65	1.180	11.360	0.65	1.180	11.360
0.85	1.542	11.466	0.85	1.542	11.466
1.05	1.898	4.722	1.05	1.898	4.722
1.25	2.169	2.397	1.25	2.169	2.397
1.45	2.319	1.979	1.45	2.319	1.979
1.65	2.397	1.867	1.65	2.397	1.867
1.85	2.433	-	1.85	2.433	-

Restraint coefficient = 2.0					
Aspect	Buckling	Wave	Aspect	Buckling	Wave
Ratio	Coefficient	Length	Ratio	Coefficient	Length
l/m	K	Ratio	l/m	K	Ratio
		A/m			A/m
0.25	0.609	11.360	0.25	0.795	11.360
0.45	1.095	11.360	0.45	1.431	11.360
0.65	1.582	11.360	0.65	2.066	11.360
0.85	2.067	11.465	0.85	2.700	11.464
1.05	2.529	3.133	1.05	3.271	2.393
1.25	2.821	1.960	1.25	3.551	1.674
1.45	2.941	1.718	1.45	3.624	1.544
1.65	2.992	-	1.65	3.635	-

Restraint coefficient = $\infty$					
Aspect	Buckling	Wave	Aspect	Buckling	Wave
Ratio	Coefficient	Length	Ratio	Coefficient	Length
l/m	K	Ratio	l/m	K	Ratio
		A/m			A/m
0.25	1.001	11.360	0.25	1.001	11.360
0.45	1.802	11.360	0.45	1.802	11.360
0.65	2.603	11.360	0.65	2.603	11.360
0.85	3.401	11.463	0.85	3.401	11.463
1.05	4.062	1.955	1.05	4.062	1.955
1.25	4.294	1.486	1.25	4.294	1.486
1.45	4.318	-	1.45	4.318	-

Table A.2 (cont.)



Aspect Ratio	Buckling Coefficient	Wave Length Ratio	Aspect Ratio	Buckling Coefficient	Wave Length Ratio
$l/m$	K	$A/m$	$l/m$	K	$A/m$

Loaded length ratio =  $C/m = 0.50$

Restraint coefficient = 0.0					
0.50	0.502	11.610	0.50	0.633	11.610
0.70	0.703	11.610	0.70	0.885	11.610
0.90	0.902	11.610	0.90	1.137	11.610
1.10	1.101	11.610	1.10	1.387	11.610
1.30	1.288	4.170	1.30	1.610	3.324
1.50	1.434	2.968	1.50	1.768	2.549
1.70	1.539	2.587	1.70	1.871	2.295
1.90	1.614	2.442	1.90	1.941	2.216
2.10	1.671	2.403	2.10	1.986	-
2.30	1.699	-			
Restraint coefficient = 1.0					
			0.50	0.908	11.610
			0.70	1.270	11.610
			0.90	1.632	11.610
			1.10	1.985	4.247
			1.30	2.256	2.473
			1.50	2.416	2.074
			1.70	2.505	1.960
			1.90	2.552	-

Restraint coefficient = 2.0					
0.50	1.217	11.610	0.50	1.589	11.610
0.70	1.703	11.610	0.70	2.224	11.610
0.90	2.187	11.610	0.90	2.857	5.143
1.10	2.641	2.989	1.10	3.410	1.983
1.30	2.939	2.048	1.30	3.713	1.593
1.50	3.082	1.814	1.50	3.824	1.527
1.70	3.152	1.773	1.70	3.851	-
1.90	3.154	-			
Restraint coefficient = $\infty$					
			0.50	2.002	11.610
			0.70	2.802	11.610
			0.90	3.598	5.143
			1.10	4.234	1.983
			1.30	4.517	1.593
			1.50	4.592	1.527
			1.70	4.594	-

Table A.2 (cont.)

Aspect	Buckling	Wave	Aspect	Buckling	Wave	Aspect	Buckling	Wave
Ratio	Coefficient	Length	Ratio	Coefficient	Length	Ratio	Coefficient	Length
l/m	K	Ratio	l/m	K	Ratio	l/m	K	Ratio
		A/m			A/m			A/m

Loaded length ratio =  $C/m = 0.75$

Restraint coefficient = 0.0			Restraint coefficient = 0.4			Restraint coefficient = 1.0		
0.75	0.753	11.860	0.75	0.949	11.860	0.75	1.362	11.860
0.95	0.953	11.860	0.95	1.201	11.860	0.95	1.723	11.860
1.15	1.151	11.860	1.15	1.451	11.860	1.15	2.079	5.336
1.35	1.343	4.936	1.35	1.682	3.777	1.35	2.370	2.760
1.55	1.498	3.259	1.55	1.854	2.784	1.55	2.557	2.264
1.75	1.612	2.779	1.75	1.970	2.465	1.75	2.665	2.108
1.95	1.693	2.593	1.95	2.048	2.353	1.95	2.735	2.079
2.15	1.753	2.528	2.15	2.106	2.334	2.15	2.742	-
2.35	1.798	-	2.35	2.114	-			

Restraint coefficient = 2.0			Restraint coefficient = 5.0			Restraint coefficient = $\infty$		
0.75	1.825	11.860	0.75	2.384	11.860	0.75	3.003	11.860
0.95	2.310	11.860	0.95	3.016	11.860	0.95	3.800	11.860
1.15	2.774	3.486	1.15	3.594	2.705	1.15	4.481	2.270
1.35	3.109	2.281	1.35	3.960	1.979	1.35	4.860	1.782
1.55	3.293	1.983	1.55	4.130	1.797	1.55	5.010	1.674
1.75	3.388	1.909	1.75	4.199	-	1.75	5.039	-
1.95	3.415	-						

Table A.2 (cont.)

Aspect Ratio	Buckling Coefficient	Wave Length Ratio	Aspect Ratio	Buckling Coefficient	Wave Length Ratio
$l/m$	K	$A/m$	$l/m$	K	$A/m$

Loaded length ratio =  $C/m = 1.0$

Restraint coefficient = 0.0			Restraint coefficient = 0.4			Restraint coefficient = 1.0		
1.00	1.004	12.110	1.00	1.265	12.110	1.00	1.815	12.110
1.20	1.203	12.110	1.20	1.515	12.110	1.20	2.174	12.110
1.40	1.399	9.128	1.40	1.760	5.347	1.40	2.502	3.487
1.60	1.571	3.874	1.60	1.955	3.236	1.60	2.729	2.585
1.80	1.699	3.099	1.80	2.090	2.731	1.80	2.866	2.323
2.00	1.790	2.814	2.00	2.181	2.548	2.00	2.951	2.246
2.20	1.856	2.702	2.20	2.245	2.492	2.20	2.991	-
2.40	1.908	2.675	2.40	2.280	-			
2.60	1.927	-						

Restraint coefficient = 2.0			Restraint coefficient = 5.0			Restraint coefficient = $\infty$		
1.00	2.434	12.110	1.00	3.179	12.110	1.00	4.004	12.110
1.20	2.915	9.106	1.20	3.802	4.576	1.20	4.775	3.410
1.40	3.313	2.780	1.40	4.263	2.366	1.40	5.285	2.107
1.60	3.555	2.246	1.60	4.510	2.024	1.60	5.528	1.878
1.80	3.686	2.097	1.80	4.631	1.945	1.80	5.632	-
2.00	3.759	-	2.00	4.659	-			

Table A.2 (cont.)

Aspect Ratio	Buckling Coefficient	Wave Length	Aspect Ratio	Buckling Coefficient	Wave Length	Aspect Ratio	Buckling Coefficient	Wave Length
l/m	K	Ratio	l/m	K	Ratio	l/m	K	Ratio
		A/m			A/m			A/m

Loaded length ratio = C/m = 1.5

Restraint coefficient = 0.0      Restraint coefficient = 0.4      Restraint coefficient = 1.0

1.50	1.506	12.610	1.50	1.897	12.610	1.50	2.723	12.610
1.70	1.701	12.610	1.70	2.144	12.610	1.70	3.072	5.830
1.90	1.882	4.963	1.90	2.354	4.068	1.90	3.321	3.229
2.10	2.013	3.671	2.10	2.494	3.247	2.10	3.467	2.788
2.30	2.105	3.265	2.30	2.586	3.978	2.30	3.555	2.654
2.50	2.170	3.104	2.50	2.649	2.883	2.50	3.615	2.631
2.70	2.218	3.050	2.70	2.696	2.868	2.70	3.617	-
2.90	2.250	-	2.90	2.699	-			

Restraint coefficient = 2.0

Restraint coefficient = 5.0

Restraint coefficient =  $\infty$

1.50	3.650	12.610	1.50	4.768	12.610	1.50	6.006	12.610
1.70	4.102	4.186	1.70	5.327	3.408	1.70	6.667	2.967
1.90	4.375	2.807	1.90	5.615	2.535	1.90	6.962	2.359
2.10	4.520	2.536	2.10	5.755	2.367	2.10	7.096	2.254
2.30	4.604	2.472	2.30	5.820	-	2.30	7.127	-
2.50	4.625							

Table A.2 (cont.)

Aspect Ratio	Buckling Coefficient	Wave Length	Aspect Ratio	Buckling Coefficient	Wave Length	Aspect Ratio	Buckling Coefficient	Wave Length
l/m	K	Ratio A/m	l/m	K	Ratio A/m	l/m	K	Ratio A/m

Loaded length ratio = C/m 2.0

Restraint coefficient = 0.0			Restraint coefficient = 0.4			Restraint coefficient = 1.0		
2.00	2.007	13.110	2.00	2.529	13.110	2.00	3.630	13.110
2.20	2.200	13.110	2.20	2.769	7.698	2.20	3.958	5.105
2.40	2.357	4.809	2.40	2.943	4.169	2.40	4.149	3.510
2.60	2.460	3.930	2.60	3.048	3.572	2.60	4.253	3.175
2.80	2.529	3.623	2.80	3.116	3.368	2.80	4.316	3.078
3.00	2.578	3.502	3.00	3.163	3.301	3.00	4.349	-
3.20	2.615	3.467	3.20	3.189	-			
3.40	2.629	-						

Restraint coefficient = 2.0			Restraint coefficient = 5.0			Restraint coefficient = $\infty$		
2.00	4.866	13.110	2.00	6.356	13.110	2.00	8.007	13.110
2.20	5.277	4.142	2.20	6.848	3.587	2.20	8.571	3.247
2.40	5.474	3.158	2.40	7.044	2.927	2.40	8.761	2.775
2.60	5.572	2.953	2.60	7.136	2.802	2.60	8.849	2.702
2.80	5.632	2.913	2.80	7.162	-	2.80	8.855	-
3.00	5.634	-						

Table A.2 (cont.)



Aspect Ratio	Buckling Coefficient K	Wave Length Ratio A/m	Aspect Ratio l/m	Buckling Coefficient K	Wave Length Ratio A/m
--------------	------------------------	-----------------------	------------------	------------------------	-----------------------

Loaded length ratio = C/m = 2.5

Restraint coefficient = 0.0			Restraint coefficient = 0.4			Restraint coefficient = 1.0		
2.50	2.509	13.610	2.50	3.161	13.610	2.50	4.537	13.610
2.70	2.696	9.274	2.70	3.391	6.949	2.70	4.843	5.217
2.90	2.832	5.043	2.90	3.536	4.495	2.90	4.994	3.910
3.10	2.915	4.311	3.10	3.619	3.984	3.10	5.072	3.617
3.30	2.969	4.044	3.30	3.670	3.806	3.30	5.119	3.535
3.50	3.007	3.941	3.50	3.707	3.752	3.50	5.138	-
3.70	3.037	3.915	3.70	3.722	-			
3.90	3.043	-						

Restraint coefficient = 2.0			Restraint coefficient = 5.0			Restraint coefficient = ∞		
2.50	6.082	13.610	2.50	7.945	13.610	2.50	10.009	13.610
2.70	6.455	4.438	2.70	8.380	3.959	2.70	10.498	3.656
2.90	6.605	3.589	2.90	8.523	3.375	2.90	10.632	3.234
3.10	6.676	3.409	3.10	8.589	3.268	3.10	10.691	-
3.30	6.715	-	3.30	8.605	-			

Table A.2 (cont.)



Aspect Ratio	Buckling Coefficient	Wave Length	Aspect Ratio	Buckling Coefficient	Wave Length	Aspect Ratio	Buckling Coefficient	Wave Length
1/m	K	Ratio	1/m	K	Ratio	1/m	K	Ratio
		A/m			A/m			A/m

Loaded length ratio =  $C/m = 3.0$

Restraint coefficient = 0.0			Restraint coefficient = 0.4			Restraint coefficient = 1.0		
3.00	3.010	14.110	3.00	3.793	14.110	3.00	5.444	14.110
3.20	3.191	8.581	3.20	4.012	6.956	3.20	5.728	5.530
3.40	3.309	5.401	3.40	4.135	4.900	3.40	5.852	4.354
3.60	3.378	4.740	3.60	4.201	4.430	3.60	5.912	4.081
3.80	3.421	4.495	3.80	4.242	4.267	3.80	5.948	4.007
4.00	3.452	4.400	4.00	4.271	4.219	4.00	5.960	-
4.20	3.476	4.379	4.20	4.280	-			
4.40	3.477	-						

Restraint coefficient = 2.0			Restraint coefficient = 5.0			Restraint coefficient = $\infty$		
3.00	7.298	14.110	3.00	9.533	14.110	3.00	12.010	14.110
3.20	7.638	4.833	3.20	9.924	4.392	3.20	12.441	4.108
3.40	7.756	4.050	3.40	10.032	3.846	3.40	12.541	3.711
3.60	7.810	3.882	3.60	10.082	3.747	3.60	12.583	-
3.80	7.837	-	3.80	10.091	-			

Table A.2 (cont.)

Aspect Ratio	Buckling Coefficient	Wave Length Ratio	Aspect Ratio	Buckling Coefficient	Wave Length Ratio	Aspect Ratio	Buckling Coefficient	Wave Length Ratio
l/m	K	A/m	l/m	K	A/m	l/m	K	A/m

Loaded length ratio =  $C/m = 3.5$

Restraint coefficient = 0.0

3.50	3.511	14.610
3.70	3.685	8.531
3.90	3.788	5.813
4.10	3.846	5.193
4.30	3.882	4.960
4.50	3.907	4.871
4.70	3.926	-

Restraint coefficient = 0.4

3.50	4.424	14.610
3.70	4.633	7.193
3.90	4.738	5.340
4.10	4.793	4.895
4.30	4.826	4.740
4.50	4.850	4.695
4.70	4.855	-

Restraint coefficient = 1.0

3.50	6.351	14.610
3.70	6.616	5.921
3.90	6.718	4.817
4.10	6.766	4.557
4.30	6.795	4.487
4.50	6.803	-

Restraint coefficient = 2.0

3.50	8.514	14.610
3.70	8.826	5.270
3.90	8.921	4.524
4.10	8.964	4.364
4.30	8.983	-

Restraint coefficient = 5.0

3.50	11.122	14.610
3.70	11.475	4.851
3.90	11.561	4.327
4.10	11.599	4.233
4.30	11.605	-

Restraint coefficient =  $\infty$

3.50	14.011	14.610
3.70	14.397	4.579
3.90	14.475	4.196
4.10	14.505	-

Table A.2 (cont.)

Aspect Ratio	Buckling Coefficient	Wave Length Ratio	Aspect Ratio	Buckling Coefficient	Wave Length Ratio
l/m	K	A/m	l/m	K	A/m

Loaded length ratio = C/m = 4.0

Restraint coefficient = 0.0			Restraint coefficient = 0.4			Restraint coefficient = 1.0		
4.00	4.012	15.110	4.00	5.056	15.110	4.00	7.257	15.110
4.20	4.179	8.716	4.20	5.253	7.531	4.20	7.505	6.350
4.40	4.270	6.253	4.40	5.345	5.799	4.40	7.591	5.293
4.60	4.319	5.659	4.60	5.391	5.370	4.60	7.630	5.040
4.80	4.349	5.435	4.80	5.418	5.220	4.80	7.654	4.973
5.00	4.370	5.349	5.00	5.438	5.177	5.00	7.660	-
5.20	4.385	-	5.20	5.441	-			

Restraint coefficient = 2.0			Restraint coefficient = 5.0			Restraint coefficient = $\infty$		
4.00	9.730	15.110	4.00	12.710	15.110	4.00	16.012	15.110
4.20	10.018	5.729	4.20	13.032	5.324	4.20	16.361	5.059
4.40	10.096	5.007	4.40	13.101	4.814	4.40	16.423	4.686
4.60	10.130	4.851	4.60	13.132	4.723	4.60	16.446	-
4.80	10.145	-	4.80	13.136	-			

Table A.2 (cont.)